MycoKeys 81: 1–44 (2021)
doi: 10.3897/mycokeys.81.67785
https://mycokeys.pensoft.net

RESEARCH ARTICLE

A peer-reviewed open-access journal
MycoKeys
Launched to accelerate biodiversity research

Phylogeny and taxonomy of *Catenularia* and similar fungi with catenate conidia

Martina Réblová[1], Jana Nekvindová[2], Andrew N. Miller[3]

1 *Czech Academy of Sciences, Institute of Botany, Průhonice 252 43, Czech Republic* **2** *Department of Clinical Biochemistry and Diagnostics, University Hospital Hradec Králové, Hradec Králové 500 05, Czech Republic* **3** *Illinois Natural History Survey, University of Illinois Urbana-Champaign, Champaign, Illinois 61820, USA*

Corresponding author: Martina Réblová (martina.reblova@ibot.cas.cz)

Academic editor: Thorsten Lumbsch | Received 23 April 2021 | Accepted 23 May 2021 | Published 11 June 2021

Citation: Réblová M, Nekvindová J, Miller AN (2021) Phylogeny and taxonomy of *Catenularia* and similar fungi with catenate conidia. MycoKeys 81: 1–44. https://doi.org/10.3897/mycokeys.81.67785

Abstract

The genus *Catenularia* (Chaetosphaeriaceae) was reviewed, and its relationships with morphologically similar fungi were evaluated using molecular and morphological data. Eleven species are accepted, four of which have been verified with molecular DNA data. The correct epithet '*cupulifera*' is proposed for the type species *C. cupulifera* **comb. nov.** Four other combinations are proposed, namely *C. catenulata* **comb. nov.**, *C. elsikii* **comb. nov.**, *C. minor* **comb. nov.** and *C. novae-zelandiae* **comb. nov.** *Catenularia* is an uncommon fungus inhabiting mainly decaying bark, wood and bamboo culms of various hosts and shows a widespread geographical distribution. It is circumscribed for fungi with mononematous, macronematous, simple conidiophores with terminal monophialides, usually accompanied with capitate hyphae. The conidia are aseptate, brown, cuneiform to rounded-obconic with an angular outline, adhering in chains. The diagnostic values of taxonomic characteristics of capitate hyphae and conidia (i.e. colour, shape in transverse section, setulae and formation) at the generic level were evaluated. An account of morphology, taxonomy and phylogeny of species accepted in *Catenularia* is provided. Based on ribosomal DNA sequences, *Chalarodes obpyramidata* **sp. nov.**, characterised by catenate, angular, hyaline conidia with apical setulae, is revealed as closely related to *Catenularia*. The new genus *Fuscocatenula* **gen. nov.** is proposed for catenularia-like fungi having pigmented conidia with protracted maturation and round outline, with two species accepted, *F. submersa* **comb. nov.** and *F. variegata* **comb. nov.** A new species *Nawawia antennata* **sp. nov.** is introduced and *Nawawia* is compared with morphologically similar taxa.

Keywords

angular conidia, basipetal chain, *Chaetosphaeria*, lignicolous, molecular systematics, phialidic conidiogenesis, 10 taxonomic novelties

Introduction

Catenularia (Saccardo 1886) is one of the oldest genera classified in the Chaetosphaeriaceae. In April 1886, Saccardo introduced '*Catenularia* Grove in litt.' with two species, '*C. simplex* Grove in litt.' and *C. atra* (= *Spadicoides atra*, Hughes 1958), of which *C. simplex* is regarded as the type (Clements and Shear 1931). Grove (1886) intended the genus to be monotypic, and later that year published *Catenularia* again with *C. simplex* as the only species observed on wood in the United Kingdom. However, *C. simplex* has previously been described by Berkeley and Broome (1871) as the presumed but nameless conidial state of *Sphaeria cupulifera* on decaying elm roots also in the United Kingdom. The species was illustrated with pigmented conidiophores arising singly from ascomata and in tufts around them, with a funnel-shaped collarette and cuneiform, dark brown, aseptate conidia adhering in chains. The anamorph was named *Psilonia cuneiformis* by Richon (1877) based on a collection on wood in France and later transferred to the monotypic genus *Psiloniella* (Costantin 1888). Mason (1941) concluded that *P. cuneiformis* and *C. simplex* are conspecific and accepted *P. cuneiformis* in *Catenularia* with *C. simplex* listed as a synonym. De Seynes (1886) and Booth (1958) confirmed that *S. cupulifera* (= *Chaetosphaeria cupulifera*, Saccardo 1883) and *C. cuneiformis* belong to the life cycle of the same species (Fig. 1). Booth (1958) noted that the conidiophores develop from the modified outer cells of the ascomatal wall and arise from hyphae at the ascomatal bases.

Linder (1933) erected *Haplochalara* based on *H. angulospora* for fungi morphologically similar to *Catenularia* and compared it with *Chalaropsis* and *Thielaviopsis* based on the similar pigmented, phialidic conidia in chains. Both latter genera are currently accepted in the Ceratocystidaceae (De Beer et al. 2014). Mason (1941) was the first to suggest the remarkable similarity of *H. angulospora* to *Catenularia* and transferred it to the latter genus.

Hughes (1965) presented the first comprehensive treatise of *Catenularia* and accepted four species. The genus was circumscribed for lignicolous hyphomycetes with simple, pigmented conidiophores arising solitary or in tufts, with dark stromatic cells around their bases, accompanied by capitate hyphae and with monophialidic conidiogenous cells extending percurrently. The conidia adhere in chains; they are aseptate, brown, cuneiform to rounded-obconic in side view, polygonal in transverse section with a small, circular, thin-walled, pale area at each corner. Capitate hyphae, a term coined by Hughes (1949), were originally proposed for sterile hyphae scattered among conidiophores of *Sporoschisma*. These are erect, brown, septate hyphae that extend percurrently and terminate into a paler, swollen apex. The apical cell bears a mucilaginous hyaline cap or pale coloured droplets that may disappear with age. Capitate hyphae also occur on the ascomatal wall of the teleomorphs.

Hughes (1965) did not accept the synonymy of *Catenularia* and *Haplochalara*. He considered capitate hyphae to be one of the main diagnostic features at the generic level, but which were missing in *H. angulospora*. Hughes (1965) excluded from *Catenularia* another nine species with ellipsoidal or globose, hyaline or slightly pig-

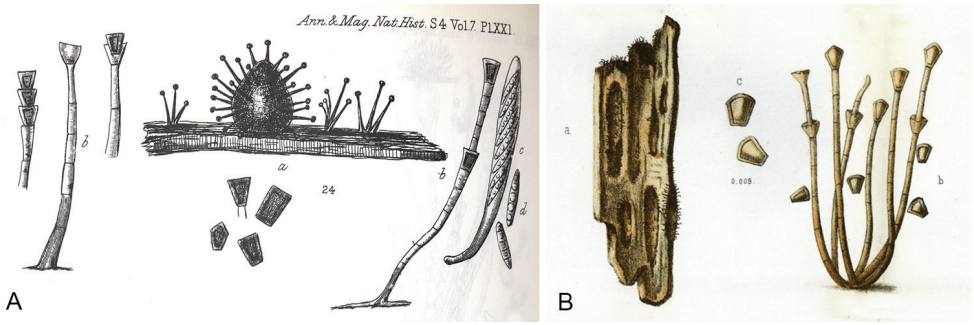

Figure 1. Illustrations of teleomorph and anamorph of *Catenularia cupulifera* **A** *Sphaeria cupulifera*: ascoma, ascus and ascospores with sporulating conidiophores (holotype, Berkeley and Broome 1871) **B** *Psilonia cuneiformis*: conidiophores with conidia (holotype, Richon 1877).

mented conidia, different conidiogenous cell morphology and modes of conidiogenesis. Some of these species have been reclassified and are currently attributed to genera such as *Chloridium*, *Exochalara*, *Gliomastix*, *Monilochaetes*, *Periconia*, *Spadicoides*, *Sporoschismopsis* and *Thielaviopsis* (Mangenot 1952; Booth 1957; Hughes 1958, 1965; Von Arx 1970; Holubová-Jechová and Hennebert 1972; Gams and Holubová-Jechová 1976; Schoknecht and Crane 1977; Rong and Gams 2000; Mbenoun et al. 2014; De Beer et al. 2014). Other authors did not follow such a narrow generic circumscription and several species without capitate hyphae were introduced in *Catenularia*, namely *C. catenulata* (Luo et al. 2019), *C. hughesii* (Sharma 1980), *C. kalakadensis* and *C. malabrica* (Subramanian and Bhat 1989), and *C. variegata* (Li et al. 2017). Admission of *C. variegata* in *Catenularia* introduced further heterogeneity into the genus. This species has a protracted maturation of conidia that are cuneiform or obovoid in the side view, but have round outline and lack typical corners with pore-like areas at the apex.

Species with the *Catenularia* morphotype have been named inconsistently as *Catenularia* or *Chaetosphaeria*. To date, 24 species and varieties have been referred to as *Catenularia* and six as their *Chaetosphaeria* counterparts (Berkeley and Broome 1871; Saccardo 1886; Linder 1933; Booth 1958; Hughes 1965; Sharma 1980; Holubová-Jechová 1982, 1983; Subramanian and Bhat 1989; Réblová and Seifert 2003; Li et al. 2017; Luo et al. 2019). They have a saprobic lifestyle and occur on decaying bark, wood or bamboo culms in terrestrial, less often freshwater habitats worldwide. Pound et al. (2019) published *Ch. elsikii*, a fossil species similar to the *Catenularia* anamorph of *Ch. novae-zelandiae*. After the abolishment of dual nomenclature and subsequent changes to the International Code of Nomenclature for algae, fungi, and plants (ICN; McNeill et al. 2012), *Catenularia* has never been formally accepted as a holomorphic genus, along with the correct taxonomic treatment of its type species.

The characteristics of conidia, conidiogenous cells, conidiophores and the mode of conidiogenesis are the main diagnostic traits that distinguish genera of the Chaetosphaeriaceae, while their teleomorphs are usually morphologically uniform. Among members of the family, *Catenularia*, *Nawawia* (Marvanová 1980) and

Phialosporostilbe (Mercado Sierra and Mena Portales 1985) share a basic pattern of turbinate to obpyramidal, angular and aseptate conidia. The conidia of *Catenularia* are brown and without setulae, conidia of the latter genera are hyaline with several setulae at the apex, occasionally also at the base. *Nawawia* contains species with mononematous conidiophores, terminal monophialides elongating percurrently, and conidia aggregated in heads. In contrast, *Phialosporostilbe* has synnematous conidiophores associated with setae, terminal monophialides and conidia aggregated in heads, rarely in chains (Mercado Sierra and Mena Portales 1985; Sureshkumar et al. 2005). *Nawawia* and *Phialosporostilbe* are saprobes on decaying plant material, often submerged in freshwater, occasionally isolated from soil (e.g. Marvanová 1980; Mercado Sierra and Mena Portales 1985; Bhat and Kendrick 1993; Mel'nik and Hyde 2006; Wu and Zhang 2009; Goh et al. 2014). In characters of conidia, they closely resemble *Chalarodes* (McKenzie 1991) and *Obeliospora* (Nawawi and Kuthubutheen 1990), whose systematic placement remains unexplored. The genus *Chalarodes* includes fungi inhabiting decaying palm leaves, and is widespread in Australasia (McKenzie 1991). The conidia adhere in basipetal chains and are borne on terminal monophialides on mononematous conidiophores. The colonies of *Obeliospora* are composed of dark, acute setae accompanied by short, monilioid conidiophores with doliiform conidiogenous cells and conspicuous cup-shaped collarettes. The genus accommodates species that thrive on submerged wood or plant litter in freshwater biotopes, occasionally they occur in terrestrial habitats, in South America and Southeast Asia (Nawawi and Kuthubutheen 1990; Kuthubutheen and Nawawi 1994; Wu and Mckenzie 2003; Cantillo-Pérez et al. 2018).

This study is based on nuc rDNA sequences combined with a comparative analysis of phenotypic data. It aims to evaluate the generic concept of *Catenularia* and its relationships with morphologically similar taxa. Another aim is to assess whether phenotypic characteristics such as the presence or absence of capitate hyphae and selected conidial features (i.e. colour, shape in transverse section, setulae and formation at the tip of the conidiogenous cell) are congruent with phylogenetic relationships.

Materials and methods

Fungal strains, morphology and DNA extraction and PCR amplification

Specimens of *Catenularia*, *Chalarodes*, *Nawawia* and *Sporoschisma* were collected in various localities in temperate and tropical geographical areas in Cuba, Czech Republic, France, Belgium, Martinique, New Zealand, Slovak Republic and Thailand. Other specimens were obtained from the Canadian National Mycological Herbarium (DAOM, Ottawa, Canada), Farlow herbarium (FH, Harvard University, Cambridge, Massachusetts, USA), New Zealand Fungarium (PDD, Auckland, New Zealand), Herbarium of the National Museum (PRM, Prague, Czech Republic), and Herbarium of the Naturhistorisches Museum Wien (W, Vienna, Austria). Holotypes and specimens (as dried voucher specimens) were deposited at PDD and Herbarium of the

Institute of Botany (PRA, Průhonice, Czech Republic). Fungal novelties were registered in MycoBank.

For morphological study, isolation and cultivation we follow Réblová et al. (2021a) and references cited therein. Axenic cultures were derived from freshly collected material. Strains were inoculated on potato-carrot agar (PCA) (Crous et al. 2019).

Protocols for the DNA extraction and PCR amplification followed Huhndorf et al. (2004), Hustad and Miller (2015) and Réblová et al. (2020). Automated sequencing was carried out by Eurofins GATC Biotech Sequencing Service (Cologne, Germany), Ottawa Research and Development Centre, Biodiversity (Mycology and Microbiology), Agriculture and Agri-Food Canada (Ottawa, Ontario, Canada) and the Roy J. Carver Biotechnology Center at the University of Illinois Urbana-Champaign (Champaign, Illinois, USA). Raw sequence data were analysed using Sequencher v.5.4.6 (Gene Codes Corp., USA, Michigan, Ann Arbor).

Alignments and phylogenetic analyses

In order to assess relationships of *Catenularia* with similar fungi, sequences of the internal transcribed spacer region (ITS1-5.8S-ITS2) (ITS) of the nuclear rRNA cistron and the large subunit 28S rDNA gene (28S) (ca. 1800 base pairs at the 5'-end) were analysed. Isolates, their sources and GenBank accession numbers of sequences generated in this study and those retrieved from GenBank and published in other studies (Réblová and Winka 2000, 2001; Fernández et al. 2006; Somrithipol et al. 2008; Shenoy et al. 2010; Magyar et al. 2011; Crous et al. 2012; Hashimoto et al. 2015; Hernández-Restrepo et al. 2016, 2017; Liu et al. 2016; Lu et al. 2016; Ma et al. 2016; Yang et al. 2018; Lin et al. 2019; Luo et al. 2019; Vu et al. 2019; Réblová et al. 2020, 2021a, b) are listed in the Suppl. material 1: Table S1.

Consensus secondary structure (2D) models for the ITS1 and ITS2 for members of the Chaetosphaeriaceae were built using the Ppfold program v.3.0 (Sukosd et al. 2012). The obtained 2D consensus models were further improved using the program Mfold (Zuker 2003) and RNAfold web server through the ViennaRNA Web Services (Gruber et al. 2015) and adjusted manually if necessary. The predicted 2D RNA structures were obtained in a dot bracket notation and were visualised and drawn using the program VARNA: Visualisation Applet for RNA (Darty et al. 2009).

Sequences were aligned manually in Bioedit v.7.1.8 (Hall et al. 1999). Consensus 2D structure models for the ITS1 and ITS2 were used to compare nucleotides at homologous positions (in helices and loops) and construct a reliable multiple sequence alignment. A predicted 2D model of the 28S of *Saccharomyces cerevisiae* (Gutell et al. 1993) was used to improve the alignment of this gene. The models were highly consistent in all species.

The ITS and 28S datasets, for which we assumed rate heterogeneity, were evaluated using PartitionFinder2 (Lanfear et al. 2017), implemented in the CIPRES Science Gateway v.3.3 (Miller et al. 2010), to find the best partitioning scheme for our datasets and to select best-fit models under corrected Akaike information criteria. Phylogenetic

reconstructions were performed using Bayesian Inference (BI) and Maximum Likelihood (ML) analyses through the CIPRES Science Gateway v.3.3. ML analysis was conducted with RAxML-HPC v.8.2.12 (Stamatakis 2014) with a GTRCAT approximation. BI analysis was executed in a likelihood framework as implemented in MrBayes v.3.2.6 (Huelsenbeck and Ronquist 2001). The phylogenetic analyses were performed as described in Réblová et al. (2021a).

The conflict-free single locus data sets were concatenated and the ITS-28S alignment (deposited in TreeBASE) was subjected to the phylogenetic analysis. Ninety nucleotides (nt) at the 5'-end of 28S were excluded from the alignment because of the incompleteness in the majority of sequences. The full dataset consisted of 2386 characters including gaps (ITS = 612 characters; 28S = 1774) and 1038 unique character sites (RAxML). For the BI analysis, GTR+I+G model was selected for both partitions. *Tracylla aristata* and *T. eucalypti* (Tracyllales) were selected as outgroup taxa.

Results

Phylogenetic analyses

In the phylogenetic analysis of the combined ITS-28S sequences, we evaluated systematic placement of *Catenularia* in the Chaetosphaeriaceae and its relationships with morphologically similar taxa. The ML and BI trees were largely congruent; the ML tree is shown in Fig. 2. The Chaetosphaeriaceae included 49 well supported clades that correspond to individual genera or natural groups of species. The genus *Catenularia* was resolved as a monophyletic, strongly supported clade (95% ML, BS 1.0 PP) with four species, *C. angulospora*, *C. cubensis*, *C. minor* and *C. catenulata*. *Catenularia* resided in a statistically well supported clade at the base of the tree. This clade contained six other genera and natural groups of species, including *Exserticlava vasiformis* and *Stanjehughesia hormiscioides*, known to form capitate hyphae on ascomata of their teleomorphs. *Catenularia* was shown as a sister (95/1.0) to an unknown species of *Chalarodes*, described as *Cha. obpyramidata* below. Morphologically similar genera *Nawawia* and *Phialosporostilbe* were resolved as separate lineages. *Chaetosphaeria submersa*, superficially resembling *Catenularia*, was clustered in a distantly related clade containing *Phaeostalagmus*, and also *Ch. innumera* and another two *Chaetosphaeria* species with anamorphs with catenate conidia, i.e. *Chloridium clavaeforme* and *Ch. phaeophorum*.

Taxonomy

***Catenularia* Grove, Syll. fung. 4: 303. 1886.**

Synonyms. *Psiloniella* Costantin, Mucéd. Simpl.: 25, 190. 1888.
Haplochalara Linder, Mycologia 25: 347. 1933.

Type species. *Catenularia cupulifera* (Berk. & Broome) Réblová & A.N. Mill.

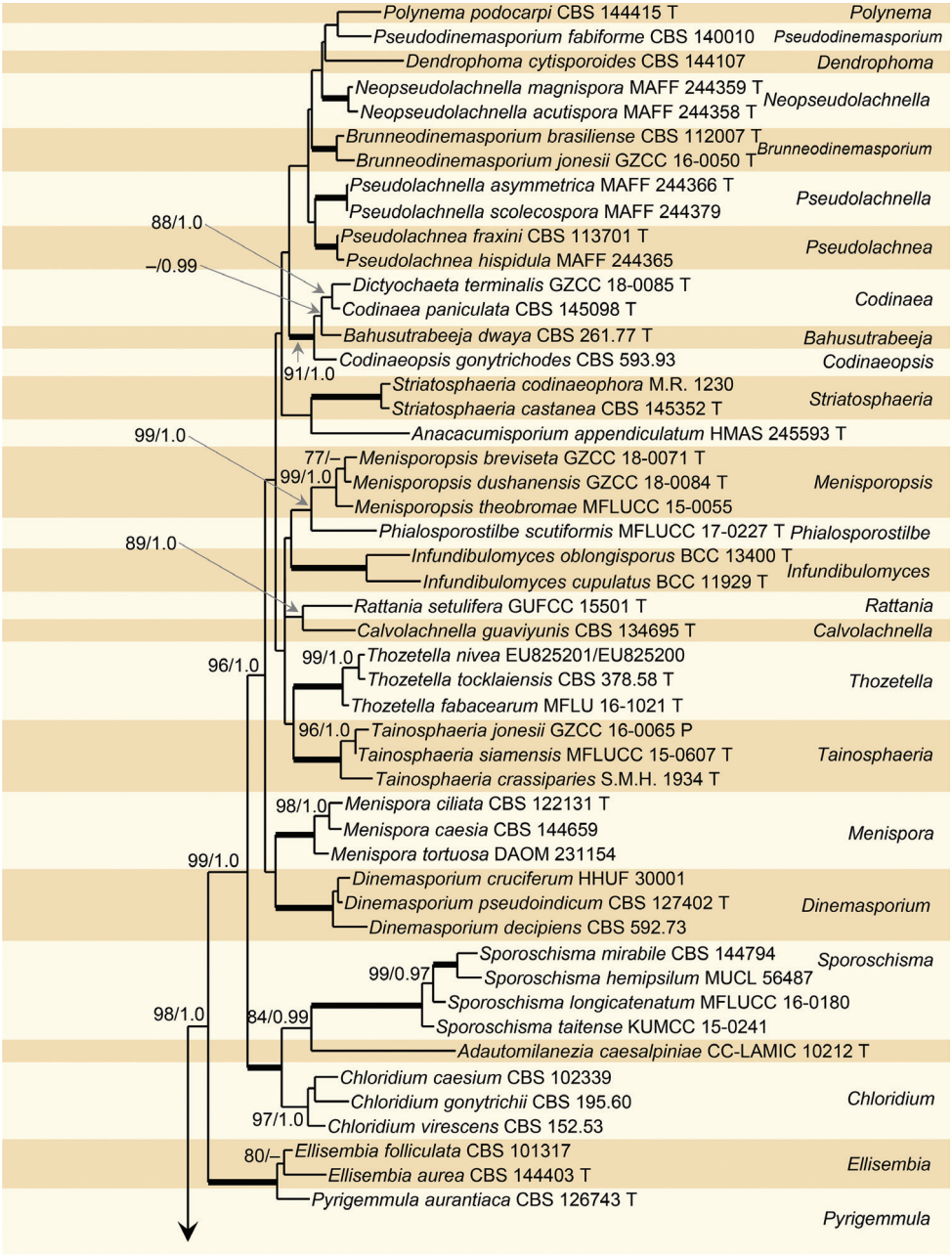

(2A)

Figure 2. A Phylogenetic analysis of the combined ITS and 28S sequences of members of the Chaetosphaeriaceae. Species names given in bold are taxonomic novelties; T, E, I, N and P indicate ex-type, ex-epitype, ex-isotype, ex-neotype and ex-paratype strains; * holotype of *Chaetosphaeria triangulaconidia*; # *Catenularia cubensis fide* Luo et al. (2019). Thickened branches indicate branch support with ML BS = 100%, PP values = 1.0. Branch support of nodes ≥ 75% ML BS and ≥ 0.95 PP is indicated above and below branches **B** phylogenetic analysis of ITS and 28S of the Chaetosphaeriaceae (continued). For legend refer to (**A**). Abbreviation: p.p. after a genus name (*pro parte*).

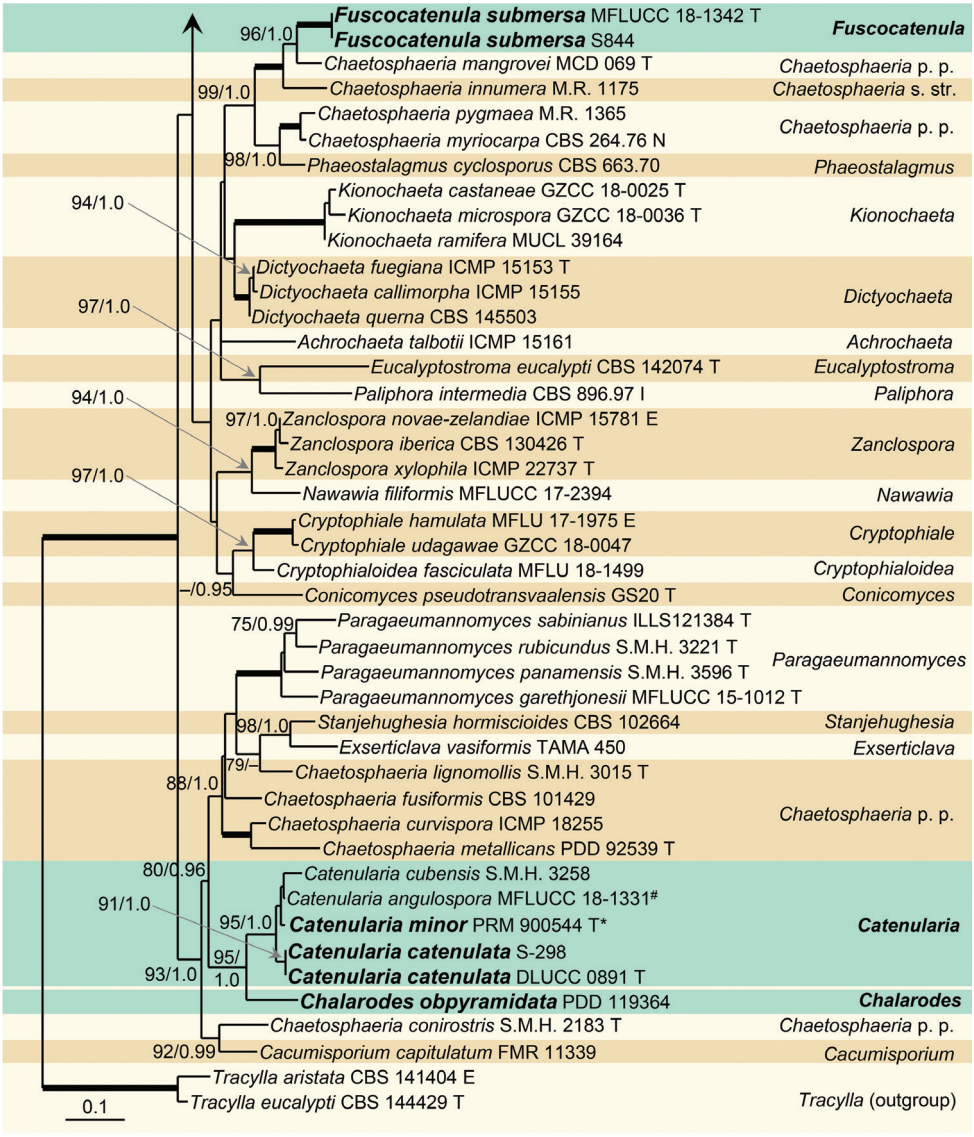

Figure 2. Continued.

Emended description. Colonies effuse, hairy to velutinous, brown, dark brown to black, mycelium partly immersed, partly superficial; composed of conidiophores, capitate hyphae and sometimes ascomata. ***Anamorph.*** Conidiophores macronematous, mononematous, solitary or in tufts, with dark stromatic hyphal cells around the bases, erect, straight or flexuous, unbranched, brown to dark brown, thick-walled, paler and thinner-walled towards the apex. Capitate hyphae scattered among the conidiophores, occasionally absent, erect, brown, extending percurrently, paler towards

the apex, apical cell sterile, thin-walled, subhyaline to hyaline, slightly swollen, broadly rounded with a hyaline mucilaginous cap that may disappear with age. Conidiogenous cells integrated, terminal, monophialidic, extending percurrently, cylindrical, subcylindrical or somewhat lageniform, brown, conidia produced successively; collarettes cup- or funnel-shaped, brown, smooth or slightly roughened, margin entire or frayed. Conidia cuneiform, obclavate, rounded-obconic to broadly obovoid in side view, with an angular outline when viewed from above with 3–6 blunt corners, broadly rounded to flattened at the apex, truncate at the distinctive, hyaline basal hilum, with a small, circular, thin-walled, pore-like area visible in the cell wall at each corner, sometimes with a visible central pore at the base, aseptate, hyaline when young, fuscous, fulvous, brown to dark brown at maturity, thick-walled, smooth; formed singly, adhered in basipetal chains, occasionally in clusters. ***Teleomorph.*** Ascomata perithecial, nonstromatic, superficial, globose, subglobose to conical, papillate, glabrous occasionally with a powdery layer that disappears with age, sometimes covered with conidiophores and capitate hyphae. Ostiolar canal periphysate. Ascomatal wall carbonaceous, two-layered. Paraphyses persistent, branching, anastomosing, hyaline, longer than the asci. Asci unitunicate, short-stipitate, apical annulus non-amyloid, with eight ascospores. Ascospores fusiform, transversely septate, hyaline, smooth, without mucilaginous sheath or appendages.

Habitat and geographical distribution. Saprobe on decaying bark, wood and bamboo culms of various hosts. Members of *Catenularia* have a worldwide distribution in temperate, subtropical and tropical geographic areas.

Notes. Hughes (1965) considered capitate hyphae to be an important diagnostic characteristic of *Catenularia*. These structures have long escaped attention, and mycologists began to notice them only after they were described by Hughes (1949). We studied holotype material of several species and original descriptions and illustrations to examine and trace this character in *Catenularia*. Capitate hyphae have not been mentioned in the original descriptions of *C. cupulifera* (Berkeley and Broome 1871; Richon 1877; Grove 1886). In studying collections of this species, we observed a variation in the presence of capitate hyphae. In some specimens, capitate hyphae are abundantly present, but may be scarce and difficult to find in others. Revision of the holotypes of *C. cuneiformis* var. *minor* (Holubová-Jechová 1983) and *Ch. triangulo-conidia* (Réblová and Seifert 2003) not only revealed that both fungi are conspecific, but also led to the discovery of capitate hyphae, although they were not mentioned in the protologues of either species. They are scattered among conidiophores and easy to overlook. Phylogenetic analysis of several *Catenularia* representatives with capitate hyphae (*C. cubensis* and *C. minor*) and those without them (*C. angulospora*, *C. catenulata*) provided compelling evidence to consider these species congeneric.

In this study, we present a taxonomic circumscription of *Catenularia* using molecular and phenotypic data. The generic concept has been emended and species with and without capitate hyphae are accepted in *Catenularia*. We were unsuccessful in obtaining *C. cupulifera* into axenic culture from fresh material. The available non-type strain CBS 419.80 of this species is a contaminant (In the Blast search, ITS and

Table 1. Species of *Catenularia*: accepted species (in bold) and disposition of morphologically similar taxa previously treated in *Catenularia* and *Chaetosphaeria*.

Name in *Catenularia* and *Chaetosphaeria*	Current name	Current classification	Reference
Catenularia angulospora (Linder) E.W. Mason*	***Catenularia angulospora*** (Linder) E.W. Mason	Chaetosphaeriales	Mason (1941)
C. antarctica Henn.*	*Periconia antarctica* (Henn.) S. Hughes	Pleosporales	Hughes (1965)
C. atra (Corda) Sacc.*	*Spadicoides atra* (Corda) S. Hughes	Xenospadicoidales	Hughes (1958)
C. cubensis Hol.-Jech.	***Catenularia cubensis*** Hol.-Jech.	Chaetosphaeriales	Holubová-Jechová (1982)
C. cuneiformis var. *cuneiformis* (Richon) E.W. Mason	***Catenularia cupulifera*** (Berk. & Broome) Réblová & A.N. Mill.	Chaetosphaeriales	Mason (1941), this study
C. cuneiformis var. *minor* Hol.-Jech.	***Catenularia minor*** (Hol.-Jech.) Réblová & A.N. Mill.	Chaetosphaeriales	Holubová-Jechová (1983), this study
C. echinata Wakker*	*Thielaviopsis ethacetica* Went	Microascales	De Beer et al. (2014)
C. elasticae Koord.*	*Gliomastix elasticae* (Koord.) Crane & Schoknecht	Hypocreales	Schoknecht and Crane (1977)
C. fuliginea Saito*	*Wallemia sebi* (Fr.) Arx	Wallemiales	Von Arx (1970)
C. fuliginea var. *lunzinensis* Szilv.*	*Catenularia fuliginea* var. *lunzinensis* Szilv.	unknown	Von Szilvinyi (1941)
C. guadalcanalensis Matsush.	*Monilochaetes guadalcanalensis* (Matsush.) I.H. Rong & W. Gams	Glomerellales	Rong and Gams (2000)
C. heimii F. Mangenot*	*Chloridium clavaeforme* (Preuss) W. Gams & Hol.-Jech.	Chaetosphaeriales	Gams and Holubová-Jechová (1976)
C. hughesii N.D. Sharma	***Catenularia angulospora*** (Linder) E.W. Mason	Chaetosphaeriales	Sharma (1980)
C. kalakadensis Subram. & Bhat	***Catenularia kalakadensis*** Subram. & Bhat	Chaetosphaeriales	Subramanian and Bhat (1989)
C. longispora S. Hughes	***Catenularia longispora*** S. Hughes	Chaetosphaeriales	Hughes (1965)
C. macrospora S. Hughes	***Catenularia macrospora*** S. Hughes	Chaetosphaeriales	Hughes (1965)
C. malabarica Subram. & Bhat	***Catenularia malabarica*** Subram. & Bhat	Chaetosphaeriales	Subramanian and Bhat (1989)
C. megalospora Speg.*	*Catenularia megalospora* Speg.	unknown	Spegazzini (1898)
C. piceae M.B. Ellis	*Exochalara longissima* (Grove) W. Gams & Hol.-Jech.	Helotiales	Gams and Holubová-Jechová (1976)
C. pidopliczkoi (Zhdanova) M.A. Litv.	*Haplochalara pidoplitschkoi* Zhdanova	unknown	Litvinov (1967)
C. simmonsii Morgan-Jones	*Sporoschismopsis simmonsii* (Morgan-Jones) Hol.-Jech. & Hennebert	Glomerellales	Holubová-Jechová and Hennebert (1972)
C. simplex Grove	***Catenularia cupulifera*** (Berk. & Broome) Réblová & A.N. Mill.	Chaetosphaeriales	Saccardo (1886), this study
C. variegata H.H. Li & X.G. Zhang	*Fuscocatenula variegata* (H.H. Li & X.G. Zhang) Réblová & A.N. Mill.	Chaetosphaeriales	Li et al. (2017), this study
C. velutina Syd. & P. Syd.*	*Catenularia velutina* Syd. & P. Syd.	unknown	Sydow and Sydow (1914)
Chaetosphaeria catenulata Z.L. Luo, K.D. Hyde & H.Y. Su	***Catenularia catenulata*** (Z.L. Luo, K.D. Hyde & H.Y. Su) Réblová & A.N. Mill.	Chaetosphaeriales	Luo et al. (2019), this study
Ch. cubensis Hol.-Jech.	***Catenularia cubensis*** Hol.-Jech.	Chaetosphaeriales	Holubová-Jechová (1983), this study
Ch. cupulifera (Berk. & Broome) Sacc.	***Catenularia cupulifera*** (Berk. & Broome) Réblová & A.N. Mill.	Chaetosphaeriales	Berkeley and Broome (1871), this study
Ch. elsikii M.J. Pound et al.	***Catenularia elsikii*** (M.J. Pound et al.) Réblová & A.N. Mill.	Chaetosphaeriales	Pound et al. (2019), this study
Ch. novae-zelandiae S. Hughes & Shoemaker	***Catenularia novae-zelandiae*** (S. Hughes & Shoemaker) Réblová & A.N. Mill.	Chaetosphaeriales	Hughes (1965), this study
Ch. trianguloconidia Réblová & Seifert	***Catenularia minor*** (Hol.-Jech.) Réblová & A.N. Mill.	Chaetosphaeriales	Réblová and Seifert (2003), this study

Notes: Species marked with an asterisk (*) were excluded from the genus by Hughes (1965). Note that some species listed among currently accepted names are included more than once due to the revealed synonymy.

28S sequences derived from this strain showed 100% identity with sequences of various strains of *Calycina citrina*.). Eleven species are accepted in *Catenularia* and listed below, four of which have been verified with molecular DNA data. Other species are accepted based on morphological similarity, but have to be confirmed as members of *Catenularia* by molecular data. So far, the teleomorph has been observed in *C. cubensis*, *C. cupulifera*, *C. minor* and *C. novae-zelandiae*. *Catenularia variegata* (Li et al. 2017) is excluded from *Catenularia* and transferred to a new segregate genus *Fuscocatenula* in this study. Disposition of *Catenularia* and morphologically similar taxa previously attributed to the genus is presented in Table 1.

Haplochalara (Linder 1933) and *Psiloniella* (Costantin 1888) are accepted as generic synonyms of *Catenularia*. The systematic placement of *H. pidoplitschkoi* (Litvinov 1967) is unknown. The species was characterised by dematiaceous, erect, simple conidiophores producing ellipsoidal, hyaline conidia that accumulate in slimy droplets and formation of dark chlamydospores in culture. Based on these characteristics, the species shows affinity to *Chloridium* (Gams and Holubová-Jechová 1976) and would be better placed in this genus.

Key to *Catenularia* species

1	Capitate hyphae present	**2**
–	Capitate hyphae absent or this character is unknown	**7**
2	Conidia 5.5–8.5 µm long, 3.5–5.5 µm wide at the apical end, 1.5–2 µm wide at base, with three bluntly rounded corners	***C. cubensis***
–	Conidia 9 µm and longer	**3**
3	Conidia up to 13.5 µm long and up to 11.5 µm wide	**4**
–	Conidia 13.5 µm and longer, wider than 11.5 µm	**5**
4	Conidia (9–)10.5–13.5 µm long, 7–9.5 µm wide at the apical end, 3.5–4.5 µm wide at the basal hilum, with (3–)4(–5) blunt corners	***C. cupulifera***
–	Conidia (6.5–)7.5–10.5(–13) µm long, 6.5–11.5 µ wide at the apical end, 1.5–2.5 µm wide at the base, with 3–5 blunt corners	***C. minor***
5	Conidia 11.5–17.5 µm long, 14.5–18.5 µm wide at the apical end, 4–5.5 µm wide at the base, with 4–5 blunt corners	***C. novae-zelandiae***
–	Conidia longer than 17.5 µm	**6**
6	Conidia 21–28 µm long, 19–28 µm wide at the apical end, 4–7 µm wide at the base, with (3–)4(–5) blunt corners	***C. macrospora***
–	Conidia 27–45 µm long, 16.8–24 µm wide at the apical end, 7–10 µm wide at the base, with three blunt corners	***C. longispora***
7	Conidia up to 9 µm long	**8**
–	Conidia longer than 9 µm	**9**
8	Conidia 6–8(–9) µm long, 4.5–6(–7) µm wide at the apical end, ca. 2 µm wide at the base, with three blunt corners	***C. angulospora***
–	Conidia up to 8 µm long, 6–7 µm wide at the apical end, 1.5–3.5 µm side at the base, with six corners	***C. kalakadensis***

9	Conidia 13–15 µm long, 12–14 µm wide at the apical end, with 3–4 corners ..... ***C. catenulata***
–	Conidia wider than 15 µm **10**
10	Conidia 12–18 µm long, 18–21 µm wide, 3–4 µm wide at the base, with 4–5 corners ..... ***C. malabrica***
–	Conidia 23–24.5 µm long, 20.8–24 µm wide, 3–4 µm wide at the base, with five corners ..... ***C. elsikii***

Catenularia angulospora **(Linder) E.W. Mason, Mycol. Pap. 5: 121. 1941.**
Fig. 3

Basionym. *Haplochalara angulospora* Linder, Mycologia 25: 347. 1933.
Synonym. ? *Catenularia hughesii* N.D. Sharma, J. Indian bot. Soc. 59: 73. 1980.

Description. Colonies on natural substrate effuse, hairy to velutinous, dark brown to almost black. ***Anamorph.*** Conidiophores 77–220 × 4.5–6(–7) µm wide, 7–8 µm above the base, macronematous, solitary or arise in tufts, erect, straight or slightly flexuous, unbranched, dark brown, paler towards the apex, septate. Capitate hyphae absent. Conidiogenous cells 18–25 × 3.5–4.5 µm tapering to ca. 2.5 µm, integrated, terminal, monophialidic, extending percurrently, obclavate to subcylindrical or slightly lageniform, pale brown, paler towards the apex; collarettes 3–4 µm wide, 1.5(–2) µm deep, funnel-shaped, subhyaline, smooth, margin entire. Conidia 6–8(–9) µm long, 4.5–6(–7) µm wide at the apical end, ca. 2 µm wide at the basal hilum (mean ± SD = 7.4 ± 1.1 × 6.0 ± 1.2 µm × 2.0 ± 0.0 µm), rounded-obconic in side view, with three blunt corners when viewed from above, broadly rounded to flattened at the apex, truncate at the basal scar, pale brown to pale fuscous, thick-walled, smooth; formed singly, adhered in basipetal chains. ***Teleomorph.*** Unknown.

Specimen examined. USA – Kentucky • near Louisville; on decaying beech log; 23 Mar. 1928; D.H. Linder (***holotype*** of *C. angulospora* FH herbarium 00965375, as microscopic slides).

Habitat and geographical distribution. Saprobe on dead culms of *Bambusa* sp., decaying wood of *Fagus* sp. and other unknown hosts in freshwater and terrestrial habitats. It is known in China, India and the USA (Linder 1933; Sharma 1980; Luo et al. 2019 as *C. cubensis*).

Notes. For additional description and illustration, see Luo et al. (2019, as *C. cubensis*). Hughes (1965) revised the type material of *H. angulospora*, and despite the striking similarities to other *Catenularia*, he kept the species in *Haplochalara* due to the absence of capitate hyphae. Sharma (1980) described *C. hughesii* on dead bamboo culms in India with pale brown to brown conidia 6–8 × 4.5–5.8 µm and conidiophores up to 270 × 5–7 µm. Although the holotype of this species was not available for study, a detailed morphological comparison of its original description and illustration with *C. angulospora* suggests that they are conspecific. Luo et al. (2019) reported this species

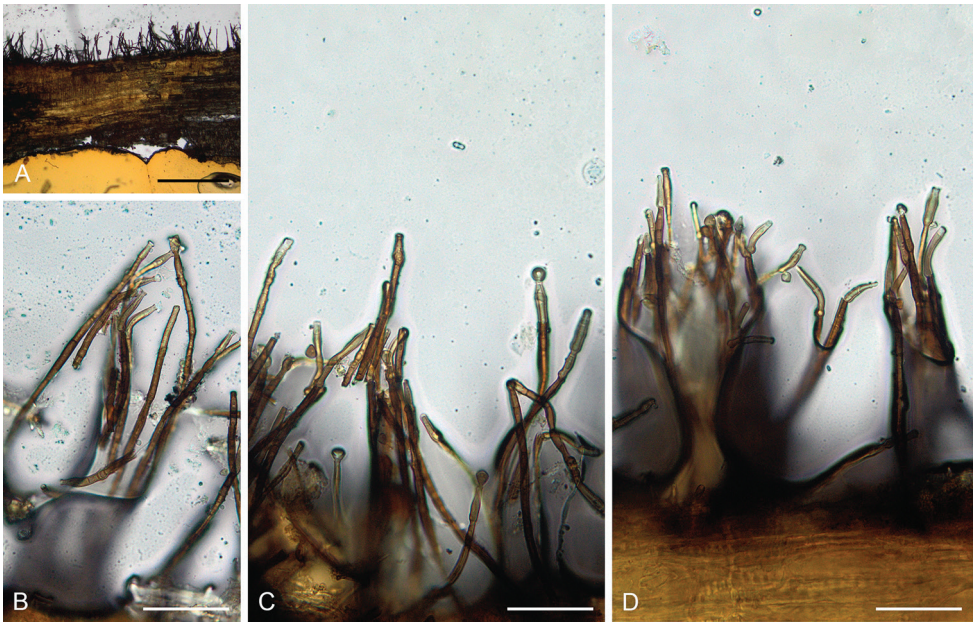

Figure 3. *Catenularia angulospora* (holotype FH 00965375) **A** vertical section of the wood with colony **B–D** conidiophores with conidia. Scale bars: 500 µm (**A**); 50 µm (**B–D**).

as *C. cubensis* (strain MFLUCC 18-1331) from China, characterised by the absence of capitate hyphae and cuneiform, greyish-brown to brown conidia 6–8 × 4–6 µm.

In the phylogenetic analysis, the strain of *C. angulospora* MFLUCC 18-1331 clustered as a sister to *C. cubensis* S.M.H. 3258, but their relationship is not statistically supported. Both species are, however, very similar. *Catenularia cubensis* (Holubová-Jechová 1982) differs from *C. angulospora* in brown to dark brown conidia, slightly narrower at the apical end (5.5–8.5 × 3.5–5.5 µm), and presence of capitate hyphae scattered among the conidiophores. The ITS sequence identity between *C. cubensis* and *C. angulospora* is 96.5% and supports our conclusion to treat them as separate species.

***Catenularia catenulata* (Z.L. Luo, K.D. Hyde & H.Y. Su) Réblová & A.N. Mill., comb. nov.**
MycoBank No: 839462

Basionym. *Chaetosphaeria catenulata* Z.L. Luo, K.D. Hyde & H.Y. Su, Fungal Divers. 99: 582. 2019.

Habitat and geographical distribution. Saprobe on submerged wood, known only in China (Luo et al. 2019).

Notes. *Catenularia catenulata* is characterised by solitary conidiophores, absence of capitate hyphae and conidia 13–15 × 12–14 µm, greyish-brown, turbinate, triangular in side view with 3–4 corners when viewed from above (Luo et al. 2019). It resembles *C. malabrica* (Subramanian and Bhat 1989), but the latter species has larger conidia 12–18 × 18–21 µm with 4–5 corners.

Catenularia cubensis **Hol.-Jech., Mycotaxon 15: 278. 1982.**
Fig. 4

Synonym. *Chaetosphaeria cubensis* Hol.-Jech., Mycotaxon 15: 278. 1982.

Description. Colonies on natural substrate effuse, hairy to velutinous, dark brown, mycelium partly immersed, partly superficial, brown; colonies composed of conidiophores, capitate hyphae and sometimes ascomata. ***Anamorph.*** Conidiophores 115–200 × 4–4.5 µm, 4.5–6 µm wide above the base, macronematous, solitary or arise in tufts, erect, straight or flexuous, unbranched, thick-walled, brown to dark brown, slightly paler towards the apex. Capitate hyphae 104–165 × 4–4.5 µm, 4–5.5 µm wide above the base, arise among the conidiophores, extending percurrently, erect, straight, brown to dark brown, paler towards the apex, apical cell sterile, thin-walled, subhyaline, slightly swollen, ca. 3.5 µm wide, broadly rounded, the hyaline gelatinous cap was not observed. Conidiogenous cells 22–38 × 3.5–4.5 µm tapering to 2–2.5 µm below the collarette, terminal, integrated, monophialidic, extending percurrently, cylindrical, pale brown to brown, producing conidia successively; collarettes 3.5–4 µm wide, 1–2 µm deep, shallow, funnel-shaped, pale brown, smooth, margin entire. Conidia 5.5–8.5 µm long, 3.5–5.5 µm wide at the apical end, 1.5–2 µm wide at the basal hilum (mean ± SD = 7.5 ± 0.7 × 4.3 ± 0.4 × 1.8 ± 0.2 µm), rounded-obconic to broadly obovoid in side view, with three bluntly rounded corners when viewed from above, broadly rounded to flattened at the apex, truncate at the basal scar, aseptate, brown to dark brown, thick-walled, smooth; formed singly, adhered in basipetal chains. ***Teleomorph.*** Ascomata 150–200 µm diam, 160–210 µm high, superficial, solitary or in groups, subglobose to conical, papillate, dark brown to black, covered with conidiophores and capitate hyphae. Ostiole periphysate. Ascomatal wall fragile, carbonaceous, 15–25 µm thick, two-layered. Outer layer consisting of brown, polyhedral cells with opaque walls. Inner layer consisting of several rows of thin-walled, hyaline cells. Paraphyses 2.5–3.5 µm wide, septate, hyaline, longer than the asci. Asci 62–84.5 × (6–)7–8.5 µm (mean ± SD = 72.2 ± 7.8 × 13.9 ± 0.9 µm), cylindrical-clavate, short-stipitate, apically rounded to obtuse, ascal apex with a non-amyloid apical annulus 2–2.5 µm wide, 1.5(–2) µm high. Ascospores 12–16(–17.5) × 3–4 µm (mean ± SD = 13.9 ± 0.9 × 3.5 ± 0.2 µm), fusiform, straight or slightly curved, hyaline, 3-septate, smooth, 2-seriate in the ascus.

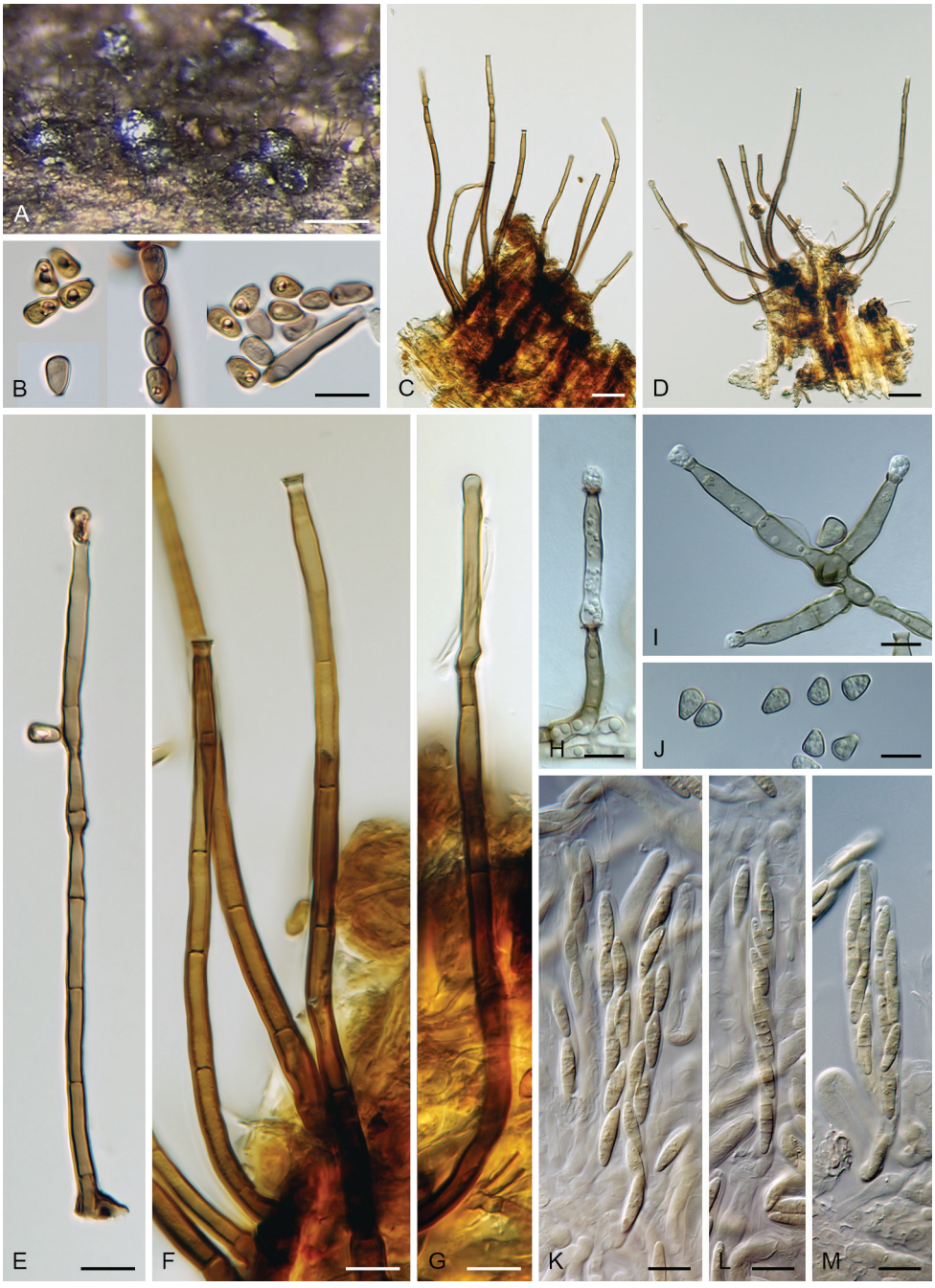

Figure 4. *Catenularia cubensis* **A** ascomata accompanied by conidiophores and capitate hyphae **B, J** conidia **C, D** tufts of conidiophores with scattered capitate hyphae **E–I** conidiophores **K–M** asci with ascospores. Images: S.M.H. 3258 (**A, H–J**), PRM 825347 holotype (**B–D, F, G, K–M**); PRA-19884 (**E**); on natural substrate (**A–G, K–M**); in culture (**H–J**). Scale bars: 200 µm (**A**); 10 µm (**B, E–M**); 25 µm (**C, D**).

Specimens examined. Costa Rica • Guanacaste, Liberia ACG, Sector Santa Maria, Estacion Biologica, trail to Bosque Encantado; 10.7647N, -85.3033W; alt. 750 m; on 5 cm diam branch on ground; 26 Jun. 1997; S.M. Huhndorf (S.M.H. 3258). Costa Rica • Alajuela, Cantón Upala, District Bijagua, Heliconias Station, Heliconias trail; 10.7081N, -85.0453W; on 25 cm diam log on ground; alt. 1190 m; 12 Jul. 2001; S.M. Huhndorf, F.A. Fernández, A.N. Miller & M. Darin (S.M.H. 4454). Cuba – Isla de la Juventud (Isla de Pinos) • Sierra de Casas, in a valley near El Abra, 2 km SW of Nueva Gerona; on dead trunk of Palmaceae; 22 Jan. 1981; V. Holubová-Jechová (***holotype*** PRM 825347). Cuba – Isla de la Juventud (Isla de Pinos) • in forest near village Caryo Piedra; on wood of a trunk of a deciduous tree; 21 Jan. 1981; V. Holubová-Jechová (PRA-19884).

Habitat and geographical distribution. Saprobe on decaying wood of palm *Euterpe oleracea* and other hosts in Brazil, Cuba and Costa Rica (Holubová-Jechová 1982; De Castro et al. 2011; Miller and Huhndorf, unpubl.; this study), and on fallen leaves in India (Dubey and Pandey 2017).

Notes. The description is based on Cuban collections. In the Costa Rican material, conidia were 6–8.5 µm long, 3–5 µm wide at the widest point, 1.5–2 µm wide at the basal hilum, brown to dark brown, broadly obovoid or cuneiform, asci 60–80 × 7–9 µm, ascospores 12–20 × 3–5 µm, fusiform, 3-septate (Huhndorf and Miller, unpubl.). For additional details, see Holubová-Jechová (1982).

Catenularia cubensis closely resembles *C. angulospora*; for comparison see notes for the latter species. *Catenularia minor* can also be compared with *C. cubensis*, but differs in longer and wider conidia (6.5–)7.5–10.5(–13) × 6.5–11.5 µm with 3–5 blunt corners and conidiophores that form two distinct layers.

Catenularia cupulifera **(Berk. & Broome) Réblová & A.N. Mill., comb. nov.**
MycoBank No: 839463
Fig. 5

Basionym. *Sphaeria cupulifera* Berk. & Broome, Ann. Mag. nat. Hist., Ser. 4, 7: 435. 1871.
Synonyms. *Lasiosphaeria cupulifera* (Berk. & Broome) Cooke & Plowr., Grevillea 7(43): 85. 1879.
Chaetosphaeria cupulifera (Berk. & Broome) Sacc., Syll. fung. 2: 94. 1883.
Psilonia cuneiformis Richon, Bull. Soc. Sci. Vitry-le-Franç. 8: 219. 1877.
Monotospora cuneiformis (Richon) Sacc., Syll. fung. 4: 300. 1886.
Psiloniella cuneiformis (Richon) Costantin, Mucéd. Simpl.: 86. 1888.
Catenularia cuneiformis (Richon) E.W. Mason, Mycol. Pap. 5: 121. 1941.
Catenularia simplex Grove, Syll. fung. 4: 303. 1886.
Psilonia simplex (Grove) Costantin, Mucéd. Simpl.: 86. 1888.
Synonymy adopted from Mason (1971) and Booth (1958).

Description. Colonies on natural substrate effuse, hairy or tufted, dark brown to black, mycelium partly immersed, partly superficial, brown; colonies composed of

Figure 5. *Catenularia cupulifera* **A, B** ascomata accompanied by conidiophores and capitate hyphae **C** colony composed of conidiophores and capitate hyphae **D–F** conidiophores **G** capitate hypha **H–J** upper parts of conidiophores with conidia **K, L** conidia **M, N** asci with ascospores. Images: W7972 (**A, B, M**); W7973 (**C, D, H, I**); PRA-19893 (**E–G, J–L**); JF 99018 (**N**); on natural substrate (**A–N**). Scale bars: 500 µm (**A–C**); 50 µm (**D**); 25 (**E**); 20 µm (**F–L**); 10 µm (**M, N**).

conidiophores, capitate hyphae and sometimes ascomata. ***Anamorph.*** Conidiophores 100–350(–530) × 6–7.5(–8) µm, 8.5–10.5 wide above the base, macronematous, solitary or in tufts, with dark brown stromatic hyphal cells around the bases, erect, straight or flexuous, unbranched, brown to dark brown, thick-walled, slightly paler towards the apex. Capitate hyphae 110–160 × 5.5–6 µm, 6.5–7 µm wide above the base, scattered among the conidiophores, erect, straight, brown to dark brown, paler towards the apex, apical cell sterile, thin-walled, subhyaline, slightly swollen, ca. 7 µm wide, broadly rounded with a hyaline gelatinous cap that disappears with age. Conidiogenous cells 40–59 × 5.5–6.5 µm, not tapering, terminal, integrated, monophialidic, extending percurrently, cylindrical, brown, producing conidia successively; collarettes 9.5–12.5 µm wide and 10–12.5 µm deep, funnel-shaped, brown, slightly roughened, with an irregularly frayed margin. Conidia (9–)10.5–13.5 µm long, 7–9.5 µm wide at the apical end, 3.5–4.5 µm wide at the basal hilum (mean ± SD = 11.8 ± 0.7 × 8.0 ± 0.6 µm × 4.0 ± 0.3 µm), cuneiform in side view, with (3–)4(–5) blunt corners when viewed from above, flattened to broadly rounded at the apex, truncate at the base, aseptate, fulvous, brown to dark brown, thick-walled, smooth; formed singly, adhered in basipetal chains. ***Teleomorph.*** Ascomata 150–220 µm diam, 200–250 µm high, superficial with a base immersed, solitary or in groups or densely aggregated forming a crust, conical to subglobose, papillate, dark brown to black, rugose, sometimes covered with conidiophores and capitate hyphae or in a dense subiculum consisting of partly decumbent conidiophores. Ostiole periphysate. Ascomatal wall fragile, carbonaceous, 22–33 µm thick, two-layered. Outer layer consisting of brown, polyhedral to angular cells with opaque walls. Inner layer consisting of several rows of thin-walled, hyaline cells. Paraphyses 3–4 µm wide tapering to 2–2.5 µm, septate, hyaline, longer than the asci. Asci 110–140 × (8–)10–11(–12.5) µm (mean ± SD = 162.2 ± 11.1 × 10.5 ± 1.2 µm), cylindrical-clavate, short-stipitate, apically narrowly rounded to obtuse, ascal apex with a non-amyloid apical annulus 2–2.5(–3) µm wide, ca. 1.5 µm high. Ascospores 21–28.5 × 4.5–5.5 µm (mean ± SD = 25.3 ± 1.7 × 5.5 ± 0.4 µm), fusiform, straight or slightly curved, hyaline, 1–4-septate, smooth, 2-seriate in the ascus.

Specimens examined. Belgium • West Flanders province, Adinkerke, Cabour; on decaying wood of *Populus* sp.; 21 Oct. 2007; B. Declerque (IFBL D0.16.23). Czech Republic – Moravia • Lanžhot, Ranšpurk National nature reserve; alt. 150 m; on decaying wood of *Carpinus betulus*; 14. Aug. 1979; V. Holubová-Jechová (PRA-19887) • *Ibid.*; on decaying wood of *Populus alba*, 28 Jul. 1970, V. Holubová-Jechová (PRA-19888) • *Ibid.*; on decaying wood *Quercus robur*, 28. Aug. 1976, V. Holubová-Jechová (PRA-19889). Czech Republic – Moravia • Bílé Karpaty, Velká Javořina Mt. near Kamenná Bouda; alt. 660 m; on decaying wood of a branch of *Fagus sylvatica*; 27 Jul. 1970; V. Holubová-Jechová (PRA-19886). France – Ariège • Pyreneés Mts., Rimont, Las Muros, alt. 480 m; on decaying wood of *Fraxinus excelsior*; 4 Feb. 1999; J. Fournier J.F. 99018 (PRA-19890). France – Ariège • Pyreneés Mts., Rimont, Las Muros, valley of the Peyrau brook, alt. 400 m; on decaying wood of *Buxus sempervivens*; 9 Nov. 1999, J. Fournier J.F. 99261 (PRA-19892) • *Ibid.*; on decaying wood of *Salix caprea*;

12 Mar. 2000; J. Fournier J.F. 00026 (PRA-19891). France – Ariège • Pyrénées Mts., Rimont, La Maille brook; alt. 550 m; on submerged wood; 28 May 2018; J. Fournier M.R. 4104 (PRA-19893). Slovak Republic • Brezová near Senica; on decaying wood of a trunk of *Salix alba*; 6 Aug. 1976; V. Holubová-Jechová (PRA-19885). United Kingdom – Somerset • Langridge, on decaying wood of roots of *Ulmus* sp.; Apr. 1869; C.E. Broome (***holotype*** of *S. cupulifera* K(M) 57177). United Kingdom • on decaying wood; 14 Apr. 1873; ex Herbarium C.E. Broome 1886 (W 7972) • *Ibid.*; ex Herbarium C.E. Broome 1886, no. 366 (W 7973).

Habitat and geographical distribution. Saprobe on decaying wood of *Carpinus betulus*, *Fagus sylvatica*, *Fraxinus excelsior*, *Hedera* sp., *Ilex* sp., *Quercus* sp., *Salix alba*, *Ulmus* sp. and other unknown hosts. Most of the records originate from Europe in Belgium, Czech Republic, France, Slovak Republic and the United Kingdom (Berkeley and Broome 1871; Hughes 1965; Holubová-Jechová 1973; this study). Hughes (1965) suggested that *C. cupulifera* is apparently only known from Europe. However, findings of this species also come from other continents. *Catenularia cupulifera* has been reported from foam in a river in Venezuela (Fernández and Smits 2018), wood of *Ulmus americana* in the USA, Illinois (Shim 1969) and decaying leaves of *Pandanus* sp. in Mauritius (Whitton et al. 2012).

Notes. Our observations of the teleomorph-anamorph connection between *Ch. cupulifera* and *C. cuneiformis* agree with those of Berkeley and Broome (1871), De Seynes (1886) and Booth (1958). Although this relationship has not yet been verified experimentally, both morphs occur together in nature. Since the anamorph and teleomorph represent two different stages of the life cycle of one organism, we propose a new combination in *Catenularia* based on *Sphaeria cupulifera* with *C. cuneiformis* and *C. simplex* as synonyms.

Catenularia novae-zelandiae resembles *C. cupulifera* but differs in larger and rounded-obconic conidia, 11.5–17.5 µm long, 14.5–18.5 µm wide. Both species have conspicuous collarettes with a frayed margin, which is larger in *C. novae-zelandiae*, 19–27 µm wide and 12.2–19 µm deep, funnel- to cup-shaped.

Catenularia elsikii **(M.J. Pound, J.M.K. O'Keefe, N.B. Nuñez Otaño & J.B. Riding) Réblová & A.N. Mill., comb. nov.**
MycoBank No: 839464

Basionym. *Chaetosphaeria elsikii* M.J. Pound, J.M.K. O'Keefe, N.B. Nuñez Otaño & J.B. Riding, Palynology 43: 603. 2019.

Habitat and geographical distribution. On fossil wood, known only in the United Kingdom.

Notes. *Catenularia elsikii* was isolated from the material containing clay, charcoal and wood fragments present in the cracks of a large sample of fossil wood discovered in the United Kingdom (Pound et al. 2019). Thick-walled, dark brown conidia

were the only structure that has been preserved in material dated to the Miocene. In the conidial characteristics, *C. elsikii* is remarkably similar to *C. macrospora* known from Canada and New Zealand and *C. novae-zelandiae* known only from New Zealand. These species share dark brown, rounded-obconic conidia with (3–)4–5 corners when viewed from above. In addition, *C. elsikii* and *C. novae-zelandiae* have a visible pore at the basal hilum. Conidia of *C. elsikii* (23.1–24.4 μm high, 20.8–23.9 μm wide with a basal scar 3–4 μm wide) are longer and wider than those of *C. novae-zelandiae*, but shorter than those of *C. macrospora*. For detailed comparison, see notes to the two latter species.

***Catenularia kalakadensis* Subram. & Bhat, Kavaka 15(1–2): 49. 1989 [1987].**

Habitat and geographical distribution. Saprobe on decaying wood, known only in China, India and Mexico (Subramanian and Bhat 1989; Heredia et al. 2004; Xia et al. 2013).

Notes. For descriptions and illustrations, refer to Subramanian and Bhat (1989) and Xia et al. (2013). *Catenularia kalakadensis* is unique among other species in conidia with six blunt corners when viewed from above. It resembles *C. cubensis* but differs in the absence of capitate hyphae and wider conidia (6–7 μm) with more corners at the apex (Subramanian and Bhat 1989).

***Catenularia longispora* S. Hughes, N. Z. J. Bot. 3: 141. 1965.**

Habitat and geographical distribution. Saprobe on decaying wood, known only in New Zealand (Hughes 1965).

Notes. *Catenularia longispora* is well recognisable by narrowly rounded-obconic, brown to dark brown conidia that are the longest in the genus, 27–45 μm long, 16.8–24 μm wide at the apical end, 7–10 μm wide at the basal hilum, with usually three blunt corners when viewed from above (Hughes 1965).

***Catenularia macrospora* S. Hughes, N. Z. J. Bot. 3: 143. 1965.**

Habitat and geographical distribution. Saprobe on decaying bark and wood of *Dacrydium cupressinum*, *Fuscospora cliffortioides*, *Vitex lucens* and other unknown hosts, known in Canada and New Zealand (Hughes 1965).

Notes. *Catenularia macrospora* has broadly obovoid to rounded-obconic, brown to dark brown conidia, 21–28 μm long, 19–28 μm wide at the apical end and 4–7 μm wide at the basal hilum, with (3–)4(–5) blunt corners when seen from above (Hughes 1965). The conidial length is comparable with those of *C. longispora* and *C. elsikii*, but the former species differs in conidia narrowly rounded-obconic, narrower at the apical

end (16.8–24 µm) with only (2–)3 corners. Although the length of conidia of *C. elsikii* and *C. macrospora* overlap and the number of corners is comparable, conidia of *C. elsikii* are slightly shorter and narrower in their upper range (23–24.5 × 21–24 µm) and narrower at the truncate base (3–4 µm) (Pound et al. 2019).

***Catenularia malabarica* Subram. & Bhat, Kavaka 15(1–2): 49. (1989) [1987].**

Habitat and geographical distribution. Saprobe on decaying wood of *Magnolia liliifera* and an unknown host, known only in India and Thailand (Subramanian and Bhat 1989; Kodsueb et al. 2008).

Notes. For descriptions and illustrations, see Subramanian and Bhat (1989). *Catenularia malabrica* produces one of the tallest conidiophores in the genus, 320–620 × 6–11 µm arising singly or in tufts. It resembles *C. novae-zelandiae* in dark brown conidia with 4–5 corners, but conidia of *C. malabrica* are wider (18–21 µm) and the capitate hyphae are absent.

***Catenularia minor* (Hol.-Jech.) Réblová & A.N. Mill., comb. nov.**
MycoBank No: 839465
Fig. 6

Basionym. *Catenularia cuneiformis* var. *minor* Hol.-Jech., Česká Mykol. 37: 14. 1983.
Synonym. *Chaetosphaeria triangulocondidia* Réblová & Seifert, Sydowia 55: 333. 2003.

Description. Colonies on the natural substrate effuse, tufted or hairy, dark brown to black, mycelium partly immersed, partly semi-immersed, pale brown to brown; colonies composed of conidiophores, capitate hyphae and sometimes ascomata. ***Anamorph.*** Conidiophores macronematous, solitary or arise in tufts, with dark brown stromatic hyphal cells around the base, erect, straight or flexuous, unbranched, thick-walled, paler towards the apex, forming two layers. Conidiophores of the lower layer 95–212 × 3.5–4.5(–5) µm, 4.5–5.5(–8.5) µm wide above the base, pale brown to brown; conidiophores of the upper layer 260–527 × 4.5–7 µm long, 7.5–10 µm wide above the base, dark brown. Capitate hyphae 122–186 × 3.5–5 µm, 5–5.5 µm wide above the base, scattered among the conidiophores, erect, straight, brown, extending percurrently, paler towards the apex, apical cell subhyaline, slightly swollen, 3.5–4 µm wide, broadly rounded, thin-walled; the hyaline gelatinous cap was not observed. Conidiogenous cells 15–40 × 3.5–5.5 µm tapering to 2.5–3 µm below the collarette, integrated, terminal, monophialidic, extending percurrently, cylindrical to slightly lageniform, pale brown to brown, producing conidia successively; collarettes 3.5–5(–6) µm wide, 1.5–2.5 µm deep, shallow, funnel-shaped, pale brown to subhyaline, smooth, margin entire. Conidia (6.5–)7.5–10.5(–13) µm long, 6.5–11.5 µ wide at the apical end, 1.5–2.5 µm wide

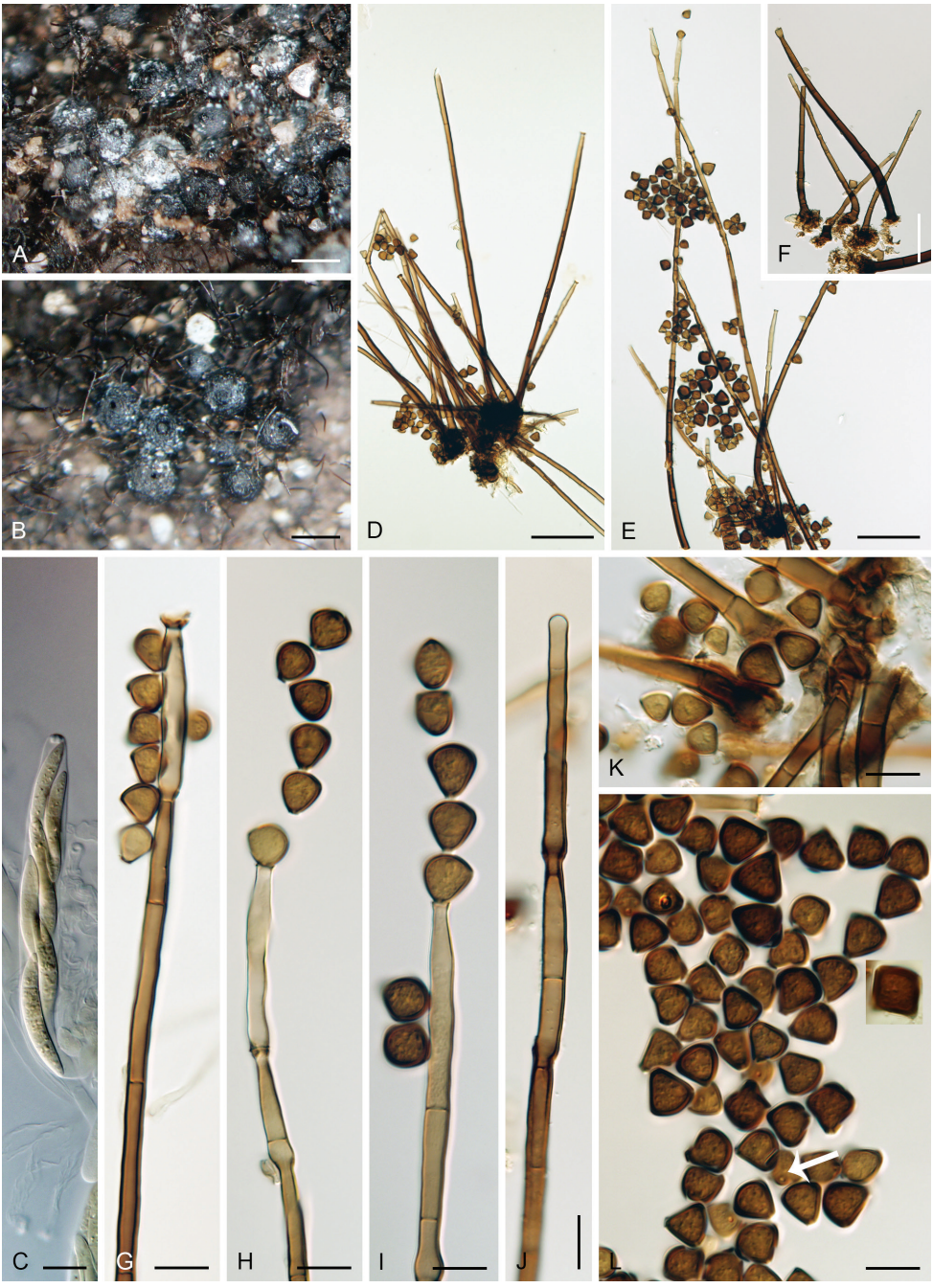

Figure 6. *Catenularia minor* **A, B** colonies composed of ascomata, conidiophores and capitate hyphae **C** ascus with ascospores **D–F** conidiophores with capitate hyphae **G–J** upper parts of conidiophores with conidia in chains **J** capitate hypha **K, L** conidia (arrow indicates central pore in the basal scar). Images: PRM 828704 holotype of *C. minor* (**D, E, G, K**); PRM 900544 holotype of *Ch. trianguloconidia* (**A–C, F, H–J, L**); on natural substrate (**A–L**). Scale bars: 250 µm (**A, B**); 10 µm (**C, G–L**); 50 µm (**D–F**).

at the base (mean ± SD = 8.9 ± 0.9 × 9.0 ± 1.2 × 2.1 ± 0.2 µm), cuneiform to rounded-obconic to obtriangular in side view, with 3–5 blunt corners when viewed from above, broadly rounded to flattened at the apex, truncate at the basal scar with a central pore, aseptate, pale brown to dark brown, thick-walled, smooth; formed singly, adhered in basipetal chains or clusters. ***Teleomorph.*** Ascomata 230–250 µm diam, 250–275 µm high, superficial, solitary or densely aggregated, subglobose to globose, covered by a whitish-grey powder except for the black glabrous papilla; the powdery covering is ca. 5–15 µm thick, disappearing with age, leaving the perithecia dark and glabrous. Ascomata sparsely covered with conidiophores. Ostiole periphysate. Ascomatal wall fragile, carbonaceous, 30–37.5 µm thick, two-layered. Outer layer consisting of dark brown, opaque, thin-walled, polyhedral cells. Inner layer consisting of hyaline, thinner-walled, elongated, compressed cells. Paraphyses 3–4 µm wide, tapering to ca. 2 µm, branching, anastomosing, septate, hyaline, longer than asci. Asci 102–112 × 8–9(–9.5) µm (mean ± SD = 106 ± 1.6 × 8.9 ± 0.2 µm), cylindrical-clavate, short-stipitate, rounded apically, ascal apex with a non-amyloid apical annulus 3 µm diam, 1.5–2 µm high. Ascospores 25–29(–30) × (3.5–)4–4.5 µm (mean ± SD = 27 ± 0.5 × 4 ± 0.7 µm), fusiform, straight or curved, hyaline, 1–3-septate, smooth, 1–2-seriate in the ascus (adapted from Réblová and Seifert 2003).

Specimens examined. Cuba – Sancti Spiritus province • Soledad, Cienfuegos Province Botanical Garden; on decaying stem of *Bambusa vulgaris*; 19 Mar. 1981; M.A. Bondarceva & S. Herrera (***holotype*** of *C. cuneiformis* var. *minor* PRM 828704). Thailand – Nakhon Nayok Province • Khao Yai National Park, trail to Haew Suwat waterfall, elev. 720 m; on decaying bamboo culm; 2 Sep. 2001; M. Réblová, Gary J. Samuels & R. Nasit M.R. 2186/TH 438 (***holotype*** of *Ch. trianguloconidia* PRM 900544).

Habitat and geographical distribution. Saprobe on dead culms of bamboo, known in Cuba and Thailand (Holubová-Jechová 1983; Réblová and Seifert 2003).

Notes. For characteristics in culture, see Réblová and Seifert (2003). The apparent similarity of *C. cuneiformis* var. *minor* (Holubová-Jechová 1983) and *Ch. trianguloconidia* (Réblová and Seifert 2003) and their habitat on dead bamboo culms prompted a revision of both species. Examination of their holotypes revealed that they are conspecific. Additionally, we discovered capitate hyphae in the type material of both species, although they were not described in the protologues. They are scattered among the conidiophores and easy to overlook. The hyaline gelatinous cap around the swollen apex of the capitate hyphae was not observed. Conidia slightly vary in size and colour, and often smaller and pale brown conidia occur together with slightly larger and darker brown conidia.

Holubová-Jechová (1983) distinguished var. *minor* from var. *cuneiformis* (= *C. cupulifera*, this study) in shorter collarettes, smaller conidia and the absence of capitate hyphae. Based on their different morphology, a new combination for var. *minor* is proposed at the species level with *Ch. trianguloconidia* reduced to synonymy.

Catenularia angulospora is similar to *C. minor*, and it is challenging to distinguish both species, especially if capitate hyphae may rarely occur in some specimens of the

latter species. *Catenularia angulospora* differs in fuscous to brown conidia that are narrower (4.5–6(–7)) µm and the lack of capitate hyphae. *Catenularia cupulifera* is comparable to *C. minor* but differs in larger collarettes (9.5–12.5 µm wide and 10–12.5 µm deep) with a frayed margin, and longer (10.5–13.5 µm) conidia that are wider (3.5–4.5 µm) at the basal hilum. Conidia of *C. cupulifera* are cuneiform in side view, whereas conidia of *C. minor* are more rounded-obconic to obtriangular.

***Catenularia novae-zelandiae* (S. Hughes & Shoemaker) Réblová & A.N. Mill., comb. nov.**

MycoBank No: 839466

Fig. 7

Basionym. *Chaetosphaeria novae-zelandiae* S. Hughes & Shoemaker, N. Z. J. Bot. 3: 138. 1965.

Description. Colonies on natural substrate effuse, tufted or velutinous, dark brown, mycelium partly immersed, partly superficial, brown; colonies composed of conidiophores, capitate hyphae and sometimes ascomata. ***Anamorph.*** Conidiophores 90–354 × 7.5–9.5 µm, 7–10.5 µm wide near the swollen base, macronematous, solitary or arise in tufts, with dark stromatic hyphal cells around the base, erect, straight or flexuous, unbranched, brown to dark brown, thick-walled. Capitate hyphae 95–215 × 5–7 µm, 6.5–9 µm wide above the base, 4.5–5.5 µm wide at the apex, solitary or in tufts, arise among the conidiophores, erect, straight to slightly flexuous, dark brown, paler towards the apex, apical cell pale brown to subhyaline, slightly swollen, broadly rounded, thin-walled, with a hyaline, mucilaginous cap that disintegrates with age. Conidiogenous cells 22.5–41(–65) × 7–11 µm, 7.5–9.5 µm wide below the collarette, terminal, integrated, monophialidic, extending percurrently, cylindrical, subcylindrical or slightly lageniform, brown, producing conidia successively; collarettes 19–27 µm wide and 12.2–19 µm deep, funnel-shaped or cup-shaped, brown to dark brown, roughened, with a frayed margin, the margin deteriorates, and the collarette becomes reduced in size 11.5–15.8 µm wide and 4.5–6 µm deep. Conidia 11.5–17.5 µm long, 14.5–18.5 µm wide at the apical end, 4–5.5 µm wide at the basal hilum, (mean ± SD = 15.8 ± 1.8 × 15.9 ± 1.3 × 5.5 ± 0.9 µm), cuneiform to rounded-obconic in side view, with 4–5 blunt corners when viewed from above, flattened to broadly rounded at the apex, truncate at the base, aseptate, brown to dark brown, thick-walled, smooth; formed singly, adhered in basipetal chains. ***Teleomorph.*** Ascomata 160–210 µm diam, 180–220 µm high, superficial, solitary or in small groups, subglobose to globose, papillate, dark brown, sometimes covered with capitate hyphae and conidiophores; capitate hyphae 80–130 × 5–5.5 µm, erect, simple, apical cell 6–6.5 µm wide, slightly inflated, broadly rounded apically, subhyaline, with a mucilaginous cap that disappears with age. Ostiole periphysate. Ascomatal wall fragile, carbonaceous, 17–22 µm thick, two-layered. Outer layer consisting of dark brown, polyhedral to angular cells with opaque walls. Inner layer consisting of rows of thin-walled, hyaline cells. Paraphyses 4–5 µm wide

Figure 7. *Catenularia novae-zelandiae* **A** ascomata **B** colony composed of conidiophores and capitate hyphae **C, D, O, P** conidiophores **E** capitate hypha arising among conidiophores **F–I** upper parts of conidiophores with conidia (arrow indicates central pore at the basal scar) **J, K** conidia in chain (arrow indicates appendages) **L, M** asci with ascospores and paraphyses **N** capitate hypha arising from the ascomal wall **Q** conidia. Images: PDD 81883 (**A–C, F–I, L–Q**); PDD 119362 (**D, E, J, K**); on natural substrate (**A–N**); in PCA culture after 2 wk (**O–Q**). Scale bars: 250 µm (**A, B**); 50 µm (**C–E**); 20 µm (**F–Q**).

tapering to 1.5–2 µm, septate, hyaline, longer than the asci. Asci 102–130 × 11–13 µm (mean ± SD = 117.6 ± 9.8 × 12.3 ± 0.8 µm), 74–100(–110) µm in the sporiferous part (mean ± SD = 83.7 ± 12 µm), cylindrical-clavate, narrowly truncate apically, ascal apex with a non-amyloid apical annulus 3.5–4 µm wide, ca. 2 µm high. Ascospores 22–28(–30) × 4–5 µm (mean ± SD = 25.6 ± 1.6 × 4.7 ± 0.4 µm), fusiform, straight or slightly curved, hyaline, 3-septate, smooth, 2-seriate in the ascus.

Characteristics in culture. On PCA: colonies 8–12 mm in 14d, circular, flat, margin entire, subsurface, aerial mycelium scarce, cobwebby to mucoid, beige-brown, reverse of the same colour. Sporulation was abundant, sporulating conidiophores developed from aerial mycelium and occasionally from immersed vegetative hyphae.

Colonies on PCA effuse, hairy, vegetative mycelium subhyaline to hyaline, 2–3 µm wide. Conidiophores, conidiogenous cells and conidia similar to those from nature. Conidiophores 31–120 × 6–7 µm, solitary or arise in tufts of 2–7, erect, straight, pale brown, 1–several-septate. Capitate hyphae absent. Conidiogenous cells 22–37 × 8–10 µm, tapering to ca. 7 µm below the collarette; collarettes 12.5–15 µm wide, 4–6(–8) µm deep, funnel-shaped, pale brown to dark brown, slightly roughened with a frayed to entire margin. Conidia (13–)14–18 µm long, 13–18 µm wide at the apical end, 4.5–6 µm wide basal hilum (mean ± SD = 15.2 ± 1.2 ×14.7 ± 1.4 µm × 5.5 ± 0.9 µm), broadly rounded-obconic in side view, aseptate, brown to grey-brown, thick-walled, smooth, formed singly, adhered in short basipetal chains.

Specimens examined. New Zealand – Auckland region • Auckland district, Upper Piha Valley, Waitākere Ranges, Home track; on decaying wood of *Metrosideros robusta*; 9 Oct. 1963; J.M. Dingley (***holotype*** PDD 21603, ***isotype*** DAOM 93575). New Zealand – West Coast region • Westland district, Otira, Kelly Shelter, Cockayane Nature Walk; on decaying wood; 16 Mar. 2003; M. Réblová MR 2846/NZ 362 (PDD 81883). New Zealand – West Coast region • Buller district, Victoria Forest Park, Reefton, Big River Inanganua track ca. 14 km; on decaying wood of *Nothofagus* sp.; 6 Mar. 2003; M. Réblová MR 2723/ NZ 224A (PDD 119362).

Habitat and geographical distribution. Saprobe on decaying wood of *Coprosma lucida*, *Coprosma* spp., *Freycinetia banksii*, *Griselinia lucida*, *Leptospermum ericoides*, *Metrosideros robusta*, *Neopanax arboreum*, *Nothofagus* sp., *Olearia rani*, *Weinmannia racemosa* and other unknown hosts, known only in New Zealand (Hughes 1965; this study).

Notes. The specimen PDD 81883 of *C. novae-zelandiae* was isolated in axenic culture (Fig. 7O–Q). In vitro, conidia were paler than those from nature and broadly rounded-obconic. Unfortunately, the isolate is no longer viable. The other collection PDD 119362 has conidia slightly larger 17.5–21 × 18–19 µm, 5–6 µm wide at the truncate base. In both specimens, we observed several conidia with minute hyaline appendages arising from the pale, circular, thin-walled areas in the cell wall (Fig. 7K).

Catenularia malabarica (Subramanian and Bhat 1989) is similar to *C. novae-zelandiae* in characters of conidia, but differs in the absence of capitate hyphae, longer conidiophores up to 620 µm long and conidiogenous cells with a shallow, funnel-shaped collarette without a frayed margin.

***Chalarodes* McKenzie, Mycotaxon 42: 89. 1991.**

Description. Colonies on natural substrate effuse, hairy, mycelium partly superficial, partly immersed; colonies composed of conidiophores and sometimes ascomata. ***Anamorph.*** Setae present, mostly associated with ascomata, simple, brown, apically rounded. Conidiophores mononematous, macronematous, solitary, erect, septate, unbranched, brown. Conidiogenous cells integrated, terminal, monophialidic, extending percurrently, cylindrical-lageniform to urceolate, brown; collarettes funnel-shaped, pale brown. Conidia obpyramidal, in side view cuneiform, obovoid to obtriangular, with angular outline when viewed from above, truncate at the basal scar, with a simple setula inserted apically at each corner, aseptate, hyaline, adhered in basipetal chains. ***Teleomorph.*** Ascomata non-stromatic, perithecial, papillate, dark brown, sparsely covered by setae and conidiophores. Ostiole periphysate. Ascomatal wall fragile, carbonaceous, two-layered. Paraphyses persistent, septate, hyaline, longer than the asci. Asci unitunicate, 8-spored, cylindrical-clavate, ascal apex with a non-amyloid apical annulus. Ascospores fusiform, hyaline, transversely septate.

Habitat and geographical distribution. Saprobes on dead leaves of *Freycinetia* spp. (Pandanaceae) and decaying wood, known only in Australasia in New Caledonia and New Zealand (McKenzie 1991; this study).

Notes. The genus *Chalarodes*, typified with *Cha. bisetis*, was erected for dematiaceous hyphomycetes observed on leaf litter of *Freycinetia* spp. in New Zealand and New Caledonia (McKenzie 1991). It is characterised by mononematous, simple, dark brown conidiophores with terminal monophialidic conidiogenous cells extending percurrently and hyaline, aseptate, cuneiform, obconical to obtriangular conidia with setulae, adhered in short basipetal chains. In the protologue (McKenzie 1991), the conidia were described only in the side view with two simple setulae at the apical end. Based on the examination of newly collected material, the conidia have angular outline when viewed from above; they have (3–)4 corners with a setula inserted in each corner. Additionally, we observed sterile setae growing among the conidiophores or on the ascomatal wall. They resemble capitate hyphae of *Catenularia*, but the mucilaginous sheath around the apex was lacking.

To date, two species, *Cha. bisetis* and *Cha. obconica*, have been placed in *Chalarodes* (McKenzie 1991). A new species, *Cha. obpyramidata*, inhabiting decaying wood and originating from New Zealand is introduced below. The teleomorph-anamorph connection of *Chalarodes* is described for the first time. Based on the results of the phylogenetic study, *Cha. obpyramidata* is closely related to *Catenularia*.

***Chalarodes obpyramidata* Réblová, sp. nov.**
MycoBank No: 839467
Fig. 8

Etymology. *Pyramidatus* (L), pyramidal, prefix *ob-* (L), meaning reversely, inversely, referring to the conidial shape.

Type. New Zealand – West Coast region • Westland district, Ross, Totara forest, Totara River valley; on decaying wood of a branch; 7 Mar. 2003; M. Réblová MR 2734/NZ 236 (***holotype*** PDD 119363).

Description. Colonies on natural substrate effuse, hairy, dark brown to black, mycelium partly superficial, partly immersed, brown; colonies composed of conidiophores and sometimes ascomata. ***Anamorph.*** Setae present, mostly associated with ascomata (see below). Conidiophores 195–360 × 5–7.5 µm, 7–8.5 µm wide above the base, mononematous, macronematous, solitary, erect, straight or flexuous, unbranched, thick-walled, dark brown, paler towards the apex. Conidiogenous cells 20–54 × 5–6.5(–8) µm tapering to 3.5–4.5 µm below the collarette, integrated, terminal, monophialidic, extending percurrently, cylindrical to cylindrical-lageniform, brown, producing conidia successively; collarettes 6–7.5 µm wide, 2.5–3(–4) µm deep, funnel-shaped, pale brown. Conidia 10.5–12 µm long, 8.5–12 µm wide, 2.5–3.5 µm wide at the basal hilum (mean ± SD = 11.2 ± 0.5 × 10.3 ± 1.0 × 2.9 ± 0.3 µm), obpyramidal, in side view cuneiform to obtriangular, with four corners when viewed from above, truncate at the basal scar, with straight or curved setulae inserted at each corner 5–8 µm long, aseptate, hyaline, thin-walled, smooth; formed singly, adhered in basipetal chains. ***Teleomorph.*** Ascomata 120–140 µm diam, 130–160 µm high, subglobose, dark brown to black, superficial, solitary or aggregated, subglobose, papillate, setose. Setae 37–157 × 3.5–5.5 µm, simple, straight, cylindrical, brown, pale brown towards the apex, extending percurrently, apical cell sterile, 3.5–4 µm wide, broadly rounded, pale brown to subhyaline, similar setae arise around ascomata on the substrate. Ostiole periphysate. Ascomatal wall fragile, carbonaceous, 20–24 µm thick, two-layered. Outer layer consisting of brown, polyhedral cells with opaque walls. Inner layer consisting of several rows of thin-walled, hyaline cells. Paraphyses 4–5 µm wide, tapering to ca. 2 µm, septate, hyaline, longer than the asci. Asci 95–114 × (9–)10–12 µm (mean ± SD = 103.5 ± 6.5 × 10.9 ± 1.1 µm), cylindrical-clavate, short-stipitate, apically narrowly rounded, ascal apex with a non-amyloid apical annulus ca. 3 µm wide, 2 µm high. Ascospores 18–22(–23) × 4–5 µm (mean ± SD = 20.4 ± 1.3 × 4.4 ± 0.4 µm), fusiform, hyaline, 1–3-septate, smooth, 2-seriate in the ascus.

Culture characteristics. On PCA: colonies 7–10 mm diam in 14d, circular, raised, margin entire, velvety-lanose, brown to dark grey-brown with whitish-grey conidial masses, reverse black. Sporulation abundant at the centre of the colony.

Colonies on PCA effuse, mycelium subhyaline to pale brown, 2–3 µm wide. Setae absent. Conidiophores, conidiogenous cells and conidia similar to those from nature. Conidiophores 74–141 × (4.5–)5–6 µm, 5.5–6.5 µm wide above the base, paler brown and less septate than those from nature, erect, straight. Conidiogenous cells 18–40 × 4.5–5.5 µm tapering to 3.5–4 µm below the collarette, cylindrical, pale brown; collarettes 5–6 µm wide, 3.5–4 µm deep, pale brown. Conidia 8–10(–11) µm long, 8–9(–10) µm wide, 2–2.5 µm wide at the hyaline basal hilum (mean ± SD = 9.7 ± 0.9 × 8.4 ± 0.6 × 2.0 ± 0.1 µm), cuneiform to obpyramidal, truncate at the basal scar, setulae not observed, aseptate, hyaline, thin-walled, smooth, formed basipetally in chains.

Figure 8. *Chalarodes obpyramidata* **A** ascomata **B** colony composed of conidiophores **C, H, O–Q** conidiophores **D–G, S, T** conidia **I–L, R** upper parts of conidiophores with conidia **M** asci with ascospores **N** paraphyses. Images: PDD 119363 (**A–L**); PDD 119364 (**M–T**); on natural substrate (**A–N**); in PCA culture after 4 wk (**O–T**). Scale bars: 250 µm (**A, B**); 50 µm (**C, H**); 10 µm (**D–G, M, N, R–T**); 20 µm (**I–L, O–Q**).

Other specimen examined. New Zealand – West Coast region • Buller district, Victoria Forest Park, Reefton, Big River Inanganua track; on decaying wood of *Nothofagus* sp. (associated with *C. novae-zelandiae* PDD 119362 and *Zanclospora falcata* PDD 119365); 6 Mar. 2003, M. Réblová MR 2724/ NZ 225 (PDD 119364).

Habitat and geographical distribution. Saprobe on decaying wood, known only in New Zealand.

Notes. In the size of conidia, our species appears intermediate between *Cha. bisetis* and *Cha. obconica* (McKenzie 1991). *Chalarodes bisetis* differs from *Cha. obpyramidata* in conidia longer and narrower at the apical end, (9.5–)12–14(–15) × 4.5–6(–9) µm, while *Ch. obconica* possesses conidia slightly shorter (8–)9–10.5(–11) µm and narrower at the basal hilum 1.75–2 µm.

Fuscocatenula **Réblová & A.N. Mill., gen. nov.**
MycoBank No: 839468

Etymology. *Fuscus* (L) dark, brown, dusky, *catenula* (L), a little chain, referring to pigmented conidia in chains.

Type species. *Fuscocatenula submersa* (Z.L. Luo, K.D. Hyde & H.Y. Su) Réblová & A.N. Mill.

Description. Colonies effuse, hairy, brown, mycelium partly immersed, partly superficial. ***Anamorph.*** Conidiophores macronematous, mononematous, solitary, erect, unbranched, brown to dark brown, thick-walled, paler and thinner-walled towards the apex. Conidiogenous cells integrated, terminal, monophialidic, extending percurrently, cylindrical to lageniform, brown; collarettes funnel-shaped, brown. Conidia cuneiform to obovoid, broadly rounded apically, truncate at the base, aseptate, hyaline when young, pale brown at maturity, with protracted maturation, smooth, formed in a basipetal chain. ***Teleomorph.*** Unknown. (Description partly adapted from Li et al. 2017; Luo et al. 2019).

Habitat and geographical distribution. Members of the genus are saprobes on decaying plant matter in terrestrial and freshwater environments, known only in Asia in China.

Notes. *Fuscocatenula* is proposed as a segregate genus for fungi distantly related from *Catenularia* (Fig. 2), although morphologically similar. Conidia of *Fuscocatenula* are obovoid with a truncate base, lack an angular outline and small, circular, thin-walled pale areas in corners that are present in *Catenularia*. Conidia have a protracted maturation; at first they are hyaline and only later become pale brown, while still attached in a chain. Sometimes the chain consists of hyaline conidia with only one or a few mature pigmented conidia (Li et al. 2017: fig. 1; Luo et al. 2019: fig. 52). In *Catenularia*, conidia are also hyaline when young but mature soon and when released from the conidiogenous locus they are usually pigmented. Since *Catenularia* also includes species lacking capitate hyphae, this character alone is not reliable in the distinction of *Fuscocatenula* from *Catenularia*.

Two species are accepted in the genus. Li et al. (2017) introduced *Catenularia variegata* for a foliicolous species from China and Luo et al. (2019) described

Chaetosphaeria submersa for a dematiaceous hyphomycete from submerged wood in Thailand. Both species are similar and reminiscent of *Catenularia*. In the phylogenetic analysis based on ITS-28S sequences, relationship of *Ch. submersa* and *Catenularia* was not supported. Molecular data of *C. variegata* are not available. Based on a detailed comparison of original descriptions and illustrations of both species we conclude that *C. variegata* is congeneric with *Ch. submersa*. Therefore, *C. variegata* is excluded from *Catenularia* and both species are transferred to the new genus *Fuscocatenula*.

***Fuscocatenula submersa* (Z.L. Luo, K.D. Hyde & H.Y. Su) Réblová & A.N. Mill., comb. nov.**
MycoBank No: 839469

Basionym. *Chaetosphaeria submersa* Z.L. Luo, K.D. Hyde & H.Y. Su, Fungal Divers. 99: 585. 2019.

Habitat and geographical distribution. Saprobe on submerged decaying wood in stream, known only in China (Luo et al. 2019).

Notes. The species is characterised by conidiophores 380–596(–691) µm × 15–21 µm and cuneiform, pale brown conidia 21–27 × 12–14 µm. The size of these structures clearly distinguishes *F. submersa* from the small-spored *F. variegata* with shorter conidiophores (Luo et al. 2019).

***Fuscocatenula variegata* (H.H. Li & X.G. Zhang) Réblová & A.N. Mill., comb. nov.**
MycoBank No: 839470

Basionym. *Catenularia variegata* H.H. Li & X.G. Zhang, Mycotaxon 132: 621. 2017.

Habitat and geographical distribution. Saprobe on dead stems of an unidentified broadleaf tree, known only in China (Li et al. 2017).

Notes. *Fuscocatenula variegata* resembles *F. submersa* but differs in shorter conidia 8.5–11 × 5.5–7.5 µm and shorter conidiophores 150–270 × 4.5–8 µm (Li et al. 2017).

***Nawawia antennata* Réblová, sp. nov.**
MycoBank No: 839471
Fig. 9

Etymology. *Antennatus* (L) meaning 'having antenna(s)', referring to the presence of conidial appendages resembling insect antennas.

Type. Thailand – Nakhon Nayok Province • Khao Yai National park, Phakrajai trail, on decaying wood and bark of a twig; 17 Aug. 2001; M. Réblová & N. Hywel-Jones M.R. 2056/TH 219 (PRA-20374).

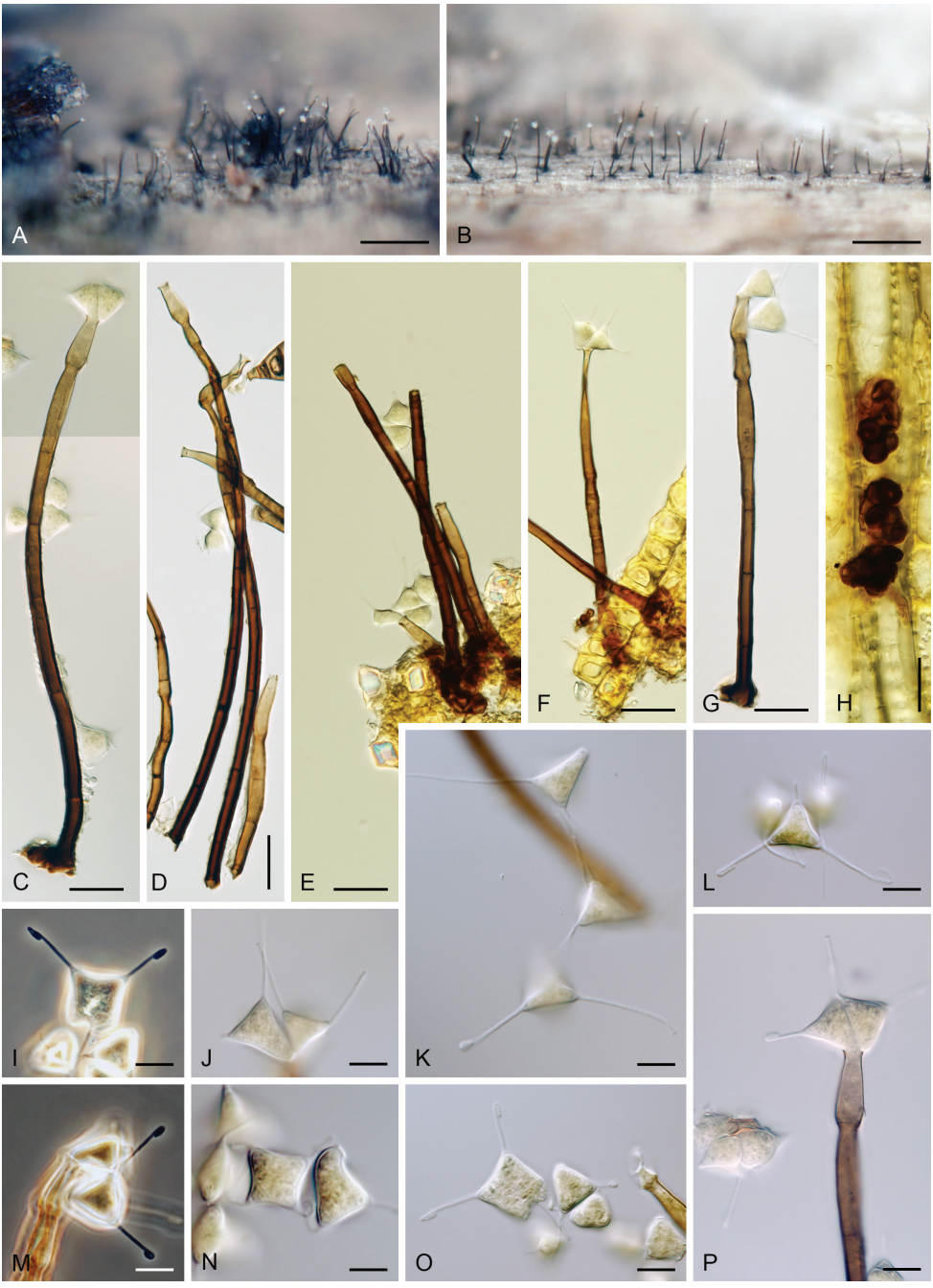

Figure 9. *Nawawia antennata* (PRA-20374 holotype) **A, B** colony **C–G** conidiophores **H** stromatic cells **I–P** conidia. Images: on natural substrate (**A–P**). Scale bars: 250 μm (**A, B**); 20 μm (**C, F, G**); 25 μm (**D, E**); 10 μm (**H–N**).

Description. Colonies on natural substrate effuse, hairy, dark brown, mycelium partly superficial, partly immersed, brown. ***Anamorph.*** Conidiophores forming two distinct layers; conidiophores of the upper layer 142–282 µm long, conidiophores of the lower layer 44–90 µm long, 5–6 µm wide, 6–8.5 wide above the base, basal cell bulbose with dark brown, thick-walled stromatic cells around the base, mononematous, macronematous, solitary or fasciculate in a group of 2–6, erect, straight or flexuous, unbranched, thick-walled, dark brown, paler towards the apex. Conidiogenous cells 19.5–29 × 5.5–7.5(–8) µm tapering to 3–5 µm below the collarette, integrated, terminal, monophialidic, extending percurrently, subcylindrical to lageniform, pale brown; collarettes 5.5–6.5 µm wide, 1.5–2.5 µm deep, funnel-shaped, pale brown. Conidia 14–17(–18) µm long, 11–14.5(–15.5) µm wide, 2.5–3.5 µm wide at the basal hilum (mean ± SD = 15.5 ± 1.2 × 12.9 ± 1.7 × 2.9 ± 0.3 µm), turbinate to obpyramidal, in side view cuneiform to obtriangular, truncate at the basal scar, flattened to slightly concave at the apical end, with (3–)4 corners when viewed from above, aseptate, hyaline, thin-walled, smooth, with simple setulae inserted at each corner, 17–43 µm long, 7.5–20 µm long when the ends are coiled, conidia accumulate in slimy droplets. ***Teleomorph.*** Not observed.

Habitat and geographical distribution. Saprobe on decaying wood, known only in Thailand.

Notes. We were unsuccessful in obtaining *N. antennata* in axenic culture. The species exhibits diagnostic characteristics of *Nawawia* such as pigmented, mononematous conidiophores with stromatic cells around the base, terminal monophialides extending percurrently and hyaline, aseptate, obtriangular conidia with an angular outline and several simple setulae at the apex. Conidia accumulate in a slimy head. Conidiophores forming two distinct layers were also documented in *N. quadrisetulata* (Goh et al. 2014: figs 2, 3).

Among *Nawawia* species, *N. antennata* is well distinguished by coiled appendages and the size of conidia. *Nawawia quadrisetulata* is similar to the new species in conidia with mostly four angles at the apex but differs in larger conidia (30–37.5 × 22.5–32.5 µm) with longer setulae (30–57.5 µm). *Nawawia antennata* resembles *N. filiformis* (Marvanová 1980) but the latter species has conidia wider at the apex (14–18 µm) and straight appendages.

Discussion

In this study, we have reviewed the generic concept of *Catenularia* and its relationships with morphologically similar genera with catenate conidia using molecular and phenotypic data. The conidial characteristics, such as the colour at maturity, the outline in transverse section and presence or absence of the setulae are the main taxonomic criteria at the generic rank for distinguishing between *Catenularia*, *Chalarodes* and

Fuscocatenula. Their conidia are formed successively; they are solitary and adhere in basipetal chains. These genera are compared with *Nawawia*, *Obeliospora* and *Phialosporostilbe*, which have similar conidia in slimy heads.

Although molecular DNA data of *C. cupulifera* are not available, four other morphologically similar species accepted in *Catenularia* were included in the analysis of ITS and 28S sequence data. *Catenularia* was resolved as a monophyletic strongly supported clade. Phylogenetic analysis indicates that *Chaetosphaeria* (Tulasne and Tulasne 1863), based on *Ch. innumera* with the *Chloridium botryoideum* anamorph (Gams and Holubová-Jechová 1976), is a phylogenetically distinct genus (Fig. 2). Therefore, *Catenularia* is proposed as the generic name for a morphologically well-delimited group of species whose teleomorphs were previously attributed to *Chaetosphaeria*. The correct epithet of the type species of *Catenularia* is '*cupulifera*' based on *Sphaeria cupulifera* 1871, the earliest available epithet at the species rank; *C. cuneiformis* 1877 and *C. simplex* 1886 are reduced to synonymy. *Catenularia* is delimited to fungi with pigmented conidiophores arising singly or in tufts, usually accompanied by capitate hyphae, terminal monophialidic conidiogenous cells extending percurrently and flared collarettes. Conidia are pigmented, aseptate, thick-walled, formed successively from the conidiogenous locus and usually adhere in chains. They are cuneiform to rounded-obconic in side view with several blunt corners when viewed from above, each with a small, thin-walled, pore-like area. The associated teleomorphs have perithecial ascomata, unitunicate 8-spored asci, persistent paraphyses and hyaline, fusiform, transversely septate ascospores. *Catenularia* grows on decaying bamboo culms and bark and wood of various hosts in terrestrial or freshwater habitats worldwide.

Eleven species are accepted in *Catenularia*, four of which have been verified with molecular DNA data. One of the accepted species, *C. elsikii*, is a fossil fungus. The conidia were preserved in a sample of fossil wood, dated to the Miocene, found in the United Kingdom (Pound et al. 2019). The substrate indicates a similar habitat as in the current species. Microscopic fossil fungi are difficult to identify, especially when only spores or fragments of reproductive structures are preserved (Taylor et al. 2015). Fortunately, *Catenularia* conidia represent a distinctive morphotype, which allows reliable identification. The majority of species of the Chaetosphaeriaceae have hyaline, thin-walled conidia and ascospores, which will likely disintegrate in the fossilized samples. On the other hand, thick-walled and heavily pigmented fungal reproductive structures are randomly present in fossil material (Pound et al. 2019). Apart from *Catenularia*, *Adautomilanezia* (Crous et al. 2016), *Ellisembia*, *Stanjehughesia* (Subramanian 1992), and *Sporoschisma* (Berkeley and Broome 1871; Hughes 1966) of the Chaetosphaeriaceae also have thick-walled and melanised conidia that may occur in fossil material or palynological preparations.

Hughes (1965) suggested that conidia of *Catenularia* may germinate through the inconspicuous, thin-walled areas in the cell wall in corners. In the newly recorded specimens of *C. novae-zelandiae*, we observed several conidia with rudimentary hyaline appendages growing from these pore-like areas (Fig. 7K). This feature has not been recorded in any other *Catenularia* species. However, we rule out the possibility that these appendages are germinating tubes after comparing the figure in Luo et al. (2019: figure

47l) depicting germinating conidium. The presence of rudimentary conidial appendages in *Catenularia* may reflect its newly revealed phylogenetic relationship.

In the ITS-28S phylogeny, *Chalarodes* was shown as a sister to *Catenularia* with high statistical support. Their close relationship is also supported by similar morphologies. *Chalarodes* differs from *Catenularia* in conidia that are hyaline at maturity and have simple setulae at the apical end. Although McKenzie (1991) described conidia of two *Chalarodes* species from the side view only, examination of our material revealed that the conidia are turbinate to obpyramidal with an angular outline. The discovery of rudimentary setulae in *C. novae-zelandiae* provides a new perspective on this characteristic. Although setulae persist in *Chalarodes*, the appendages in *Catenularia* were lost during evolution or never evolved, except in the discovered case. However, the systematic placement of *C. novae-zelandiae* has yet to be confirmed with DNA sequence data. Our observations of *Cha. obpyramidata* in culture (Fig. 8O–T) correspond to those of Marvanová (1980) on *Nawawia filiformis*. In both species, conidia that formed in culture lack setulae.

Fuscocatenula is proposed for fungi similar to *Catenularia* and readily distinguished by pigmented conidia with protracted maturation, round in transverse section, lacking minute pore-like areas at the apical end, and the absence of capitate hyphae. In the phylogenetic analysis, *Fuscocatenula* was shown as a separate lineage, related to several *Chaetosphaeria* with hyaline or slightly pigmented conidia formed singly or in chains (Gams and Holubová-Jechová 1976). Its closest relatives are *Ch. mangrovei* with an unknown conidial state, and *Ch. innumera*. *Chloridium botryoideum*, the anamorph of *Ch. innumera*, forms hyaline ellipsoidal conidia arranged in imbricate chains or large heads on sympodially elongating conidiogenous cells. *Phaeostalagmus cyclosporus* and two *Chaetosphaeria* species with *Chloridium* anamorphs are shown as a sister subclade to *Fuscocatenula*. *Chloridium clavaeforme* and *Chl. phaeophorum* belong to the section *Gongromeriza* and resemble *Fuscocatenula* in slightly pigmented, short-cuneiform or dacryoid conidia forming chains or slimy droplets. *Phaeostalagmus*, on the other hand, represents a different phenotype. Its conidiophores are branched with lateral or terminal monophialides producing hyaline, ellipsoidal conidia in slimy heads.

Capitate hyphae (Hughes 1949) are a prominent characteristic that occurs in several members of the Chaetosphaeriaceae. They accompany conidiophores of *Catenularia* and *Sporoschisma*; they are scattered on the substrate or more frequently grow in tufts among the conidiophores or on ascomata of their teleomorphs. Capitate hyphae also occur on ascomata of *Ch. capitata*, the teleomorph of *Exserticlava vasiformis*, and *Ch. conirostris* (Sivanesan and Chang 1995; Fernández and Huhndorf 2005). Similar setae with a swollen apical cell but without the mucilaginous cap were observed on and around ascomata of the teleomorph of *Cha. obpyramidata* (this study). The presence of analogous structures have been described in the teleomorph of *Stanjehughesia* (Réblová 1999); they cover ascomata and their apical part, separated by a septum, is formed by an amorphous, subhyaline, clavate to almost triangular globule. All these genera, except for *Sporoschisma*, clustered as members of a robust clade at the base of the family tree.

Because of its mononematous conidiophores and hyaline, tetrahedral conidia with setulae arranged in corners at the apical end, *Chalarodes* appears similar to *Nawawia*

(Marvanová 1980). *Nawawia* encompasses aero-aquatic fungi that form effuse, hairy colonies on decaying wood, bamboo culms and petioles. It is distinguished from *Chalarodes* by conidia that do not adhere in chains; instead they are single or accumulate in heads at the tip of the conidiogenous cells. Conidiophores often have small stromatic hyphal cells around the base. *Nawawia* accommodates five species of which only four, namely *N. antennata*, *N. filiformis*, *N. quadrisetula*, *N. sasae-kurilensis*, correspond to the generic concept based on *N. filiformis* (Marvanová 1980; Mel'nik and Hyde 2006; Goh et al. 2014; this study). The new species *N. antennata* resembles *N. quadrisetula* (Goh et al. 2014) in characters of conidiophores and conidia but differs in that the conidia are smaller and the setulae are coiled. Unfortunately, living culture or molecular data are not available to confirm its relationships. *Nawawia oviformis* (Peng et al. 2016) does not fit the circumscription of the genus; it has conidia with a round outline in transverse section with setulae arranged irregularly over the whole surface. These characteristics are typical of *Bahusutrabeeja* (Subramanian and Bhat 1977) and *N. oviformis* would be better placed in this genus. In the ITS-28S phylogenetic tree (Fig. 2), *Nawawia* and *Bahusutrabeeja* form separate lineages. Three species originally attributed to *Nawawia* have been reclassified and placed in other genera as *Neonawawia malaysiana* (Yang et al. 2018), *Obeliospora nitida* (Cantillo-Pérez et al. 2018) and *Phialosporostilbe dendroidea* (Yang et al. 2018). *Neonawawia* is particularly interesting by its formation of sporodochial conidiomata and hyaline to light brown conidiophores; it resembles *Nawawia* only in the characteristics of conidia. Based on phylogenetic evidence, its placement has been confirmed outside the Chaetosphaeriaceae (Yang et al. 2018).

Hyaline, turbinate conidia with an angular outline and apical setulae represent an uncommon morphotype in the Chaetosphaeriaceae. Apart from *Chalarodes* and *Nawawia*, similar conidia borne on monophialides occur only in species of *Phialosporostilbe*. The latter genus is distantly related to both genera and is distinguished by synnematous conidiophores associated with setae, conidial setulae occasionally formed at the base and a chloridium-like synanamorph (Mercado Sierra and Mena Portales 1985; Bhat and Kendrick 1993). The synnemata are indeterminate and although in most species the stalk is formed by compact conidiophores that climb upwards along the seta and diverge at their fertile apices, the arrangement of conidiophores of *P. gregariclavata* (Shirouzu and Harada 2004) is unusual within the genus. The central setiform conidiophore is accompanied by a group of shorter, parallel conidiophores that are solitary or tightly adhering to each other and may fuse. Therefore, the conidiophores of *P. gragariclava* may be interpreted as a poorly developed synnemata (Shirouzu and Harada 2004: fig. 10). In the characters of conidiophores, *P. gregariclavata* resembles members of *Nawawia*.

In characteristics of conidia, *Chalarodes*, *Nawawia* and *Phialosporostilbe* are comparable with *Obeliospora*, whose systematic placement remains unknown. The genus was emended by Cantillo-Pérez et al. (2018) and is readily distinguished by the absence of stromatic hyphal cells, and the presence of dark acute setae accompanied by monilioid conidiophores with terminal doliiform conidiogenous cells and flared, cup- or funnel-shaped collarettes. The conidia vary in shape ranging from round-tetrahedral, conical, pyramidal to subglobose and are hyaline, although in some species older conidia become light brown.

Although we emphasised characteristics of conidia in chains or heads to support delimitation of *Catenularia*, *Chalarodes* and *Nawawia*, we should look at this diagnostic trait with caution. For example, in *C. minor* conidia adhere in chains but in older parts of the colony conidia may form clusters. The chains break into smaller fragments, which appear as a cluster at the tip of the conidiogenous cell. In microscopic preparation, the chains readily break up into solitary conidia (Fig. 6E, L). A similar variability occurs in *Phialosporostilbe*. Although the majority of species have conidia arranged in slimy heads, the conidia of *P. catenata* form chains (Sureshkumar et al. 2005). Réblová et al. (2011) discussed this phenomenon using the example of *Monilochaetes camelliae* observed with an ESEM (Environmental Scanning Electron Microscope). The authors showed that there is a continuum from conidial chains to slimy heads on the phialides in culture. *Chloridium* is another example, e.g. *Chl. clavaeforme* and *Chl. virescens*, in which chains, cirrhi, and slimy heads can all be observed in one species in culture (Gams and Holubová-Jechová 1976; pers. obs.). It is apparently caused by the osmolarity of the medium that may affect the proportion between chains and heads.

The present investigation contributes to the knowledge of *Catenularia* and similar fungi with catenate conidia placed in the Chaetosphaeriaceae. Sampling of other species in the genera *Catenularia*, *Chalarodes*, *Nawawia* and *Phialosporostilbe*, which have not yet been verified by molecular data, are needed to address their systematic placement.

Acknowledgements

Peter Johnston is thanked for his assistance to M.R. in obtaining the Manaaki Whenua Fellowship and collecting permits for New Zealand. Genevieve Tocci (FH) is thanked for her assistance to M.R. in revising the holotype of *C. angulospora*. We thank Sabine Huhndorf for the use of her collections and DNA extracts. We thank Jacques Fournier and Bernard Declerque for valuable collections of *Catenularia* and *Sporoschisma*. Curators of herbaria, Jan Holec (PRM), Anton Igersheim (W), Ludmila Kirschnerová (PRA), Scott Redhead (DAOM) and Adrienne Stanton (PDD), are acknowledged for assistance with obtaining herbarium loans and depositing new herbarium material. We thank Konstanze Bensch and Shaun Pennycook for their grammatical review of new names. We thank Kazuaki Tanaka for discussion on *Phialosporostilbe*.

This study was supported by the project of the Czech Science Foundation (GAČR 20-14840S), and as long-term research development projects of the Czech Academy of Sciences, Institute of Botany (RVO 67985939) (M.R.) and the University Hospital Hradec Králové MH CZ – DRO (UHHK, 00179906) (J.N.). This study was also supported by a National Science Foundation award (DEB-0515558) to A.N.M. The Roy J. Carver Biotechnology Center at the University of Illinois Urbana-Champaign is thanked for sequencing services. The field work of M.R. in New Zealand was partly supported by Studienstiftung für mykologische Systematik und Ökologie (2003) and Manaaki Whenua Fellowship, Landcare Research Auckland (2005). The authors have declared that no competing interests exist.

References

Arx JA von (1970) The genera of fungi sporulating in pure culture. Verlag J. Cramer, Lehre, 288 pp.

Berkeley MJ, Broome CE (1871) Notices on British fungi. The Annals and Magazine of Natural History IV 7: 425–436. https://doi.org/10.1080/00222937108696408

Bhat DJ, Kendrick WB (1993) Twenty-five new conidial fungi from the Western Ghats and the Andaman Islands (India). Mycotaxon 49: 19–90.

Booth C (1957) Studies of Pyrenomycetes: I. Four species of *Chaetosphaeria*, two with *Catenularia* conidia. II. *Melanopsamma pomiformis* and its *Stachybotrys* conidia. Mycological Papers 68: 1–27.

Booth C (1958) The genera *Chaetosphaeria* and *Thaxteria* in Britain. The Naturalist London: 83–90.

Cantillo-Pérez T, Oliveira Fiuza P, Mena-Portales J, Gusmão LFP (2017) [2018]. Emendation of the genus *Obeliospora*: new species, combinations and new records from Brazil. Nova Hedwigia 106: 325–335. https://doi.org/10.1127/nova_hedwigia/2017/0439

Clements FE, Shear CL (1931) Genera of Fungi. H.W. Wilson Company, New York, 496 pp.

Costantin JN (1888) Les Mucédinées Simples. Histoire, Classification, Culture et Rôle des Champignons Inférieurs dans les Maladies des Végétaux et des Animaux. i–viii. P. Klincksieck, Paris, 210 pp.

Crous PW, Verkley GJM, Christensen M, Castañeda-Ruíz RF, Groenewald JZ (2012) How important are conidial appendages? Persoonia 28: 126–137. https://doi.org/10.3767/003158512X652624

Crous PW, Verkley GJM, Groenewald JZ, Houbraken J (2019) Fungal biodiversity. CBS laboratory manual series 1. CBS-KNAW Fungal Biodiversity Centre, Utrecht, 425 pp.

Crous PW, Wingfield MJ, Burgess TI, Hardy GEStJ, Crane C, Barrett S, Cano-Lira JF, Le Roux JJ, Thangavel R, Guarro J, Stchigel AM, Martín MP, Alfredo DS, Barber PA, Barreto RW, Baseia IG, Cano-Canals J, Cheewangkoon R, Ferreira RJ, Gené J, Lechat C, Moreno G, Roets F, Shivas RG, Sousa JO, Tan YP, Wiederhold NP, Abell SE, Accioly T, Albizu JL, Alves JL, Antoniolli ZI, Aplin N, Araújo J, Arzanlou M, Bezerra JDP, Bouchara J-P, Carlavilla JR, Castillo A, Castroagudín VL, Ceresini PC, Claridge GF, Coelho G, Coimbra VRM, Costa LA, da Cunha KC, da Silva SS, Daniel R, de Beer ZW, Dueñas M, Edwards J, Enwistle P, Fiuza PO, Fournier J, García D, Gibertoni TB, Giraud S, Guevara-Suárez M, Gusmão LFP, Haituk S, Heykoop M, Hirooka Y, Hofmann TA, Houbraken J, Hughes DP, Kautmanová I, Koppel O, Koukol O, Larsson E, Latha KPD, Lee DH, Lisboa DO, Lisboa WS, López-Villalba Á, Maciel JLN, Manimohan P, Manjón JL, Marincowitz S, Marney TS, Meijer M, Miller AN, Olariaga I, Paiva LM, Piepenbring M, Poveda-Molero JC, Raj KNA, Raja HA, Rougeron A, Salcedo I, Samadi R, Santos TAB, Scarlett K, Seifert KA, Shuttleworth LA, Silva GA, Silva M, Siqueira JPZ, Souza-Motta CM, Stephenson SL, Sutton DA, Tamakeaw N, Telleria MT, Valenzuela-Lopez N, Viljoen A, Visagie CM, Vizzini A, Wartchow F, Wingfield BD, Yurchenko E, Zamora JC, Groenewald JZ (2016) Fungal Planet description sheets: 469–557. Persoonia 37: 218–403. https://doi.org/10.3767/003158516X694499

Darty K, Denise A, Ponty Y (2009). VARNA: Interactive drawing and editing of the RNA secondary structure. Bioinformatics 25: 1974–1975. https://doi.org/10.1093/bioinformatics/btp250

De Beer ZW, Duong TA, Barnes I, Wingfield BD, Wingfield MJ (2014) Redefining *Ceratocystis* and allied genera. Studies in Mycology 79: 187–219. https://doi.org/10.1016/j.simyco.2014.10.001

De Castro CC, Hernández Gutiérrez A, Maria Pontes Sotão HM (2011) Novos registros de fungos anamorfos (hifomicetos) para o Neotrópico e América do Sul. Revista Brasileira de Botanica 34: 515–521. https://doi.org/10.1590/S0100-84042011000400005

De Seynes J (1886) Recherches pour Servir a l'Histoire Naturelle des Vegetaux Inferieurs. III (Ire Partie). De la Formation des Corps Reproducteurs Appeles Acrospores. G. Masson, Libraire de L'Académie de Médicine, Paris, 51 pp.

Dubey R, Pandey AD (2017) Percentage distribution of foliicolous fungi of Maharashtra, India with respect to their disease symptoms: a novel study. Mycologia Iranica 4: 103–120. https://doi.org/10.22043/MI.2018.117293

Fernández FA, Huhndorf SM (2005) New species of *Chaetosphaeria*, *Melanopsammella* and *Tainosphaeria* gen. nov. from the Americas. Fungal Diversity 18: 15–57.

Fernández FA, Miller AN, Huhndorf SM, Lutzoni FM, Zoller S (2006) Systematics of the genus *Chaetosphaeria* and its allied genera: morphological and phylogenetic diversity in north temperate and neotropical taxa. Mycologia 98: 121–130. https://doi.org/10.1080/15572536.2006.11832718

Fernández R, Smits G (2018) Registro de hifomicetos acuáticos en el río Guáquira de la Reserva Ecológica Guáquira (San Felipe, Venezuela). Gestión y Ambiente 21: 121–128. https://doi.org/10.15446/ga.v21n1.71778

Gams W, Holubová-Jechová V (1976) *Chloridium* and some other dematiaceous hyphomycetes growing on decaying wood. Studies in Mycology 13: 1–99.

Goh TK, Lau WP, Teo KC (2014) A new species of *Nawawia* from Malaysia, with a synopsis of the genus. Mycotaxon 129: 109–118. https://doi.org/10.5248/129.109

Grove WB (1886) New or Noteworthy Fungi: Part III. Journal of Botany 24: 197–206.

Gruber AR, Bernhart SH, Lorenz R (2015) The ViennaRNA web services. Methods in Molecular Biology 1269: 307–26. https://doi.org/10.1007/978-1-4939-2291-8_19

Gutell RR, Gray MW, Schnare MN (1993) A compilation of large subunit (23S and 23Slike) ribosomal RNA structures. Nucleic Acids Research 21: 3055–3074. https://doi.org/10.1093/nar/21.13.3055

Hall TA (1999) BioEdit 5.0.9: a user-friendly biological sequence alignment editor and analysis program for Windows 95/98/NT. Nucleic Acids Symposium Series 41: 95–98.

Hashimoto A, Sato G, Matsuda T, Matsumura M, Hatakeyama S, Harada Y, Ikeda H, Tanaka K (2015) Taxonomic revision of *Pseudolachnea* and *Pseudolachnella*, and establishment of *Neopseudolachnella* and *Pseudodinemasporium* genera nova. Mycologia 107: 383–408. https://doi.org/10.3852/14-171

Heredia G, Reyes M, Arias RM, Mena-Portales J, Mercado-Sierra A (2004) Adiciones al conocimiento de la diversidad de los hongos conidiales del bosque mesófilo de montana del estado de Veracruz. Acta Botánica Mexicana 66: 1–22. https://doi.org/10.21829/abm66.2004.969

Hernández-Restrepo M, Gené J, Castañeda-Ruíz RF, Mena-Portales J, Crous PW, Guarro J (2017) Phylogeny of saprobic microfungi from Southern Europe. Studies in Mycology 86: 53–97. https://doi.org/10.1016/j.simyco.2017.05.002

Hernández-Restrepo M, Schumacher RK, Wingfield MJ, Ahmad I, Cai L, Duong TA, Edwards J, Gené J, Groenewald JZ, Jabeen S, Khalid AN, Lombard L, Madrid H, Marin-Felix Y, Marincowitz S, Miller AN, Rajeshkumar KC, Rashid A, Sarwar S, Stchigel AM, Taylor PWJ, Zhou N, Crous PW (2016) Fungal systematics and evolution: FUSE 2. Sydowia 68: 193–230. https://doi.org/10.12905/0380.sydowia68-2016-0193

Holubová-Jechová V (1973) Lignicolous hyphomycetes from Czechoslovakia 3. *Sporoschisma*, *Sporoschismopsis* and *Catenularia*. Folia Geobotanica and Phytotaxonomica 8: 209–218. https://doi.org/10.1007/BF02854564

Holubová-Jechová V (1982) New or interesting phialidic hyphomycetes from Cuba. Mycotaxon 15: 277–292.

Holubová-Jechová V (1983) Studies on hyphomycetes from Cuba I. Česká Mykologie 37: 12–18. https://doi.org/10.1007/BF02857456

Holubová-Jechová V, Hennebert GL (1972) *Sporoschismopsis*, a new genus of lignicolous hyphomycetes. Bulletin du Jardin Botanique National de Belgique 42: 385–391. https://doi.org/10.2307/3667664

Huelsenbeck JP, Ronquist F (2001) MrBayes: Bayesian inference of phylogenetic trees. Bioinformatics 17: 754–755. https://doi.org/10.1093/bioinformatics/17.8.754

Hughes SJ (1949) Studies on micro-fungi. II. The genus *Sporoschisma* Berkeley & Broome and a redescription of *Helminthosporium rousselianum* Montagne. Mycological Papers 31: 1–34. https://doi.org/10.1016/S0007-1536(49)80034-9

Hughes SJ (1958) Revisiones hyphomycetum aliquot cum appendice de nominibus rejiciendis. Canadian Journal of Botany 36: 727–836. https://doi.org/10.1139/b58-067

Hughes SJ (1965) New Zealand fungi 3. *Catenularia* Grove. New Zealand Journal of Botany 3: 136–150. https://doi.org/10.1080/0028825X.1965.10876990

Hughes SJ (1966) New Zealand fungi. 6. *Sporoschisma* Berk. & Br. New Zealand Journal of Botany 4: 77–85. https://doi.org/10.1080/0028825X.1966.10443955

Huhndorf SM, Miller AN, Fernández FA (2004) Molecular systematics of the Sordariales: The order and the family Lasiosphaeriaceae redefined. Mycologia 96: 368–387. https://doi.org/10.1080/15572536.2005.11832982

Hustad VP, Miller AN (2015) Studies in the genus *Glutinoglossum*. Mycologia 107: 647–657. https://doi.org/10.3852/14-328

Kodsueb R, McKenzie EHC, Lumyong S, Hyde KD (2008) Fungal succession on woody litter of *Magnolia liliifera* (Magnoliaceae). Fungal Diversity 30: 55–72. https://doi.org/10.3852/14-328

Kuthubutheen AJ, Nawawi A (1994) *Henicospora longissima* sp. nov., *Obeliospora triappendiculata* sp. nov., *Paraulocladium fabisporum* sp. nov. and other hyphomycetes from Malaysia. Mycological Research 98: 677–685. https://doi.org/10.1016/S0953-7562(09)80416-4

Lanfear R, Frandsen PB, Wright AM, Senfeld T, Calcott B (2017) PartitionFinder 2: new methods for selecting partitioned models of evolution for molecular and morphological phylogenetic analyses. Molecular Biology and Evolution 34: 772–773. https://doi.org/10.1093/molbev/msw260

Li HH, Zhang K, Xia JW, Wang JY, Yang CL, Zhang XG (2017) *Catenularia variegata* sp. nov. from southern China, and a first Chinese record of *Xylocladium clautriavii*. Mycotaxon 132: 621–634. https://doi.org/10.5248/132.621

Lin CG, McKenzie EHC, Liu JK, Jones EBG, Hyde KD (2019) Hyaline-spored chaetosphaeriaceous hyphomycetes from Thailand and China, with a review of the family Chaetosphaeriaceae. Mycosphere 10: 655–700. https://doi.org/10.5943/mycosphere/10/1/14

Linder DH (1933) North American Hyphomycetes. I. Two new Helicosporeae and the new genera *Haplochalara* and *Paspalomyces*. Mycologia 25: 342–349. https://doi.org/10.1080/00275514.1933.12020675

Litvinov MA (1967) Opredelitel' Mikroskopicheskikh Pochvennykh Gribov. Nauka, Leningrad, 475 pp.

Liu JK, Yang J, Maharachchikumbura SSN, McKenzie EHC, Jones EBG, Hyde KD, Liu ZY (2016) Novel chaetosphaeriaceous hyphomycetes from aquatic habitats. Mycological Progress 15: 1157–1167. https://doi.org/10.1007/s11557-016-1237-1

Lu YZ, Liu KJ, Hyde KD, Bhat DJ, Xiao YP, Tian Q, Wen TC, Boonmee S, Kang JC (2016) *Brunneodinemasporium jonesii* and *Tainosphaeria jonesii* spp. nov. (Chaetosphaeriaceae, Chaetosphaeriales) from southern China. Mycosphere 7: 1322–1331. https://doi.org/10.5943/mycosphere/7/9/6

Luo ZL, Hyde KD, Liu J-K, Maharachchikumbura SSN, Rajesh J, Bao D-F, Bhat DJ, Lin C-G, Li W-L, Yang J, Liu N-G, Lu Y-Z, Jayawardena RS, Li J-F, Su H-Y (2019) Freshwater Sordariomycetes. Fungal Diversity 99: 451–660. https://doi.org/10.1007/s13225-019-00438-1

Ma YR, Xia JW, Gao JM, Li Z, Zhang XG (2016) *Anacacumisporium*, a new genus based on morphology and molecular analyses from Hainan, China. Cryptogamie Mycologie 37: 45–59. https://doi.org/10.7872/crym/v37.iss1.2016.45

Magyar D, Shoemaker RA, Bobvos J, Crous PW, Groenewald JZ (2011) *Pyrigemmula*, a novel hyphomycete genus on grapevine and tree bark from Hungary. Mycological Progress 10: 307–314. https://doi.org/10.1007/s11557-010-0703-4

Mangenot F (1952) Recherches méthodiques sur les champignons de certains bois en décomposition. Revue Génerale de Botanique 59: 1–115.

Mason EW (1941) Annotated account of fungi received at the Imperial Bureau of Mycology. Mycological Papers 5: 1–144.

Marvanová L (1980) New or noteworthy aquatic hyphomycetes. Transactions of the British Mycological Society 75: 221–231. https://doi.org/10.1016/S0007-1536(80)80083-0

Mbenoun M, De Beer ZW, Wingfield MJ, Wingfield BD, Roux J (2014) Reconsidering species boundaries in the *Ceratocystis paradoxa* complex, including a new species from oil palm and cacao in Cameroon. Mycologia 106: 757–784. https://doi.org/10.3852/13-298

McKenzie EHC (1991) Dematiaceous hyphomycetes on *Freycinetia* (Pandanaceae). 3: *Chalarodes* gen. nov. Mycotaxon 42: 89–93.

McNeill J, Barrie FF, Buck WR, Demoulin V, Greuter W, et al. [Eds] (2012) International Code of Nomenclature for algae, fungi, and plants (Melbourne Code). [Regnum vegetabile no. 154.]. Koeltz Scientific Books, Königstein, 208 pp.

Mel'nik VA, Hyde KD (2006) *Nawawia sasae-kurilenses* sp. nov. from the Russian Far East. Mikologiya i Fitopatologiya 40: 411–414.

Mercado Sierra A, Mena Portales J (1985) Nuevo género de hifomicete fialídico de Cuba. Revista del Jardín Botánico Nacional Universidad de la Habana 6: 57–60.

Miller MA, Pfeiffer W, Schwartz T (2010) Creating the CIPRES Science Gateway for inference of large phylogenetic trees. Proceedings of the Gateway Computing Environments Workshop (GCE), 14 Nov. 2010, New Orleans, 8 pp. https://doi.org/10.1109/GCE.2010.5676129

Nawawi A, Kuthubutheen AJ (1990) *Obeliospora*, a new genus of setose, phialosporous hyphomycetes with appendaged conidia. Mycotaxon 37: 395–400.

Peng J, Chang D, Huang Y, Yu ZF (2016) *Nawawia oviformis* sp. nov. from China. Mycotaxon 131: 735–738. https://doi.org/10.5248/131.735

Pound MJ, O'Keefe JMK, Nuñez Otaño NB, Riding JB (2019) Three new Miocene fungal palynomorphs from the Brassington Formation, Derbyshire, UK. Palynology 43: 596–607. https://doi.org/10.1080/01916122.2018.1473300

Réblová M (1999) Studies in *Chaetosphaeria* sensu lato III. *Umbrinosphaeria* gen. nov. and *Miyoshiella* with *Sporidesmium* anamorphs. Mycotaxon 71: 13–43.

Réblová M, Gams W, Seifert KA (2011) *Monilochaetes* and allied genera of the Glomerellales, and a reconsideration of families in the Microascales. Studies in Mycology 68: 163–191. https://doi.org/10.3114/sim.2011.68.07

Réblová M, Kolařík M, Nekvindová J, Miller AN, Hernández-Restrepo M (2021b) Phylogeny, global biogeography and pleomorphism of *Zanclospora*. Microorganisms 9(4): e706. https://doi.org/10.3390/microorganisms9040706

Réblová M, Nekvindová J, Fournier J, Miller AN (2020) Delimitation, new species and teleomorph-anamorph relationships in *Codinaea*, *Dendrophoma*, *Paragaeumannomyces* and *Striatosphaeria* (Chaetosphaeriaceae). MycoKeys 74: 17–74. https://doi.org/10.3897/mycokeys.74.57824

Réblová M, Nekvindová J, Kolařík M, Hernández-Restrepo M (2021a) Delimitation and phylogeny of *Dictyochaeta*, and introduction of *Achrochaeta* and *Tubulicolla*, genera nova. Mycologia 113: 390–433. https://doi.org/10.1080/00275514.2020.1822095

Réblová M, Seifert KA (2003) Six new species of *Chaetosphaeria* from tropical rain forests in Thailand and redescription of *Chaetosphaeria hiugensis*. Sydowia 55: 313–347.

Réblová M, Winka K (2000) Phylogeny of *Chaetosphaeria* and its anamorphs based on morphological and molecular data. Mycologia 92: 939–954. https://doi.org/10.1080/00275514.2000.12061238

Réblová M, Winka K (2001) Generic concepts and correlations in ascomycetes based on molecular and morphological data: *Lecythothecium duriligni* gen. et sp. nov. with a *Sporidesmium* anamorph, and *Ascolacicola austriaca* sp. nov. Mycologia 93: 478–493. https://doi.org/10.1080/00275514.2001.12063181

Rong IH, Gams W (2000) The hyphomycete genera *Exochalara* and *Monilochaetes*. Mycotaxon 76: 451–462.

Richon C (1877) Description et Dessins de Quelques Plantes Cryptogames Nouvelles ou Extremement Rares. Bulletin de la Société des sciences et arts Vitry-le-François 8: 211–222.

Saccardo PA (1883) Sylloge Pyrenomycetum. Sylloge Fungorum 2: 1–813.

Saccardo PA (1886) Sylloge Hyphomycetum. Sylloge Fungorum 4: 1–807.

Schoknecht JD, Crane JL (1977) Revision of *Torula* and *Hormiscium* species. *Torula occulta*, *T. diversa*, *T. eliastticae*, *T. bigemina* and *Hormiscium condensatum* reexamined. Mycologia 69: 533–546. https://doi.org/10.1080/00275514.1977.12020092

Sharma ND (1980) Some additions to fungi of India – VIII. Journal of the Indian Botanical Society 59: 72–77.

Shenoy BD, Jeewon R, Wang H, Amandeep K, Ho HW, Bhat DJ, Crous PW, Hyde KD (2010) Sequence data reveals phylogenetic affinities of fungal anamorphs *Bahusutrabeeja*, *Diplococcium*, *Natarajania*, *Paliphora*, *Polyschema*, *Rattania* and *Spadicoides*. Fungal Diversity 44: 161–169. https://doi.org/10.3767/003158511X617435

Shim JJ (1969) Lignicolous fungi on *Ulmus americana* L. Korean Journal of Microbiology 7: 91–106.

Shirouzu T, Harada Y (2004) Bambusicolous fungi in Japan (2): *Phialosporostilbe gregariclava*, a new anamorphic fungus from *Sasa*. Mycoscience 45: 390–394. https://doi.org/10.1007/S10267-004-0200-1

Sivanesan A, Chang HS (1995) *Pseudofuscophialis lignicola* gen. et sp. nov. and *Chaetosphaeria capitata* sp. nov. from wood in Taiwan. Mycological Research 99: 711–716. https://doi.org/10.1016/S0953-7562(09)80534-0

Somrithipol S, Sakayaroj J, Rungjindamai N, Plaingam N, Jones EBG (2008) Phylogenetic relationship of the coelomycete genus *Infundibulomyces* based on nuclear rDNA data. Mycologia 100: 735–741. https://doi.org/10.3852/07-040

Spegazzini C (1898) Fungi Argentini novi vel critici. Anales del Museo Nacional de Historia Natural Buenos Aires 6: 81–365.

Stamatakis A (2014) RAxML Version 8: A tool for Phylogenetic Analysis and Post-Analysis of Large Phylogenies. Bioinformatics 30: 1312–1313. https://doi.org/10.1093/bioinformatics/btu033

Sukosd Z, Knudsen B, Kjems J, Pedersen CN (2012) PPfold 3.0: Fast RNA secondary structure prediction using phylogeny and auxiliary data. Bioinformatics 28: 2691–2692. https://doi.org/10.1093/bioinformatics/bts488

Subramanian CV (1992) A reassessment of *Sporidesmium* (Hyphomycetes) and some related taxa. Proceedings of the Indian Academy of Sciences (Plant Sciences) 58: 179–190.

Subramanian CV, Bhat DJ (1977) *Bahusutrabeeja*, a new genus of the hyphomycetes. Canadian Journal of Botany 55: 2202–2206. https://doi.org/10.1139/b77-249

Subramanian CV, Bhat DJ (1989) [1987] Hyphomycetes from South India I. Some new taxa. Kavaka 15: 41–74.

Sureshkumar G, Sharath Babu K, Kunwar IK, Manoharachary C (2005) Two new hyphomycetous fungal species from India. Mycotaxon 92: 279–283.

Sydow H, Sydow P (1914) Enumeration of Philippine fungi with notes and descriptions of new species. II. Philippine Journal of Science Section C Botany 8: 475–508.

Szilvinyi A von (1941) Mikrobiologische Boden untersuchungen im Lunzer Gebiet. Zentralblatt für Bakteriologie und Parasitenkunde, Abteilung 2. 103: 133–189.

Taylor TN, Krings M, Taylor E (2015) Fossil fungi. Academic Press, London, 398 pp.

Tulasne ELR, Tulasne C (1863) Selecta Fungorum Carpologia, Tomus Secundus. Xylariei – Valsei – Sphaeriei. Paris, Imperial, Typograph, I–XIX, 319 pp.

Vu D, Groenewald M, de Vries M, Gehrmann T, Stielow B, Eberhardt U, Al-Hatmi A, Groenewald JZ, Cardinali G, Houbraken J, Boekhout T, Crous PW, Robert V, Verkley GJM (2019) Large-scale generation and analysis of filamentous fungal DNA barcodes boosts coverage for kingdom fungi and reveals thresholds for fungal species and higher taxon delimitation. Studies in Mycology 92: 135–154. https://doi.org/10.1016/j.simyco.2018.05.001

Whitton SR, McKenzie EHC, Hyde KD (2012) Fungi Associated with Pandanaceae. Springer: Dordrecht, 125–353. https://doi.org/10.1007/978-94-007-4447-9

Wu WP, McKenzie EHC (2003) *Obeliospora minima* sp. nov. and four other hyphomycetes with conidia bearing appendages. Fungal Diversity 12: 223–234.

Wu YM, Zhang TY (2009) New species of *Phialosporostilbe* and *Pleurothecium*. Mycotaxon 110: 1–4. https://doi.org/10.5248/110.1

Xia JW, Ma LG, Ma YR, Castañeda-Ruíz RF, Zhang XG (2013) *Corynesporopsis curvularioides* sp. nov. and new records of microfungi from southern China. Cryptogamie Mycologie 34: 281–288. https://doi.org/10.7872/crym.v34.iss3.2013.281

Yang J, Liu NG, Liu JK, Hyde KD, Jones EBG, Liu ZY (2018) Phylogenetic placement of *Cryptophiale*, *Cryptophialoidea*, *Nawawia*, *Neonawawia* gen. nov. and *Phialosporostilbe*. Mycosphere 9: 1132–1150. https://doi.org/10.5943/mycosphere/9/6/5

Zuker M (2003) Mfold web server for nucleic acid folding and hybridization prediction. Nucleic Acids Research 31: 3406–3415. https://doi.org/10.1093/nar/gkg595

Supplementary material 1

Table S1. Taxa, isolate information and accession numbers for sequences retrieved from GenBank

Authors: Martina Réblová1, Jana Nekvindová2, Andrew N. Miller

Data type: molecular data

Explanation note: New sequences determined for this study and taxonomic novelties are given bold

Link: https://doi.org/10.3897/mycokeys.81.67785.suppl1

MycoKeys 81: 45–68 (2021)
doi: 10.3897/mycokeys.81.66249
https://mycokeys.pensoft.net

RESEARCH ARTICLE

A peer-reviewed open-access journal
MycoKeys
Launched to accelerate biodiversity research

Soil fungal communities of ectomycorrhizal dominated woodlands across West Africa

Peter Meidl[1*], Brendan Furneaux[2*], Kassim I. Tchan[3*], Kerri Kluting[1*], Martin Ryberg[2], Marie-Laure Guissou[4], Bakary Soro[5], Aïssata Traoré[6], Gbamon Konomou[7], Nourou S. Yorou[3], Anna Rosling[1]

1 *Department of Ecology and Genetics, Evolutionary Biology, Uppsala University, Norbyvägen 18D, Uppsala 752 36, Sweden* **2** *Department of Organismal Biology, Systematic Biology, Uppsala University, Norbyvägen 18D, Uppsala 752 36, Sweden* **3** *Research Unit in Tropical Mycology and Plant-Soil Fungi Interactions, LEB, University of Parakou, Parakou, Benin* **4** *Université Norbert Zongo, Unité de Formation et de Recherches en Sciences et technologies. BP 376 Koudougou, Burkina Faso* **5** *Université Nangui Abrogoua, URF Sciences de la Nature, Laboratoire d'écologie et de Développement Durable, Abidjan, Ivory Coast* **6** *Institut d'Economie Rurale (IER), Rue Mohammed V, Bozola, BP 258, Bamako, Mali* **7** *Herbier National de Guinée / Université Gamal Abdel Nasser de Conakry BP: 1147, Conakry, Guinée*

Corresponding author: Anna Rosling (Anna.Rosling@ebc.uu.se)

Academic editor: R.H. Nilsson | Received 21 March 2021 | Accepted 24 May 2021 | Published 11 June 2021

Citation: Meidl P, Furneaux B, Tchan KI, Kluting K, Ryberg M, Guissou M-L, Soro B, Traoré A, Konomou G, Yorou NS, Rosling A (2021) Soil fungal communities of ectomycorrhizal dominated woodlands across West Africa. MycoKeys 81: 45–68. https://doi.org/10.3897/mycokeys.81.66249

Abstract

Forests and woodlands in the West African Guineo-Sudanian transition zone contain many tree species that form symbiotic interactions with ectomycorrhizal (ECM) fungi. These fungi facilitate plant growth by increasing nutrient and water uptake and include many fruiting body-forming fungi, including some edible mushrooms. Despite their importance for ecosystem functioning and anthropogenic use, diversity and distribution of ECM fungi is severely under-documented in West Africa. We conducted a broad regional sampling across five West African countries using soil eDNA to characterize the ECM as well as the total soil fungal community in gallery forests and savanna woodlands dominated by ECM host tree species. We subsequently sequenced the entire ITS region and much of the LSU region to infer a phylogeny for all detected soil fungal species. Utilizing a long read sequencing approach allows for higher taxonomic resolution by using the full ITS region, while the highly conserved LSU gene allows for a more accurate higher-level assignment of species hypotheses, including species without ITS-based taxonomy assignments. We detect no overall difference in species richness between gallery forests and woodlands.

* Peter Meidl and Brendan Furneaux contributed equally as first authors. Kassim Tchan and Kerri Kluting contributed equally as second authors.

However, additional gallery forest plots and more samples per plot would have been needed to firmly conclude this pattern. Based on both abundance and richness, species from the families Russulaceae and Inocybaceae dominate the ECM fungal soil communities across both vegetation types. The community structure of both total soil fungi and ECM fungi was significantly influenced by vegetation types and showed strong correlation within plots. However, we found no significant difference in fungal community structure between samples collected adjacent to different host tree species within each plot. We conclude that within plots, the fungal community is structured more by the overall ECM host plant community than by the species of the individual host tree that each sample was collected from.

Keywords
biodiversity, eDNA, fungal community, gallery forest, Guineo-Sudanian woodlands

Introduction

Throughout West Africa, forests, woodlands and savannas represent ecosystems of great biodiversity and economic importance as resources for food, fuel and fiber (Sinsin and Kampmann 2010). In many parts of the region, forest land is under pressure from grazing, conversion to cropland, fuelwood extraction and replacement by plantations of non-native trees, often resulting in fragmentation of the landscape (Assédé et al. 2020). These threatened ecosystems harbor a tremendous undescribed diversity of fungi, a group of organisms that is particularly understudied in tropical regions, and particularly so in West Africa (Gryzenhout et al. 2012; Piepenbring et al. 2020). Ectomycorrhizal (ECM) symbiosis is a mutualistic relationship in which fungal hyphae surround and grow between the cortical cells of specialized fine plant roots. The relationship benefits both organisms, with the fungal partner providing nutrients in exchange for carbon from the plant partner. Although only certain groups of fungi and plants can form ECM, this capacity has evolved convergently in around 80 fungal lineages (Tedersoo and Smith 2017) and 30 plant lineages (Tedersoo and Brundrett 2017), the latter of which are often dominant trees in forests and woodlands. ECM fungi play an important role for plant health and forest regeneration by facilitating nutrient and water uptake to their host plants. Globally, ECM fungi represent about 8% of described fungal species (Ainsworth 2008; Rinaldi et al. 2008; Hawksworth and Lücking 2017). Despite their importance both in nature and the anthropogenic world, fungal diversity remains poorly characterized, particularly in tropical regions (Tedersoo et al. 2014). Increased knowledge about existing fungal biodiversity of wooded ecosystems is an important step towards building sustainable land use management that balances production and conservation.

Wooded vegetation covers much of West Africa south of the Sahelian savanna and is geographically structured largely based on water availability (Swaine 1992). In the West Sudanian savanna and Guinean forest-savanna mosaic ecoregions, which together form the Guineo-Sudanian transition zone (Fig. 1), woodland growth is water limited due to seasonal drought, and canopy coverage is typically between 15–40% (Swaine 1992; Paré et al. 2008). Drought and fire are important factors determining plant

community structure in these woodlands (Savadogo 2007). Characteristic Guineo-Sudanian woodland trees (Adomou 2005; Assédé et al. 2020) include species in the genera *Isoberlinia*, *Afzelia* and *Anthonotha* (Fabaceae), *Uapaca* (Phyllanthaceae) and *Monotes* (Dipterocarpaceae), all of which form symbiotic associations with ECM fungi (Yorou et al. 2014; Tedersoo and Brundrett 2017; Houdanon et al. 2019). Gallery forests are another characteristic vegetation type in the region. Gallery forests form narrow corridors in riparian areas (i.e., along rivers), typically in areas which are too dry for closed-canopy forest to grow outside of the riparian area (Natta et al. 2003). Thus, the gallery forest edge is distinct in relation to surrounding habitat types (Paré et al. 2008). While only a small proportion of African tree species form ECM associations, the total number of tree species is much higher than in boreal and temperate regions (Bâ et al. 2012). Despite this, Africa has the highest number of tree species forming associations with ECM fungi of all tropical regions, and these ecosystems are often characterized by the dominance or co-dominance of ECM trees such that these trees represent a critical ecological component (Corrales et al. 2018). The occurrence of stands of predominantly ECM forming tree species (Houdanon et al. 2019) has led to the hypothesis that ECM fungi facilitate establishment of other ECM seedlings (Corrales et al. 2018). Further, low levels of host specificity have been demonstrated for ECM fungi in Africa, potentially allowing for the formation of common ECM networks linking different host species below ground (Diédhiou et al. 2010; Tedersoo et al. 2011).

Fungal diversity in West Africa is understudied and only recently was a fungal check list for West Africa completed to facilitate monitoring and communication of fungal diversity (Piepenbring et al. 2020). The checklist is an important first step to assess the role and prevalence of fungal diversity in West Africa (Yorou and De Kesel 2011). The checklist contains only already described fruiting body-forming fungi, which represent only a fraction of the estimated fungal diversity (Hawksworth and Lücking 2017). In fact, global estimates based on environmental sequencing indicate that the majority of extant soil fungi remain undescribed (Tedersoo et al. 2017).

The recent proliferation of environmental DNA-based studies has overcome many limitations of fruiting body-based surveys, advancing knowledge of large-scale patterns of fungal diversity (Sato et al. 2012; Tedersoo et al. 2014; Barberán et al. 2015; Davison et al. 2015). Molecular identification of fungi from soil and roots has greatly improved our ability to characterize ECM fungal communities independently from fruiting bodies, whose formation varies with various temporal and spatial factors. Such studies suggest that, contrary to biodiversity patterns of animals and plants, ECM fungi decrease in species richness towards the equator, with lower diversity in tropical compared to temperate forests (Tedersoo and Nara 2010). In West Africa, ECM fungal communities are dominated by species in the four families Russulaceae, Thelephoraceae, Boletaceae and Sclerodermataceae (Bâ et al. 2012; Tedersoo and Smith 2013, 2017). Species in the Amanitaceae are also widespread throughout the tropics (Corrales et al. 2018). Surveys based on fruiting bodies confirm this pattern, reporting numerous members of these families (Ducousso et al. 2003; Yorou 2008; Bâ et al. 2011; Sanon et al. 2014; Yorou et al. 2016; Piepenbring et al. 2020).

Although woodlands and gallery forests in the Guineo-Sudanian transition zone are known to host many ECM fungi, little is known about how ECM tree composition and density affect the abundance and composition of ECM and other fungi in soil. The majority of existing studies describing fungal biodiversity in West Africa rely on observation and collection of fruiting bodies. Because these structures are highly ephemeral, and many species don't produce them at all, sequencing DNA from soil samples is a more reliable means of providing a more complete perspective of a given soil fungal community. As ECM-dominated vegetation in West Africa varies widely in tree species composition and structure (Houdanon et al. 2019), we suspect similar differences in the below-ground fungal community. To capture the regional diversity of ECM fungi, we collected soil samples in vegetation dominated by ECM host trees across the five West African countries Benin, Burkina Faso, Mali, Guinea and the Ivory Coast. We leveraged the capability of the PacBio Sequel system to provide high quality reads of over 1 kb in length to sequence the full internal transcribed spacer (ITS) and partial large subunit (LSU) of the nuclear ribosomal DNA. This allowed a model-based approach to generating species hypotheses, based on a phylogenetic tree generated from the more conserved LSU region, as well as a combined approach to taxonomic identification involving both similarity-based assignment on the ITS region and reference to the LSU-based phylogenetic tree. We analysed how ECM host tree species community structure, total soil fungal communities and ECM fungal communities varied in two different vegetation types. Our data provide an important baseline resource for future biodiversity studies of soil fungal communities in West Africa.

Methods

Field site characteristics and soil sampling

Field collections were carried out during June and July of 2018 in five West African countries: Benin, Burkina Faso, Mali, Guinea and Ivory Coast. Sites were selected opportunistically from natural areas where ECM host trees were present, with relatively uniform vegetation and slope. A total of seven locations with nine sites were sampled: Kota Waterfall (KOTA-G and KOTA-W) in Benin, Kou Forest Reserve (KOUF-G) and Niangoloko Forest Reserve (NIAN-W) in Burkina Faso, Farako Forest Reserve (FA01-W and FA15-W) in Mali, Bissandougou Forest Reserve (BISS-W) and Moussaya Forest Reserve (MOUS-W) in Guinea and Kouadianikro Forest Reserve (KDNK-W) in Ivory Coast (Fig. 1, Table 1, Suppl. material 1: datafile 1). Sites were classified in the field as gallery forest (-G sites) or woodland (-W sites) based on proximity to a flowing river. At each woodland site, a 50 by 50 m plot was established, but at the gallery forests sites, 30 by 80 m plots were established instead because uniform vegetation did not extend for 50 m perpendicular to the flow of the river. In order to characterize the tree community of each plot, we measured tree girth at a height above the ground

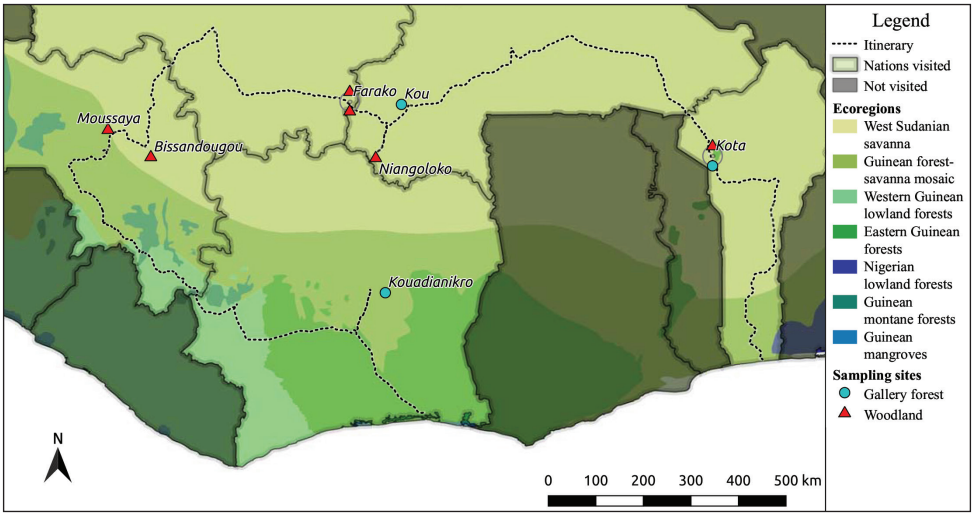

Figure 1. Sampling sites of the West African Centre for Tropical Mycology's 2018 National Geographic Explorer Grant expedition. Shapes and colors separate the different woodland types with blue circles for gallery forests and red triangles for woodlands. With site names (abbreviations): Bissandougou (BISS-W), Moussaya (MOUS-W), Kota (KOTA-G and KOTA-W), Kouadianikro (KDNK-W), Kou (KOUF-G), Niangoloko (NIAN-W) and Farako (FA01-W and FA15-W). The dotted line represents the route taken on the sampling trip, beginning on the coast of Benin and concluding in Ivory Coast. Ecoregions are from White (1983), digitized in Olson et al. (2001).

of approximately 1.4 m for all trees with a girth larger than 15 cm, and used these measurements to calculate basal areas (basal area = girth$^2/4\pi$). Trees were categorized as ECM or non-ECM (Brundrett 2017) based on species identification by members of the team. The species identity and girth of all ECM trees was recorded in order to provide an accurate representation of the ECM tree community within each site. Non-ECM trees were not identified to species, but were treated as a pool. The initial grouping into gallery forest and woodland sites based on the presence of a stream was later reassessed based on ordination of the tree communities, as described under statistics below.

In each plot, soil sample locations were selected according to the protocol used in Tedersoo et al. (2014). Ten ECM trees were chosen in proportion to the relative abundance of ECM tree species in the plot, while ensuring that each species in the plot was represented at least once, and that all sampled trees were at least eight meters apart. At each selected tree, two soil samples were collected roughly one meter on either side of the stem using a small sterilized spade to collect the top 5 cm of soil. The two soil samples were pooled in a plastic bag and homogenized by hand for roughly ten seconds. A sub-sample of around 250 mg of soil was placed in a separate 2.0 ml tube containing 750 ml of field lysis and preservation buffer (Xpedition Soil/Fecal DNA miniprep, Zymo Research Corporation, Irvine, California, USA) and lysed in the field using a portable bead beater (TeraLyser, Zymo Research Corporation).

Table 1. Site characteristics.

Vegetation type and site	Country	Lat./Lon.	Elev (m)	MAT (°C)	MAP (mm)	All trees		Av. Girth		% ECM		ECM trees		Dom. ECM tree spp. (Rel abund)
						BA (m^2/ha)	n	ECM (cm)	non (cm)	BA	Nr.	n	Sp	
Gallery forest			**375**	**26.7**	**1070**	**28.2**	**110**	**99**	**49**	**83%**	**59%**	**56**	**2**	
Kota-G	Benin	10°12.76"N, 1°26.77"E	500	26.5	1190	35.9	107	110	56	80%	56%	60	3	*B. grandiflora* (51%), *U. guineensis* (48%)
Kou	Burkina Faso	11°11.25"N, 4°26.48"W	375	27.4	980	26.4	113	86	48	77%	46%	54	1	*B. grandiflora* (100%)
Kouadianikro	Ivory Coast	7°37.77"N, 4°44.81"W	250	26.3	1030	22.3	72	102	42	94%	76%	53	1	*B. grandiflora* (100%)
Woodland			**440**	**26.4**	**1240**	**12.7**	**160**	**58**	**32**	**56%**	**40%**	**65**	**3**	
Bissandougou	Guinea	10°11.33"N, 9°11.60"W	425	25.9	1520	8.3	205	29	34	59%	62%	125	4	*U. togoensis* (54%), *I. doka* (43%)
Moussaya	Guinea	10°42.24"N, 9°59.71"W	430	25.8	1460	14.3	297	39	26	51%	37%	115	3	*U. togoensis* (71%)
Farako 01	Mali	11°14.12"N, 5°25.25"W	460	26.7	1080	9.1	58	91	37	46%	35%	15	2	*I. tomentosa* (70%)
Farako 15	Mali	11°14.38"N, 5°25.15"W	460	26.7	1080	8.4	121	63	17	66%	42%	20	3	*I. doka* (52%), *I. tomentosa* (40%)
Kota-W	Benin	10°12.54"N, 1°26.73"E	515	26.5	1190	18.1	200	60	45	44%	27%	54	3	*I. tomentosa* (86%)
Niangoloko	Burkina Faso	10°10.33"N, 4°55.74"W	345	27.0	1140	18.0	168	67	32	69%	38%	60	3	*I. doka* (89%)

Abbreviations: Lat./Lon.: Latitude and longitude; Elev: Elevation; MAT: Mean annual temperature; MAP: Mean annual precipitation; Tot. BA: Total basal area for all trees with girth larger than 15 cm; % ECM: Percentage of trees (girth > 15 cm) belonging to ectomycorrhizal (ECM) host species, by total basal area (BA) and total number (Nr); Av. Girth: Average girth of trees, separated into ECM host species (ECM) and other species (non); ECM trees: number of ECM host trees present (n), and number of species represented (Sp); Dom. ECM tree spp.: (co-)dominant ECM host species, as fraction of all ECM host trees. Numbers in bold are means for each vegetation type across sites.

DNA extraction, amplification and sequencing the soil fungal communities

Field lysed samples were returned to Uppsala University (Sweden) for DNA extraction using the Xpedition Soil/Fecal Prep kit following the manufacturer's protocol. DNA concentration and integrity were verified by 0.8% agarose gel electrophoresis in 0.5% Tris Acetate-EDTA buffer (Sigma-Aldrich, St. Louis, Missouri, USA) stained with 1× GelRed (Biotium Inc., Hayward, California, USA). Approximately 1500 bases of the rDNA ITS and LSU regions were amplified from all soil DNA extracts using the primer set ITS1 (White et al. 1990) and LR5 (Hopple Jr and Vilgalys 1994) with Phusion High-Fidelity DNA polymerase (Thermo Fisher Scientific, Waltham, Massachusetts, USA). We ran a thermo-cycling protocol as follows: an initial denaturation at 95 °C for 10 min followed by 30 cycles of denaturation at 95 °C for 45 s, annealing at 58 °C for 45 s and elongation at 72 °C for 90 s, with a final elongation at 72 °C for 10 min. Both primers were indexed for multiplexing (Suppl. material 2: datafile 2). Each PCR run included a blank sample and a positive control with DNA extracted from a commercially purchased fruit body of *Agaricus bisporus*. PCR products from a total of 90 samples as well as controls were purified using Sera-Mag SpeedBeads (GE Healthcare, Life Science, Chicago, IL, USA) and quantified using Nanodrop 2000C (ThermoScientific, Waltham, USA) before pooling the samples at equimolar proportions together with samples from another unpublished study for sequencing at Uppsala Genome Center (Sweden) using two cells on a Sequel system (Pacific Biosciences,

Menlo Park, CA, USA). Sequences were delivered to us as circular consensus sequence FASTQ files. Raw reads are available in the European Nucleotide Archive (samples ERS5551933–ERS5552022).

Bioinformatic sequence analyses

Rather than applying the typical OTU clustering approach using a preselected sequence dissimilarity threshold to control both sequencing error and intraspecies variation, we used model-based approaches to address sequencing errors and intraspecies variation separately. We first generated denoised amplicon sequence variants (ASVs) in DADA2 (Callahan et al. 2016), where variation due to sequencing error is removed or reduced. We then grouped ASVs into phylogeny-based species hypotheses (SHs) using a Poisson tree process model (PTP; Zhang et al. 2013), based on a phylogenetic tree built from the reads.

Denoised ASVs were generated from the dataset using the procedure established in Kalsoom-Khan et al. (2020) after assessing general read quality and ensuring that the majority of reads fell within the expected length (1–2 kb). Raw sequence reads were filtered and trimmed using the tool cutadapt (version 1.18; Martin 2011) to demultiplex reads based on the forward and reverse barcodes, to keep only reads with both primers present, and to remove the actual primer sequences from the reads. Amplicons sequenced in reverse were reverse complemented before continuing the analyses. PacBio-type chimeras were detected and removed using cutadapt (version 2.3; Martin 2011). Reads were filtered using DADA2 (version 1.9.3; Callahan et al. 2016), discarding sequences with more than 3 expected errors as well as those with a length outside the range of 1200–1800 bases. Filtered sequences were then denoised using DADA2, with complete pooling to increase the detection of low-abundance ASVs, and an increased alignment band size of 32 (default 16) due to the tendency of PacBio sequences to include indels. Singleton ASVs are not included in DADA2 denoising output. *De novo* chimera detection and removal were also performed in DADA2, with a minimum parent overabundance of 3.5 (default 1.5) and allowing detection of chimeras with a single base difference from their parent sequence. After denoising and chimera removal, 1147 ASVs representing 3.6% of initial reads remained in the dataset (Suppl. material 5: Table S1). An ASV occurrence table was generated with read count for each ASV across samples.

The tool ITSx (version 1.1-beta; Bengtsson-Palme et al. 2013) was used to identify the different regions (ITS1, ITS2 and the LSU gene) of the ribosomal rDNA within each ASV. Taxonomy was assigned to the ITS1 and ITS2 regions separately using SINTAX (Edgar 2016) in VSEARCH (version 2.10.4; Rognes et al. 2016) and the UNITE sequence database (release date 2019-02-02; Kõljalg et al. 2013).

In order to create a phylogenetic tree to assist in grouping ASVs into species hypotheses and identification of sequences without good ITS database matches, we utilized the highly conserved LSU region of each sequence. All LSU regions were aligned using MAFFT (version 7.402; Katoh and Standley 2013). Three accuracy-based algorithms (L, G and E) were tested within MAFFT. The alignment generated with the

G algorithm was selected after visual inspection of all three alignments, because it was determined to most consistently align homologous regions. Alignments were visualized in Aliview (version 1.25; Larsson 2014), manually trimmed and checked prior to tree generation. To aid in taxonomy assignment and delineation of species hypotheses, a maximum likelihood tree was inferred using RAxML in the CIPRES portal (Miller et al. 2010). The maximum likelihood tree contained multiple issues including non-fungal lineages and possible chimeras. Class-level taxonomic assignments with a SINTAX confidence value of 0.8 or higher were added to the ASV name in the tree file using a customized script (Kalsoom Khan et al. 2020) in order to aid pruning of non-fungal lineages from the initial phylogenetic tree. A series of alignments and trees were generated by stepwise removal of ASVs that were determined to be non-fungal based on SINTAX taxonomy assignment and their placement in the tree. The non-fungal ASV_1147 was maintained in the alignment to serve as an outgroup. This procedure identified a total of 1,014 fungal ASVs in the dataset and the lowest-rank taxonomy assignment available (confidence value of 0.8 or higher) was amended to each ASV name (Suppl. material 3: datafile 3). Additionally, the SH Matching tool (development version) from the PlutoF platform (Kõljalg et al. 2019) was used to assign ASVs to UNITE species hypotheses (SH) when possible. ASVs were assigned to the narrowest UNITE SH whose inclusivity threshold they satisfied. ASV sequences are deposited in the European Nucleotide Archive (accession numbers LR993318-LR994464).

We used the Poisson-tree process (PTP) method to generate phylogenetic SHs based on branch length distribution in a ML tree based on the LSU region, including all fungal ASVs (Zhang et al. 2013) (Suppl. material 4: datafile 4). The ML tree, described above, was uploaded to the bPTP online server (https://species.h-its.org/ptp/) and run for 500,000 generations, with a range of burn-in rates being tested, before settling on 0.15 as the final burn-in rate. Convergence of MCMC chains was examined manually using Tracer (version 1.7.1; Rambaut et al. 2018). The resulting SHs were manually checked on a per-SH basis by aligning the ITS2 regions of the included ASVs to ensure they represent relevant units of similarity across ITS2 (>98%) and to detect possible chimeras across ASVs. An SH occurrence table across samples was calculated based on combined read counts for all remaining ASVs that mapped into an SH.

Functional guilds were assigned to SHs based on their taxonomic annotation using the FUNGuild database (Nguyen et al. 2016) via FUNGuildR (version 0.1.0; http://github.com/brendanf/FUNGuildR), where genus-level taxonomy generally allows for reasonably robust assignment of functional guild. For statistical analysis of the ECM community, all SHs that were assigned to the ectomycorrhizal guild with a confidence level of Probable or Highly Probable were included.

Statistical analyses

The robustness of vegetation type site classification was tested using a non-metric multidimensional scaling (NMDS) ordination based on Bray-Curtis distances calculated on total basal area in m^2/ha for each ECM species and the total basal area for all non-ECM trees at each site. NMDS was calculated using the metaMDS function from

vegan (version 2.5.6; Oksanen et al. 2013), using stepacross distances for sites with no shared species and without the automatic community normalization procedures, which are intended for count-based analyses.

Mean annual temperature and precipitation for each site were extracted from 1970–2000 historical averages in 2.5-minute maps from WorldClim 2.1 (Fick and Hijmans 2017) using the RGDAL package (version 1.5-16; Bivand et al. 2020). Differences in climate variables, tree number and tree girth between vegetation types were tested using the non-parametric Wilcoxon-Mann-Whitney test, employing plot as a blocking variable for tests using individual trees as sampling units.

Species accumulation curves and asymptotic diversity estimates were calculated using the iNEXT package (version 2.0.20; Hsieh et al. 2016). Curves were calculated at three different spatial scales: for each soil sample based on the number of sequencing reads; for each sampling plot based on the number of sequencing reads and the number of soil samples; and for each vegetation type based on the number of sequencing reads, the number of soil samples and the number of sampling plots.

The SH occurrence table was normalized to relative read abundance within each sample. Variation in the total fungal communities and ECM fungal communities were visualized using unconstrained NMDS based on Bray-Curtis dissimilarities between relative read abundances of SHs. NMDS was calculated using metaMDS as above, with stepacross distances for the ECM communities, where high beta diversity led to some samples having no shared species. The number of dimensions in each NMDS was increased until the stress was below 0.2. Correlations between vegetation type, host species and plot identity and the community composition of the total fungal as well as the ECM fungal community composition were tested for significance in a series of three permutation tests (Anderson 2001; McArdle and Anderson 2001) using the dbrda and anova.cca functions in vegan (Oksanen et al. 2013) based again on Bray-Curtis dissimilarities between relative read abundances of SHs. The combination of dbrda and anova.cca gives identical results to the more commonly used adonis and adonis2 functions when used for the same models but also allow the test to be applied to the residuals of known effects and the use of stepacross distances. First, the existence of plot-level effects between the nine sampling plots was assessed by an unconstrained permutation test on a dbRDA with plot as the only explanatory variable. Then, differences between the two vegetation types were confirmed by permuting plots but keeping the samples within each plot together, with vegetation type as the only explanatory variable. Finally, differences between the fungal communities associated with different host trees were tested by using a dbRDA model with the host tree species as the explanatory variable, fit to the residuals of the model based on site, and tested by permuting samples within plots. All permutation tests used 9999 permutations.

All statistical analysis and resultant figure generation was conducted in R (version 3.6.3; R Core Team 2020). Plots were generated using ggplot2 version 3.3.1 (Wickham 2016). Arrangement of multiple subplots as well as calculation of confidence ellipses were done with ggpubr version 0.3.0 (Kassambara 2020). Labels inside plots were placed using ggrepel version 0.8.2 (Slowikowski 2020). Color palettes are from ColorBrewer v2.0 (Harrower and Brewer 2003) via the RColorBrewer package (Neuwirth 2014) and I Want Hue (Jacomy 2013) via the hues package (Baumgartner and Dinnage 2019).

Results

Ectomycorrhizal hosts of two vegetation types in the Guineo-Sudanian transition zone

In order to verify our initial visual classifications of sites into gallery forests and woodlands, sites were condensed using the basal area of ECM tree species separately and all non-ECM trees combined. This classified the nine sites into two distinct vegetation types, gallery forest and woodlands, for further analysis in this study (Figs 1, 2). Three sites were classified as gallery forests in accordance with the initial classification of both Kota (KOTA-G) and Kou (KOUF-G), while Kouadianikro (KDNK-W) was initially classified as a woodland. Despite the location of Kouadianikro, several hundred meters from the nearest river on a sloping hillside, the closed canopy and high dominance of large *Berlinia grandiflora* trees at the site (100% of ECM trees, and 94% of all tree basal area) rendered it the most similar to the gallery forest sites, in particular KOUF-G. *B. grandiflora* was the most common ECM host tree at all three gallery forest sites (Table 1).

While all ECM host trees were *B. grandiflora* at Kou and Kouadianikro, three host species were present at Kota-G, with *Uapaca guineensis* being co-dominant with *B. grandiflora.* Across the gallery forest sites, the total basal area was on average 28.2 m^2/ha, with ECM hosts making up 46–76% of total basal area (Table 1). The other six sites were classified as woodland, featuring a greater variation of host trees between sites and characterized by an open canopy and an average total basal area of 12.7 m^2/ha. All woodland sites had more than one ECM host tree species, with dominant hosts including *Isoberlinia tomentosa*, *Isoberlinia doka* and *Uapaca togoensis* (Table 1). Less abundant ECM host tree species encountered at these sites include *Monotes kerstingii*, *Anthonotha crassifolia* and *Afzelia africana*.

There were no statistically significant differences between the two vegetation types in elevation (Z = -0.77, p = 0.44), mean annual temperature (Z = 0.39, p = 0.70) or mean annual precipitation (Z = -1.4, p = 0.15). The average girth of ECM host trees was generally larger than that of non-ECM trees in both gallery forests (Z = 6.17, p = 8.2e-7) and woodlands (Z = 10.025, p < 2.2e-16). Trees in gallery forests tended to have greater girth than those in woodlands for both ECM host trees (Z = 4.93, p = 8.7e-12) and non-ECM trees (Z = 2.68, p = 0.0073). The total basal area of all trees (Z = 2.32, p = 0.020) and the fraction of the total basal area represented by ECM trees (Z = 2.32, p = 0.020) were both greater in gallery forest plots than woodland plots. There was no significant difference in the total number of trees (Z = -1.55, p = 0.12), or the number of ECM trees (Z = -0.39, p-value = 0.70) between vegetation types (Table 1).

Soil fungal communities in gallery forests and woodlands

Across the nine plots, a total of 520 soil fungal taxa were detected as SHs based on branch length distribution in a ML tree generated from an alignment of the LSU region of 1,014 fungal ASVs (Suppl. material 3: datafile 3). Almost 70% of these

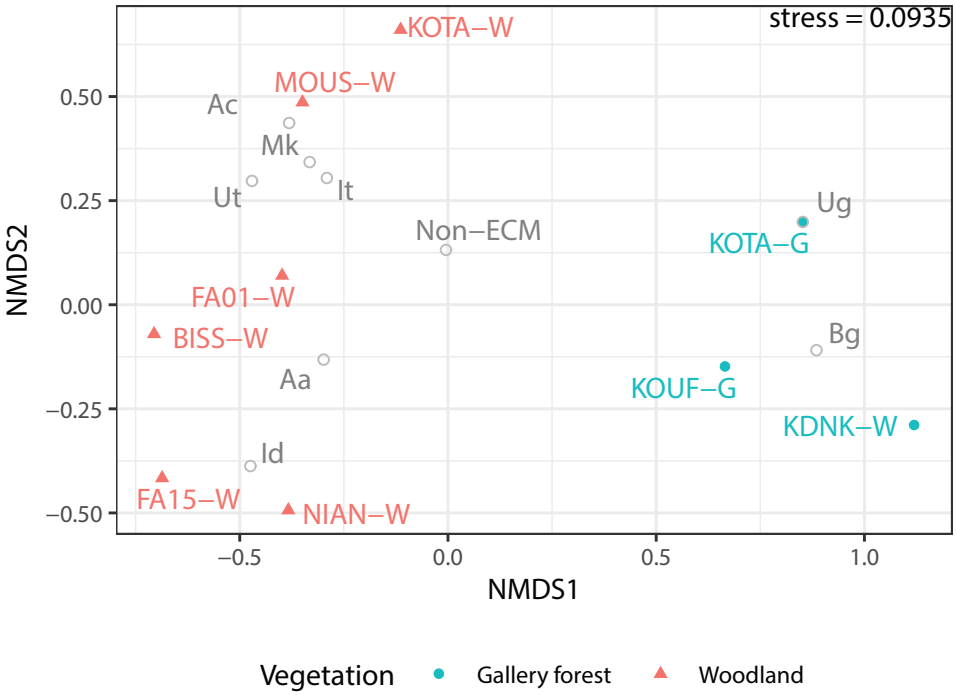

Figure 2. NMDS ordination of tree communities based on Bray-Curtis dissimilarities between sites, based on total basal areas of each ECM trees species separately and all non-ECM trees combined. The nine sites were classified into two distinct woodland types, woodlands in red and gallery forests in blue. Site abbreviations: Bissandougou Forest Reserve (BISS-W), Moussaya Forest Reserve (MOUS-W), Kota Waterfall (KOTA-G and KOTA-W), Kouadianikro Forest Reserve (KDNK-W), Kou Forest Reserve (KOUF-G), Niangoloko Forest Reserve (NIAN-W) and Farako Forest Reserve (FA01-W and FA15-W). ECM tree species abbreviations: Afzelia africana (Aa), Ac: Anthonotha crassifolia (Ac), Bg: Berlinia grandiflora (Bg), Id: Isoberlinia doka (Id), I. tomentosa (It), Monotes kerstingii (Mk), Uapaca guineensis (Ug) and Uapaca togoensis (Ut).

were represented by only one ASV, together accounting for 17.5% of all reads. Species accumulation curves for the nine plots demonstrate that sampling was close to saturation with regard to sequencing depth (Fig. 3A). While more species would have been detected in each sample had we sequenced more (Suppl. material 5: Fig. S1), this is not predicted to translate into higher richness detected per site. On the other hand, species accumulation curves based on the number of samples were nowhere near saturated (Fig. 3B). These results indicate that we would have recovered more taxa per site if we had sampled 30 instead of 10 trees at each site. Estimated species richness from read-based species accumulation curves ranged from close to 200 to 250 soil fungal taxa per site (Fig. 3A) and does not appear to differ between the two vegetation types. Species richness estimated per vegetation type suggest an overall higher species richness in gallery forests compared to woodlands, however, confidence intervals for the estimates overlap (Suppl. material 5: Fig. S2).

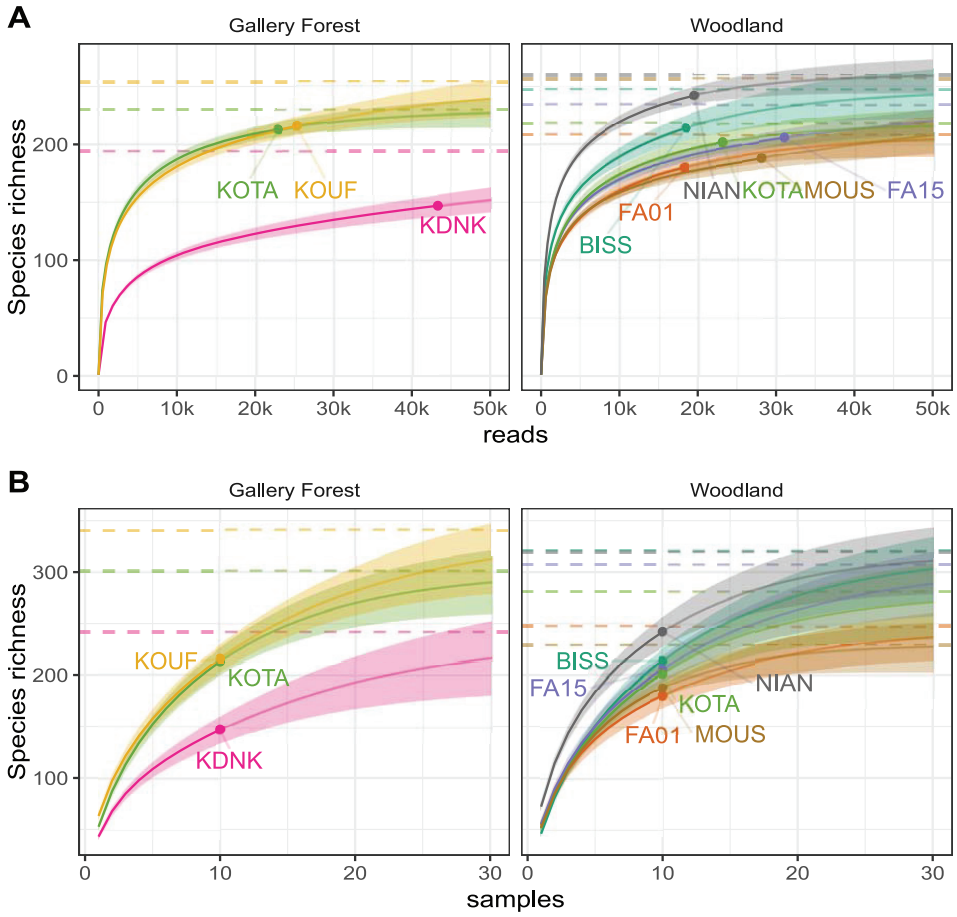

Figure 3. Species accumulation curves for each plot. Curves are based on SHs, by sequencing depth (**A**) and number of trees sampled (**B**), presented separately for three gallery forest sites (left panels) and six woodland sites (right panels). Points represent the observed species richness at the actual sequencing depth and trees sampled in **A, B** respectively. Thin lines represent the accumulation curve calculated by rarefaction (darker) and extrapolation (lighter); shaded regions represent the associated 95% confidence intervals. Dotted lines represent the asymptotic estimate for each site.

Ordination analysis based on relative abundance of soil fungal SHs show that community structure is affected by vegetation type (Fig. 4) and host species (Suppl. materials 5: Fig. S3, Table S2). Permutation tests confirmed the effect of vegetation type (P=0.012 for both ECM and total fungal communities). However, within plots, the effect of host species is not significant (P=0.44 and P=0.040 for ECM and total soil fungi respectively). At plot level, ECM host community composition is likely more important for shaping local fungal communities relative to the closest host tree sampled.

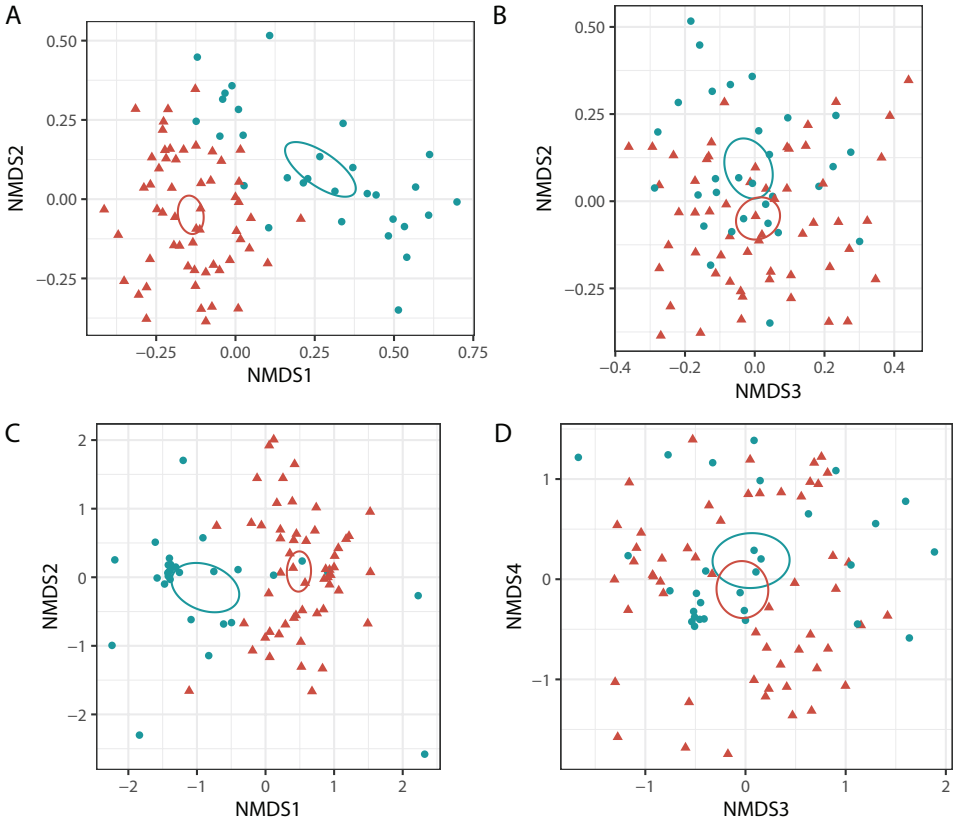

Figure 4. NMDS ordination of fungal communities based on Bray-Curtis dissimilarity of species hypothesis-based community composition, grouped into woodland (W) and gallery forests (GF) samples, for All fungi, axis 1–2 (**A**) and axis 2–3 (**B**), and for ECM fungi, axis 1–2 (**C**) and axis 3–4 (**D**). Stress value = 0.1902 for all fungi and 0.1723 for ECM fungi. Ellipses represent 95% confidence intervals around the mean of each vegetation type.

Soil fungal communities in gallery forests and woodlands

After evaluating the taxonomic affiliation of all ASVs based on their phylogenetic placement in the tree (Suppl. material 3: datafile 3), class-level taxonomy was assigned to 83% of the SHs, together representing 97% of the fungal reads in both vegetation types (Suppl. material 5: Fig. S5). The most abundant group was by far the Agaricomycetes, representing 71% of the reads in woodlands and 84% in gallery forests. Agaricomycetes was also the most species-rich class; with 174 taxa it represented 33% of the detected SHs in both vegetation types. The second most species-rich class was the Dothideomycetes, with 103 species, encompassing only 5.3% of the reads across all samples (Suppl. material 5: Fig. S5). In woodlands, 85% of the reads could be assigned to a fungal guild, and for gallery forest the corresponding number was

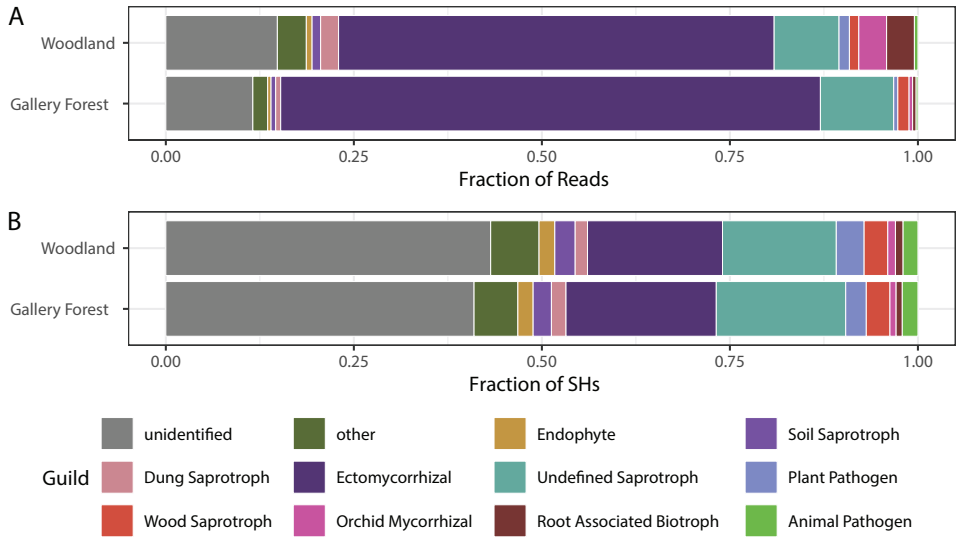

Figure 5. Fungal guild assignment of the soil fungal community in gallery forest and woodlands. Abundance measured as fraction of reads (**A**) and richness measured as fraction of species hypotheses (SH) (**B**) Guilds representing less than 2% of both abundance and richness are grouped together in "other".

88% (Fig. 5A). The vast majority of guild-assigned reads were identified as ECM fungi: 58% in woodlands and 72% in gallery forests. Across both vegetation types, 57% of the SHs were assigned to a fungal guild, with 17% of the SHs representing ECM fungi (Fig. 5B).

Except for two SHs in the family Elaphomycetaceae (Ascomycota), the ECM fungal communities in both vegetation types are made up of species in the phylum Basidiomycota (Fig. 6), and nine ECM lineages were identified to family level in that phylum. Based on both abundance and richness, the Russulaceae and Inocybaceae dominate the ECM fungal soil communities across both vegetation types (Fig. 6). A total of 29 SHs in Russulaceae were detected in both vegetation types, but the family Russulaceae was more abundant in gallery forests, accounting for 58% of the reads assigned to ECM, compared to 41% in woodlands (Fig. 6A). The families Thelephoraceae, Amanitaceae, Clavulinaceae and Hymenochaetaceae were all more abundant and more species-rich in woodlands compared to gallery forest. The families Boletaceae and Sclerodermataceae, on the other hand, were more abundant and diverse in gallery forest (Fig. 6). Sebacinaceae accounted for an average of 11% of reads and 3.3% of SHs in woodland sites, but only 1.4% of reads and 2.5% of SHs in gallery forest. However, of these only a few rare SHs, all in woodlands, were assigned to guild as probable ECM. Guild assignments are listed along with accession numbers and taxonomy assignment in Suppl. material 3: datafile 3.

The overall ordination patterns of the ECM communities are similar to those of the total soil fungal community (Fig. 4, Suppl. material 5: Figs S3, S4), and ECM communities are significantly affected by vegetation type (Fig. 4C). Interestingly, the

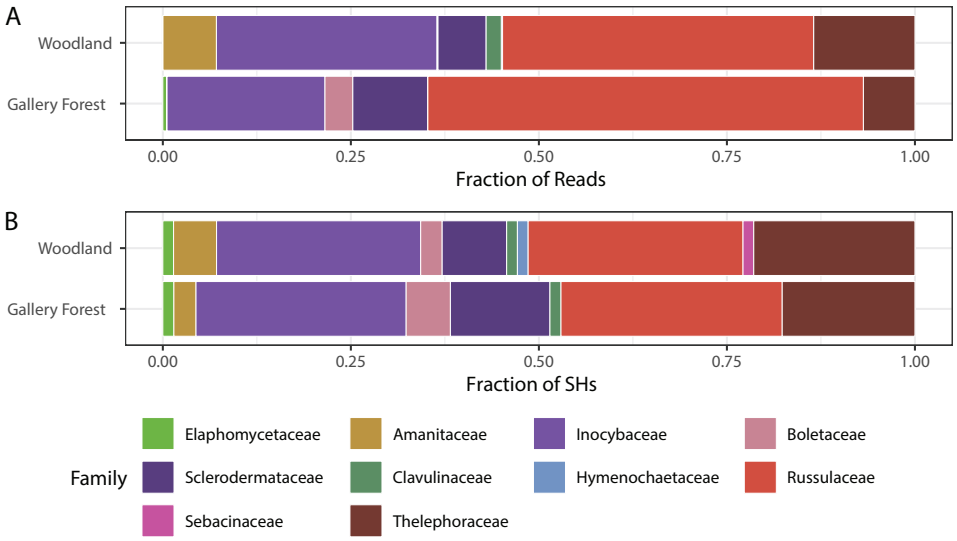

Figure 6. Taxonomic composition to family level of ECM fungi in gallery forest and woodlands. Abundance measured as fraction of reads (**A**) and richness measured as fraction of species hypotheses (SH) (**B**).

species of ECM host tree located closest to each sample does not significantly (p=0.44) affect the ECM fungal community composition once site-level effects are excluded (Suppl. material 5: Fig. S3C, D). However, *B. grandiflora* seems to have the most distinct fungal communities, especially when it comes to the ECM fungal community (Suppl. material 5: Fig. S3C).

Discussion

Most tropical tree species form symbiotic interactions with arbuscular mycorrhizal fungi (Smith and Read 2010). The fraction of tropical trees that instead interact with ectomycorrhizal fungi commonly form characteristic monodominant stands (Corrales et al. 2018). Indeed, ECM host trees make up 77–94% of the basal area in gallery forest plots of our study, and are dominated by *B. grandiflora* that is the only ECM host species in two of the three gallery forest plots (Table 1). The woodlands are an exception to this pattern, where monodominant stands are not observed (Lykke and Sambou 1998; Kakaï and Sinsin 2009; Houdanon et al. 2019). Instead, ECM host trees made up on average 56% of the basal area in these plots with two to four different host species in each plot (Table 1).

The total fungal community as well as the ECM fungal communities in gallery forest soils are different from those in woodland soils (Fig. 4). This effect is likely driven by the dominance of *B. grandiflora* which is the only host tree species that appears to have a distinct soil fungal community based on our ordination analysis (Suppl. mate-

rial 5: Fig. S3A,C). However, abiotic factors such as soil moisture and soil chemistry were not determined in the present study and could also explain at least part of the observed differences. The overall species richness is not different between the vegetation types (Fig. 3). The gallery forest site Kouadianikro stands out with the lowest estimated richness of all sites. This is also the site from which we generated the highest number of sequences, although the number of samples collected, rather than the sequencing depth, appears to limit species detection in our study.

Spatial effects influence beta diversity of ECM fungi, more so in tropical ecosystems than in boreal forests (Bahram et al. 2013). The patchy distribution of ECM-dominated stands in tropical woodlands and forests has been suggested as one explanation for this observation, but other drivers include different soil characteristics, altitude and host specificity (Corrales et al. 2018). We also captured high beta diversity, especially for the ECM fungal community, in both vegetation types. In our survey, we sampled woodland more intensely than gallery forests. Even so, the species accumulation curves indicate that we would have needed to sample at least twice as many sites for our sampling to reach saturation.

Our data largely confirms earlier observations that the ECM fungal communities of West Africa are dominated by fungi in the families Russulaceae and Thelephoraceae (Bâ et al. 2012; Tedersoo and Smith 2013, 2017). In our data, Inocybaceae is the second most abundant and species-rich ECM lineage after Russulaceae. While both of these families contain predominantly fruiting body-forming fungi (De Kesel et al. 2002; Yorou and De Kesel 2011), many SHs could not be identified even to genus level. Assignment of ECM status in Sebacinales based on taxonomy is problematic due to the presence of multiple mycorrhizal types and recent taxonomic changes in the order (Weiss et al. 2004; Garnica et al. 2016), which have not been uniformly propagated into database annotations. However, based on their abundance in ECM woodlands, it is probable that at least some of the detected Sebacinaceae taxa are, in fact, ECM. Many fungal species in West Africa lack reference sequences and our dataset thus provides a mycological resource for future analysis of both described and hitherto undescribed or at least unsequenced fungal species of ECM-dominated woodlands and gallery forests in the Guineo-Sudanian transition zone.

Based on fruiting body inventories in Benin, Yorou and De Kesel (2011) demonstrated that gallery forests dominated by ECM trees represent unique, ECM species-rich habitats in West Africa. In the present study, soil fungal communities from gallery forests were enriched in Boletaceae relative to woodland sites. This corroborates the findings of Yorou and De Kesel (2011) that the Kota gallery forest (including sample site KOTA-G) features the most diverse assemblage of Boletaceae in Benin. In contrast, the lack of sequences from *Cantharellus* (Hydnaceae, Cantharellales) in the present study is striking, and likely due to primer mismatches (Tedersoo et al. 2015). In the Guinean and Sudanian ecozones, fruiting bodies of cantharelloid taxa are commonly found associated with gallery forests dominated by *B. grandiflora* and *U. guineensis* (De Kesel et al. 2011, 2016; Buyck et al. 2020). In Benin, gallery forests host a higher diversity of cantharelloid taxa compared to woodlands (Yorou and De Kesel 2011).

Conclusion

Gallery forest and woodlands in the Guineo-Sudanian transition zone harbor partially overlapping and differently structured soil fungal communities. Site-specific composition of ECM host tree species shapes ECM fungal communities and total soil fungal communities. Our data provides a baseline, albeit incomplete, for phylogenetic placement and taxonomic resolution of environmental sequences from ECM-dominated forests in the Guineo-Sudanian transition zone. Sampling of more samples per site and more sites of the gallery forest is needed for a more complete characterization of the studied ecosystems.

Acknowledgements

Sampling was funded by the National Geographic Society as part of exploration grant #CP-126R-17. B. Sulistyo assisted with sampling, and the molecular laboratory work was performed by Dr Y. Strid at UU. Dr J. Tångrot assisted us in raw data and ASV submission as part of the Biodiversity Atlas Sweden which is made possible by its partners and by grants from the Swedish Research Council. We acknowledge support for sequencing at the National Genomics Infrastructure (NGI) / Uppsala Genome Centre and SciLife Laboratory, Uppsala, supported by the Swedish Research Council and the KAW. Bioinformatic analysis was possible thanks to the National Bioinformatics Infrastructure Sweden (NBIS) and enabled by resources provided by the Swedish National Infrastructure for Computing (SNIC), partially funded by the Swedish Research Council through grant agreement no. 2018-05973.

References

Adomou A (2005) Vegetation patterns and environmental gradients in Benin: implications for biogeography and conservation. PhD Thesis, Wageningen University, Wageningen. https://edepot.wur.nl/121707

Ainsworth GC (2008) Ainsworth & Bisby's Dictionary of the Fungi (10th edn.). CABI, Wallingford, 640 pp.

Altschul SF, Gish W, Miller W, Myers EW, Lipman DJ (1990) Basic local alignment search tool. Journal of Molecular Biology 215(3): 403–410. https://doi.org/10.1016/S0022-2836(05)80360-2

Anderson MJ (2001) A new method for non-parametric multivariate analysis of variance. Austral Ecology 26(1): 32–46. https://doi.org/10.1111/j.1442-9993.2001.01070.pp.x

Assédé ESP, Azihou AF, Geldenhuys CJ, Chirwa PW, Biaou SSH (2020) Sudanian versus Zambezian woodlands of Africa: Composition, ecology, biogeography and use. Acta Oecologica 107: e103599. https://doi.org/10.1016/j.actao.2020.103599

Bâ AM, Duponnois R, Diabaté M, Dreyfus B (2011) Les champignons ectomycorhiziens des arbres forestiers en Afrique de l'Ouest: méthodes d'étude, diversité, écologie, utilisation

en foresterie et comestibilité. IRD Editions, Marseille, 252 pp. https://doi.org/10.4000/books.irdeditions.10404

Bâ AM, Duponnois R, Moyersoen B, Diédhiou AG (2012) Ectomycorrhizal symbiosis of tropical African trees. Mycorrhiza 22(1): 1–29. https://doi.org/10.1007/s00572-011-0415-x

Bahram M, Kõljalg U, Courty PE, Diedhiou AG, Kjøller R, Polme S, Ryberg M, Veldre V, Tedersoo L (2013) The distance decay of similarity in communities of ectomycorrhizal fungi in different ecosystems and scales. Journal of Ecology 101(5): 1335–1344. https://doi.org/10.1111/1365-2745.12120

Barberán A, Ladau J, Leff JW, Pollard KS, Menninger HL, Dunn RR, Fierer N (2015) Continental-scale distributions of dust-associated bacteria and fungi. Proceedings of the National Academy of Sciences 112(18): 5756–5761. https://doi.org/10.1073/pnas.1420815112

Baumgartner J, Dinnage R (2019) hues: Distinct colour palettes based on "iwanthue." R package version 0.2.0. https://CRAN.R-project.org/package=hues

Bengtsson-Palme J, Ryberg M, Hartmann M, Branco S, Wang Z, Godhe A, De Wit P, Sánchez-García M, Ebersberger I, de Sousa F (2013) Improved software detection and extraction of ITS1 and ITS2 from ribosomal ITS sequences of fungi and other eukaryotes for analysis of environmental sequencing data. Methods in Ecology and Evolution 4(10): 914–919. https://doi.org/10.1111/2041-210X.12073

Bivand R, Tim Keitt T, Rowlingson B (2020) rgdal: Bindings for the 'Geospatial' Data Abstraction Library. R package version 1.5–16. https://CRAN.R-project.org/package=rgdal

Brundrett MC (2017) Global diversity and importance of mycorrhizal and nonmycorrhizal plants. Ecological Studies 230: 533–556. https://doi.org/10.1007/978-3-319-56363-3_21

Buyck B, Ebika STN, De Kesel A, Hofstetter V (2020) Tropical African *Cantharellus* Adans.: Fr. (Hydnaceae, Cantharellales) with lilac-purplish tinges revisited. Cryptogamie, Mycologie 41(10): 161–177. https://doi.org/10.5252/cryptogamie-mycologie2020v41a10

Callahan BJ, McMurdie PJ, Rosen MJ, Han AW, Johnson AJA, Holmes SP (2016) DADA2: high-resolution sample inference from Illumina amplicon data. Nature Methods 13(7): 581–583. https://doi.org/10.1038/nmeth.3869

Corrales A, Henkel TW, Smith ME (2018) Ectomycorrhizal associations in the tropics – biogeography, diversity patterns and ecosystem roles. New Phytologist 220(4): 1076–1091. https://doi.org/10.1111/nph.15151

Davison J, Moora M, Öpik M, Adholeya A, Ainsaar L, Bâ AM, Burla S, Diedhiou A, Hiiesalu I, Jairus T (2015) Global assessment of arbuscular mycorrhizal fungus diversity reveals very low endemism. Science 349(6251): 970–973. https://doi.org/10.1126/science.aab1161

De Kesel A (2011) *Cantharellus solidus*, a new species from Benin (West-Africa) with a smooth hymenium. Cryptogamie, Mycologie 32(3): 277–283. https://doi.org/10.7872/crym.v32.iss3.2011.277

De Kesel A, Amalfi M, Ngoy BKW, Yorou NS, Raspé O, Degreef J, Buyck B (2016) New and interesting *Cantharellus* from tropical Africa. Cryptogamie, Mycologie 37(3): 283–327. https://doi.org/10.7872/crym/v37.iss3.2016.283

De Kesel A, Codjia JTC, Yorou NS (2002) Guide des champignons comestibles du Bénin. Meise Botanic Garden, Meise.

Diédhiou AG, Selosse MA, Galiana A, Diabaté M, Dreyfus B, Bâ AM, De Faria SM, Béna G (2010) Multi-host ectomycorrhizal fungi are predominant in a Guinean tropical rainforest and shared between canopy trees and seedlings. Environmental Microbiology 12(8): 2219–2232. https://doi.org/10.1111/j.1462-2920.2010.02183.x

Ducousso M, Bâ AM, Thoen D (2003) Les champignons ectomycorhiziens des forêts naturelles et des plantations d'Afrique de l'Ouest: une source de champignons comestibles. Bois et Forets des Tropiques 275: 51–63. https://agritrop.cirad.fr/511421/

Edgar RC (2016) SINTAX: a simple non-Bayesian taxonomy classifier for 16S and ITS sequences. bioRxiv 074161. https://doi.org/10.1101/074161

Fick SE, Hijmans RJ (2017) WorldClim 2: new 1-km spatial resolution climate surfaces for global land areas. International Journal of Climatology 37: 4302–4315. https://doi.org/10.1002/joc.5086

Gryzenhout M, Jefwa JM, Yorou NS (2012) The status of mycology in Africa: A document to promote awareness. IMA Fungus 3(1): 99–102. https://doi.org/10.5598/imafungus.2012.03.01.11

Harrower M, Brewer CA (2003) ColorBrewer.org: An Online Tool for Selecting Colour Schemes for Maps. The Cartographic Journal 40: 27–37. https://doi.org/10.1179/000870403235002042

Hawksworth DL, Lücking R (2017) Fungal diversity revisited: 2.2 to 3.8 million species. Microbiology Spectrum 5(4): 79–95. https://doi.org/10.1128/microbiolspec.FUNK-0052-2016

Hopple Jr JS, Vilgalys R (1994) Phylogenetic relationships among coprinoid taxa and allies based on data from restriction site mapping of nuclear rDNA. Mycologia 86(1): 96–107. https://doi.org/10.2307/3760723

Houdanon R, Tchan I, Laourou G, Codjia J, Badou S, Aignon L, Boni S, Yorou NS (2019) Spatial structure of ectomycorrhizal trees in wooded savannas of Guineo-Sudanian ecozone in West Africa. Journal of Tropical Forest Science 31(1): 1–11. https://doi.org/10.26525/jtfs2019.31.1.001011

Hsieh T, Ma K, Chao A (2016) iNEXT: an R package for rarefaction and extrapolation of species diversity (Hill numbers). Methods in Ecology and Evolution 7(12): 1451–1456. https://doi.org/10.1111/2041-210X.12613

Jacomy M (2013) I Want Hue. médialab. http://medialab.github.io/iwanthue/

Kakaï RG, Sinsin B (2009) Structural description of two *Isoberlinia* dominated vegetation types in the Wari-Maro Forest Reserve (Benin). South African Journal of Botany 75(1): 43–51. https://doi.org/10.1016/j.sajb.2008.07.003

Kalsoom Khan F, Kluting K, Tångrot J, Urbina H, Ammunet T, Eshghi Sahraei S, Rydén M, Ryberg M, Rosling A (2020) Naming the untouchable – environmental sequences and niche partitioning as taxonomical evidence in fungi. IMA Fungus 11: 1–23. https://doi.org/10.1186/s43008-020-00045-9

Kassambara A (2020) ggpubr: 'ggplot2' based publication ready plots. R Package version 0.3.0. https://CRAN.R-project.org/package=ggpubr

Katoh K, Standley DM (2013) MAFFT multiple sequence alignment software version 7: improvements in performance and usability. Molecular Biology and Evolution 30(4): 772–780. https://doi.org/10.1093/molbev/mst010

Kõljalg U, Nilsson RH, Abarenkov K, Tedersoo L, Taylor AF, Bahram M, Bates ST, Bruns TD, Bengtsson-Palme J, Callaghan TM (2013) Towards a unified paradigm for sequence-based identification of fungi. Molecular Ecology 22(21): 5271–5277. https://doi.org/10.1111/mec.12481

Kõljalg U, Abarenkov K, Zirk A, Runnel V, Piirmann T, Pöhönen R, Ivanov F (2019) PlutoF: Biodiversity data management platform for the complete data lifecycle. Biodiversity Information Science and Standards 3: e37398. https://doi.org/10.3897/biss.3.37398

Larsson A (2014) AliView: a fast and lightweight alignment viewer and editor for large datasets. Bioinformatics 30(22): 3276–3278. https://doi.org/10.1093/bioinformatics/btu531

Lykke A, Sambou B (1998) Structure, floristic composition, and vegetation forming factors of three vegetation types in Senegal. Nordic Journal of Botany 18(2): 129–140. https://doi.org/10.1111/j.1756-1051.1998.tb01859.x

Martin M (2011) Cutadapt removes adapter sequences from high-throughput sequencing reads. EMBnet.journal 17(1): 10–12. https://doi.org/10.14806/ej.17.1.200

McArdle BH, Anderson MJ (2001) Fitting multivariate models to community data: a comment on distance-based redundancy analysis. Ecology 82(1): 290–297. https://doi.org/10.1890/0012-9658(2001)082[0290:FMMTCD]2.0.CO;2

Miller MA, Pfeiffer W, Schwartz T (2010) Creating the CIPRES Science Gateway for inference of large phylogenetic trees. 2010 Gateway Computing Environments Workshop (GCE), New Orleans (USA), Nov 2010. IEEE, 8 pp. https://doi.org/10.1109/GCE.2010.5676129

Natta A, Sinsin B, Van der Maesen L (2003) Riparian forests and biodiversity conservation in Benin (West Africa). In: Proceedings of the XII World Forestry Congress, Québec City (Canada), 2003. FAO. http://http://www.fao.org/3/XII/0356-B2.htm

Neuwirth E (2014) RColorBrewer: ColorBrewer palettes. R package version 1.1-2. https://CRAN.R-project.org/package=RColorBrewer

Nguyen NH, Song Z, Bates ST, Branco S, Tedersoo L, Menke J, Schilling JS, Kennedy PG (2016) FUNGuild: an open annotation tool for parsing fungal community datasets by ecological guild. Fungal Ecology 20: 241–248. https://doi.org/10.1016/j.funeco.2015.06.006

Oksanen J, Blanchet FG, Kindt R, Legendre P, Minchin PR, O'Hara R, Simpson GL, Solymos P, Stevens MHH, Wagner H (2013) Package 'vegan'. Community ecology package, version 2.5-4. https://CRAN.R-project.org/package=vegan

Olson DM, Dinerstein E, Wikramanayake ED, Burgess ND, Powell GVN, Underwood EC, D'Amico JA, Itoua I, Strand HE, Morrison JC, Loucks CJ, Allnutt TF, Ricketts TH, Kura Y, Lamoreux JF, Wettengel WW, Hedao P, Kassem KR (2001) Terrestrial ecoregions of the world: a new map of life on Earth. BioScience 51: 933–938. https://doi.org/10.1641/0006-3568(2001)051[0933:TEOTWA]2.0.CO;2

Paré S, Söderberg U, Sandewall M, Ouadba JM (2008) Land use analysis from spatial and field data capture in southern Burkina Faso, West Africa. Agriculture, Ecosystems & Environment 127(3–4): 277–285. https://doi.org/10.1016/j.agee.2008.04.009

Piepenbring M, Maciá-Vicente JG, Codjia JEI, Glatthorn C, Kirk P, Meswaet Y, Minter D, Olou BA, Reschke K, Schmidt M (2020) Mapping mycological ignorance – checklists and diversity patterns of fungi known for West Africa. IMA Fungus 11(1): 1–22. https://doi.org/10.1186/s43008-020-00034-y

R Core Team (2020) R: A language and environment for statistical computing. Version 3.6.3. R Foundation for Statistical Computing, Vienna.

Rambaut A, Drummond AJ, Xie D, Baele G, Suchard MA (2018) Posterior summarization in Bayesian phylogenetics using Tracer 1.7. Systematic Biology 67(5): 901–904. https://doi.org/10.1093/sysbio/syy032

Rinaldi A, Comandini O, Kuyper TW (2008) Ectomycorrhizal fungal diversity: seperating the wheat from the chaff. Fungal Diversity 33: 1–45. https://www.fungaldiversity.org/fdp/sfdp/33-1.pdf

Rognes T, Flouri T, Nichols B, Quince C, Mahé F (2016) VSEARCH: a versatile open source tool for metagenomics. PeerJ 4: e2584. https://doi.org/10.7717/peerj.2584

Sanon E, Guissou KML, Yorou NS, Buyck B (2014) Le genre *Russula* au Burkina Faso (Afrique de l'Ouest): quelques espèces nouvelles de couleur brunâtre. Cryptogamie, Mycologie 35(4): 377–397. https://doi.org/10.7872/crym.v35.iss4.2014.377

Sato H, Tsujino R, Kurita K, Yokoyama K, Agata K (2012) Modelling the global distribution of fungal species: new insights into microbial cosmopolitanism. Molecular Ecology 21(22): 5599–5612. https://doi.org/10.1111/mec.12053

Savadogo P (2007) Dynamics of Sudanian savanna-woodland ecosystem in response to disturbances. PhD Thesis. Swedish Agricultural University, Umeå. http://urn.kb.se/resolve?urn=urn:nbn:se:slu:epsilon-1585

Sinsin B, Kampmann D (2010) Atlas de la Biodiversité de l'Afrique de l'Ouest. Tome I: Benin. BIOTA, Cotonou & Frankfurt/Main.

Slowikowski K (2020) ggrepel: Automatically position non-overlapping text labels with "ggplot2." R package version 0.8.2. https://CRAN.R-project.org/package=ggrepel

Smith SE, Read DJ (2010) Mycorrhizal Symbiosis. Academic Press, London, 787 pp.

Swaine M (1992) Characteristics of dry forest in West Africa and the influence of fire. Journal of Vegetation Science 3(3): 365–374. https://doi.org/10.2307/3235762

Tedersoo L, Bahram M, Jairus T, Bechem E, Chinoya S, Mpumba R, Leal M, Randrianjohany E, Razafimandimbison S, Sadam A (2011) Spatial structure and the effects of host and soil environments on communities of ectomycorrhizal fungi in wooded savannas and rain forests of Continental Africa and Madagascar. Molecular Ecology 20(14): 3071–3080. https://doi.org/10.1111/j.1365-294X.2011.05145.x

Tedersoo L, Bahram M, Puusepp R, Nilsson RH, James TY (2017) Novel soil-inhabiting clades fill gaps in the fungal tree of life. Microbiome 5(1): 1–42. https://doi.org/10.1186/s40168-017-0259-5

Tedersoo L, Bahram M, Ryberg M, Otsing E, Kõljalg U, Abarenkov K (2014) Global biogeography of the ectomycorrhizal /sebacina lineage (Fungi, Sebacinales) as revealed from comparative phylogenetic analyses. Molecular Ecology 23(16): 4168–4183. https://doi.org/10.1111/mec.12849

Tedersoo L, Brundrett MC (2017) Evolution of Ectomycorrhizal Symbiosis in Plants. In: Tedersoo L (Ed.) Biogeography of Mycorrhizal Symbiosis. Ecological Studies (Analysis and Synthesis) (Vol. 230). Springer, Cham. https://doi.org/10.1007/978-3-319-56363-3_19

Tedersoo L, May TW, Smith ME (2010) Ectomycorrhizal lifestyle in fungi: global diversity, distribution, and evolution of phylogenetic lineages. Mycorrhiza 20(4): 217–263. https://doi.org/10.1007/s00572-009-0274-x

Tedersoo L, Nara K (2010) General latitudinal gradient of biodiversity is reversed in ectomycorrhizal fungi. The New Phytologist 185(2): 351–354. https://doi.org/10.1111/j.1469-8137.2009.03134.x

Tedersoo L, Smith ME (2013) Lineages of ectomycorrhizal fungi revisited: foraging strategies and novel lineages revealed by sequences from belowground. Fungal Biology Reviews 27(3–4): 83–99. https://doi.org/10.1016/j.fbr.2013.09.001

Tedersoo L, Smith ME (2017) Ectomycorrhizal fungal lineages: detection of four new groups and notes on consistent recognition of ectomycorrhizal taxa in high-throughput sequencing studies. Ecological Studies 230: 125–142. https://doi.org/10.1007/978-3-319-56363-3_6

White F (1983) The vegetation of Africa: a descriptive memoir to accompany the UNESCO/AETFAT/UNSO vegetation map of Africa. UNESCO.

Wickham H (2016) ggplot2: Elegant Graphics for Data Analysis. Springer-Verlag, New York. https://doi.org/10.1007/978-3-319-24277-4_9

Yorou NS, De Kesel A (2011) Larger fungi. In: Neuenschwander P, Sinsin B, Goergen G (Eds) Nature Conservation in West Africa: Red List for Benin. IITA, Ibadan, Nigeria, 47–60.

Yorou NS (2008) Miscellaneous contributions to the anatomy and molecular phylogeny of tropical African resupinate Thelephorales. PhD Thesis. Ludwig-Maximilians-Universität München, Munich. https://edoc.ub.uni-muenchen.de/8133/2/SOULEMANE_YOROU_Nourou.pdf

Yorou NS, Koné A, Guissou M, Guelly N, Maba D, Ekué M, De Kesel A (2014) Biodiversity and Sustainable Use of Wild Edible Fungi in the Sudanian Centre of Endemism: A Plea for Valorisation. In: Ba AM, McGuire KL, Diedhiou AG (Eds) Ectomycorrhizal Symbioses in Tropical and Neotropical Forests. CRC Press, Boca Raton/London/New York, 255–284. https://doi.org/10.1201/b16536-14

Zhang J, Kapli P, Pavlidis P, Stamatakis A (2013) A general species delimitation method with applications to phylogenetic placements. Bioinformatics 29(22): 2869–2876. https://doi.org/10.1093/bioinformatics/btt499

Supplementary material 1

Datafile 1

Authors: Peter Meidl, Brendan Furneaux, Kassim Tchan, Kerri Kluting, Martin Ryberg, Marie-Laure Guissou, Soro Bakary, Aïssata Traoré, Gbamon Konomou, Nourou Yorou, Anna Rosling

Data type: Site and sample information

Explanation note: This file contains site and host tree information from ECM dominated woodlads of West Africa sampled during the National Geographic Society exploration grant #CP-126R-17.

Link: https://doi.org/10.3897/mycokeys.81.66249.suppl1

Supplementary material 2

Datafile 2

Authors: Peter Meidl, Brendan Furneaux, Kassim Tchan, Kerri Kluting, Martin Ryberg, Marie-Laure Guissou, Bakary Soro, Aïssata Traoré, Gbamon Konomou, Nourou Yorou, Anna Rosling

Data type: Barcodes and primer sequences

Explanation note: This file contains the primer barcode sequence information for forward primer ITS1 and reverse primer LR5 used for amplification of total fungal (and other eukaryotes) from soil samples collected in ECM dominated woodlands of West Africa collected during the National Geographic Society explorer grant #CP-126R-17.

Link: https://doi.org/10.3897/mycokeys.81.66249.suppl2

Supplementary material 3

Datafile 3

Authors: Peter Meidl, Brendan Furneaux, Kassim Tchan, Kerri Kluting, Martin Ryberg, Marie-Laure Guissou, Bakary Soro, Aïssata Traoré, Gbamon Konomou, Nourou Yorou, Anna Rosling

Data type: ASV list with accession nr, taxonomy and functional guild assignment

Explanation note: This file contains a list of all 1147 ASVs with accession nr and the taxonomy assignment inlcuding UNITE SH when assigned and functional guild assignment. Generated from soil samples collected in ECM dominated woodlands of West Africa collected during the National Geographic Society explorer grant #CP-126R-17.

Link: https://doi.org/10.3897/mycokeys.81.66249.suppl3

Supplementary material 4

Datafile 4

Authors: Peter Meidl, Brendan Furneaux, Kassim Tchan, Kerri Kluting, Martin Ryberg, Marie-Laure Guissou, Bakary Soro, Aïssata Traoré, Gbamon Konomou, Nourou Yorou, Anna Rosling

Data type: Phylogenetic tree for inference of SHs

Explanation note: A Phylogenetic tree of all fungal ASVs in the study.

Link: https://doi.org/10.3897/mycokeys.81.66249.suppl4

Supplementary material 5

Table S1 and Figs S1–S4

Authors: Peter Meidl, Brendan Furneaux, Kassim Tchan, Kerri Kluting, Martin Ryberg, Marie-Laure Guissou, Bakary Soro, Aïssata Traoré, Gbamon Konomou, Nourou Yorou, Anna Rosling

Data type: table and images

Explanation note: Supplementary tables and figures.

Link: https://doi.org/10.3897/mycokeys.81.66249.suppl5

MycoKeys 81: 69–138 (2021)
doi: 10.3897/mycokeys.81.67850
https://mycokeys.pensoft.net

RESEARCH ARTICLE

A peer-reviewed open-access journal
MycoKeys
Launched to accelerate biodiversity research

Unravelling unexplored diversity of cercosporoid fungi (Mycosphaerellaceae, Mycosphaerellales, Ascomycota) in tropical Africa

Yalemwork Meswaet[1], Ralph Mangelsdorff[1], Nourou S. Yorou[2], Meike Piepenbring[1]

1 *Department of Mycology, Institute of Ecology, Evolution and Diversity, Faculty of Biosciences, Goethe University Frankfurt am Main, Biologicum, Max-von-Laue-Str. 13, 60438 Frankfurt am Main, Germany* **2** *Faculty of Agronomy, University of Parakou, BP 123 Parakou, Benin*

Corresponding author: Meike Piepenbring (Piepenbring@bio.uni-frankfurt.de)

Academic editor: Huzefa Raja | Received 28 April 2021 | Accepted 29 May 2021 | Published 17 June 2021

Citation: Meswaet Y, Mangelsdorff R, Yorou NS, Piepenbring M (2021) Unravelling unexplored diversity of cercosporoid fungi (Mycosphaerellaceae, Mycosphaerellales, Ascomycota) in tropical Africa. MycoKeys 81: 69–138. https://doi.org/10.3897/mycokeys.81.67850

Abstract

Cercosporoid fungi (Mycosphaerellaceae, Mycosphaerellales, Ascomycota) are one of the largest and most diverse groups of hyphomycetes causing a wide range of diseases of economically important plants as well as of plants in the wild. Although more than 6000 species are known for this group, the documentation of this fungal group is far from complete. Especially in the tropics, the diversity of cercosporoid fungi is poorly known. The present study aims to identify and characterise cercosporoid fungi collected on host plants belonging to Fabaceae in Benin, West Africa. Information on their morphology, host species and DNA sequence data (18S rDNA, 28S rDNA, ITS and *tef1*) is provided. DNA sequence data were obtained by a simple and non-culture-based method for DNA isolation which has been applied for cercosporoid fungi for the first time in the context of the present study. Among the loci used for the phylogenetic analysis, *tef1* provided the best resolution together with the multigene dataset. Species delimitation in many cases, however, was only possible by combining molecular sequence data with morphological characteristics. Based on forty specimens recently collected in Benin, 18 species are presented with morphological descriptions, illustrations and sequence data. Among these, six species in the genus *Cercospora* and two species in *Pseudocercospora* are proposed as species new to science. The newly described species are *Cercospora* (*C.*) *beninensis* on *Crotalaria macrocalyx*, *C. parakouensis* on *Desmodium tortuosum*, *C. rhynchophora* on *Vigna unguiculata*, *C. vignae-subterraneae* on *Vigna subterranea*, *C. tentaculifera* on *Vigna unguiculata*, *C. zor-*

niicola on *Zornia glochidiata*, *Pseudocercospora sennicola* on *Senna occidentalis* and *Pseudocercospora tabei* on *Vigna unguiculata*. Eight species of cercosporoid fungi are reported for Benin for the first time, three of them, namely *C.* cf. *canscorina*, *C.* cf. *fagopyri* and *C. phaseoli-lunati* are new for West Africa. The presence of two species of cercosporoid fungi on Fabaceae previously reported from Benin, namely *Nothopassalora personata* and *Passalora arachidicola*, is confirmed.

Keywords

Benin, *Cercospora*, Fabaceae, Leguminosae, molecular phylogenetic analysis, *Nothopassalora*, *Passalora*, *Pseudocercospora*, West Africa

Introduction

Hyphomycetous anamorphs of *Mycosphaerella*-like teleomorphs are generally referred to as cercosporoid fungi and are classified in genera with concepts that often changed (Crous and Braun 2003; Braun et al. 2013; Kirschner 2014). Cercosporoid fungi include about 6000 recognized species (Braun et al. 2015), in more than ten genera, with *Cercospora* Fresen. (*C.*), *Nothopassalora* U.Braun, C.Nakash., Videira & Crous (*N.*), *Passalora* Fr. (*P.*) and *Pseudocercospora* Speg. (*Ps.*) being the genera relevant for the present publication.

Cercosporoid fungi belonging to Mycosphaerellaceae (Mycosphaerellales, Ascomycota) are one of the largest and most diverse groups of hyphomycetes and cause a wide range of diseases, on numerous economically important plants such as cereals, vegetables and fruits as well as on wild plants. Major diseases include the angular leaf spot of bean caused by *Pseudocercospora griseola*, black leaf streak of banana caused by *Ps. fijiensis* (M.Morelet) Deighton, fruit and leaf spot disease of citrus caused by *Ps. angolensis* (T.Carvalho & O.Mendes) Crous & U.Braun, leaf spot disease of celery (*Cercospora apii* Fresen.), of sugar beet (*C. beticola* Sacc.), and foliar diseases of groundnut caused by *Nothopassalora personata* (Berk. & M.A.Curtis) U.Braun, C.Nakash., Videira & Crous or *Passalora arachidicola* (Hori) U.Braun (Braun et al. 2013; Videira et al. 2017). Infections by these fungi are mostly evident by leaf spots, but cercosporoid fungi can also cause necrotic lesions on flowers, fruits, seeds and pedicels of numerous hosts in most climatic regions (Agrios 2005). Cercosporoid fungi are known from all parts of the world but they are more abundant and diverse in tropical and subtropical regions (Beilharz et al. 2002; Braun and Freire 2004; Hernández-Gutiérrez and Dianese 2008, 2009).

Cercosporoid fungi are dematiaceous hyphomycetes with conidiophores formed singly or in groups, arranged in sporodochia or in synnemata, with integrated, terminal or intercalary conidiogenous cells (Crous and Braun 2003; Ávila et al. 2005; Braun et al. 2013). Most of the cercosporoid species were previously assigned to a single genus, *Cercospora*, which was later split into several smaller genera mainly by Deighton (1967, 1973, 1974, 1976, 1979), Braun (1993) and Crous and Braun (2003). Crous and Braun (2003) recognized four genera, namely *Cercospora*, *Passalora*, *Pseudocercospora* and *Stenella* Syd as important cercosporoid genera. Later, the genus *Stenella* was

assigned to the Teratosphaeriaceae based on the phylogenetic placement of the type species. *Stenella*-like species remaining in Mycosphaerellaceae were classified in the genus *Zasmidium* Fr. (Arzanlou et al. 2007; Braun et al. 2013). In the present paper, we follow generic concepts defined by Crous and Braun (2003) and recently updated by Braun et al. (2013), Crous et al. (2013a), Groenewald et al. (2013) and Videira et al. (2017). However, according to recent molecular sequence analyses, most genera of the cercosporoid fungi are not monophyletic (Videira et al. 2017). As many cercosporoid fungi have a strong impact on cultivated plants, a better understanding and stabilisation of the taxonomy of these fungi are urgently needed.

The genus *Cercospora* was established by Fresenius in 1863 (Fuckel 1863) based on the type species *Cercospora apii* (Braun and Crous 2016; Videira et al. 2017). It is one of the most species-rich genera of the hyphomycetes and contains numerous important plant pathogenic fungi throughout the world (Crous and Braun 2003). In 1954, the genus was monographed by Chupp (1954), who treated 1419 *Cercospora*-species using a broad generic concept. Later, several attempts have been made to split *Cercospora* s. lat. into smaller genera by using characteristics of conidiomatal structure, hyphae, conidiophores, conidiogenous cells, conidiogenous loci and conidia (Ellis 1971, 1976; Deighton 1973, 1979, 1983; Braun 1995a, 1998; Crous and Braun 2003). Currently, *Cercospora* species are morphologically characterised by pigmented conidiophores, unpigmented conidia, as well as thickened and darkened conidiogenous loci and conidial hila (Crous and Braun 2003; Groenewald et al. 2013). A significant problem in the taxonomy of *Cercospora* is the host specificity of its species. Most *Cercospora* species are considered to be distinct based on the host and thus assumed to be specific to a host species or to a host genus (Chupp 1954; Braun 1995a). Some species, such as *C. apii* and *C. beticola*, however, were isolated from a high number of host species belonging to several families (Groenewald M et al. 2006). Moreover, phylogenetic approaches based on multi-locus sequences can be problematic for species delimitation in *Cercospora* due to a high level of conservation in DNA sequences of commonly used loci (i.e., ITS, *tef1*, actA, cmdA and his3) (Bakhshi et al. 2018).

The genus *Pseudocercospora* was introduced by Spegazzini (1910) based on the type species *Ps. vitis* (Lév.) Speg., a foliar pathogen of grapevine. The majority of *Pseudocercospora* species are known as pathogens occurring on many different plants, mainly in tropical and sub-tropical regions (Chupp 1954; Crous and Braun 2003; Crous et al. 2013). In contrast to *Cercospora* spp., they are characterised by pigmented conidiophores and conidia, without thickened and darkened conidiogenous loci and conidial hila (Deighton 1976). The monophyly of the genus has not yet been fully resolved (Kirschner 2014). According to molecular sequence data, most species of *Pseudocercospora* appear to be host specific (Crous et al. 2013).

The genus *Passalora* Fr. was introduced by Fries (1849) based on the type species *Passalora bacilligera* (Mont. & Fr.) Mont. & Fr. (≡ *Cladosporium bacilligerum* Mont. & Fr.) (Videira et al. 2017). Species of *Passalora* are characterised by pigmented conidiophores and conidia as well as thickened and darkened conidiogenous loci and conidial hila (Crous and Braun 2003).

Several molecular phylogenetic studies are available on species of cercosporoid fungi that are represented by strains in culture collections (Świderska-Burek et al. 2020). These, however, only represent a small fraction of several hundreds of taxa of cercosporoid fungi that are valid species defined by morphological characteristics (Braun et al. 2016; Świderska-Burek et al. 2020). Therefore, the number of cercosporoid species known by detailed morphological characteristics as well as molecular sequence data has to be increased.

Although cercosporoid fungi cause a wide range of diseases on major agricultural crops, the study of cercosporoid fungi in West Africa is still at an early pioneer stage and only very incomplete information is currently available (Piepenbring et al. 2020). To date, approximately 320 species of cercosporoid hyphomycetes are known from 14 West African countries (Piepenbring et al. 2020, Suppl. materials 1, 2). Among these, 12 species of cercosporoid fungi have been reported for Benin (Turner 1971; Marley et al. 2002; Crous and Braun 2003; Houessou et al. 2011; Piątek and Yorou 2018; Soura et al. 2018; Meswaet et al. 2019; Farr and Rossman 2021). Morphological characteristics and molecular sequence data are lacking for most cercosporoid species known for Benin and other West African countries. Although cercosporoid fungi have been investigated for more than 150 years and are important in the agricultural sector, almost no, or only inadequate, studies have been carried out in most West African countries such as Benin. In addition to this lack of species knowledge in tropical regions, many species of cercosporoid fungi are characterised morphologically only. Since many cercosporoid species are known as pathogens on cultivated plants, an accurate diagnosis, identification and documentation of these fungi are a prerequisite and urgent for their control and epidemiological surveys.

As a first step towards a systematic documentation of cercosporoid fungi in tropical Africa, we focus on species infecting hosts belonging to the Fabaceae (Leguminosae) in the present publication. Fabaceae are the third largest family of angiosperms (Gepts et al. 2005). This family includes peas, lentils, beans, peanuts and other plants with pods and/or seeds that are consumed as food (Messina 1999). Several species belonging to *Vigna* originate from West Africa (Benin, Burkina Faso, Cameroon, Ghana, Niger, Nigeria and Togo) including two important cultivated crops *Vigna unguiculata* (L.) Walp. and *Vigna subterranea* (L.) Verdc. (Hepper 1963; Faris 1965; Padulosi and Ng 1990). They provide important nutrients such as proteins, low glycemic index carbohydrates, minerals and vitamins. Legumes are richer in protein than other cultivated plants because of nitrogen-fixing bacteria living in nodules of their roots (Kouris-Blazos and Belski 2016).

We apply an integrative approach that includes sampling in Benin, detailed descriptions and illustrations of collected specimens and herbarium specimens, examination of closely related known species on the same or closely related host species based on herbarium specimens and the isolation, sequencing and analysis of nuclear DNA sequence data. For the isolation of DNA, a new, simple method for DNA isolation has been developed and is presented for the first time for cercosporoid fungi.

Methods

Collections and morphological studies

Samples of leaves infected by cercosporoid fungi were randomly collected in farmlands and fallows in Benin from July–August 2016, July–September 2017 and August–September 2019. Infected leaves were dried in a plant press and deposited in the herbaria Botanische Staatssammlung München (M) and University of Parakou (**UNIPAR**).

Dried specimens were observed by stereomicroscopy and by light microscopy, using a Zeiss Axioscope 40 microscope. For light microscopy, leaf sections were made with razor blades and mounted in distilled water or 5% KOH without staining. Semipermanent preparations of sections of the infected leaves were made by a microtome (Leica CM 1510-1) and mounted in lactophenol with cotton blue. For approximately 50 ml lactophenol cotton blue solution we mixed 10 mg phenol, 0.025 mg cotton blue, 10 ml lactic acid, 20 ml glycerin and 10 ml distilled water. Measurements of 30 conidia, conidiophores and other structures have been made for each specimen at a magnification of ×1000. Measurements are presented as mean value ± standard deviation with extreme values in parentheses. Line drawings were made freehand on scaled paper. Images and drawings were edited with Photoshop CS5 (Adobe, San Jose, California). Critical taxa were determined with the help of type specimens and other specimens loaned from the US National Fungus Collections (BPI), the Herbarium of the University of Illinois (ILL) and the New York Botanical Garden (NY).

Host plant identification

Host plants were identified by morphological characteristics and in some cases by molecular methods. Morphological identifications were made by comparison with herbarium specimens, literature (e.g., Akoégninou et al. 2006) and with the help of local botanists. Molecular sequence data for species identifications were obtained by polymerase chain reaction (PCR) for the amplification of the partial region of chloroplast rbcL with the primer pairs rbcLa-F (Levin et al. 2003) and rbcLa-R (Kress et al. 2009). DNA was extracted from approx. 0.05 g of leaf tissue dried with silica gel using the innuPREP Plant DNA Kit (Analytik Jena, Germany) and following the manufacturer's instructions. Protocols for PCR were carried out as described by Fazekas et al. (2012).

DNA Extraction and PCR amplification of fungal DNA

DNA was isolated from caespituli taken with a needle from dry specimens using the E.Z.N.A Forensic DNA Extraction Kit following the manufacturer's instructions. Small pieces of leaves containing several clean caespituli, with as little contaminations as possible, were selected under the stereomicroscope. Precautions were taken to avoid picking cells of any other organism (fungi, algae) associated with the leaves. To extract total genomic DNA from caespituli, a small amount of clean hyphae from the leaf sur-

face was transferred into a sterile Eppendorf tube using a sterilized needle or adhesive mini-tapes. The sample was homogenized for 7–10 min. using a Retsch Mixer Mill MM301 with TL buffer and 2.5 mm Zirconia beads. Isolated DNA was re-suspended in elution buffer and stored at -20 °C. DNA concentration was checked by a NanoDrop 2000c spectrophotometer (Thermo Fisher Scientific, USA).

Four partial nuclear gene regions (three ribosomal loci and one protein-coding gene) were amplified and sequenced: For the large subunit nuclear ribosomal DNA (nrLSU, 28S rDNA) the primers LSU1Fd and LSU3Rd (Crous et al. 2009a), for the small subunit nuclear ribosomal DNA (nrSSU, 18S rDNA) the primers SSU1Fd and SSU1Fd (Crous et al. 2009a), for the internal transcribed spacer region of ribosomal DNA (ITS) the primers V9G (de Hoog and van den Ende 1998) and ITS4 (White et al. 1990) and for the translation elongation factor 1-α (*tef1*) the primers EF1- 728F and EF1-986R (Carbone and Kohn 1999) were used. PCR amplification and sequencing were conducted following the protocols of Hunter et al. (2006), Crous et al. (2009a, 2012) and Videira et al. (2017). The PCR mixtures consisted of 1 µL genomic DNA, 15× $MgCl_2$ reaction buffer (Bioline, Luckenwalde, Germany), 25 mM $MgCl_2$, 25 µM of each dNTP, 10 µM of each primer and 5 U Taq DNA polymerase (VWR) in a total volume of 25 µL. Cycling parameters of the PCR for LSU, SSU and ITS were as follows: initial denaturation at 94 °C for 3 min, followed by 35 cycles of amplification [denaturation at 94 °C for 30 s, primer annealing at 52 °C for 30 s and primer extension at 72 °C for 45 s] and a final extension at 72 °C for 5 min, followed by storage at 8 °C. The PCR mixture for *tef1* contained 2 µL of template DNA and the cycling parameters to obtain the partial *tef1* were as follows: an initial denaturation at 96 °C for 2 min; followed by 35 cycles of amplification [denaturation at 94 °C for 30 s, primer annealing at 56 °C for 30 s and primer extension at 72 °C for 30 s] and a final extension at 72 °C for 7 min, followed by storage at 8 °C. PCR-products were checked on 1.5% agarose electrophoresis gels containing HDGreenPlus DNA stain. Amplified PCR products were purified with the Cycle Pure Kit (VWR-Omega, USA). Sequencing was performed at Seqlab GmbH, Germany.

Molecular phylogeny

Amplification of the SSU, LSU, ITS and *tef1* gene regions for all isolates used in this study yielded fragments of approximately 1100 bp, 900 bp, 650 bp and 300 bp, respectively. Consensus sequences of trace files were generated with Geneious 10.2.2 (https://www.geneious.com, Kearse et al. 2012) and searched against GenBank (https://www.ncbi.nlm.nih.gov/, Benson et al. 2014) with MegaBLAST. Sequences with a high similarity (65 sequences of LSU, ITS and *tef1* regions) were retrieved (Table 1). A total of 148 sequences for 65 specimens were obtained from GenBank (Table 1) and 92 sequences for 28 specimens from Benin were generated in this study (Table 2). They were aligned with MAFFT v. 7 using the L-INS-i algorithm (Nakamura et al. 2018). The alignments were manually checked by using MEGA v. 7 (Kumar et al. 2016). Gblocks v. 0.91b (Talavera and Castresana 2007) was used to remove poorly aligned positions and divergent regions from the DNA alignment using the parameters for a less stringent

Table 1. Data of DNA sequences of cercosporoid fungi downloaded from GenBank and used in this study.

Species	Host	Host family	Country	Source	GenBank Accession Numbers			Reference
					nrLSU	ITS	*tef1*	
Cercospora cf. *apii* Fresen.	*Cajanus cajan* (L.) Millsp.	Fabaceae	S. Africa	CBS 115411	JN941171	JN942278	–	Groenewald JZ et al. (2013)
Cercospora asparagi Sacc.	*Asparagus* sp.	Asparagaceae	USA	AS16-02	KY549100	KY549098	KY549102	Hay et al. (2017)
Cercospora canescens Ellis & G.Martin	*Vigna radiata* (L.) R.Wilczek.	Fabaceae	India	Cer70-18	–	MN795675	–	Das et al. 2019
Cercospora capsica Heald & F.A.Wolf	*Capsicum annuum* L.	Solanaceae	S. Korea	CBS 132622	–	JX143568	JX143323	Groenewald JZ et al. (2013)
Cercospora cf. *citrulline* Cooke	*Citrullus lanatus* (Thunb.) Matsum. & Nakai	Cucurbitaceae	Japan	MUCC 576	–	JX143579	JX143337	Groenewald JZ et al. (2013)
Cercospora dubia Speg.	*Chenopodium* sp.	Amaranthaceae	Mexico	CPC 15600	KX286968	KX287277	–	Videira et al. (2016)
Cercospora kikuchii (Tak. Matsumoto & Tomoy.) M.W.Gardner	*Glycine max* (L.) Merr.	Fabaceae	USA	DLS5070-3A		AY373573	AY373582	Cai and Schneider (2008)
Cercospora lactucae-sativae Sawada	*Lactuca sativa* L.	Asteraceae	Japan	MUCC 570	–	JX143623	JX143382	Groenewald JZ et al. (2013)
Cercospora malayensis F.Stevens & Solheim	*Abelmoschus esculentus* (L.) Moench	Malvaceae	S. Korea	KACC 47769	–	MH129519	MH129517	Ju et al. (2020)
Cercospora cf. *maloti* Ellis & Everh.	*Cucumis melo* L.	Cucurbitaceae	Japan	MUCC 575	–	JX143625	JX143384	Groenewald JZ et al. (2013)
Cercospora cf. *nicotianae* Ellis & Everh.	*Nicotiana tabacum* L.	Solanaceae	–	CBS 570.69	–	DQ835074	DQ835100	Groenewald JZ et al. (2010)
Cercospora olivascens Sacc.	*Aristolochia clematitis* L.	Aristolochiaceae	Romania	CBS 253.67	–	JX143632	JX143391	Groenewald JZ et al. (2013)
Cercospora physalidis Ellis	*Solanum melongena* L.	Solanaceae	India	Cer 69-18	MK027095	MK029358	–	Sinha et al., unpublished
Cercospora rodmanii Conway	*Eichhornia* sp.	Pontederiaceae	Mexico	15-GTOX	GQ884187	GQ884185	–	Montenegro-Calderón et al. (2011)
Cercospora sojina Hara	*Glycine soja* Siebold & Zucc.	Fabaceae	S. Korea	CBS 132615	–	JX143659	JX143419	Groenewald JZ et al. (2013)
Cercospora sp. Q JZG-2013	*Acacia mangium* Willd.	Fabaceae	Thailand	CPC 10550	–	AY752139	AY752172	Groenewald JZ et al. (2013)
Cercospora vignigena C.Nakash., Crous, U.Braun & H.D.Shin	*Vigna unguiculata* (L.) Walp.	Fabaceae	Japan	MUCC 579	–	JX143736	JX143495	Groenewald JZ et al. (2013)
Cercospora zebrina Pass.	*Trifolium subterraneum* L.	Fabaceae	Australia	CBS 118790	KF251651	KF251147	–	Quaedvlieg et al. (2013)
Cladosporium sphaerospermum Penz.	–	–	Russia	G402	KJ443113	KJ443245	KJ443201	Grum-Grzhimaylo et al. (2016)
Mycosphaerella keniensis Crous & T.A.Cout.	*Eucalyptus grandis* W.Hill	Myrtaceae	Kenya	CMW5147	DQ246259	–	DQ235100	Hunter et al. (2006)
Mycosphaerella microsora Syd.	*Tilia platyphyllos* Scop.	Malvaceae	Romania	CBS 552.71	MH872022	MH860260		Vu et al. (2019)
Mycosphaerella valgourgensis Crous	*Yucca* sp.	Asparagaceae	France	CPC:18385	JF951175	JF951152	–	Crous et al. (2011)
Nothopassalora personata (Berk. & M.A.Curtis) U. Braun, C.Nakash., Videira & Crous	*Arachis hypogaea* L.	Fabaceae	Australia	CBS 142236	NG_058496	NR_156379	–	Videira et al. (2017)
Paracercospora egenula (Syd.) Deighton	*Solanum melongena* L.	Solanaceae	India	CBS 485.81	JQ324940	GU269699	GU384415	Crous et al. (2013a)
Passalora arctostaphyli Moreno-Rico & Crous	*Arctostaphylos pungens* Kunth	Ericaceae	Mexico	CPC 22067	KJ152785	KJ152782	–	Moreno-Rico et al. (2014)
Neocercosporidium smilacis (Thüm.) U.Braun, C. Nakash., Videira & Crous	*Smilax aspera* L.	Smilacaceae	Italy	CBS 556.71	KJ633269	KJ633265	–	Collemare et al. (2015)
Pseudocercospora abelmoschi (Ellis & Everh.) Deighton	*Hibiscus syriacus* L.	Malvaceae	S.Korea	CBS 132103	GU253696	GU269647	GU384365	Crous et al. (2013a)

Species	Host	Host family	Country	Source	GenBank Accession Numbers			Reference
					nrLSU	ITS	*tef1*	
Pseudocercospora atromarginalis (G.F.Atk.) Deighton	*Solanum* sp.	Solanaceae	New Zealand	CBS 114640	GU253706	GU269658	GU384376	Crous et al. (2013a)
Pseudocercospora cercidicola Crous, U.Braun & C. Nakash.	*Cercis chinensis* Bunge	Fabaceae	Japan	MUCC 896	GU253719	GU269671	GU384388	Crous et al. (2013a)
Pseudocercospora chengtuensis (F.L.Tai) Deighton	*Lycium chinense* Mill.	Solanaceae	S. Korea	CBS 131924	MH877506	MH866053	–	Vu et al. (2019)
Pseudocercospora chiangmaiensis Cheew., K.D.Hyde & Crous	*Eucalyptus camaldulensis* Dehnh.	Myrtaceae	Thailand	CBS 123244	MH874812	MH863288	–	Vu et al. (2019)
Pseudocercospora cruenta (Sacc.) Deighton	*Phaseolus vulgaris* L.	Fabaceae	Taiwan	CBS 117232	GU253730	GU269689	GU384405	Crous et al. (2013a)
Pseudocercospora cydoniae (Ellis & Everh.) Y.L.Guo & X.J.Liu	*Chaenomeles speciosa* (Sweet) Nakai	Rosaceae	S. Korea	CBS 131923	MH877505	MH866052	–	Vu et al. (2019)
Pseudocercospora dingleyae U.Braun & C.F.Hill	*Haloragis erecta* (Murray) Oken	Haloragaceae	New Zealand	CBS 114645	KX286997	KX287299	–	Videira et al. (2016)
Pseudocercospora dovyalidis (Chupp & Doidge) Deighton	*Dovyalis zeyheri* (Sond.) Warb.	Salicaceae	S. Africa	CBS 126002	MH875338	MH863877	–	Vu et al. (2019)
Pseudocercospora encephalarti Y.Meswaet, Mangelsdorff, Yorou & M.Piepenbr.	*Encephalartos barteri* Carruth. ex Miq.	Zamiaceae	Benin	YMMAS78	–	MK397016	–	Meswaet et al. (2019)
Pseudocercospora flavomarginata G.C.Hunter, Crous & M.J.Wingf.	*Eucalyptus camaldulensis* Dehnh.	Myrtaceae	Thailand	CBS 118824	–	NR_111805	–	Quaedvlieg et al. (2012)
Pseudocercospora fuligena (Roldan) Deighton	*Solanum lycopersicum* L.	Solanaceae	Japan	MUCC 533	GU253749	GU269712	GU384428	Crous et al. (2013a)
Pseudocercospora griseola f. griseola (Sacc.) Crous & U.Braun	*Phaseolus vulgaris* L.	Fabaceae	S. Korea	CBS 131929	MH877495	MH866046	–	Vu et al. (2019)
Pseudocercospora hakeae (U.Braun & Crous) U. Braun & Crous	*Hakea* sp.	Proteaceae	Australia	CBS:144520	MK442553	MK442617	MK442708	Crous et al. (2019)
Pseudocercospora humuli (Hori) Y.L.Guo & X.J.Liu	*Humulus lupulus* L.	Cannabaceae	Japan	MUCC 742	GU253758	–	GU384439	Crous et al. (2013a)
Pseudocercospora kaki Goh & W.H.Hsieh	*Diospyros kaki* L.f.	Ebenaceae	Japan	MUCC 900	GU253761	GU269729	GU384442	Crous et al. (2013a)
Pseudocercospora madagascariensis Crous & M.J.Wingf.	*Eucalyptus camaldulensis* Dehnh.	Myrtaceae	Madagascar	CBS 124155	MH874880	MH863357	–	Vu et al. (2019)
Pseudocercospora metrosideri U.Braun	*Metrosideros collina* (J.R.Forst. & G.Forst.) A.Gray	Myrtaceae	New Zealand	CBS 118795	GU253774	GU269746	GU384458	Crous et al. (2013a)
Pseudocercospora neriicola Crous, Frisullo & Camele	*Nerium oleander* L.	Apocynaceae	Italy	CPC 23765	KJ869222	KJ869165	KJ869240	Crous et al. (2014)
Pseudocercospora pallida (Ellis & Everh.) H.D.Shin & U.Braun	*Campsis grandiflora* (Thunb.) K.Schum.	Bignoniaceae	S. Korea	CBS 131889	–	–	GU384469	Crous et al. (2013a)
Pseudocercospora paraguayensis (Tak. Kobay.) Crous	*Eucalyptus nitens* (H.Deane & Maiden) Maiden	Myrtaceae	Brazil	CBS:111286	KF901945	KF901619	KF903205	Quaedvlieg et al. (2014)
Pseudocercospora parapseudarthriae Crous & A.R.Wood	*Pseudarthria hookeri* Wight & Arn.	Fabaceae	S. Africa	CPC 23449	KJ869208	KJ869151	KJ869238	Crous et al. (2014)
Pseudocercospora pittospori (Plakidas) Y.L.Guo & X.J.Liu	*Pittosporum* sp.	Pittosporaceae	USA	HI-018	MK210475	MK210511	–	Vaghefi et al. 2021

Species	Host	Host family	Country	Source	GenBank Accession Numbers			Reference
					nrLSU	ITS	*tef1*	
Pseudocercospora proteae Crous	*Protea mundii* Klotzsch	Proteaceae	S. Africa	CBS 131587	–	–	GU384519	Crous et al. (2013a)
Pseudocercospora prunicola (Ellis & Everh.) U.Braun	*Prunus* sp.	Rosaceae	China	BJFU ZYP141005.9	KX853057	KX853048	KX853066	Liu et al. (2016)
Pseudocercospora ranjita (S.Chowdhury) Deighton	*Gmelina* sp.	Lamiaceae	Indonesia	CBS 126005	MH875340	MH863879	GU384500	Crous et al. (2013a)
Pseudocercospora ravenalicola G.C.Hunter & Crous	*Ravenala madagascariensis* Sonn.	Strelitziaceae	India	CBS 122468	GU253828	–	GU384521	Crous et al. (2013a)
Pseudocercospora schizolobii (M.J.Wingf. & Crous) M.J.Wingf. & Crous	*Eucalyptus camaldulensis* Dehnh.	Myrtaceae	Thailand	CBS 124990	KF251827	KF251323	KF253270	Verkley et al. (2013)
Pseudocercospora sennae-multijugae Meir. Silva, R.W.Barreto & Crous	*Senna multijuga* (Rich.) H.S.Irwin & Barneby	(Fabaceae)	Brazil	CPC 25206	KT290169	KT290142	KT290196	Silva et al. (2016)
Pseudocercospora sp.	*Citrus grandis* (L.) Osbeck	Rutaceae	China	ZJUM 75	KP895896	KP896026	KP896073	Huang et al. (2015)
Pseudocercospora sp.	*Eichhornia azurea* (Sw.) Kunth	Pontederiaceae	Brazil	CPC 19537	KX287003	KX287304	–	Videira et al. (2016)
Pseudocercospora sp.	*Eichhornia azurea* (Sw.) Kunth	Pontederiaceae	Brazil	CPC 19535	KX287001	KX287303	–	Videira et al. (2016)
Pseudocercospora sp. A MB-2015	*Phaseolus vulgaris* L.	Fabaceae	Iran	CCTU 1166	KP717028	KM452864	KM452886	Bakhshi et al. (2014)
Pseudocercospora stizolobii (Syd. & P.Syd.) Deighton	*Eucalyptus camaldulensis* Dehnh.	Myrtaceae	Thailand	CPC 25217	KT290170	KT290143	KT290197	Silva et al. (2016)
Pseudocercospora tereticornis Crous & Carnegie	*Eucalyptus tereticornis* Sm.	Myrtaceae	Australia	CBS 125214	MH874960	MH863460	–	Vu et al. (2019)
Pseudocercospora vitis (Lév.) Speg.	*Vitis vinifera* L.	Vitaceae	S. Korea	CPC 11595	–	–	JX901702	Quaedvlieg et al. (2012)
Pseudocercosporella bakeri (Syd. & P.Syd.) Deighton	*Ipomoea indica* (Burm.) Merr.	Convolvulaceae	New Zealand	CBS 119488	KX287005	KX287306	KX287862	Videira et al. (2016)
Pseudocercosporella myopori U.Braun & C.F.Hill	*Myoporum laetum* G.Forst.	Scrophulariaceae	New Zealand	CBS 114644	KX287000	KX287302	JX143491	Groenewald JZ et al. (2013)
Zasmidium daviesiae (Cooke & Massee) U.Braun, C.Nakash., Videira & Crous	*Daviesia latifolia* R.Br.	Fabaceae	Australia	CBS:116002	KF901928	KF901603	KF903373	Quaedvlieg et al. (2014)

Table 2. Data of sequences of cercosporoid fungi from Benin generated during the present study. Names of species proposed as new in this study are written in bold.

Species	Voucher	Host	Host family	GenBank Accession Numbers			
				nrSSU	nrLSU	ITS	tef1
Cercospora beninensis	YMM11	*Crotalaria macrocalyx* Benth.	Fabaceae	MW834445	MW834433	MW834437	MW848615
Cercospora aff. *canescens* Ellis & G.Martin	YMM07	*Calopogonium* sp.	Fabaceae	MW834475	–	MW834492	MW848605
	YMM01	*Vigna subterranea* (L.) Verdc.	Fabaceae	MW834473	MW834457	MW834490	MW848603
Cercospora cf. *canscorina* Chidd.	YMM05	*Vigna* sp.	Fabaceae	MW834474	MW834458	MW834491	MW848604
Cercospora cf. *fagopyri* K.Nakata & S.Takim.	YMM23A	*Lablab* sp.	Fabaceae	–	–	MW861543	MW848607
Cercospora parakouensis	YMM296A	*Desmodium tortuosum* (Sw.) DC.	Fabaceae	–	MW834436	MW834442	MW848621
Cercospora phaseoli-lunati U.Braun & Crous	YMM289	*Vigna radiata* (L.) R.Wilczek	Fabaceae	MW834471	–	MW834483	MW848601
Cercospora rhynchophora	YMM03B	*Vigna unguiculata* (L.) Walp.	Fabaceae	MW834447	MW834431	MW834443	MW848619
Cercospora sp.1	YMM3S	*Sorghum bicolor* (L.) Moench	Poaceae	MW834466	MW834452	MW834484	MW848600
Cercospora sp.2	YMM48S	*Sorghum bicolor* (L.) Moench	Poaceae	MW834467	MW834453	MW834485	MW848608
Cercospora sp.3	YMM229	*Spigelia* sp.	Loganiaceae	–	MW834462	MW834500	MW848599
Cercospora sp.4	YMM297B	*Phaseolus lunatus* L.	Fabaceae	MW834481	MW834464	MW834501	MW848612
Cercospora tentaculifera	YMM75	*Vigna unguiculata* (L.) Walp.	Fabaceae	MW834448	–	MW834440	MW848614
Cercospora vignae-subterraneae	YMM293	*Vigna subterranea* (L.) Verdc.	Fabaceae	MW834446	–	MW834438	MW848618
Cercospora zorniicola	YMM299	*Zornia glochidiata* DC.	Fabaceae	–	–	–	MW848616
Nothopassalora personata (Berk. & M.A.Curtis) U.Braun, C.Nakash., Videira & Crous	YMM49A	*Arachis hypogaea* L.	Fabaceae	MW834479	MW844038	MW834497	–
Passalora arachidicola (Hori) U.Braun	YMM49B	*Arachis hypogaea* L.	Fabaceae	MW845059	MW844039	MW834498	–
Pseudocercospora bradburyae E.Young	YMM275	*Centrosema pubescens* Benth.	Fabaceae	MW834465	–	–	MW848609
Pseudocercospora cruenta (Sacc.) Deighton	YMM288	*Phaseolus* sp.	Fabaceae	MW834472	MW834456	MW834489	MW848602
	YMM04	*Vigna unguiculata* (L.) Walp.	Fabaceae	MW834478	MW834461	MW834496	MW848606
	YMM03A	*Vigna unguiculata* (L.) Walp.	Fabaceae	MW834482	MW834460	MW834495	MW848613
	YMM294B	*Vigna unguiculata* (L.) Walp.	Fabaceae	MW834480	MW834463	MW834493	MW848611
	YMM125	*Vigna unguiculata* (L.) Walp.	Fabaceae	MW834476	MW834451	MW834499	MW848610
Pseudocercospora griseola (Sacc.) Crous & U.Braun	YMM297A	*Phaseolus lunatus* L.	Fabaceae	MW834477	MW834459	MW834494	–
Pseudocercospora sennicola	YMM12	*Senna occidentalis* (L.) Link	Fabaceae	MW834444	MW834432	MW850550	–
Pseudocercospora sp.3	YMM19	*Abelmoschus* sp.	Malvaceae	MW834470	–	MW834488	–
Pseudocercospora sp.1	YMM123	*Abelmoschus* sp.	Malvaceae	MW834468	MW834454	MW834486	–
Pseudocercospora tabei	YMM220	*Vigna unguiculata* (L.) Walp.	Fabaceae	MW834450	MW834434	MW834439	MW848617

selection. Subsequently, a four-locus concatenated alignment (SSU, LSU, ITS and *tef1*) dataset was assembled for phylogenetic analyses using Geneious 10.2.2. *Cladosporium sphaerospermum* (G402) served as outgroup taxon, because the genus *Cladosporium* s. str. was shown to be the sister group of *Mycosphaerella* s. str. (Braun et al. 2003). PartitionFinder2 v.2.1.1 (Lanfear et al. 2014) on XSEDE (Miller et al. 2010) was used to select the best-fit model of evolution for each gene fragment separately. Data were partitioned by gene and by codon position in the case of protein-coding sequences. The TRNEF+G model was applied to 28S rDNA, K80 model to 18S rDNA, K81+G to ITS and TRN+G model to *tef1*. The alignment and the tree were deposited in TreeBASE (http://purl.org/phylo/treebase/phylows/study/TB2:S28032). Phylogenetic analyses of this study were conducted by applying Maximum Likelihood (ML) in RAxML-HPC2 v.8.2.12 (Stamatakis 2014) on XSEDE (Miller et al. 2010) and Bayesian with the program MrBayes 3.2.6 (Ronquist et al. 2012) on XSEDE (Miller et al. 2010) on the CIPRES Science Gateway web portal. (http://www. phylo.org/sub_sections/portal/).

For Maximum Likelihood analyses one thousand nonparametric bootstrap iterations were used with the generalised time-reversible model with a discrete gamma distribution (GTRGAMMA) (Stamatakis et al. 2008). For Bayesian phylogenies, two parallel runs with eight chains of Metropolis-coupled Markov chain Monte Carlo iterations were performed with the heat parameter being set at 0.2. Analyses were run for 100 million generations, with trees sampled every 1000th generation until the average standard deviation of split frequencies reached 0.01 (stop value). The first 25% of saved trees were discarded as the 'burn-in' phase. Posterior probabilities (PP) were determined from the remaining trees. Bayesian posterior probabilities (BPP) ≥ 94% and Bootstrap values (BS) ≥ 70% are considered as significant.

Data availability

The specimen data is available through the Dryad Digital Repository https://datadryad.org/ (https://doi.org/10.5061/dryad.73n5tb2x9).

Results

Phylogeny

We isolated DNA from a total of 28 specimens of cercosporoid fungi recently collected in Benin (Table 2). These specimens represent 18 species found on species of Fabaceae for which 76 sequences are provided: 20 sequences of 18S rDNA, 16 of 28S rDNA, 21 of ITS and 19 of *tef1*. The separately aligned data sets for each marker consisted of 35 sequences/893 base pairs for 18S rDNA, 60/719 for 28S rDNA, 82/437 for ITS and 74/160 for *tef1*.

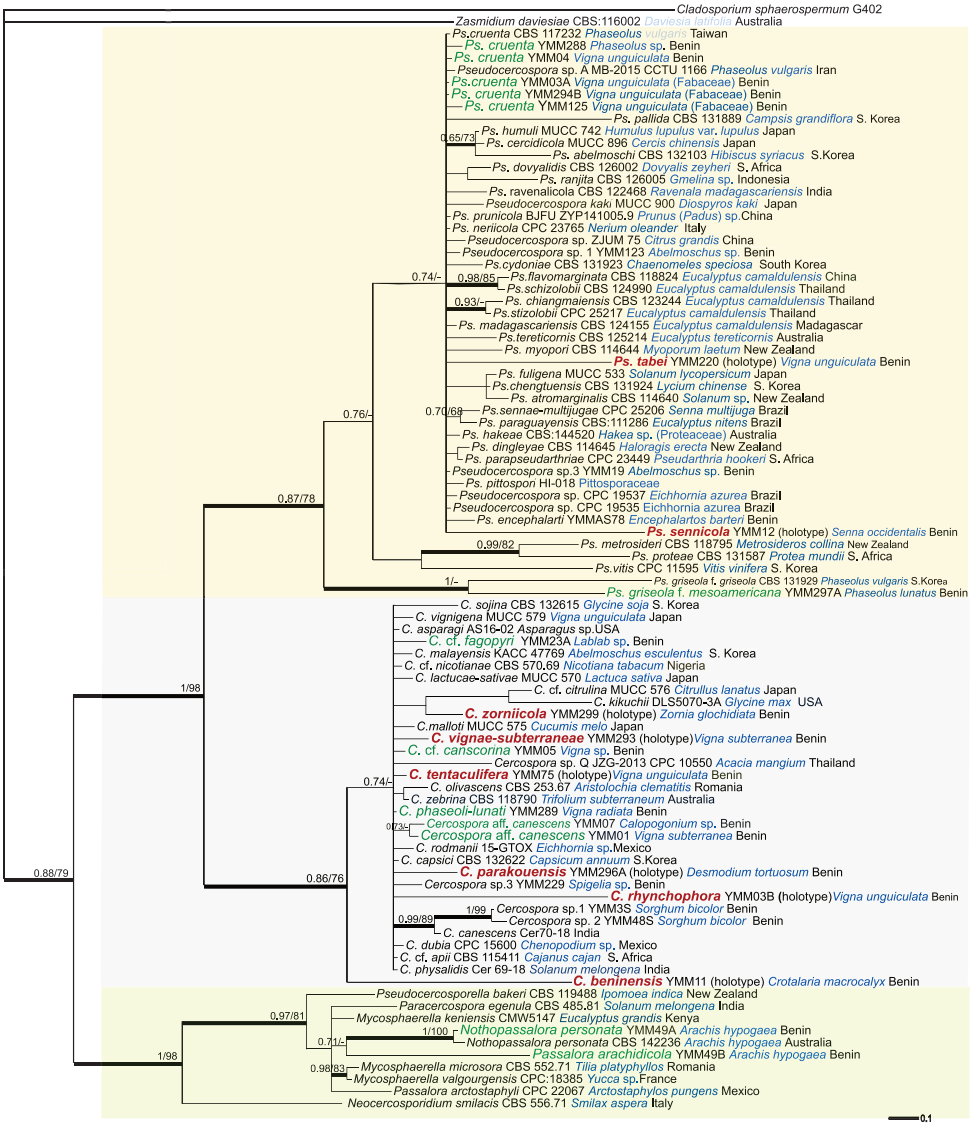

Figure 1. The Bayesian phylogenetic tree inferred from DNA sequence data from the multigene alignment (SSU rDNA, LSU rDNA, ITS and *tef1*) of cercosporoid species. Nodes receiving Bayesian PP ≥ 0.94 or ML BS ≥ 70% are considered as strongly supported and are indicated by thickened branches. Names of newly described species are written in bold and red. Species newly reported for Benin are indicated by green letters. Names of host plants are written with blue letters.

For the four-locus data analysis, DNA sequence data from the 18SrDNA, 28SrDNA, ITS and *tef1* gene regions were combined and submitted to Bayesian and Maximum Likelihood (ML) analyses. The final concatenated alignment contained a total of 91 specimens including the out-group (65 specimens from NCBI and 26 specimens from this study) and had an aligned length of 2212 characters including alignment

gaps. As the ML analyses produced tree topologies mostly identical to results of Bayesian analyses, bootstrap support values of the ML trees were incorporated into the tree that resulted from Bayesian analyses (Fig. 1). In this tree, the cercosporoid fungi are grouped in three major clades: *Cercospora* (86/76), *Pseudocercospora* (87/78) and *Passalora* together with other species of other genera (100/98) (Fig. 1). Phylogenetic analyses of individual loci are deposited in TreeBASE. Details of results concerning the delimitation of species are mentioned and discussed as part of species notes below.

Tef1 sequence data showed differences between closely related species in the genera *Cercospora* and *Pseudocercospora* and are more informative than ITS and LSU rDNA sequence data. Therefore, we provide molecular phylogenetic analyses based on new *tef1* sequences as well as sequences from GenBank for some newly described species, namely *Cercospora rhynchophora*, *C. parakouensis*, *C. zorniicola* and *Pseudocercospora tabei*. For *Ps. sennicola*, we provide an analysis based on ITS sequence data, because we were not able to obtain *Tef1* sequence data.

Taxonomy

Based on morphological, molecular phylogenetic and host evidence, the cercosporoid fungi recently collected in Benin are assigned to 18 different taxa belonging to four genera. Among these, eight species are proposed as new to science, six in the genus *Cercospora* and two in *Pseudocercospora*. Eight species represent new reports for Benin, three of them are new for the whole of West Africa, namely *Cercospora* cf. *canscorina*, *C.* cf. *fagopyri* and *C. phaseoli-lunati*. Two species of cercosporoid fungi were previously reported in Benin and are confirmed.

Cercospora beninensis **Y.Meswaet, Mangelsdorff, Yorou & M.Piepenbr., sp. nov.**
MycoBank No: 839170
Figs 2A, 3

Etymology. The epithet *beninensis* refers to the country of origin of the type specimens, Benin.

Diagnosis. *Cercospora beninensis* differs from four *Cercospora* spp. known on *Crotalaria* spp. by having only internal hyphae, darker, shorter and narrower conidiophores [(14.5–)28.5–160(–168) × (3–)3.5–4.5(–5) µm] and mostly smaller and narrower conidia [(19–)23.5–122(–150) × (2.5–)3–4(–4.5) µm] (Table 3).

Type. Benin. Borgou: Parakou, c. 363 m a.s.l., 9°20'29"N, 2°37'28"E, on *Crotalaria macrocalyx* Benth. (Fabaceae), 21 Sep 2019, Y. Meswaet and R. Dramani, YMM11 (***Holotype*****:** M-0312640; ***Isotype*****:** UNIPAR). ***Ex holotype sequences.*** MW834445 (SSU), MW834433 (LSU), MW834437 (ITS), MW848615 (*tef1*).

Description. ***Leaf spots*** amphigenous, subcircular to angular-irregular, (0.5–)1.5–5.5 mm diam., brown to reddish brown, more evident on the adaxial surface of the leaves than on the abaxial side, occasionally with a chlorotic halo, the outermost ring darker than the inner ring, often with indefinite margin. ***Caespituli*** amphigenous,

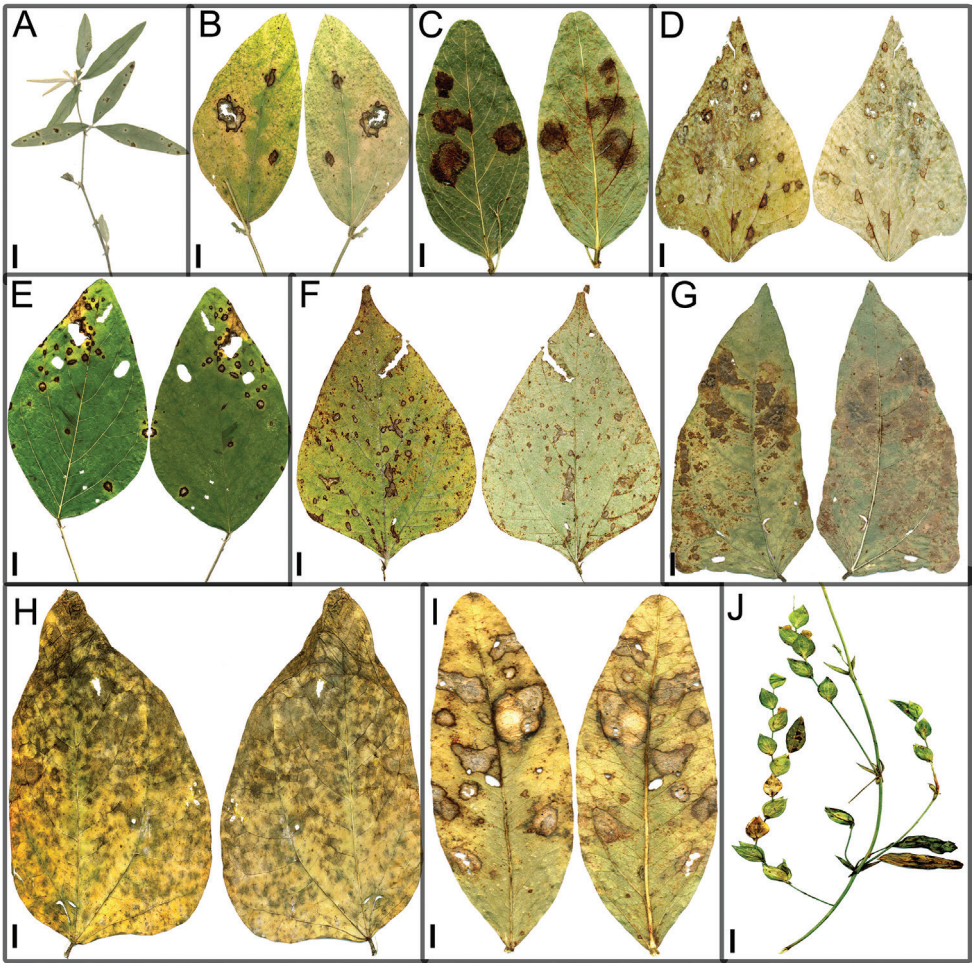

Figure 2. Leaf spot symptoms associated with *Cercospora* spp. **A** *Cercospora beninensis* on *Crotalaria macrocalyx* (YMM11) **B** *Cercospora* aff. *canescens* on *Calopogonium* sp. (YMM07) **C** *Cercospora* aff. *canescens* on *Vigna subterranea* (YMM01) **D** *Cercospora fagopyri* on *Lablab* sp. (YMM23A) **E** *Cercospora parakouensis* on *Desmodium tortuosum* (YMM296A) **F** *Cercospora phaseoli-lunati* on *Vigna radiata* (YMM289) **G** *Cercospora rhynchophora* on *Vigna unguiculata* (YMM03B) **H** *Cercospora tentaculifera* on *Vigna unguiculata* (YMM75) **I** *Cercospora vignae-subterraneae* on *Vigna subterranea* (YMM293) **J** *Cercospora zorniicola* on *Zornia glochidiata* (YMM299). Scale bars: 10 mm (**A, C, F, G**); 12 mm (**B, D, E, H, J**); 6 mm (**I**).

mainly epiphyllous, greyish brown to dark brown. ***Mycelium*** internal. Internal hyphae conspicuous, branched, 2.5–3.5 µm wide, septate, pale brown. ***Stromata*** lacking or formed by few aggregated swollen hyphal cells. ***Conidiophores*** in small, loose to moderately dense fascicles of up to approx. 16 conidiophores, occasionally solitary, arising from internal hyphae breaking through the adaxial epidermis of the leaves or penetrating through stomatal openings, erect, straight, subcylindrical, 1–2(–3) times geniculate, sometimes attenuated towards the tips, occasionally branched, (14.5–)28.5–160(–168) × (3–)3.5–4.5(–5) µm, 0–6(–8)-septate, brown to dark brown. ***Conidiogenous***

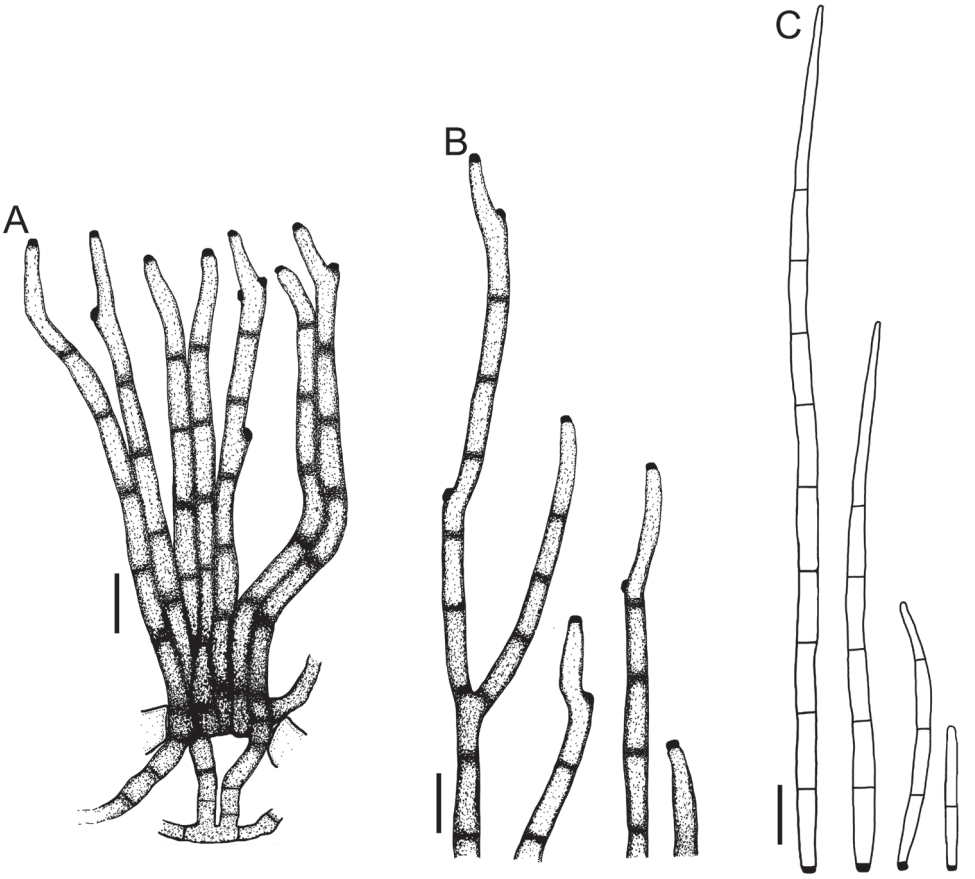

Figure 3. *Cercospora beninensis* on *Crotalaria macrocalyx* (YMM11) **A** fascicle of conidiophores **B** individual conidiophores **C** conidia. Scale bars: 15 µm (**A**); 10 µm (**B, C**).

cells monoblastic or proliferating sympodially, sometimes distinctly subdenticulate; loci 1.5–2.5(–3.5) µm wide, thickened and darkened. ***Conidia*** solitary, acicular to narrowly obclavate, straight to curved, (19–)23.5–122(–150) × (2.5–)3–4(–4.5) µm, 1–7(–9)-septate, hyaline, smooth, tip acute, base truncate to short obconically truncate, 2.5–3(–4) µm wide, hila thickened and darkened.

Additional specimens examined. Benin. Borgou: Parakou, on the way to Okpara forest, c. 323 m a.s.l., 9°18'11"N, 2°43'50"E, on *Crotalaria macrocalyx*, 3 Sep 2019, Y. Meswaet and R. Dramani, YMM274 (***Paratypes*****:** M-0312641; UNIPAR). Benin. Borgou: N'Dali, c. 380 m a.s.l., 9°52'33"N, 2°41'20"E, same host, 31 Aug 2019, Y. Meswaet and A. Tabé, YMM272 (M-0312642).

Host and distribution. On *Crotalaria macrocalyx* (Fabaceae) in Benin.

Notes. Currently, three species and one form of *Cercospora* are known on *Crotalaria* spp., namely *C. apii*, *C. canescens*, *C. demetrioniana* G.Winter and *C. demetrioniana* f. *minor* Gonz. Frag. & Cif. (Farr and Rossman 2021). *C. beninensis* is morphologically distinct from all of them (Table. 3). *C. apii* differs by conidiophores that are more

Table 3. Comparison of *Cercospora beninensis* (YMM11) on *Crotalaria macrocalyx* with *Cercospora* spp. known from *Crotalaria* spp. based on literature [a–f].

Cercospora species	Leaf spots colour, size	Stromata	Conidiophore size (in µm), branching, septa, colour	Conidium sizes (in µm), septa
Cercospora beninensis (YMM11)	Brown to reddish brown, 0.5(1.5–)–5.5 mm diam.	Small or lacking	(14.5–)28.5–160(–168) × (3–)3.5–4.5(–5), branched, 0–6(–8)-septate, dark brown	(19–)23.5–122(–150) × (2.5–)3.5–4(–4.5), 1–7(–9) septa
C. apii [ab]	Present	Often small or lacking, occasionally developed, (up to 50 µm diam.)	20–300 × 4–6.5, rarely branched, multi-septate, pale brown, uniform in colour and width	25–315 × 3–6, (0–)3–25(–30) septa[b]
C. canescens [a]	3–15 mm	Often small	20–200 × 3–6.5, rarely branched, multi-septate, pale to medium dark brown	25–300 × 2.5–5.5, indistinctly multi-septate
C. demetrioniana [cde]	Rusty brown to dark brown, 1–1.5 mm.	Present	40–350 × 4–6 (–7) [c] or up to 1 mm[de], 1–10-septate, unbranched, pale brown	50–210 × 3.5–5.5 /75–230 × 4–7, 7–16, very closely and indistinctly septate
C. demetrioniana f. *minor*[f]	No information	No information	110–130 × 5–6	35–70(–170) × 5–5.5

[a] Hsieh and Goh (1990), [b] Crous and Braun (2003), [c] Chupp (1954), [d] Saccardo (1886), [e] Winter (1884), [f] Ciferri and González-Fragosa (1926).

abundant on the abaxial surface of the leaves, in large and dense fascicles and longer [20–300 µm versus (14.5–)28.5–160(–168) in *C. beninensis*] as well as by longer and wider conidia [(25–315 × 3–6 µm versus (19–)23.5–122(–150) × (2.5–)3–4(–4.5) in *C. beninensis*] with more numerous septa (Chupp 1954; Crous and Braun 2003). *C. canescens* causes larger leaf spots often along the leaf margin, paler conidiophores that are more abundant on the abaxial leaf surface and longer conidia [(30–300) µm versus (19–)23.5–122(–150) µm in *C. beninensis*] (Chupp 1954). The distinctness is confirmed by molecular data. *C. demetrioniana* produces unbranched, paler, longer and wider conidiophores [40–350 × 4–6(–7) µm, in the original description a length of up to 1 mm is mentioned, versus (14.5–)28.5–160(–168) × (3–)3.5–4.5(–5) in *C. beninensis*] and above all, longer and wider conidia (75–230 × 4–7 µm with 7–16 indistinct septa versus (19–)23.5–122(–150) × (2.5–)3–4(–4.5) µm with 1–7(–9) distinct septa in *C. beninensis*] (Winter 1884; Saccardo 1886; Chupp 1954). *C. demetrioniana* f. *minor* differs from the present species by shorter and wider conidiophores (110–130 × 5–6 µm) and wider conidia (5–5.5 µm) (Ciferri and González-Fragoso 1926).

C. beninensis is distinct from all known species for which DNA sequence data are available based on its position in the multi-gene (Fig. 1) and in the *tef1* phylogeny (see Suppl. material 4). In the ITS phylogeny, *C. beninensis* cannot be distinguished from other *Cercospora* spp. (see Suppl. material 3).

***Cercospora* aff. *canescens* Ellis & G.Martin, Am. Nat. 16(12): 1003 (1882).**
MycoBank No: 179841
Figs 2B, C, 4

Type. USA (no further data available), on *Phaseolus* sp. (Fabaceae), 1882, s.n. ("Type?" NY, n.v.).

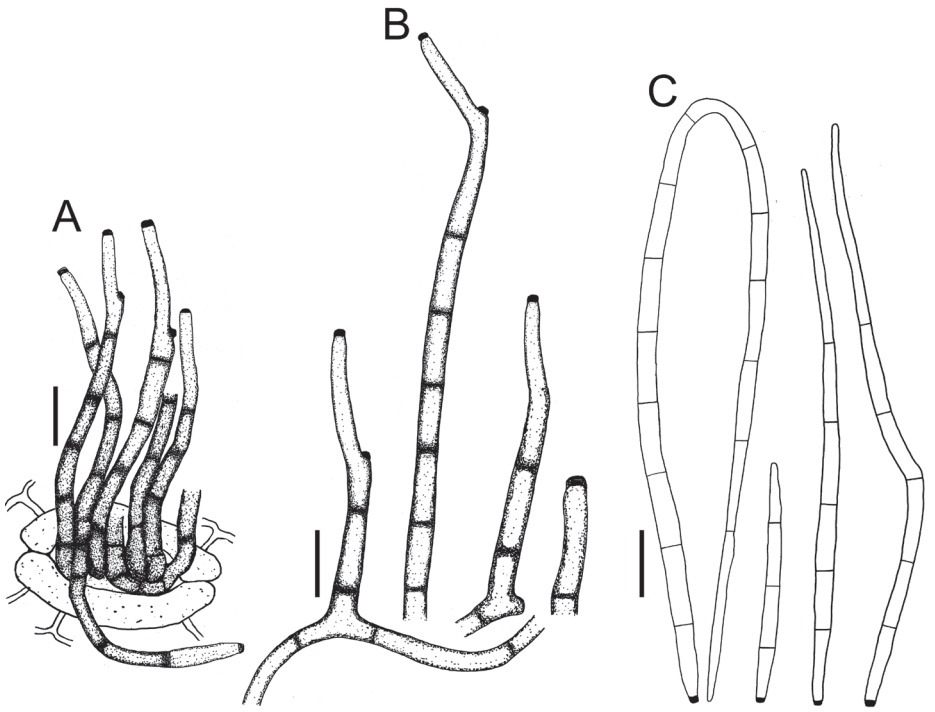

Figure 4. *Cercospora* aff. *canescens* on *Calopogonium* sp. (YMM07) **A** fascicle of conidiophores protruding from a stomatal opening **B** solitary conidiophores **C** conidia. Scale bars: 15 µm (**A, C**); 10 µm (**B**).

For synonyms see Crous and Braun (2003) or MycoBank.

Description. ***Leaf spots*** amphigenous, subcircular to irregularly angular, 3–11.5(–13) mm diam., occasionally crossing veins, reddish brown to slightly dark brown, with dark margin. ***Caespituli*** amphigenous, greyish brown to dark brown. ***Mycelium*** internal and external. Internal hyphae often indistinct. External hyphae branched, 2.5–3.5 µm wide, septate, olivaceous brown to brown, smooth. **Stromata** lacking or formed by few aggregated swollen hyphal cells, immersed in the mesophyll or in substomatal cavities, dark brown. ***Conidiophores*** in small, loose fascicles of up to 8, arising from stromata, breaking through the adaxial epidermis of the leaves or penetrating through stomatal openings, sometimes solitary arising through stomatal openings or erumpent through the cuticle, erect, straight to sinuous or somewhat geniculate, rarely branched, (16.5–)21–152(–165) × (4–)4.5–5.5 µm, 1–6-septate, brown to dark brown. ***Conidiogenous cells*** terminal, monoblastic to polyblastic, brown; loci 1.5–2.5 (–3) µm wide, thickened and darkened. ***Conidia*** solitary, narrowly obclavate to subacicular, straight to curved, (34–)38–280(–330) × (3–)3.5–4(–4.5) µm, 3–12(–14)-septate, hyaline to subhyaline, smooth, apex subacute or acute, base truncate to short obconically truncate, up to 2.5 µm wide, hila thickened and darkened.

Specimens examined. Benin. Borgou: Parakou, c. 363 m a.s.l., 9°20'29"N, 2°37'28"E, on *Calopogonium* sp., 21 Sep 2019, Y. Meswaet and A. Tabé, YMM07 (M-0312643,

UNIPAR). Benin. Borgou: Parakou, c. 395 m a.s.l., 9°21'27"N, 2°36'44"E, *Calopogonium* sp., 17 Sep 2019, Y. Meswaet and A. Tabé, YMM08 (M-0312644). Benin. Borgou: Parakou, c. 395 m a.s.l., 9°21'27"N, 2°36'44"E, on *Vigna subterranea*, 16 Sep 2019, Y. Meswaet and R. Dramani, YMM01 (M-0312645, UNIPAR).

Herbarium specimens examined for comparison. *C. canescens*. On *Vigna unguiculata* (as *V. sinensis* L.): El Salvador. Sacocoyo, 3 Jul 1943, Wellman F. L. 140 (BPI 434127B). On *V. unguiculata* (as *V. sinensis*): USA. Illinois: Gallatin County, 8 Sep 1932, G.H. Boewe B331 (ILL23703 ***Holotype*** of *C. vignicaulis* Tehon). On *V. unguiculata*: USA. Illinois: Pulaski, Olmstead, 17 Sep 1933, G.H. Boewe s.n. (ILL24809 ***Paratype*** of *C. vignicaulis*). On *V. unguiculata* (as *V. sinensis*): USA. Illinois: White, Carmi., 10 Sep 1934, G.H. Boewe B588 (ILL 25450 ***Paratype*** of *C. vignicaulis*).

Hosts and distribution. On many species of Fabaceae and of other families (Crous and Braun 2003), known worldwide, from Australia, Bangladesh, Brazil, Bolivia, Brunei, Cambodia, China, Colombia, Costa Rica, Cuba, Dominican Republic, Ecuador, Fiji, Ghana, Guyana, Haiti, Hong Kong, India, Indonesia, Iran, Japan, Kenya, Korea, Malawi, Malaysia, Malawi, Mauritius, Myanmar, Nepal, New Caledonia, New Zealand, Nigeria, Pakistan, Panama, Papua New Guinea, Peru, Philippines, Puerto Rico, Russia, Senegal, Sierra Leone, Solomon Islands, Somalia, South Africa, Saint Vincent and the Grenadines, Sudan, Tadzhikistan, Taiwan, Tanzania, Thailand, Trinidad and Tobago, Togo, Uganda, USA, Uzbekistan, Vanuatu, Venezuela, Zambia, Zimbabwe (Chupp 1954; Ellis 1976; Shin and Kim 2001; Crous and Braun 2003; Farr and Rossman 2021).

Notes. The present *Cercospora* sp. on *Calopogonium* sp. also occurs on *Vigna subterranea* with different leaf spot appearances and caespituli. The lesions on *Calopogonium* sp. appear to be associated with a species of Pleosporales, whereas the leaf lesions on *V. subterranea* apparently are not associated with any other fungus and are dark reddish brown to dark brown with a dark margin, which are typical symptoms caused by *Cercospora* spp. The lesions on *V. subterranea* are larger and more abundant than those on *Calopogonium* sp., with abundant, dense caespituli and with dark greyish brown pigmentation (Fig. 2C).

Cercospora canescens is the only species of *Cercospora* known for *Calopogonium* spp. (Farr and Rossman 2021) and has been reported from West Africa (Guinea) on *Calopogonium mucunoides* (Lenné 1990). Apart from having slightly narrower conidia [(3–)3.5–4(–4.5) µm versus 2.5–5.5(–6) µm in *C. canescens*] as described by Chupp (1954), Hsieh and Goh (1990) and Mulder and Holliday (1975), the present specimen from Benin is morphologically identical to *C. canescens*. In the phylogenetic analyses, however, DNA sequences of the two specimens from Benin cluster together but separately from sequences of *C. canescens* available from India. In the multi-gene tree (Fig. 1), *C. canescens* is located on a branch in a clade together with sequences of *Cercospora* spp. YMM3SO and YMM48SO on *Sorghum bicolor* (Poaceae) from Benin. *C. canescens* is known to correspond to a species complex that shows diverse morphological characteristics and genetic diversity (Joshi et al. 2006; Groenewald et al. 2013). Although *C. canescens* is an economically important species, no sequence data from the

type or a neotype specimen are available (e.g., Groenewald et al. 2013). These are indispensable to resolve the *C. canescens* species complex. The specimens collected in Benin are tentatively placed into the species complex of *C. canescens* until DNA sequence data from the type locality (USA) and from diverse host species are available. *C.* aff. *canescens* is cited here for the first time for Benin (Piepenbring et al. 2020).

***Cercospora* cf. *canscorina* Chidd., Sydowia 13 (1–6): 155. 1959.**
MycoBank No: 294326
Fig. 5

Type. India. R. Br. Khandala (Maharashtra), on *Canscora diffusa* (Vahl) R.Br. ex Roem. & Schult. (Gentianaceae), 9 Nov 1956, Chiddarwar 4 (***Holotype*:** IMI 83165, n.v.; ***Isotypes*:** HCIO, BPI, n.v.).

Description. ***Leaf spots*** amphigenous, subcircular to irregularly angular, 2.5–8 mm diam., brown to reddish brown, with a dark margin. ***Caespituli*** amphigenous, greyish brown to brown. ***Mycelium*** internal. **Stromata** lacking or formed by few substomatal aggregated swollen hyphal cells. ***Conidiophores*** in small, loose fascicles to moderately large and dense fascicles of up to approx. 22 conidiophores, arising from internal hyphae breaking through the adaxial epidermis of the leaves or penetrating through stomatal openings, sometimes solitary, erect, straight, subcylindrical, 1–2 times geniculate, unbranched, (12–)20.5–68(–72) × (3–)3.5–4.5 µm, 0–6-septate, brown to dark brown. ***Conidiogenous cells*** terminal, usually monoblastic, sometimes polyblastic; loci apical or sometimes located on the shoulders of geniculations, 1.5–2.5(–3) µm wide, thickened and darkened. ***Conidia*** solitary, acicular to narrowly obclavate, straight to curved, 22–76(–80) × 2.5–3.5 µm, 1–7-septate, hyaline, smooth, tip acute, base truncate to short obconically truncate, 2–3 µm wide, hila thickened and darkened.

Specimens examined. Benin. Borgou: Parakou, c. 386 m a.s.l., 9°20'35"N, 2°36'37"E, on *Vigna* sp., 14 Sep 2019, Y. Meswaet and R. Dramani, YMM05 (M-0312646; UNIPAR).

Hosts and distribution. On *Canscora diffusa* (Gentianaceae) from Khandala, West India (Chiddarwar 1959) and on *Vigna unguiculata* (as *Vigna catjang* (Burm.f.) Walp.) from India (Bhat and Pratibha 2010). *C.* cf. *canscorina* is reported here for the first time for Benin and for Africa.

Notes. Seven species of *Cercospora* have previously been recorded on *Vigna* spp., namely *C. apii*, *C. canescens*, *C. canscorina*, *C. caracallae* (Speg.) Vassiljevsky & Karak., *C. kikuchii*, *C. longispora* Peck and *C. vignigena* C.Nakash., Crous, U.Braun & H.D. Shin (Farr and Rossman 2021). The present species from Benin is morphologically identical to *C. canscorina* (Chiddarwar 1959; Bhat and Pratibha 2010) except for narrower conidiophores with (3–)3.5–4.5 µm versus 3–7 µm in *C. canscorina* as mentioned by Bhat and Pratibha (2010). The original specimen of *C. canscorina* was not available for morphological examination and no DNA sequence data are currently published for this species.

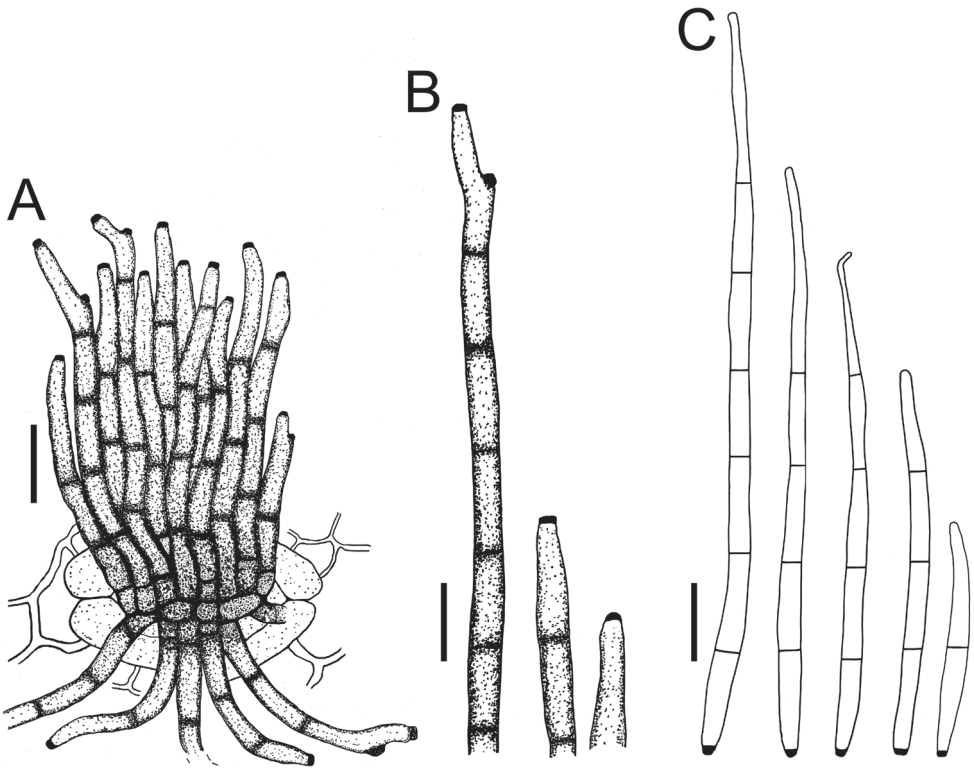

Figure 5. *Cercospora* cf. *canscorina* on *Vigna* sp. (YMM05) **A** fascicle of conidiophores protruding from a stomatal opening **B** solitary conidiophores **C** conidia. Scale bars: 15 μm (**A**); 10 μm (**B, C**).

Therefore, a reliable species identification is not possible. The application of the name for the collections from Benin is tentative and must be verified based on sequences derived from the Indian type specimen or similar samples. *C.* cf. *canscorina* differs from all species of *Cercospora* on other members of Fabaceae from Benin by producing unbranched, relatively pale conidiophores and above all, shorter conidiophores [(12–)20.5–68(–72) μm] and conidia [22–76(–80) μm]. Based on the multi-gene tree (Fig. 1) it is not possible to distinguish *Cercospora* cf. *canscorina* from many other *Cercospora* spp.

***Cercospora* cf. *fagopyri* K.Nakata & S.Takim., J. Agric. Exp. Stat. Gov. Gen. Chosen 15: 29. 1928.**
MycoBank No: 456931
Figs 2D, 6

Type. South Korea. Suwon, on *Fagopyrum esculentum* Moench (Polygonaceae), Sep 1934, K. Nakata & S. Takimoto (holotype specimen, not located and not preserved according to Groenewald et al. (2013), ***neotype*:** CBS H-21008, n.v).

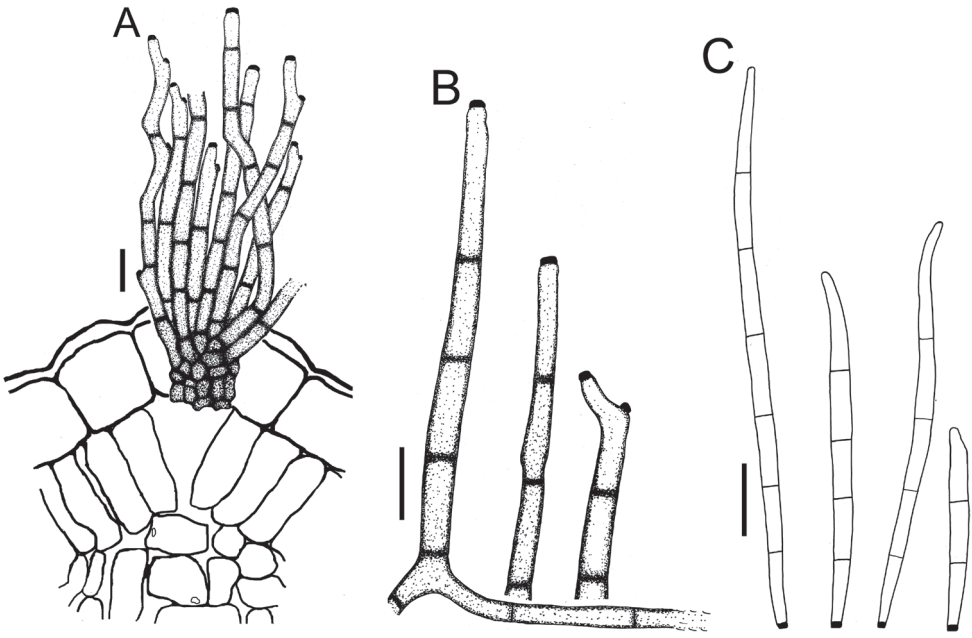

Figure 6. *Cercospora* cf. *fagopyri* on *Lablab* sp. (YMM23A) **A** fascicle of conidiophores growing out from a slightly developed stroma in the epidermis shown as part of a transverse section of a leaf **B** solitary conidiophores **C** conidia. Scale bars: 15 µm (**A**); 10 µm (**B, C**).

For synonyms see Groenewald et al. (2013) or MycoBank.

Description. ***Leaf spots*** amphigenous, circular to subcircular or rarely irregularly angular, 2–5 mm diam., more or less limited by veins, reddish to pale brown, margin dark brown on the adaxial surface, less conspicuous on the abaxial surface. ***Caespituli*** amphigenous, conspicuous, greyish brown to dark brown. ***Mycelium*** internal and external. External hyphae branched, often inconspicuous, 1.5–3 µm wide, septate, olivaceous brown to brown, smooth. ***Stromata*** lacking to well-developed, 10–45 µm diam., dark brown, substomatal or breaking through the epidermis. ***Conidiophores*** in small, loose to moderately dense fascicles of up to approx. 14 conidiophores, arising from stromata breaking through the adaxial epidermis of the leaves or through stomatal openings, sometimes solitary arising from external hyphae, erect, straight, subcylindrical to geniculate, unbranched, (22.5–)36–157(–168) × 3–4(–5) µm, 2–6(–8)-septate, brown to dark brown. ***Conidiogenous cells*** terminal, with 1–2 loci; loci mainly apical, sometimes located on the shoulders of geniculations, 1.5–2(–3) µm wide, thickened and darkened. ***Conidia*** solitary, acicular to narrowly obclavate, straight to somewhat curved, (24–)27.5–70(–78) × (2–)2.5–3(–4) µm, with 2–5(–6) somewhat indistinct septa, hyaline, smooth, tip acute, base truncate to short obconically truncate, 1.5–2.5 µm wide, hila thickened and darkened.

Specimens examined. Benin. Donga: Taneka-Koko, c. 441 m a.s.l., 9°51'30"N, 1°29'34"E, on *Lablab* sp., 29 Jul 2017, Y. Meswaet, M. Piepenbring, N. S. Yorou and

participants of the summer school 2017, YMM23A ((M-0312647; UNIPAR). Same locality and host, 03 Aug 2016, Y. Meswaet, M. Piepenbring, N. S. Yorou and participants of the summer school 2016, YMM02 (M-0312648).

Hosts and distribution. On *Cercis chinensis* (Fabaceae), *Cosmos bipinnata* Cav. (Asteraceae), *Fallopia dumetorum* (L.) Holub and *Fagopyrum esculentum* (Polygonaceae), *Hibiscus syriacus* (Malvaceae), *Viola mandshurica* W. Becker (Violaceae), from China, Japan, South Korea, Taiwan, Uganda and Venezuela (Hsieh and Goh 1990; Groenewald et al. 2013). *C.* cf. *fagopyri* is cited here for the first time on *Lablab* sp. and the first time for Benin and West Africa.

Notes. Currently there are two species of the genus *Cercospora* known on hosts belonging to *Lablab*, namely *C. canescens* and *C. apii*. The present *Cercospora* sp. (YMM23A) differs from *C. canescens* in leaf spot size, stromata and septation characteristics, as well as unbranched conidiophores. Above all, the sizes of the conidia of the present species are different [(24–)27.5–70(–78) × (2–)2.5–3(–4) µm versus 30–300 × 2.5–5 (–6) µm in *C. canescens*]. *C. apii* differs by often small or lacking stromata, dense fascicules of up to 30 conidiophores, branched, longer conidiophores [20–300 µm versus (22.5–)36–157(–168) µm in *C.* cf. *fagopyri*] and above all, longer and wider conidia [25–315 × 3–6 µm versus (24–)27.5–70(–78) × (2–)2.5–3(–4) µm in *C.* cf. *fagopyri*] (Chupp 1954).

Our sequence of the *tef1* region of the specimen YMM23A from Benin is 100% similar to a sequence of *Cercospora fagopyri* on *Fallopia dumetorum* (GenBank JX143353) (Identities 233/233, i.e., 100%) and 99% similar to a further sequence of *C. fagopyri* on *Fagopyrum esculentum* (GenBank JX143352; Identities; 233/234, i.e., 99%). The identification of the present specimen as *C.* cf. *fagopyri* is only based on molecular data. Morphologically, descriptions of specimens of *C. fagopyri* on diverse host species in the literature differ and are quite confusing (Hsieh and Goh 1990; Groenewald et al. 2013). In order to establish a morphological concept and to know the host range of *C. fagopyri*, fresh specimens need to be collected once again on *Fagopyrum esculentum* in Korea, where this species was originally collected and pathogenicity needs to be proven for diverse host species.

Cercospora parakouensis **Y.Meswaet, Mangelsdorff, Yorou & M.Piepenbr., sp. nov.**
MycoBank No: 839171
Figs 2E, 7

Type. Benin. Borgou: Parakou, Tankaro, c. 360 m a.s.l., 9°23'01"N, 2°30'36"E, on *Desmodium tortuosum* (Sw.) DC. (Fabaceae), 20 Sep 2019, Y. Meswaet and R. Dramani, YMM296A (***Holotype*****:** M-0312649; ***Isotype*****:** UNIPAR). ***Ex holotype sequences.*** MW834436 (LSU), MW834442 (ITS), MW848621 (*tef1*).

Etymology. The epithet *parakouensis* refers to the city of the type collection, Parakou, Benin.

Diagnosis. *Cercospora parakouensis* differs from the two *Cercospora* species known on *Desmodium* spp., namely *C. canescens* and *C. kashiensis* Bharadwaj by producing al-

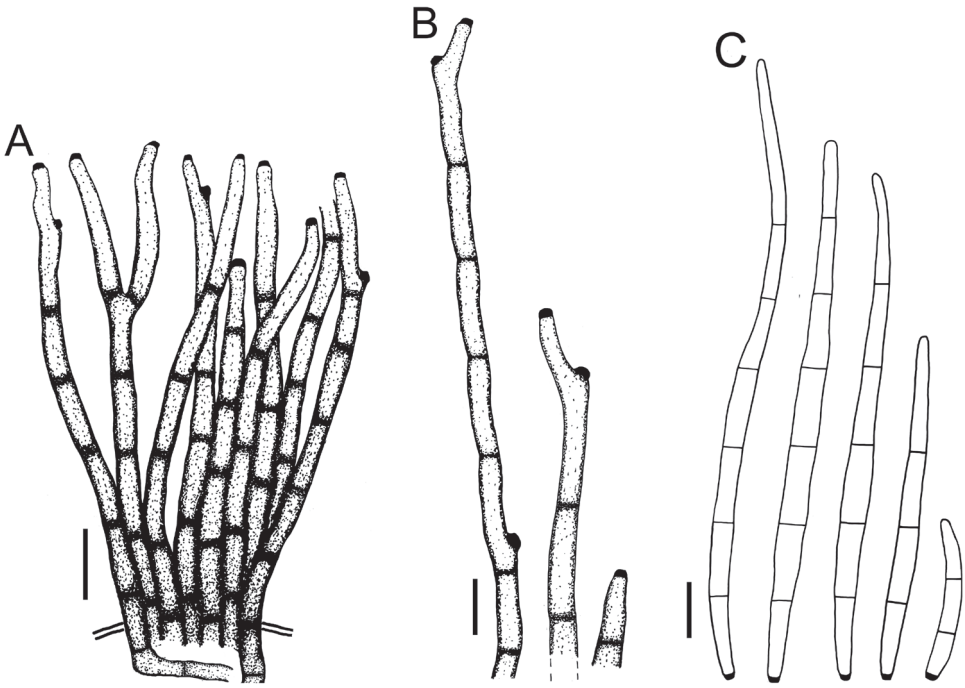

Figure 7. *Cercospora parakouensis* on *Desmodium tortuosum* (YMM296A) **A** fascicle of erumpent conidiophores **B** solitary conidiophores **C** conidia. Scale bars: 15 µm (**A**); 10 µm (**B, C**).

most no stromata, branched, darker and shorter conidiophores [(12.5–)18–178(–190) µm] and non- pigmented and shorter conidia [(14–)19–88(–113.5) × 3.5–4.5(–5) µm].

Description. ***Leaf spots*** almost lacking to well-developed, amphigenous, subcircular to irregularly angular, 1.5–5 mm diam., darkish brown to reddish brown, often with a diffuse whitish centre surrounded by a darker margin. ***Caespituli*** amphigenous, greyish brown to dark brown. ***Mycelium*** mainly internal. **Stromata** lacking. ***Conidiophores*** in small, loose fascicles, sometimes arising from internal hyphae, breaking through the adaxial epidermis of the leaves or penetrating through stomatal openings, occasionally solitary, arising through stomatal openings, erect, straight to sinuous or somewhat geniculate, occasionally branched, (12.5–)18–178(–190) × (3.5–)4–5(–5.5) µm, 1–6(–8)-septate, brown to dark brown. ***Conidiogenous cells*** terminal or rarely intercalary, usually monoblastic, rarely polyblastic; loci subcircular, 1.5–3 µm wide, thickened and darkened, refractive. ***Conidia*** solitary, narrowly obclavate to subacicular, straight to curved, (14–)19–88(–113.5) × 3.5–4.5(–5) µm, 2–6-septate, hyaline, smooth, apex subacute or acute, base truncate to short obconically truncate, 2–3(–3.5) µm wide, hila thickened and darkened.

Additional specimens examined. Benin. Borgou: Parakou, c. 395 m a.s.l., 9°21'27"N, 2°36'44"E, on *Desmodium tortuosum*, 17 Sep 2019, Y. Meswaet and A. Tabé, YMM292 (***Paratypes*****:** M-0312650; UNIPAR).

Herbarium specimens examined for comparison. See *Cercospora* aff. *canescens*.

Host and distribution. On *Desmodium tortuosum* (Fabaceae) from Benin.

Notes. Currently, two *Cercospora* species are known from *Desmodium* spp., namely *C. canescens* and *C. kashiensis* (Farr and Rossman 2021). *C. canescens* differs from the present species by causing large leaf spots often along the margin of the leaf, 3–15 mm in extent, paler conidiophores and above all, longer conidia [30–300 µm versus (14–)19–88(–113.5) µm in *C. parakouensis*] (Chupp 1954). The distinctness is also confirmed by molecular data (Fig. 1). *C. kashiensis* described on *Desmodium gangeticum* (L.) DC. from India causes different leaf spots, has unbranched and longer conidiophores (40–282 µm versus (12.5–)18–178(–190) in *C. parakouensis*) and above all, pigmented and longer conidia (16–220 µm versus (14–)19–88(–113.5) µm in *C. parakouensis*) with 2–15 septa (Bharadwaj 1971).

In the multi-gene tree (Fig. 1), the ITS and the *tef1* phylogeny (see Suppl. materials 3, 4), *C. parakouensis* forms part of a polytomy with a relatively large genetic distance (branch length) in relation to other sequences considered in the analysis.

Based on a MegaBLAST search using the *tef1* sequence, the closest matches in NCBI's GenBank nucleotide database were *Cercospora nicotianae* on *Nicotiana tabacum* (Solanaceae) from China (GenBank MK881748; Identities 283/291, i.e., 97%), *Cercospora* cf. *sigesbeckiae* on *Persicaria orientalis* L. (Polygonaceae) from South Korea (GenBank JX143412; Identities 283/291, i.e., 97%) and *Cercospora* aff. *canescens* on a species of Malvaceae from Mexico (GenBank JX143321; Identities 283/291, i.e., 97%).

Cercospora phaseoli-lunati **U.Braun & Crous, Mycotaxon 92: 396. 2005.**
MycoBank No: 500171
Figs 2F, 8

Type. USA. Alabama: Tuskegee, on *Phaseolus lunatus* (Fabaceae), 5 Jul 1897, G.W. Carver 290 (***Holotype*** NY, n.v.).

Description. ***Leaf spots*** amphigenous, subcircular to irregularly angular, 2.5–8(–12) mm diam., more or less limited by veins, whitish grey to greyish brown, with a narrow to wide dark brown margin on the adaxial surface, less conspicuous on the abaxial surface. ***Caespituli*** amphigenous, mainly epiphyllous, scattered, brown to dark brown. ***Mycelium*** internal, indistinct. External hyphae absent. ***Stromata*** lacking or formed by few aggregated swollen hyphal cells, immersed in the mesophyll or in substomatal cavities. ***Conidiophores*** in small, loose fascicles of up to 6, arising from internal hyphae of small hyphal aggregations, breaking through the adaxial epidermis of the leaves or penetrating through stomatal openings, or solitarily arising through stomatal openings, erect, rarely branched, straight to geniculate or subcylindrical to mostly attenuated towards the tips, conical or irregularly shaped, (18–)21.5–94(–102) × (3.5–)4–5 µm, 1–6-septate, smooth, brown to dark brown. ***Conidiogenous cells*** terminal, monoblastic or polyblastic; loci distinct, up to 2.5 µm wide, thickened and darkened. ***Conidia*** solitary, narrowly obclavate to subacicular, straight to curved, (16–)19–94(–105.5) ×

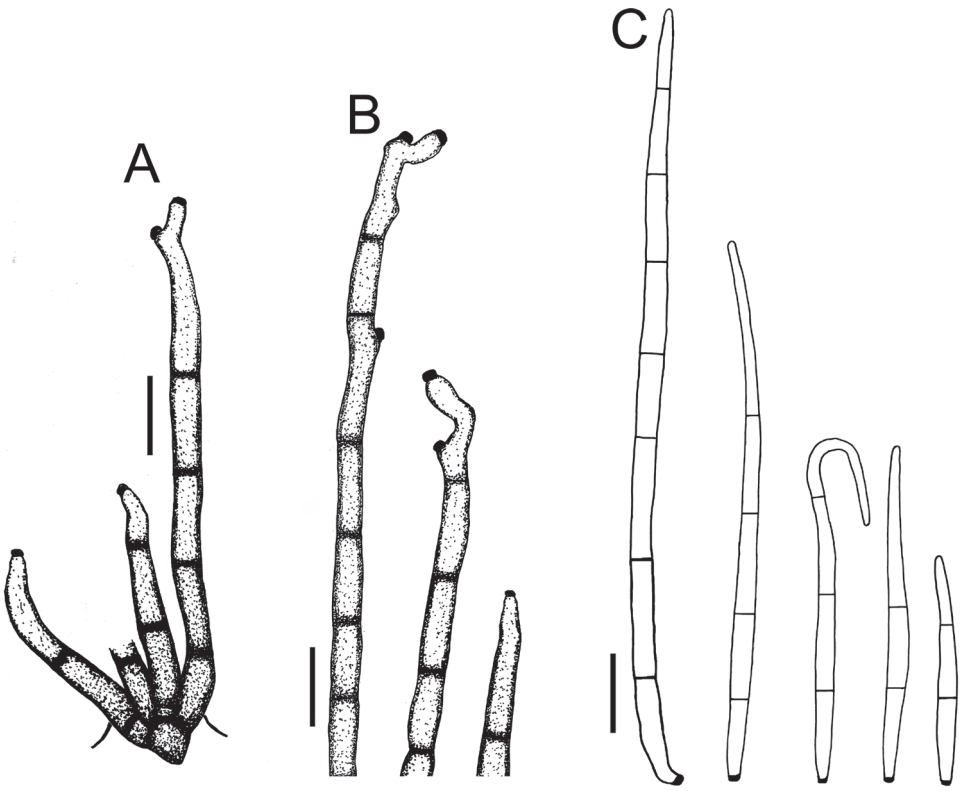

Figure 8. *Cercospora phaseoli-lunati* on *Vigna radiata* (YMM289) **A** small fascicle of conidiophores **B** solitary conidiophores **C** conidia. Scale bars: 12 µm (**A**); 10 µm (**B, C**).

2.5–3.5 µm, 2–7-septate, hyaline to subhyaline, smooth, apex subacute or acute, base truncate to short obconically truncate, up 2.5 µm wide, hila thickened and darkened.

Specimen examined. Benin. Borgou: Parakou, c. 386 m a.s.l., 9°20'35"N, 2°36'37"E, on *Vigna radiata,* 14 Sep 2019, Y. Meswaet and R. Dramani, YMM289 (M-0312651 UNIPAR).

Hosts and distribution. On *Phaseolus lunatus* from USA, Alabama, Tuskegee (type locality) (Braun and Crous 2005). This species is cited here for the first time for Benin. Thereby, it is cited for the first time for West Africa. *Vigna radiata* is a new host species.

Notes. Thirteen *Cercospora* species have previously been recorded on species of *Vigna* and *Phaseolus*, namely *C. albida* Matta & Belliard, *C. apii*, *C. canescens*, *C. canscorina*, *C. caracallae*, *C. kikuchii*, *C. longispora*, *C. olivascens*, *C. phaseoli-lunati*, *C. phaseolicola* U.Braun & Mouch., *C. phaseolina* Speg., *C. vignigena* and *C. zonata* G. Winter (Farr and Rossman 2021). Among these, *C. caracallae* and *C. phaseoli-lunati* are morphologically rather similar to the present collection. *C. caracallae*, however, differs in causing distinct leaf spots and caespituli, dense fascicules composed of unbranched and wider conidiophores [5–6 µm versus (3.5–)4–5 µm in *C. phaseoli-lunati*] and wider conidia (3–5.5 µm versus 2.5–3.5 µm in *C. phaseoli-lunati*) with less septa (3–5 versus

2–7 septa) (Chupp 1954; Spegazzini 1910). Except for the presence of distinct leaf spots and sporulation, the morphology of the present collection from Benin fits well to the original description of *C. phaseoli-lunati* on *Phaseolus lunatus* from the USA provided by Braun and Crous (2005). Based on the present phylogenies, it is not possible to distinguish *C. phaseoli-lunati* from numerous other *Cercospora* spp.

Cercospora rhynchophora **Y.Meswaet, Mangelsdorff, Yorou & M.Piepenbr., sp. nov.**
MycoBank No: 839172
Figs 2G, 9

Type. Benin. Borgou: Parakou, c. 385 m a.s.l., 9°20'34"N, 2°36'39"E, on *Vigna unguiculata* (L.) Walp. (Fabaceae), 14 Sep 2019, Y. Meswaet and R. Dramani, YMM03B (***Holotype*****:** M-0312652; ***Isotype*****:** UNIPAR). ***Ex holotype sequences*****.** MW834447 (SSU), MW834431 (LSU), MW834443 (ITS), MW848619 (*tef1*).

Etymology. The epithet *rhynchophora* refers to the beak- or hook-like tips of the conidiophores, a characteristic of this species.

Diagnosis. *Cercospora rhynchophora* differs from other *Cercospora* spp. known on *Vigna* spp. by causing distinct leaf spots, often well-developed stromata and up to 4 times geniculate conidiophores with often polyblastic conidiogenous cells with irregular, often beak-shaped tips.

Description. ***Leaf spots*** amphigenous, small to fairly large, subcircular to irregularly angular, (3–)4.5–12.5 mm diam. or confluent and larger, dark brown to reddish brown, mostly with an indefinite margin, or whitish grey to greyish brown, with a narrow to wide dark brown margin on the adaxial surface, occasionally confined by veins. ***Caespituli*** amphigenous, scattered to dense, dark brown. ***Mycelium*** mainly internal, but some external hyphae also present. External hyphae septate, brown, 2–3.5 µm wide, smooth. **Stromata** often well-developed, up to 50 µm diam., in substomatal chambers or in the mesophyll, brown to dark brown. ***Conidiophores*** in loose to moderately dense fascicles formed by 3–20 conidiophores, arising from internal hyphae or stromata breaking through the adaxial epidermis of the leaves, or penetrating through stomatal openings, or solitary, erect, straight to 1–4 times geniculate or subcylindrical, sometimes branched, mostly attenuated towards the tips that are often irregularly shaped or conical, (12.5–)26–160(–200) × (3.5–)4–5(–5.5) µm, 0–7(–9)-septate, brown to dark brown. ***Conidiogenous cells*** terminal or rarely intercalary, proliferating sympodially, mostly polyblastic, frequently distinctly subdenticulate, sometimes with bent tips looking like a beak or a hook; loci (1.5–)2–2.5(–3) µm wide, thickened and darkened. ***Conidia*** solitary, acicular to narrowly obclavate, straight to curved, (28–)40–265(–280) × (3–)3.5–4.5(–5) µm, 1–9-septate, hyaline, smooth, tip acute, base truncate to obconically truncate, sometimes long obconically truncate, 2–2.5(–3.5) µm wide, hila thickened and darkened.

Additional specimen examined. Benin. Borgou: Parakou, c. 395 m a.s.l., 9°21'27"N, 2°36'44"E, on *Vigna unguiculata*, 17 Sep 2019, Y. Meswaet and R. Dramani, YMM03C (***Paratypes*****:** M-0312653; UNIPAR).

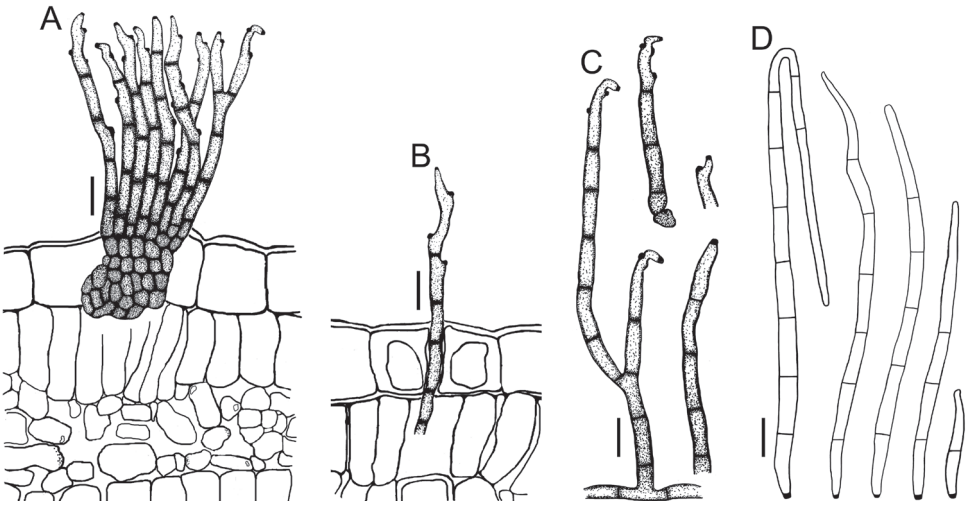

Figure 9. *Cercospora rhynchophora* on *Vigna unguiculata* (YMM03B) **A** fascicle of conidiophores growing out from a developed stroma embedded in the mesophyll **B** conidiophore penetrating through a stomatal opening **C** solitary conidiophores arising from external hyphae **D** conidia. Scale bars: 20 μm (**A, B**); 15 μm (**C, D**).

Herbarium specimens examined for comparison. See *Cercospora* aff. *canescens.*

Host and distribution. On *Vigna unguiculata* (Fabaceae) in Benin.

Notes. The infection of leaves of *Vigna unguiculata* by *Cercospora rhynchophora* was severe and caused dark brown to reddish brown large patches (Fig. 2G). This infection was frequently associated with an infection by *Pseudocercospora cruenta* (Sacc.) Deighton. Seven species of *Cercospora* have previously been recorded on *Vigna* spp. (Table 4). Among these, *C. apii*, *C. canescens*, *C. kikuchii* and *C. vignigena* have to date been reported as agents of leaf spot diseases on *V. unguiculata*. Morphologically, *C. rhynchophora* differs from these species by a specific combination of characteristics (Table 4). *C. apii* has often small or no stromata, forms non-geniculate, densely fasciculate and longer conidiophores (20–300 μm) that are uniform in colour and width and carry monoblastic conidiogenous cells (Chupp 1954; Hsieh and Goh 1990) versus developed stromata, shorter conidiophores [(12.5–)26–160(–200) μm] that are irregularly shaped with polyblastic conidiogenous cells presenting beak-shaped tips in *C. rhynchophora*. Additionally, *C. apii* has pale to olivaceous brown conidiophores (Hsieh and Goh 1990) versus the dark brown ones of *Cercospora rhynchophora*.

C. canescens causes different leaf spots and caespituli, develops small or no stromata and paler conidiophores that are uniform in colour with often monoblastic, mostly uniform conidiogenous cells (Chupp 1954; Hsieh and Goh 1990) versus irregularly shaped conidiophores with polyblastic, beaked conidiogenous cells in *C. rhynchophora*. The distinctness is also confirmed by molecular data. *C. canscorina* forms shorter conidiophores [29.8–85.0 μm versus (12.5–)26–160(–200) μm in *C. rhynchophora*] and conidia [31.2–89.9 × 3–3.4 μm versus (28–)40–265(–280) μm in *C. rhynchophora*]

Table 4. Comparison of *Cercospora rhynchophora* (YMM03B) on *Vigna unguiculata*, *Cercospora tentaculifera* (YMM75) on *Vigna unguiculata* as well as on *Phaseolus vulgaris* and *C. vignae-subterraneae* (YMM293, see below) on *Vigna subterranea* with *Cercospora* species known from *Vigna* spp. based on literature [a–f].

Cercospora species	*Leaf spots*, colour, size	Stromata	Conidiophore size (in µm), branching, septa, colour	Conidium sizes (in µm), septa
Cercospora rhynchophora (YMM03B)	Dark brown to reddish brown, (3–)4.5–12.5 mm diam.	Well-developed	(12.5–)26–160(–200) × (3.5–)4–5(–5.5), branched, 0–7(–9)-septate, dark brown	(28–)40–265(–280) × (3–)3.5–4.5(–5), 1–9 distinct septa
***C. tentaculifera* (YMM75)**	Almost absent	Small or lacking	(32.5–)40–400(–435) × (3–)3.5–4.5(–5), rarely branched, (2–)3–8(–10)-septate, brown to dark brown	(29–)38–188(–240) × (2.5–)3–3.5(–4.5), 1–9 septa
C. vignae-subterraneae (YMM293)	Brown to reddish brown, 2–6.5 mm diam.	Lacking or small	(28–)35.5–278(–340) × (3.5–)4–5, rarely branched, 2–6-septate, brown to dark brown	(19–)26.5–100(–110.5) × (2.5–)3–4, (2–)3–6 septa
C. apii [ab]	Present	Often small or lacking, occasionally developed, up to 50 µm diam.	20–300 × 4–6.5, rarely branched, multi-septate, pale brown, uniform in colour and width	25–315 × 3–6, (0–)3–25(–30) septa[b]
C. canescens [a]	3–15 mm	Often small	20–200 × 3–6.5, rarely branched, multi-septate, pale to medium dark brown	25–300 × 2.5–5.5, indistinctly multi-septate
C. canscorina [c]	Pale brown to brown, 3–6 mm	Developed	29.8–85.0 × 3.4–4.2, 1–3-septate, or rarely non-septate, pale brown	31.2–89.9 × 3–3.4, 3–9 septa
C. caracallae[d]	Present	Present	40–80 × 5–6, unbranched,	50–75 × 4, 3–5 septa
C. kikuchii[a]	Present	Small	45–200 × 3–6.5, unbranched, multi-septate	50–375 × 2.5–5, indistinctly multi-septate
C. longispora [e]	Present	Small	5–30 × 1.5–3, unbranched, multi-septate, scars indistinct or lacking	75–170 × 2–3.5, indistinctly multi-septate
C. vignigena[f]	Pale to medium brown, 8–20 mm	Small to well-developed (up to 60 µm diam.)	40–130 × 5–7(–10), 0–3-septate	(35–)45–70(–150) × (2.5–)4–6(–10), (3–)4–7(–14) septa

[a] Hsieh and Goh (1990), [b] Crous and Braun (2003), [c] Chiddarwar (1959), [d] Spegazzini (1910), [e] Chupp (1954), [f] Groenewald et al. (2013).

with pale brown and 1–3-septate conidiophores (Chiddarwar 1959). *C. caracallae* has densely fasciculate, unbranched, shorter and wider conidiophores [40–80 × 5–6 µm versus (12.5–)26–160(–200) µm in *C. rhynchophora*] and shorter conidia [50–75 µm versus (28–)40–265(–280) µm of *C. rhynchophora*] with 3–5 septa (Spegazzini 1910). *C. kikuchii* has unbranched conidiophores and longer conidia [50–375 µm versus (28–)40–265(–280) µm in *C. rhynchophora*] that are 0–22-septate (Hsieh and Goh 1990). *C. longispora* has shorter and narrower conidiophores [5–30 × 1.5–3 µm versus (12.5–)26–160(–200) × (3.5–)4–5(–5.5) µm in *C. rhynchophora*] and shorter conidia (75–170 µm versus (28–)40–265(–280) in *C. rhynchophora*] (Chupp 1954). *C. vignigena* produces pale brown and wider conidiophores [5–7(–10) µm versus (3.5–)4–5(–5.5) µm in *C. rhynchophora*] that are 0–3-septate and shorter as well as wider conidia [(35–)45–70(–150) × (2.5–)4–6(–10) µm versus (28–)40–265(–280) × (3–)3.5–4.5(–5) µm of *C. rhynchophora*] (Groenewald et al. 2013).

In the multi-gene (Fig. 1) and the ITS tree (see Suppl. material 3), *C. rhynchophora* forms part of a polytomy with a relatively large genetic distance (branch length) in rela-

tion to other sequences considered in the analysis. According to a MegaBLAST search using the *tef1* sequence, the closest matches in NCBI's GenBank nucleotide database were *Cercospora beticola* Sacc. on *Tetragonia tetragonoides* (Pall.) Kuntze (Aizoaceae) from Brazil (GenBank MN517124; Identities 272 / 279, i.e., 97%), *Cercospora kikuchii* on *Platostoma palustre* (Blume) A.J. Paton (Lamiaceae) from Taiwan (GenBank LC488192; Identities 272 / 279, i.e., 97%) and *Cercospora* sp. RF5 on *Brunfelsia hopeana* (Hook.) Benth. (Solanaceae) from Thailand (GenBank AB863025; Identities 272 / 279, i.e., 97%).

Cercospora sp. YMM297B on *Phaseolus lunatus* L.

Fig. 10

Description. ***Leaf spots*** almost lacking to well-developed, amphigenous, subcircular to irregularly angular, 2.5–8 mm diam., reddish brown, later dark brown by abundant caespituli, finally sometimes greyish brown to dark reddish brown, surrounded by dark margins, often with diffuse whitish centres. ***Caespituli*** amphigenous, greyish brown to dark brown. ***Mycelium*** mainly internal. External hyphae branched, 2–3(–4) µm wide, septate, olivaceous brown to brown, smooth. **Stromata** lacking or small, up to 20 µm diam., immersed in the mesophyll or in substomatal cavities, subcircular to irregular, olivaceous brown to darker brown. ***Conidiophores*** in small and loose fascicles, breaking through the adaxial epidermis of the leaves or penetrating through stomatal openings, sometimes solitarily arising through stomatal openings, erect, straight to sinuous, or somewhat geniculate, unbranched, (13–)17.5–195(–220) × (3.5–)4–5 µm, with 2–6(–8) septa each, occasionally slightly constricted and darker at the septa, brown to dark brown. ***Conidiogenous cells*** integrated, terminal, mainly monoblastic; loci 2–3.5 µm wide, thickened and darkened. ***Conidia*** solitary, narrowly obclavate to subacicular, straight to curved, (27–)36–148(–164) × (2.5–)3–4(–4.5) µm, with 2–7(–9) somewhat indistinct septa each, hyaline to sub-hyaline, smooth, apex subacute or acute, base truncate to short obconically truncate, 2–3(–3.5) µm wide, hila thickened and darkened.

Specimen examined. Benin. Borgou: Parakou, Tankaro, c. 360 m a.s.l., 9°23'01"N, 2°30'36"E, on *Phaseolus lunatus*, 20 Sep 2019, Y. Meswaet and R. Dramani, YMM297B (M-0312654; UNIPAR).

Notes. The infection of leaves of *Phaseolus lunatus* by *Cercospora* sp. YMM297B was associated with the infection by *Pseudocercospora griseola*. Among the *Cercospora* spp. known on *Phaseolus* and *Vigna*, *C. olivascens* is morphologically close to *Cercospora* sp. YMM297B. *C. olivascens*, however, differs from *Cercospora* sp. YMM297B by hypophyllous caespituli, no external hyphae, conidiophores that are up to five times geniculate and paler (Saccardo 1878; Chupp 1954), as well as hyaline conidia. The present specimen from Benin presents amphigenous caespituli, external hyphae, less geniculate and brown to dark brown conidiophores and often sub-hyaline conidia. *C. olivascens* also differs from the present species by being originally described from *Aristolochia clematitis* (Aristolochiaceae). According to Chupp (1954), this species was wrongly

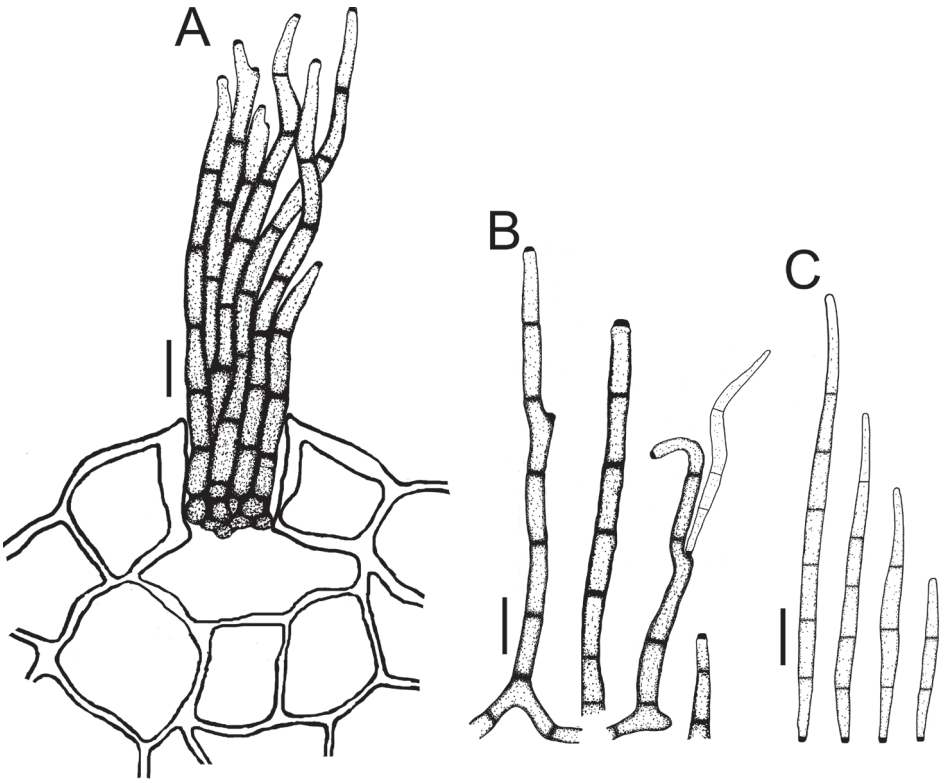

Figure 10. *Cercospora* sp. on *Phaseolus lunatus* (YMM297B) **A** fascicle of conidiophor**e**s emerging through a stomatal opening **B** solitary conidiophores **C** conidia. Scale bars: 15 μm (**A**); 10 μm (**B, C**).

reported on *Phaseolus vulgaris* by Saccardo (1886). This was confirmed by Crous and Braun (2003). In the ITS phylogeny (see Suppl. material 3), *Cercospora* sp. YMM297B forms part of a polytomy with a relatively large genetic distance (branch length) in relation to other sequences considered in the analysis. In the *tef1* phylogeny (see Suppl. material 4), it is not possible to distinguish this collection from several other *Cercospora* spp. As the description and sequence data are obtained only from a single specimen, the data are not sufficient for a final conclusion and the description as a new species. A reliable species characterisation is not possible until more collections become available.

Cercospora tentaculifera **Y.Meswaet, Mangelsdorff, Yorou & M.Piepenbr., sp. nov.**
MycoBank No: 839173
Figs 2H, 11

Type. Benin. Borgou: Parakou, c. 372 m a.s.l., 9°21'43"N, 2°36'04"E, on *Vigna unguiculata* (L.) Walp. (Fabaceae), 02 August 2017, Y. Meswaet, M. Piepenbring, N.S. Yorou and participants of the summer school 2017, YMM75 (***Holotype*****:** M-0312655;

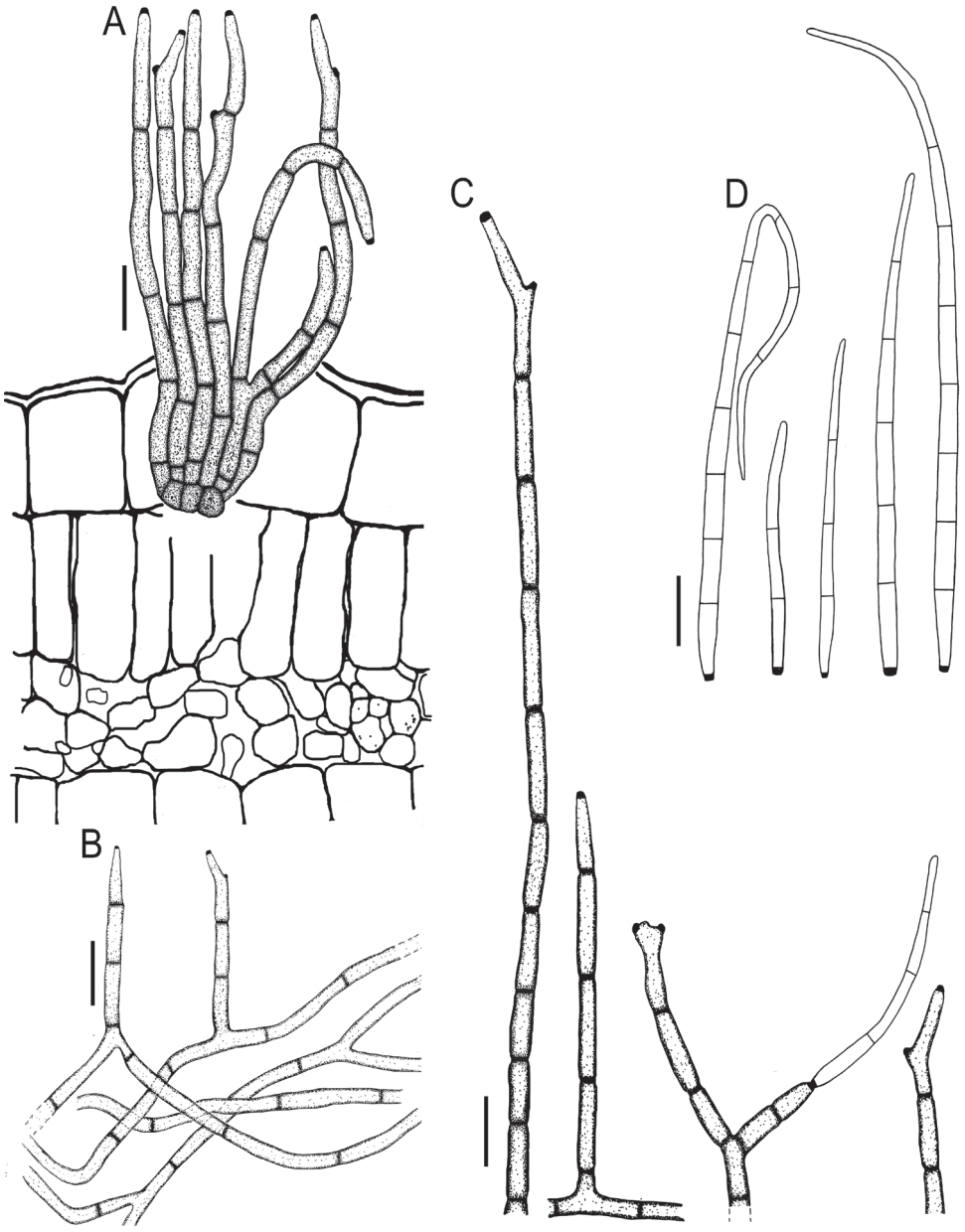

Figure 11. *Cercospora tentaculifera* on *Vigna unguiculata* (YMM75) **A** fascicle of conidiophores growing out from a small stroma immersed in the epidermis **B** external hyphae **C** solitary conidiophores **D** conidia. Scale bars: 20 µm (**A**); 12 µm (**B**); 15 µm (**C, D**).

***Isotype*:** UNIPAR). ***Ex holotype sequences*.** MW834448 (SSU), MW834440 (ITS), MW848614 (*tef1*).

Etymology. The epithet *tentaculifera* refers to the ramified and flexible hyphae.

Diagnosis. *Cercospora tentaculifera* differs from other *Cercospora* spp. on *Vigna* and *Phaseolus* in causing inconspicuous or no leaf spots, well-developed external hyphae, mainly adaxial caespituli and up to 435 µm long conidiophores that are constricted at the septa.

Description. ***Leaf spots*** almost lacking or pale brown with reddish brown discolorations. ***Caespituli*** amphigenous, mostly epiphyllous, scattered, greyish brown to dark brown. ***Mycelium*** internal and external. External hyphae branched, 2–3.5(–4) µm wide, septate, olivaceous brown to brown, smooth. ***Stromata*** lacking or formed by few substomatal swollen hyphal cells, immersed in the mesophyll or in substomatal cavities. ***Conidiophores*** in small, loose fascicles formed by up to approx. 8 conidiophores, breaking through the adaxial epidermis of the leaves or penetrating through stomatal openings, solitary when arising from external hyphae, erect, straight, curved or slightly 1–2 times geniculate, often constricted at septa, rarely branched, (32.5–)40–400(–435) × (3–)3.5–4.5(–5) µm, (2–)3–8(–10)-septate, brown to dark brown. ***Conidiogenous cells*** terminal, rarely subterminal, mostly monoblastic or with few conidiogenous loci; loci mainly apical, sometimes located on the shoulders of geniculations, 2–2.5(–3.5) µm wide, thickened and darkened, refractive, often subcircular or rarely flattened. ***Conidia*** solitary, acicular to narrowly obclavate, straight to curved, (29–)38–188(–240) × (2.5–)3–3.5(–4.5) µm, 1–9-septate, hyaline, smooth, tip acute, base truncate to short obconically truncate, 2.5–3(–3.5) µm wide, hila thickened and darkened.

Additional specimen examined. Benin. Borgou: Parakou, agricultural research site of the University of Parakou, c. 360 m a.s.l., 9°20'10"N, 2°38'53"E, on *Phaseolus vulgaris*, 20 Aug 2017, Y. Meswaet and A. Tabé, YMM130 (***Paratypes*:** M-0312656; UNIPAR).

Herbarium specimens examined for comparison. See *Cercospora* aff. *canescens.*

Hosts and distribution. Known on *Phaseolus vulgaris* and *Vigna unguiculata* (Fabaceae) from Benin.

Notes. Thirteen *Cercospora* species have previously been recorded on species of *Vigna* or *Phaseolus* (Tables 4, 5).

Among these, *C. apii*, *C. canescens* and *C. phaseolicola* have a morphology similar to the present collections, particularly by relatively long conidiophores (Tables 4, 5). *C. apii*, however, differs from the present species in causing distinct leaf spots (brown to fairly dark in colour with darker margin), the place of sporulation (caespituli more abundant on the abaxial surface of leaves versus on the adaxial surface of leaves in the case of *C. tentaculifera*), paler and shorter conidiophores [20–300 µm versus (32.5–)40–400(–435) µm in *C. tentaculifera*] that are occasionally arising from developed (up to 50 µm diam.) stromata and somewhat longer and wider conidia [25–315 × 3–6 µm versus (29–)38–188(–240) × (2.5–)3–3.5(–4) µm in *C. tentaculifera*] (Hsieh and Goh 1990). *C. canescens* differs from *C. tentaculifera* in causing different leaf spots and sporulation, producing dense fascicles, paler and shorter conidiophores [20–200 µm versus (32.5–)40–400(–435) µm in *C. tentaculifera*] and somewhat longer conidia [25–300 µm versus (29–)38–188(–240) µm in *C. tentaculifera*] (Hsieh and Goh 1990). *C. phaseolicola* differs from *C. tentaculifera* in causing zonate leaf

Table 5. Comparison of *Cercospora tentaculifera* (YMM75) on *Vigna unguiculata* and *Phaseolus vulgaris* with *Cercospora* species known from *Phaseolus* spp. based on literature [a–g].

Cercospora species	*Leaf spots*, colour, size	Stromata	Conidiophore size (in µm), branching, septa, colour	Conidium sizes (in µm), septa
***C. tentaculifera* (YMM75)**	Almost absent	Small or lacking	(32.5–)40–400(–435) × (3–)3.5–4.5(–5), rarely branched, (2–)3–8(–10)-septate, brown to dark brown	(29–)38–188(–240) × (2.5–)3–3.5(–4.5), 1–9 septa
C. albida[a]	Almost absent	Small or lacking	10–60 × 3–6, branched, 1–2-septate	(30–)50–90(–125) × (1.5–)2–3.5(–4), 0–6 septa
C. canescens[b]	3–15 mm	Often small	20-200 × 3–6.5, rarely branched, multi-septate, pale to medium dark brown	25–300 × 2.5–5.5, indistinctly multi-septate
C. caracallae[c]	Present	Present	40–80 × 5–6, unbranched	50–75 × 3–4, 3–5 septa
C. kikuchii[b]	Present	Small	45–200 × 3–6.5, unbranched, multi-septate	50–375 × 2.5–5, indistinctly multi-septate
C. olivascens[d]	Present	Small	50–200 × 4–5.5, unbranched, multi-septate	35–150 × 4–5.5, 3–9 septa
C. phaseoli-lunati[e]	Present	Present	20–100 × 2.5–5(–6), usually pluri-septate	(20–)30–100 × 1–3, pluri-septate
C. phaseolicola[f]	Present	Absent	300–600 × 4–7(–10), branched, pluri-septate	50–200 × 3–5, pluri-septate
C. phaseolina[g]	Present	No information	50–80 × 4–5, unbranched	20–45 × 3–3.5, 1–3 septa
C. zonata[d]	Present	Lacking or slightly developed	10–80 × 3–5, mostly 10–40, 0–2-septate, unbranched	40–125 × 2.5–4.5, usually 3septa

[a] Braun (1995b), [b] Hsieh and Goh (1990), [c] Spegazzini (1910) [d] Chupp (1954), [e] Crous and Braun (2005), [f] Braun et al. (1999), [g] Spegazzini (1881).

spots and producing only internal hyphae, hardly geniculate, much longer and wider conidiophores [300–600 × 4–7 µm, occasionally up to 10 µm wide versus (32.5–)40–400(–435) × (3–)3.5–4.5(–5) µm] (Braun et al. 1999).

Based on the present phylogenies, it is not possible to distinguish this species from many other *Cercospora* spp. included in this study. Nevertheless, we propose this species as new to science based on a unique combination of morphological characteristics.

***Cercospora vignae-subterraneae* Y.Meswaet, Mangelsdorff, Yorou & M.Piepenbr., sp. nov.**

MycoBank No: 839174

Figs 2I, 12

Type. Benin. Borgou: Parakou, c. 394 m a.s.l., 9°21'25"N, 2°36'45"E, on *Vigna subterranea* (L.) Verdc. (Fabaceae), 17 Sep 2019, Y. Meswaet and R. Dramani, YMM293 (***Holotype*:** M-0312657; ***Isotype*:** UNIPAR). ***Ex holotype sequences*.** MW834446 (SSU), MW834438 (ITS), MW848618 (*tef1*).

Etymology. The epithet *vignae-subterraneae* refers to the host species, *Vigna subterranea*.

Diagnosis. *Cercospora vignae-subterraneae* differs from all other *Cercospora* spp. known on *Vigna* spp. in causing often necrotic leaf spots with a pale to white greyish centre, mostly hypophyllous caespituli, external hyphae, flat conidiogenous loci and shorter conidia [(19–)26.5–100(–110.5) µm].

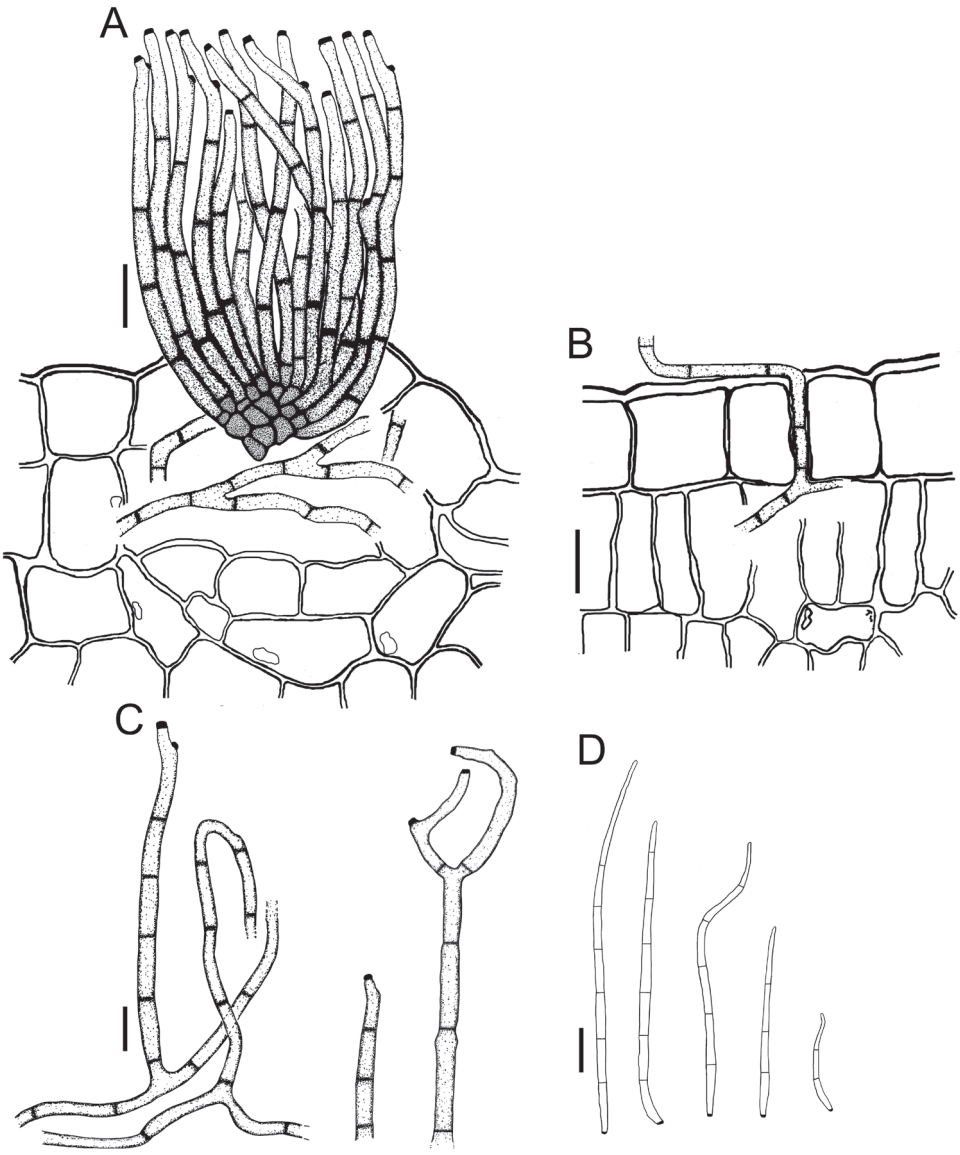

Figure 12. *Cercospora vignae-subterraneae* on *Vigna subterranea* (YMM293) **A** fascicle of conidiophores **B** external hypha penetrating through a stomatal opening **C** solitary conidiophores arising from external hyphae **D** conidia. Scale bars: 20 µm (**A, B**); 12 µm (**C**); 10 µm (**D**).

Description. ***Leaf spots*** amphigenous, circular or subcircular to irregularly angular, 2–6.5 mm diam., often limited by veins, brown to greyish brown, later necrotic with a pale to white greyish centre, surrounded by a darker margin, the outermost ring mostly darker than the inner margins. ***Caespituli*** amphigenous, but mostly hypophyllous, greyish brown to dark brown. ***Mycelium*** internal and external. External hyphae

branched, 2–3(–3.5) µm wide, septate, olivaceous brown to brown, smooth. ***Stromata*** lacking or small, immersed in the mesophyll or in substomatal cavities. ***Conidiophores*** in small to large, loose to dense fascicles or solitary, arising through stomatal openings or breaking through the epidermis, erect, subcylindrical, sinuous or somewhat geniculate, simple or rarely branched, (28–)35.5–278(–340) × (3.5–)4–5 µm, 2–6-septate, smooth, brown to dark brown with slightly paler tips. ***Conidiogenous cells*** terminal, usually monoblastic, rarely polyblastic; loci conspicuous, often flat, (1.5–)2–3 µm wide, darkened and thickened. ***Conidia*** solitary, narrowly obclavate to subacicular, straight to curved, (19–)26.5–100(–110.5) × (2.5–)3–4 µm, (2–)3–6-septate, hyaline, smooth, apex subacute or acute, base truncate to short obconically truncate, (1.5–)2–2.5(–3) µm wide, hila thickened and darkened.

Additional specimen examined. Benin. Alibori: Gogounou, c. 333 m a.s.l., 10°50'35"N, 2°49'42"E, on *Vigna subterranea* Verdc., 2 Sep 2017, Y. Meswaet and A. Tabé, YMM180 (***Paratypes*****:** M-0312658; UNIPAR).

Herbarium specimens examined for comparison. See *Cercospora* aff. *canescens.*

Host and distribution. On *Vigna subterranea* (Fabaceae) in Benin.

Notes. Seven species of *Cercospora* have previously been recorded on *Vigna* spp. (Table 4) (Farr and Rossman 2021). However, no species of *Cercospora* is known to occur on *Vigna subterranea* (Farr and Rossman 2021), a plant species native to West Africa and cultivated mainly in the warm tropics of sub-Saharan Africa (Hepper 1963). Morphologically, *C. vignae-subterraneae* is distinct from all seven species of *Cercospora* mentioned above (Table 4). *C. apii* differs from *C. vignae-subterraneae* by paler conidiophores occasionally arising from a developed stroma of up to 50 µm diam. and above all, longer and wider conidia [25–300 × 3–6 µm versus (19–)26.5–100(–110.5) × (2.5–)3–4 µm in *C. vignae-subterraneae*] that are (0–)3–25(–30)-septate (Hsieh and Goh 1990; Crous and Braun 2003). *C. canescens* causes different leaf spots and caespituli, paler and shorter conidiophores [20–200 µm versus (28–)35.5–278(–340) µm in *C. vignae-subterraneae*] as well as longer conidia [25–300 µm versus (19–)26.5–100(–110.5) µm of *C. vignae-subterraneae*] (Hsieh and Goh 1990). *C. canscorina* forms well-developed stromata as well as paler and shorter conidiophores [29.8–85 µm versus (28–)35.5–278(–340) µm in *C. vignae-subterraneae*] with 1–3 septa (Chiddarwar 1959).

C. caracallae has densely fasciculate, unbranched and shorter conidiophores [40–80 µm versus (28–)35.5–278(–340) µm in *C. vignae-subterraneae*] and slightly shorter conidia [50–75 µm versus (19–)26.5–100(–110.5) µm in *C. vignae-subterraneae*] (Spegazzini 1910). *C. kikuchii* has unbranched and shorter conidiophores [45–200 × 3–6.5 µm versus (28–)35.5–278(–340) µm in *C. vignae-subterraneae*] and larger conidia [50–375 µm versus (19–)26.5–100(–110.5) µm in *C. vignae-subterraneae*] with up to 22 septa (Hsieh and Goh 1990). *C. longispora* has unbranched, shorter and narrower conidiophores [5–30 × 1.5–3 µm versus (28–)35.5–278(–340) × (3.5–)4–5 µm in *C. vignae-subterraneae*] with inconspicuous conidiogenous loci and somewhat longer conidia [75–170 × 2–3.5 µm versus (19–)26.5–100(–110.5) µm in *C. vignae-subterraneae*] (Chupp 1954). *C. vignigena* has paler, shorter and wider conidiophores

[40–130 × 5–7(–10) µm versus (28–)35.5–278(–340) × (3.5–)4–5 µm in *C. vignae-subterraneae*] that are 0–3-septate, and wider conidia [(2.5–)4–6(–10) µm versus (2.5–)3–4 µm of *C. vignae-subterraneae*) (Mulder and Holliday 1975).

In the multi-gene (Fig. 1) and in the ITS phylogeny (see Suppl. material 3), *C. vignae-subterraneae* forms part of a polytomy with a relatively large genetic distance (branch length) in relation to other sequences considered in the analysis. In the *tef1* phylogeny (see Suppl. material 4), it is not possible to distinguish *C. vignae-subterraneae* from other *Cercospora* spp. Based on the results of our comparative study, we propose *C. vignae-subterraneae* as a species new to science.

Cercospora zorniicola **Y.Meswaet, Mangelsdorff, Yorou & M.Piepenbr., sp. nov.**
MycoBank No: 839175
Figs 2J, 13

Type. Benin. Collines: Glazoué, c. 189 m a.s.l., 7°58' 25"N, 2°14'24"E, on *Zornia glochidiata* DC. (Fabaceae), 22 Sep 2019, Y. Meswaet, A. Tabé and M. Piepenbring, YMM299 (***Holotype*****:** M-0312659; ***Isotypes*****:** UNIPAR)**.** ***Ex holotype sequences*****.** MW848616 (*tef1*).

Etymology. The epithet *zorniicola* refers to the host genus *Zornia* and "*-cola*" (lat. *colere* = to dwell).

Diagnosis. *Cercospora zorniicola* is characterised by external hyphae, unbranched conidiophores that are uniform in colour and width, with mostly monoblastic conidiogenous cells (Fig. 13).

Description. ***Leaf spots*** almost lacking or brown to dark brown discolorations, amphigenous, 0.5–2 mm diam., often located along the main veins, surrounded by a yellow discoloration of undefined size and shape. ***Caespituli*** amphigenous, greyish brown to dark brown. ***Mycelium*** internal and external. External hyphae 2–3 µm wide, septate, branched, subhyaline to pale olivaceous, smooth. ***Stromata*** lacking or formed by few substomatal aggregated swollen hyphal cells, up to 22 µm wide, in substomatal chambers or embedded in the mesophyll, dark brown. ***Conidiophores*** in small, loose fascicles of up to approx. 14 conidiophores, arising from internal hyphae breaking through the adaxial epidermis of the leaves, or penetrating through stomatal openings, occasionally solitary arising from external hyphae, erect, straight, subcylindrical to geniculate, unbranched, (15–)24.5–134(–158) × 3.5–4.5 µm, 1–5(–6)-septate, brown to dark brown, often uniform in colour and width. Conidiogenous cells usually monoblastic, rarely polyblastic; loci 1.5–3 µm wide, thickened and darkened. ***Conidia*** solitary, acicular to narrowly obclavate, straight to curved, (15–)27.5–182.5(–200) × (2–)2.5–3.5(–4) µm, 1–8(–12)-septate, hyaline, tip acute, base truncate to short obconically truncate, 1.5–3 µm wide, hila thickened and darkened.

Additional specimens examined. Benin. Borgou: Parakou, on the way to N'Dali, c. 367 m a.s.l., 9°27'53"N, 2°37'43"E, on *Zornia glochidiata*, 17 Sep 2019, Y. Meswaet

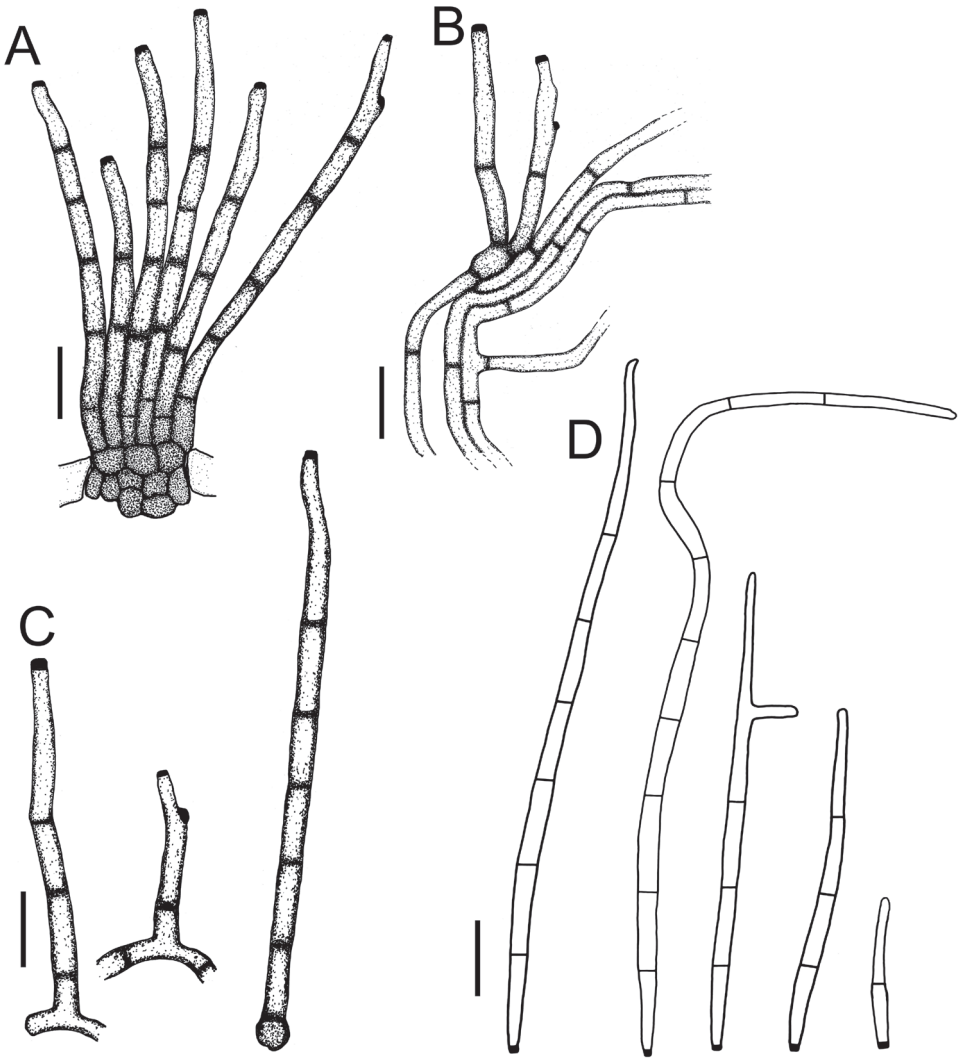

Figure 13. *Cercospora zorniicola* on *Zornia glochidiata* (YMM299) **A** fascicle of conidiophores growing out from a small stroma **B** external hyphae with two conidiophores **C** solitary conidiophores arising from external hyphae **D** conidia. Scale bars: 15 µm (**A**); 12 µm (**B**); 10 µm (**C, D**).

and R. Dramani, YMM13 (***Paratypes*:** M-0312660; UNIPAR). Benin. Borgou: Parakou, c. 391 m a.s.l., 9°22'56"N, 2°37'33"E, same host, 29 Aug 2019, Y. Meswaet and A. Tabé, YMM233 (M-0312661).

Notes. The genus *Zornia* comprises 80 species mainly distributed in tropical regions of the world (Fortuna-Perez et al. 2013). No species of *Cercospora* are currently known on hosts belonging to *Zornia* (Farr and Rossman 2021). *Pseudocercospora zorniae* (J.M. Yen & Gilles) Deighton (≡ *Cercospora zorniae* J.M. Yen & Gilles) is the only known species of cercosporoid fungi infecting species of *Zornia*.

In the multi-gene phylogeny (Fig. 1), *Cercospora zorniicola* grouped closely, but with poor support, with isolates of *Cercospora* cf. *citrullina* (MUCC 576) on *Citrullus lanatus* (Thunb.) Matsum. & Nakai (Cucurbitaceae) and *C. kikuchii* on *Glycine max*, *Phaseolus* spp., *Cyamopsis tetragonoloba* (L.) Taub., *Vigna* and other Fabaceae hosts (Mulder and Holliday 1975; Groenewald et al. 2013). However, morphologically, *C. zorniicola* is clearly distinct from *C.* cf. *citrullina* by external hyphae, unbranched, darker and longer conidiophores [(15–)24.5–134(–158) µm] and somewhat longer conidia [(15–)27.5–182.5(–200) µm], while *C.* cf. *citrullina* has pale to pale brown and short conidiophores (50–86 µm) and shorter conidia (40–130 µm) (Groenewald et al. 2013). *C. zorniicola* differs from *C. kikuchii* in having external hyphae, darker and shorter conidiophores [(15–)24.5–134(–158) µm] and shorter conidia [(15–)27.5–182.5(–200) µm], while *C. kikuchii* has paler and longer conidiophores (45–200 µm) and above all, much longer conidia (50–375 µm) with numerous indistinct septa (Mulder and Holliday 1975; Hsieh and Goh 1990). In the phylogeny based on *tef1* molecular sequence data, it is not possible to distinguish *C. zorniicola* from other *Cercospora* spp. (see Suppl. material 4).

Based on a MegaBLAST search in the NCBI GenBank nucleotide database using the *tef1* sequence data of *C. zorniicola*, the closest matches were *Cercospora* aff. *canescens* on *Dioscorea rotundata* Poir. (Dioscoreaceae) from Ghana (GenBank JX143316; Identities 294 / 300, i.e., 98%), *Cercospora* cf. *coreopsidis* W.W. Ray on *Coreopsis lanceolata* L. (Asteraceae) form South Korea (GenBank JX143344; Identities 293 / 300, i.e., 97%) and *Cercospora nicotianae* on *Nicotiana tabacum* (Solanaceae) from China (GenBank MK881748; Identities 292 / 300, i.e., 97%). This species is proposed to be new to science based on a distinct combination of morphological characteristics and because no other species of *Cercospora* is currently known on a species of this host genus.

***Nothopassalora personata* (Berk. & M.A. Curtis) U.Braun, C.Nakash., Videira & Crous, Studies in Mycology 87: 333. 2017.**

MycoBank No: 822766

Figs 14A, B, 15

Basionym. *Cladosporium personatum* Berk. & M.A. Curtis, Grevillea 3 (27): 106 (1875).

Type. USA. South Carolina: Santee River, on *Arachis hypogaea* (Fabaceae), (no date), Ravenel 1612 (***Holotype*** K n.v.; ***Isotype*** IMI 104552, n.v.; ***Epitype*** CBS H-22946, n.v.).

For more synonyms see Crous and Braun 2003; Videira et al. 2017 or MycoBank.

Description. ***Leaf spots*** amphigenous, subcircular to irregularly angular, 2–8 mm diam., reddish brown, later dark brown by abundant caespituli, finally sometimes greyish brown to blackish brown, margin indefinite. ***Caespituli*** amphigenous, greyish brown to dark brown. ***Mycelium*** mainly internal. **Stromata** small to well-developed, up to 48 µm diam., immersed in the mesophyll or in substomatal chambers, subcircular to irregular, brown to dark brown. ***Conidiophores*** in moderately dense to

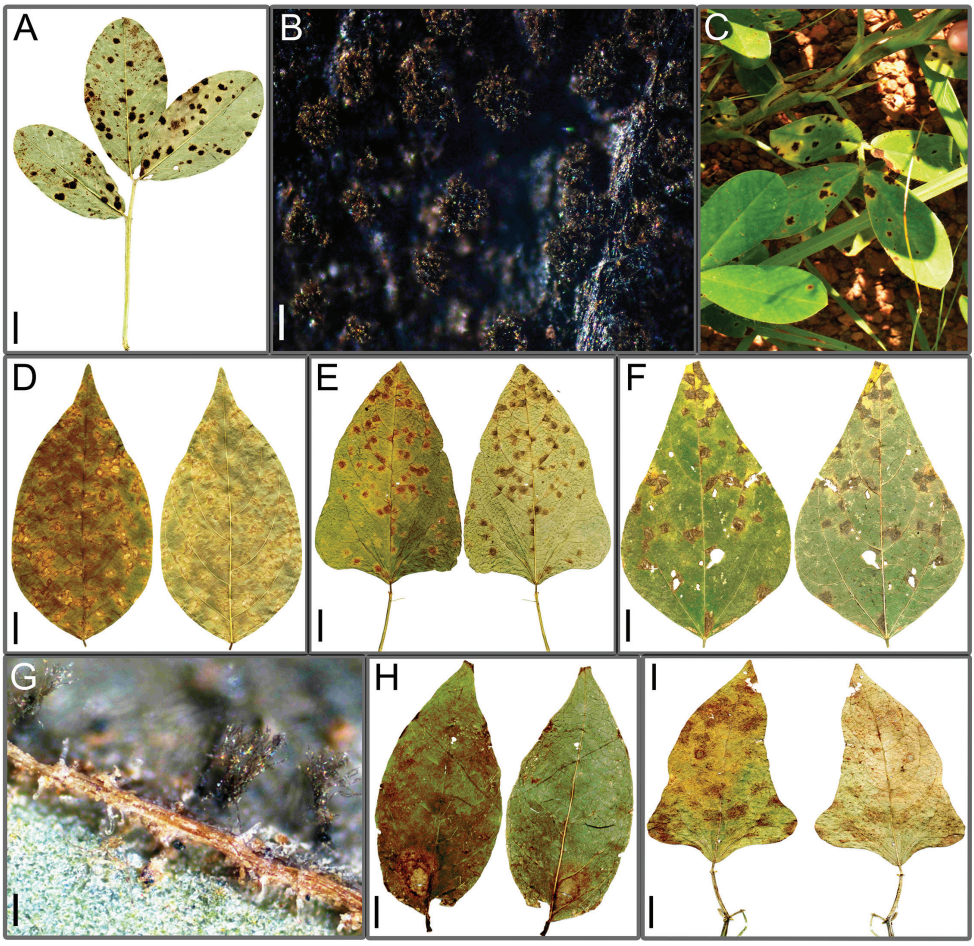

Figure 14. Leaf spot symptoms associated with cercosporoid fungi **A, B** *Nothopassalora personata* on *Arachis hypogaea* (YMM49A) **B** close-up of lesions with caespituli **C** *Passalora arachidicola* on *Arachis hypogaea* (YMM49B) **D** *Pseudocercospora bradburyae* on *Centrosema pubescens* (YMM275) **E** *Pseudocercospora cruenta* on *Phaseolus* sp. (YMM288) **F, G** *Pseudocercospora griseola* on *Phaseolus lunatus* (YMM297A) **G** close-up of lesions with sporulation **H** *Pseudocercospora sennicola* on *Senna occidentalis* (YMM12) **I** *Pseudocercospora tabei* on *Vigna unguiculata* (YMM220). Scale bars: 15 mm (**A, D, E, F, I**); 100 µm (**B, G**); 12 mm (**D, H**).

dense fascicles, arising from stromata, breaking through the adaxial epidermis of the leaves or penetrating through stomatal openings, or solitarily arising through stomatal openings, cylindrical, straight to sinuous or geniculate, conically truncate at the apex, unbranched, (12.5–)20–55.5(–58) × 5–7 µm, 1–3(–4)-septate, pale brown to brown, paler towards the apex. Conidiogenous loci 2.5 µm wide, thickened and darkened. ***Conidia*** solitary, cylindrical to long-obclavate with round apex, straight to curved, (14–)23–68(–80) × (5–)5.5–8(–9) µm, 2–6-septate, pale brown to olivaceous brown, base obconically truncate, 2–3 µm wide, hila thickened and darkened.

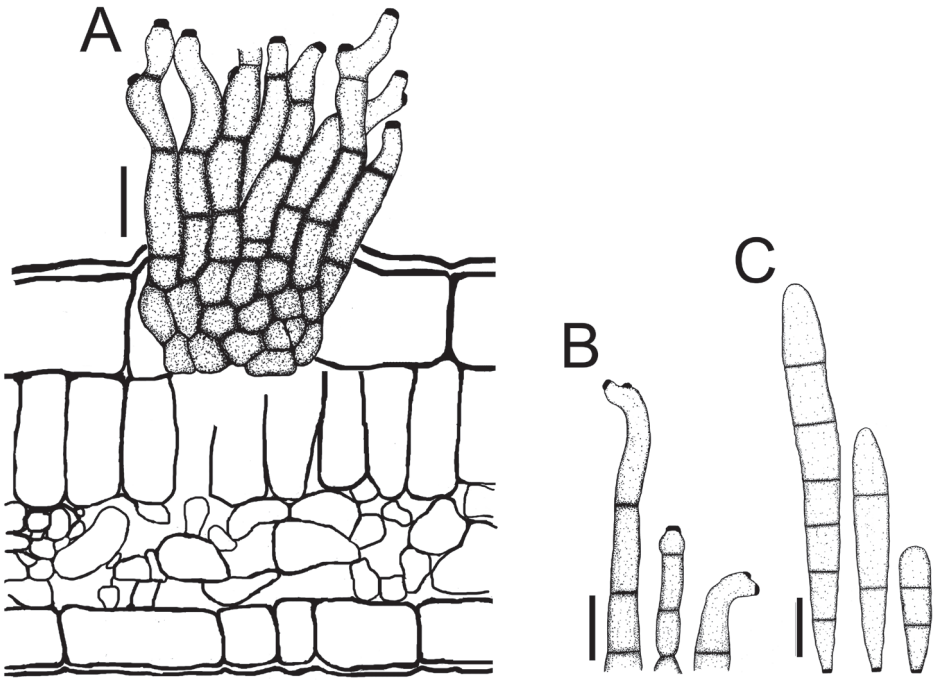

Figure 15. *Nothopassalora personata* on *Arachis hypogaea* (YMM49A) **A** fascicle of conidiophores growing out from a developed stroma embedded in the epidermis **B** solitary conidiophores **C** conidia. Scale bars: 15 µm (**A**); 12 µm (**B, C**).

Specimens examined. Benin. Donga: Taneka-Koko, c. 441 m a.s.l., 9°51'30"N, 1°29'34"E, on *Arachis hypogaea*, 29 Jul 2017, Y. Meswaet, M. Piepenbring N.S. Yorou and participants of the summer school 2017, YMM49A (M-0312662; UNIPAR). Benin. Borgou: Parakou, c. 354 m a.s.l., 9°20'02"N, 2°38'48"E, same host, 27 Aug 2019, Y. Meswaet and R. Dramani, YMM224A (M-0312663). Benin. Borgou: Parakou, Songhai (farm school), c. 333 m a.s.l., 9°24'42"N, 2°41'24"E, same host, 30 Aug 2019, Y. Meswaet and A. Tabé, YMM247 (M-0312664). Benin. Borgou: Commune of Nikki, Tontarou, c. 452 m a.s.l., 9°50'23"N, 3°14'59"E, same host, 19 Sep 2019, Y. Meswaet, A. Tabé and M. Piepenbring, YMM295 (M-0312665).

Herbarium specimens examined for comparison. *Nothopassalora personata*. On *Arachis* sp.: Democratic Republic of the Congo (Zaire). Kindu, 28 Jan 1920, Shantz H. L., 628 (BPI 439440 as *Cercospora personata* Berk. & M.A. Curtis). On *Arachis* sp.: Guinea. 5 Sep 1964, Litzenberger S. C., 91 (BPI 439443 as *C. personata*). On *A. hypogaea*: Indonesia, Java, Tegal, 28 Jan 1920, Raciborski, s.n (BPI 407235 "type?" of *Septogloeum arachidis* Racib.).

Hosts and distribution. On *Arachis glabrata* Benth., *A. hypogaea* (Fabaceae), known in tropical regions where the host is cultivated, including Afghanistan, Angola, Argentina, Australia, Azerbaijan, Bangladesh, Barbados, Benin, Bermuda, Bhutan, Bolivia, Brazil, Brunei, Burkina Faso, Cambodia, Canada, China, Cambodia, Cameroon,

Chad, Colombia, Congo, Cuba, Dominican Republic, Egypt, EI Salvador, Ethiopia, Fiji, French Polynesia, Gabon, Gambia, Georgia, Ghana, Greece, Guam, Guatemala, Guinea, Guyana, Haiti, Honduras, Hong Kong, India, Indonesia, Iran, Iraq, Israel, Ivory Coast, Jamaica, Jordan, Kenya, Korea, Laos, Lesser Antilles, Liberia, Libya, Madagascar, Malawi, Malaysia, Mali, Mauritius, Mexico, Morocco, Mozambique, Myanmar, Nepal, New Caledonia, Nicaragua, Niger, Nigeria, Pakistan, Panama, Papua New Guinea, Paraguay, Peru, Philippines, Puerto Rico, Russia, Saint Vincent and the Grenadines, Senegal, Sierra Leone, Singapore, Solomon Islands, Somalia, South Africa, Spain, Sri Lanka, Sudan, Suriname, Taiwan, Tanzania, Thailand, Togo, Tonga, Trinidad and Tobago, Turkmenistan, Turkey, Uganda, Uruguay, USA, Uzbekistan, Venezuela, Vietnam, Zambia, Zimbabwe (Yen and Lim 1980; Hsieh and Goh 1990; Shin and Kim 2001; Crous and Braun 2003; Farr and Rossman 2021).

Notes. *Nothopassalora personata* and *Passalora arachidicola* (Hori) U.Braun are the agents of the two major foliar diseases of *Arachis hypogaea* worldwide (Jenkins 1938; Kokalis-Burelle et al. 1997; Videira et al. 2017). During the collecting activities in Benin, we observed that both, *N. personata* and *P. arachidicola*, are present wherever *A. hypogaea* is grown and mixed infections are common. In addition, *N. personata* is occasionally associated with *Puccinia* sp. *N. personata* often predominates and is more destructive than *P. arachidicola*. *N. personata* differs from *P. arachidicola*, in forming wider conidiophores (5–7 µm) as well as cylindrical and wider conidia [(5–)5.5–8(–9) µm], while *P. arachidicola* forms narrower conidiophores [(3.5–)4–5 µm)] and conidia (3.5–4.5 µm). *N. personata* and *P. arachidicola* on *A. hypogaea* were previously reported from Benin (Crous and Braun 2003), but this is the first report of these pathogens in Benin including details of the two species.

Passalora arachidicola **(Hori) U.Braun, New Zealand J. Bot. 37: 303. 1999.**
MycoBank No: 459582
Figs 14C, 16

Basionym. *Cercospora arachidicola* Hori, Rep. (Annual) Nishigahara Agric. Exp. Sta. Tokyo: 26. 1917.

Type. Japan. Tokyo, Experiment Station, on *Arachis hypogaea* (Fabaceae), (no date), S. Hori. s.n. (***Holotype*** HIRO, n.v.).

For more synonyms see Crous and Braun (2003) or MycoBank.

Description. ***Leaf spots*** amphigenous, subcircular to angular-irregular, 2.5–9.5 mm diam., greyish brown to medium dark brown, occasionally limited by veins, margin indefinite. ***Caespituli*** epiphyllous, whitish brown to greyish brown. ***Mycelium*** mainly internal. Internal hyphae pale brown, smooth, 1.5–3 µm wide. ***Stromata*** small, up to approx. 32 µm diam., embedded in the mesophyll or in substomatal chambers, subcircular to irregular, brown to dark brown. ***Conidiophores*** in small, loose to moderately dense fascicles, arising from internal hyphae or stromata, or solitary, arising through stomatal openings, erect, straight to sinuous or geniculate, sim-

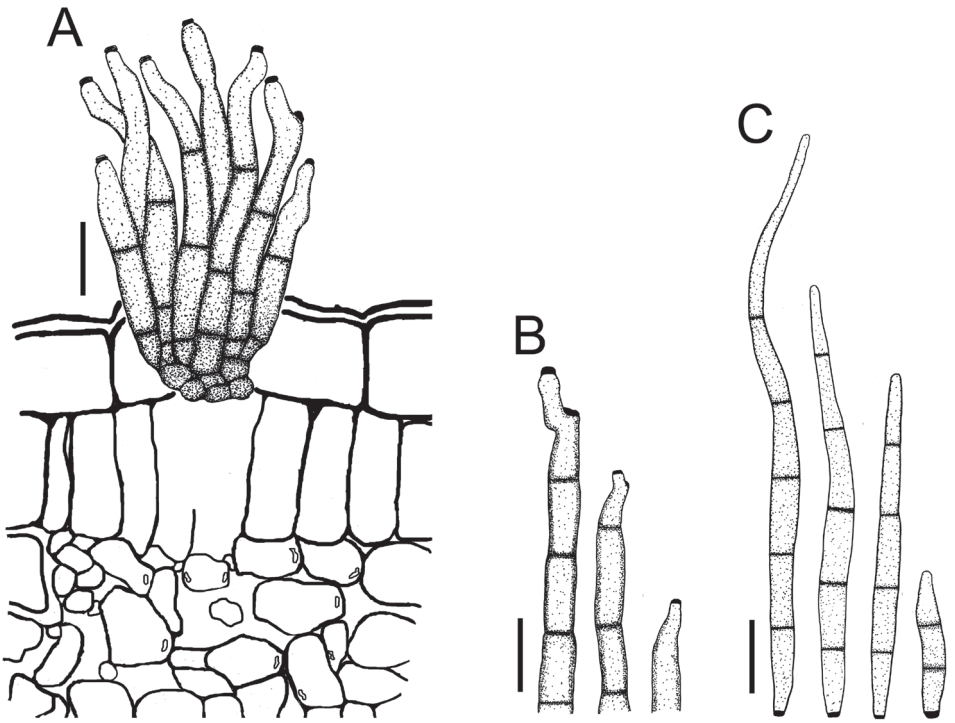

Figure 16. *Passalora arachidicola* on *Arachis hypogaea* (YMM49B) **A** fascicle of conidiophores growing out from a small stroma embedded in the epidermis **B** solitary conidiophores **C** conidia. Scale bars: 15 μm (**A**); 10 μm (**B, C**).

ple, (11.5–)14–42.5(–53) × (3.5–)4–5 μm, 0–5-septate, smooth, olivaceous brown to slightly dark brown, paler towards the tips. Conidiogenous loci 2–2.5(–3) μm wide, thickened and darkened. ***Conidia*** solitary, narrowly obclavate to subacicular, straight to slightly curved, (16–)23–76.5(–88) × 3.5–4.5 μm, 2–5-septate, olivaceous brown, apex subacute or acute, base truncate to short obconically truncate, 2–2.5(–3.5) μm wide, hila thickened and darkened.

Specimens examined. Benin. Donga: Taneka-Koko, c. 441 m a.s.l., 9°51'30"N, 1°29'34"E, on *Arachis hypogaea*, 29 Jul 2017, Y. Meswaet, M. Piepenbring, N. S. Yorou and participants of the summer school 2017, YMM49B (M-0312666; UNIPAR). Benin. Borgou: Parakou, c. 354 m a.s.l., 9°20'02"N, 2°38'48"E, same host, 27 Aug 2019, Y. Meswaet and R. Dramani, YMM224B (M-0312667).

Herbarium specimens examined for comparison. *Passalora arachidicola*. On *Arachis* sp.: Guinea. Labe, 29 Jul 1964, Litzenberger S. C. 55 (BPI 432987 as *Cercospora arachidicola*). On *Arachis* sp.: Guinea. Dubreka, 25 Jul 1964, Litzenberger S. C. 39 (BPI 432989 as *C. arachidicola*). On *Arachis* sp.: Guinea. Beyla, 2 Aug 1964, Litzenberger S. C. 47 (BPI 432990A as *C. arachidicola*). On *Arachis* sp.: Guinea. Kissidougou, 4 Aug 1964, Litzenberger S. C. 28 (BPI 432991 as *C. arachidicola*).

On *Arachis* sp.: Guinea. Dabola, 4 Aug 1964, Litzenberger S. C. 26 (BPI 432992 as *C. arachidicola*).

Host and distribution. On *Arachis hypogaea* (Fabaceae) known worldwide where the host is cultivated, including Afghanistan, Angola, Argentina, Australia, Bangladesh, Benin, Bolivia, Brazil, Brunei, Burkina Faso, China, Cuba, Cambodia, Cameroon, Colombia, Comoros, Democratic Republic Congo, Cuba, Dominican Republic, El Salvador, Fiji, Gabon, Gambia, Ghana, Guatemala, Guinea, Guyana, Hong Kong, India, Indonesia, Ivory Coast, Jamaica, Japan, Kenya, Korea, Laos, Lebanon, Libya, Madagascar, Malawi, Malaysia, Mali, Mauritius, Mexico, Mozambique, Myanmar, Nepal, New Caledonia, Nicaragua, Niger, Nigeria, Pakistan, Panama, Papua New Guinea, Philippines, Puerto Rico, Malaysia, Senegal, Sierra Leone, Solomon Islands, Somalia, South Africa, Sudan, Suriname, Taiwan, Tanzania, Thailand, Togo, Uganda, USA, Uruguay, Venezuela, Vietnam, Zambia, Zimbabwe (Chupp 1954; Hsieh and Goh 1990; Shin and Kim 2001; Crous and Braun 2003; Farr and Rossman 2021).

Notes. *Passalora arachidicola* was placed into the genus *Passalora* by Braun (1999) based on morphological characteristics that are confirmed in the context of the present study. Crous et al. (2009b, 2009c, 2013a) showed that the genus *Passalora* is paraphyletic or polyphyletic. Therefore, the present species most probably does not belong to *Passalora*. However, we refrain from drawing taxonomic conclusions here because a revision of the genus *Passalora* is beyond the scope of the present study.

***Pseudocercospora bradburyae* (E. Young) Deighton, Mycological Papers 140: 140. 1976**

MycoBank No: 321522

Figs 14D, 17

Basionym. *Cercospora bradburyae* E. Young, Mycologia 8 (1): 46 (1916).

Type. Puerto Rico. Rosario, on *Centrosema pubescens* (as *Bradburya pubescens* (Benth.) Kuntze (Fabaceae), 15 Feb 1913, F. L. Stevens 446 (***Holotype*:** ILL!).

For more synonyms see Crous and Braun 2003 or MycoBank.

Description. ***Leaf spots*** amphigenous, subcircular to irregularly angular, (2.5–)4–8.5 mm diam., limited by veins, reddish brown to brown, with indefinite margins. ***Caespituli*** mainly epiphyllous, olivaceous brown to slightly dark brown. ***Mycelium*** internal and external. External hyphae branched, 2.5–3.5 µm wide, septate, olivaceous brown to brown, smooth. ***Stromata*** lacking or small, about 10–18 µm diam., immersed in the mesophyll or in substomatal chambers. ***Conidiophores*** often in small, loose to slightly dense fascicles of up to approx. 10 conidiophores, arising from stromata or breaking through the adaxial epidermis of the leaves, occasionally solitary arising from external hyphae, straight to sinuous or somewhat geniculate, rarely branched, (11–)13–44(–48.5) × (3.5–)4–5 µm, 0–3(–4)-septate, smooth, olivaceous brown to brown, paler towards the tips. ***Conidiogenous cells*** terminal, 10–15 µm long; loci inconspicuous to distinctly denticle-like, not thickened and not darkened, 1.5–3 µm

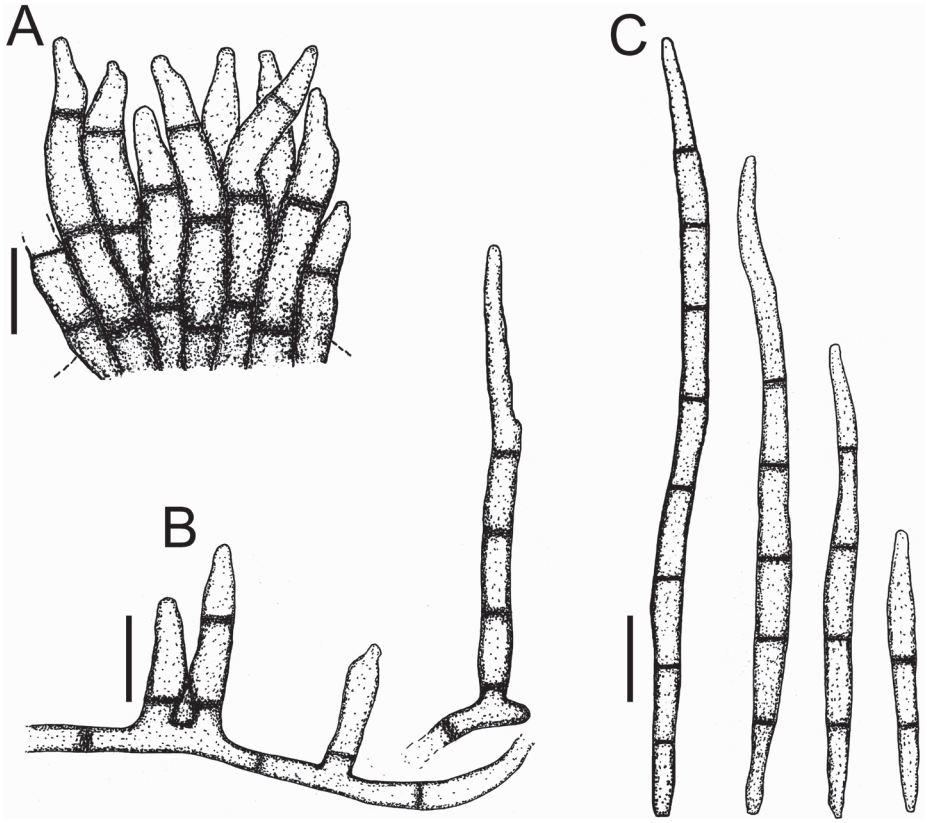

Figure 17. *Pseudocercospora bradburyae* on *Centrosema pubescens* (YMM275) **A** fascicle of conidiophores **B** solitary conidiophores arising from external hyphae **C** conidia. Scale bars: 15 µm (**A**); 10 µm (**B, C**).

wide. ***Conidia*** solitary, narrowly obclavate to subacicular, straight to curved, (30–)38–110(–130) × (2.5–)3–4(–4.5) µm, 3–9-septate, olivaceous brown, smooth, apex subacute to rounded and slightly narrower, base truncate to obconically truncate, 1.5–3 µm wide, hila not thickened and not darkened, occasionally somewhat refractive.

Specimens examined. Benin. Borgou: N'Dali, c. 380 m a.s.l., 9°52'33"N, 2°41'20"E, on *Centrosema pubescens*, 31 Aug 2019, Y. Meswaet and A. Tabé, YMM275 (M-0312668; UNIPAR). Same locality and host, 1 Sep 2019, Y. Meswaet and A. Tabé, YMM275B (M-0312669).

Herbarium specimens examined for comparison. *Pseudocercospora bradburyae*. On *Centrosema pubescens* (as *Bradburya pubescens*): Puerto Rico. Rosario, 15 Feb 1913, Stevens F. L. 446 (ILL14818 ***Holotype*** of *Cercospora bradburyae*). Puerto Rico. Mayagüez, 31 Oct 1913, Stevens F. L. 3930 (ILL10600 ***Paratype***). Puerto Rico. San Germán, 12 Dec 1913, Stevens F. L. 5833 (ILL10606 ***Paratype***). Puerto Rico. Dos Bocas, below Utuado, 30 Dec 1913, Stevens F. L. 6558(ILL10603 ***Paratype***). Puerto Rico. Hormigueros, 14 Jan 1914, Stevens F. L. 225a (ILL10609 ***Paratype***). Guinea. Kindia, May 1963, Kranz J, 2795 (BPI 1112168).

Host and distribution. On *Centrosema acutifolium* Benth., *C. arenarium* Benth., *C. brasilianum* (L.) Benth., *C. macrocarpum* Benth., *C. plumieri* Benth., *C. pubescens*, *C. virginianum* (L.) Benth, *Centrosema* spp. (Fabaceae) from Australia, Barbados, Bolivia, Brazil, Brunei, Cambodia, China, Colombia, Costa Rica, Cuba, Dominican Republic, Ecuador, Fiji, Hong Kong, Ghana, Guinea, Indonesia, Jamaica, Malaysia, Mexico, Micronesia, Mona Island, New Caledonia, Nigeria, Niue, Palau, Papua New Guinea, Peru, Philippines, Puerto Rico, Solomon Islands, St. Thomas, South Africa, Taiwan, Thailand, Togo, Tonga, Trinidad and Tobago, Vanuatu, Venezuela, Virgin Islands (Chupp 1954; Ellis 1976; Hsieh and Goh 1990; Crous and Braun 2003; Farr and Rossman 2021). This species is reported here for the first time for Benin.

Notes. Three species of *Pseudocercospora*, namely *Ps. bradburyae*, *Ps. centrosematicola* (J.M. Yen & Lim) J.M. Yen and *Ps. clitoriae* (G.F. Atk.) Deighton are known on *Centrosema* spp. (Chupp 1954; Farr and Rossman 2021). The present specimens from Benin differ from *Ps. clitoriae* by having often small fascicles formed by up to approx. 10 conidiophores and longer conidiophores [(11–)13–44(–48) µm] and wider conidia [(2.5–)3–4(–4.5) µm], while *Ps. clitoriae* has large, dense fascicles formed by 40 or more conidiophores, shorter conidiophores [8–15(–22) µm] and narrower conidia (2.5–3 µm) (Chupp 1954; Deighton 1976). Based on the descriptions made by Chupp (1954), Hsieh and Goh (1990), Young (1916) and the re-examination of the type specimen of *Ps. bradburyae,* the present specimen from Benin agrees well with *Ps. bradburyae*. In the *tef1* phylogeny (see Suppl. material 4), *Ps. bradburyae* grouped with low support with isolates of *Ps. humuli* on *Humulus lupulus* (Cannabaceae) from Japan, *Ps. cercidicola* on *Cercis chinensis* (Fabaceae) from Japan and *Ps. abelmoschi* on *Hibiscus syriacus* (Malvaceae) from South Korea.

***Pseudocercospora cruenta* (Sacc.) Deighton, Mycol. Pap. 140: 142. 1976**
MycoBank No: 321556
Figs 14E, 18

Basionym. *Cercospora cruenta* Sacc., Michelia 2:149 (1880).

Type. USA. South Carolina: (no further information on the locality), on *Phaseolus* sp. (Fabaceae), (no date), Ravenel 2156 (***Holotype***: PAD, n.v.).

For more synonyms see Crous and Braun (2003) or MycoBank.

Description. ***Leaf spots*** amphigenous, subcircular to irregularly angular, (2.5–)4–8.5 mm diam., limited by veins, reddish brown to dark brown, with an indefinite margin. ***Caespituli*** amphigenous, denser, darker olivaceous to almost sooty on the abaxial surface of the leaves than on the adaxial side. ***Mycelium*** internal and external. External hyphae branched, 2.5–3.5 µm wide, septate, olivaceous brown to brown, smooth. ***Stromata*** lacking or small, 8–14 µm diam., immersed in the mesophyll or in substomatal cavities, subcircular to irregular, brown to dark brown. ***Conidiophores*** in small, loose, moderately large and dense fascicles formed by up to approx. 10 conidiophores, arising from stromata, breaking through the adaxial epidermis of the leaves or pen-

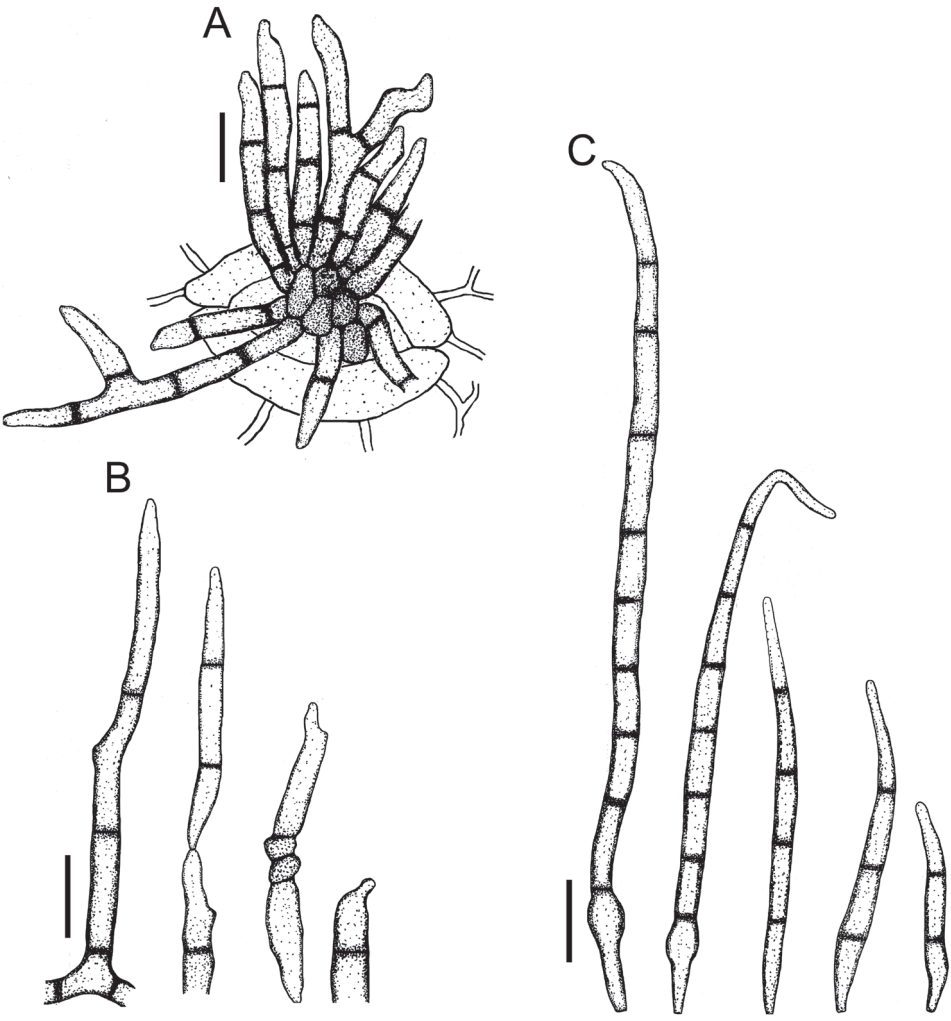

Figure 18. *Pseudocercospora cruenta* on *Phaseolus* sp. (YMM288) **A** fascicle of conidiophores protruding from a stomatal opening **B** solitary conidiophores **C** conidia. Scale bars: 15 μm (**A, C**); 10 μm (**B**).

etrating through stomatal openings, sometimes solitary, arising from external hyphae, straight to sinuous or somewhat geniculate, rarely branched, (12–)15.5–54(–58.5) × (3.5–)4–5 μm [in YMM125 up to 120 μm long], 1–3-septate, smooth, olivaceous brown to brown, paler towards the tips. ***Conidiogenous cells*** terminal or subterminal, a conidiophore can be reduced to a single conidiogenous cell; loci 2–2.5 μm wide, not thickened and not darkened. ***Conidia*** solitary, narrowly obclavate to subacicular, straight to curved, (30.5–)42–132(–154) × (3–)3.5–4.5(–5) μm, 2–10-septate, olivaceous brown, smooth, apex subacute to rounded and slightly narrower than the rest of the conidiophore, up to 2.5 μm wide, base truncate to obconically truncate, 2–2.5(–3) μm wide, hila not thickened and not darkened.

Specimens examined. Benin. Borgou: Parakou, c. 353 m a.s.l., 9°20'02"N, 2°38'48"E, on *Phaseolus* sp., 12 Sep 2019, Y. Meswaet and A. Tabé, YMM288 (M-0312670, UNIPAR). Benin. Atlantique: Commune of Allada, Sékou, c. 84 m a.s.l., 6°38'18"N, 2°13'09"E, on *Vigna unguiculata*, 15 August 2017, Y. Meswaet and A. Tabé, YMM125 (M-0312671; UNIPAR). Benin. Borgou: Parakou, c. 385 m a.s.l., 9°20'34"N, 2°36'39"E, same host, 14 Sep 2019, Y. Meswaet and R. Dramani, YMM03A (M-0312672). Borgou: Parakou, c. 394 m a.s.l., 9°21'25"N, 2°36'45"E, same host, 17 Sep 2019, Y. Meswaet and R. Dramani, YMM294B (M-0312673). Benin. Borgou: Parakou, c. 363 m a.s.l., 9°20'29"N, 2°37'28"E, same host, 21 Sep 2019, Y. Meswaet and A. Tabé, YMM04 (M-0312674).

Herbarium specimens examined for comparison. *Pseudocercospora cruenta*. On *Vigna unguiculata*: USA. Mississippi: Starkville, Sep 1888, Tracy S. M. s.n. (BPI 435817 ***Paratype*** of *Cercospora dolichi* Ellis & Everh.); On *Phaseolus* sp.: USA. South Carolina: Aiken, no date, Ravenel H. W. s.n (BPI 439619 ***Paratype*** of *C. phaseolorum* Cooke). *Pseudocercospora stizolobii* (Syd. & P. Syd.) Deighton. On *Mucuna* sp.: Philippines. Los Baños, 6 Apr 1913, Raimundo M. B. 892 (BPI 441666 ***Holotype*** of *C. stizolobii* Syd. & P. Syd.).

Hosts and distribution. On *Calopogonium* sp., *Canavalia ensiformis* (L.) DC., *C. gladiata* (Jacq.) DC., *C. maritima* Thouars, *Canavalia* sp., *Cassia lathyroides* L., *Cicer arietinum* L., *Clitoria ternatea* L., *Dolichos biflorus* L., *D. lablab* L., *Dolichos* sp., *Glycine max*, *Glycine* sp., *Lablab niger* Medik., *L. purpureus* (L.) Sweet, *Mucuna capitata* Wight & Arn., *M. deeringiana* (Bort) Merr., *Phaseolus aconitifolius* Jacq., *P. adenanthus* G. Mey., *P. aureus* Roxb., *P. calcaratus* Roxb., *P. coccineus* L., *P. lathyroides* L., *P. lunatus*, *P. radiatus* L., *P. sublobatus* Roxb., *P. vulgaris*, *Psophocarpus tetragonolobus* (L.) DC., *Pueraria* sp., *Strophostyles helvola* (L.) Elliott, *Vicia faba* L., *Vigna antillana* (Urb.) Fawc. & Rendle, *V. catjang* (Burm.f.) Walp., *V. cylindrica* (L.) Skeels, *V. luteola* (Jacq.) Benth., *V. marina* (Burm.) Merr., *V. mungo* (L.) Hepper, *V. repens* (L.) Kuntze, *V. sesquipedalis* (L.) Fruwirth, *V. sinensis* (L.) Savi ex Hausskn., *V. unguiculata* (L.) Walp., and further species in other genera of Fabaceae. It is widespread in warmer regions, including Afghanistan, Angola, Argentina, Australia, Azerbaijan, Bangladesh, Barbados, Bolivia, Brazil, Brunei, Cambodia, Canada, China, Colombia, Cuba, Dominican Republic, Egypt, EI Salvador, Ethiopia, Fiji, Ghana, Grenada, Guatemala, Guyana, Haiti, Honduras, Hong Kong, India, Indonesia, Iran, Iraq, Italy, Jamaica, Japan, Korea, Liberia, Malawi, Malaysia, Mauritius, Mexico, Mozambique, Myanmar, Nepal, New Caledonia, Niger, Nigeria, Pakistan, Panama, Papua New Guinea, Peru, Philippines, Puerto Rico, Russia, Rwanda, Saint Lucia, Saint Vincent and the Grenadines, Samoa, Saudi Arabia, Senegal, Sierra Leone, Singapore, Solomon Islands, Somalia, South Africa, Sri Lanka, Sudan, Suriname, Taiwan, Tanzania, Thailand, Togo, Tonga, Trinidad and Tobago, Uganda, USA, Venezuela, Virgin Islands, Zambia, Zimbabwe. (Saccardo 1886; Mulder and Holliday 1975; Ellis 1976; Yen and Lim 1980; Shin and Kim 2001; Crous and Braun 2003; Farr and Rossman 2021).

Notes. Except for the presence of external hyphae and mostly slightly shorter conidiophores, the present specimen from Benin is morphologically identical to *Ps. cruenta*

as known by literature (Chupp 1954; Deighton 1976). This identification is confirmed by results obtained by phylogenetic analyses based on *tef1* sequence data (see Suppl. material 4). *Ps. cruenta* is a well-known pathogen causing leaf spot diseases on species of *Vigna* and allied genera. It can cause serious yield losses of up to 40% in cowpea (Sivanesan 1990). *Ps. cruenta* is cited here for the first time for Benin.

***Pseudocercospora griseola* (Sacc.) Crous & U.Braun, Studies in Mycology 55: 169. 2006**

MycoBank No: 500855
Figs 14F, G, 19

Basionym. *Isariopsis griseola* Sacc., Michelia 1: 273. 1878.

For synonyms see Crous and Braun (2003), Crous et al. (2006) or MycoBank.

Type. Italy. Selva, on *Phaseolus vulgaris* L. (Fabaceae), Aug 1877, Saccardo, Mycotheca Veneta 1247 (***Lectotype*:** HAL, designated by Videira et al. 2017: 401, MBT378593, n.v.; ***Epitype*:** CBS H-19683, designated by Videira et al. 2017: 401, MBT378594, n.v.).

For illustrations see: Saccardo (1881), Fragoso (1927), Deighton (1990), Shin and Kim (2001) or Crous et al. (2006).

Description. ***Leaf spots*** amphigenous, subcircular to irregularly angular, 2.5–7(–9.5) mm diam., reddish brown to dark brown or sometimes greyish brown to dark reddish brown, surrounded by a narrow darker margin. ***Caespituli*** amphigenous, mainly hypophyllous, reddish brown to olivaceous brown. ***Mycelium*** internal and external. External hyphae branched, 2.5–3 µm wide, septate, olivaceous brown to brown, smooth. ***Conidiophores*** in dense synnematous fascicles, synnemata up to 250 µm high, 20–40(–65) µm wide, emerging through stomatal openings or erumpent, or conidiophores solitary, arising from external hyphae, straight to sinuous or somewhat geniculate, 3–5(–6.5) µm wide, 1–6-septate, smooth, olivaceous brown to brown. Conidiogenous loci not thickened and not darkened, rather inconspicuous. ***Conidia*** solitary, narrowly obclavate to subacicular, straight to curved, (22–)30–78(–83) × (4.5–)5–7 µm, 2–6-septate, olivaceous brown, smooth, apex subacute to rounded, base truncate to obconically truncate, (2.5–)3–4(–4.5) µm wide, hila not thickened and not darkened.

Specimen examined. Benin. Borgou: Parakou, Tankaro, c. 360 m a.s.l., 9°23'01"N, 2°30'36"E, on *Phaseolus lunatus*, 20 Sep 2019, Y. Meswaet and R. Dramani, YM-M297A (M-0312675; UNIPAR).

Herbarium specimens examined for comparison. *Pseudocercospora griseola*. On *Phaseolus* sp.: USA. Pennsylvania: West Chester, Gardens, Sep 1880, W. T. Harris 1363 (NY 00937289 ***Holotype*** of *Graphium laxum*). On *Phaseolus* sp.: USA. Pennsylvania: West Chester, Gardens, Sep 1880, W. T. Harris s.n (BPI 448758 ***Paratype*** of *G. laxum*). On *Phaseolus* sp.: USA. New Jersey: Newfield, 27 Sep 1894, Ellis, s.n (BPI 435104 ***Paratype*** of *Cercospora columnaris* Ellis & Everh.). On *P. vulgaris*: Italy. Venetia, Selva, Aug 1877, Sacc. Mycoth. Ven. s.n (BPI 449390, ***isolectotype*** of *Isariopsis griseola*).

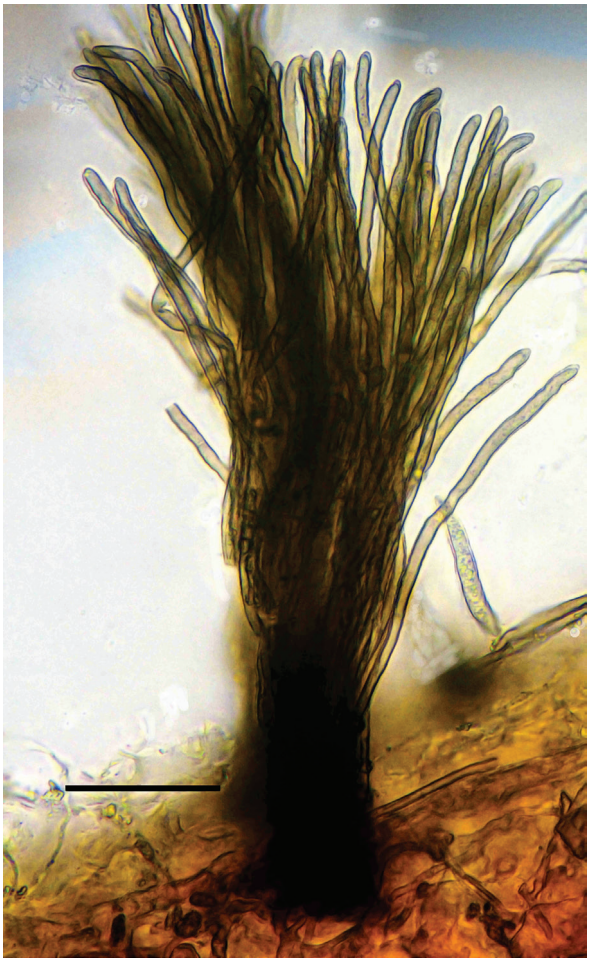

Figure 19. Synnematous fascicle of conidiophores of *Pseudocercospora griseola* on *Phaseolus lunatus* (YMM297A). Scale bar: 50 μm.

Hosts and distribution. On *Lablab purpureus* (L.) Sweet (as *Lablab niger* Medik.), *Lathyrus odoratus* L., *Macroptilium atropurpureum* (DC.) Urb., *Phaseolus acutifolius* A. Gray, *P. coccineus* L., *P. lunatus*, *P. vulgaris*, *Vigna angularis* (Willd.) Ohwi & H. Ohashi, *V. mungo*, *V. radiata*, *V. umbellata* (Thunb.) Ohwi & H. Ohashi (as *P. pubescens* Blume), *V. unguiculata* (L.) Walp. (Fabaceae) from worldwide, including Angola, Argentina, Armenia, Australia, Austria, Bhutan, Brazil, Bulgaria, Burundi, Cameroon, Canada, China, Colombia, Costa Rica, Croatia, Cuba, Democratic Republic Congo, Dominican Republic, Ecuador, El Salvador, Ethiopia, Fiji, Georgia, Germany, Ghana, Great Britain, Greece, Guatemala, Haiti, Hungary, Jamaica, Japan, India, Indonesia, Iran, Ireland, Israel, Italy, Ivory Coast, Jamaica, Japan, Kenya, Korea, Laos, Latvia, Malawi, Madagascar, Malaysia, Mauritius, Mexico, Mozambique, Nepal, Netherlands, Netherlands Antilles, New Caledonia, New Zea-

land, Nicaragua, Nigeria, Norfolk Island, Panama, Papua New Guinea, Paraguay, Peru, Philippines, Poland, Portugal, Puerto Rico, Reunion (France), Romania, Russia, Rwanda, Saint Helena (British), Senegal, Sierra Leone, Singapore, Slovenia, Solomon Islands, Somalia, South Africa, Spain, Sudan, Suriname, Swaziland, Switzerland, Taiwan, Tanzania, Thailand, Trinidad and Tobago, Turkey, Uganda, Ukraine, U.S.A., Vanuatu, Venezuela, Virgin Islands, Zambia, Zimbabwe (Crous and Braun 2003; Crous et al. 2006; Farr and Rossman 2021). *Ps. griseola* is reported here for the first time for Benin.

Notes. Four species of *Pseudocercospora*, namely *Ps. cruenta*, *Ps. glycines* (Cooke) Deighton, *Ps. griseola* and *Ps. stizolobii* are known agents of leaf spot diseases on *Phaseolus* spp. (Farr and Rossman 2021). The present *Pseudocercospora* sp. is phylogenetically (Fig. 1) and morphologically well distinguished from *Ps. cruenta*, *Ps. glycines* and *Ps. stizolobii* (Crous et al. 2006) by forming synnematous fascicles, longer and broader conidiophores and broader conidia. The morphology of this collection from Benin on *P. lunatus* fits well with the description of *Ps. griseola*.

Angular leaf spot (ALS) caused by *Ps. griseola* is a serious disease of common bean (*P. vulgaris*) all around the world (Ddamulira et al. 2014). It is reported for about 80 countries, where it can cause 45% to 80% losses of yield under conditions favourable for the fungus (Guzmán et al. 1999). The disease is also a major problem for bean production (50–60% of yield losses) in Africa, mainly in the Great Lakes Regions (Kenya, Uganda, Tanzania and Rwanda) where bean growing is popular (Golato and Meossi 1972; Wortmann et al. 1998; Aggarwal et al. 2004). According to Guzmán et al. (1995) and Crous et al. (2006), the species includes two major intraspecific groups, *Ps. griseola* f. *griseola* (Andean) and *Ps. griseola* f. *mesoamericana* (Middle-American) (Crous et al. 2006). Based on ITS sequence data (see Suppl. material 3), the present isolate from Benin clusters with *Ps. griseola* f. *mesoamericana*.

Pseudocercospora sennicola **Y.Meswaet, Mangelsdorff, Yorou & M.Piepenbr., sp. nov.**
MycoBank No: 839176
Figs 14H, 20

Type. Benin. Atlantique: Cotonou, University of Abomey-Calavi, c. 9 m a.s.l., 6°24'45"N, 2°20'41"E on *Senna occidentalis* (L.) Link (Fabaceae), 23 Sep 2019, Y. Meswaet and A. Tabé, YMM12 (***Holotype*****:** M-0312676; ***Isotype*****:** UNIPAR). ***Ex holotype sequences*****.** MW834444 (SSU), MW834432 (LSU), MW850550 (ITS).

Etymology. The epithet *sennicola* refers to the host genus *Senna* and *-cola* (lat. *colere* = to dwell).

Diagnosis. *Pseudocercospora sennicola* differs from other *Pseudocercospora* spp. known on *Senna* spp. by causing often inconspicuous spots and the combination of branched and relatively long conidiophores [16.5–)20.5–92(–98) µm] and relatively short and wide conidia [(16–)22–54.5(–65) × 3–4.5(–5) µm] that are often constricted at the septa (Table 6).

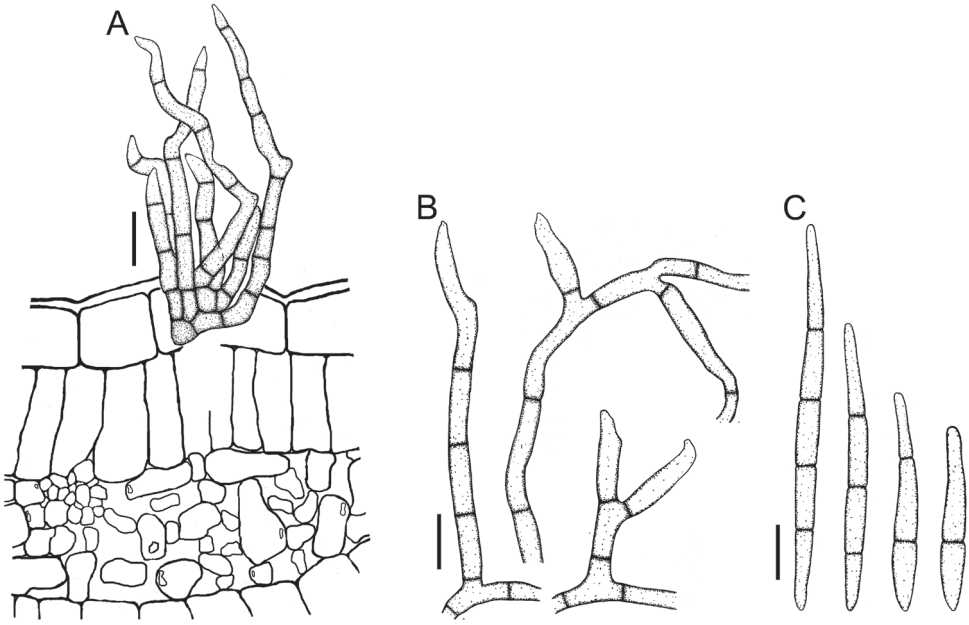

Figure 20. *Pseudocercospora sennicola* on *Senna occidentalis* (YMM12) **A** fascicle of conidiophores growing out of a small stroma embedded in the epidermis **B** solitary conidiophores arising from external hyphae **C** conidia. Scale bars: 15 µm (**A**); 10 µm (**B, C**).

Description. ***Leaf spots*** lacking or indistinct to pale brown discolorations, amphigenous, subcircular to irregularly angular, (2–)4.5–10.5 mm diam., occasionally surrounded by a darker margin. ***Caespituli*** amphigenous, loose, olivaceous brown. ***Mycelium*** internal and external. External hyphae branched, 2.5–3.5 µm wide, septate, olivaceous brown to brown, smooth. ***Stromata*** lacking to slightly developed, in substomatal cavities or partly embedded in the mesophyll, 10–20 µm diam., brown to dark brown. ***Conidiophores*** in small, loose fascicles of up to approx. 10 conidiophores, arising from internal hyphae or hyphal aggregations, breaking through the adaxial epidermis of the leaves or penetrating through stomatal openings, or solitary, arising from external hyphae, erect to decumbent, flexuous, simple or occasionally branched, subcylindrical to somewhat clavate, geniculate-sinuous, slightly narrower towards the tips, (16.5–)20.5–92(–98) × (3–)3.5–4.5 µm, 2–6(–8)-septate, smooth, olivaceous brown to slightly dark brown, paler towards the tips. ***Conidiogenous cells*** terminal or lateral, medium brown, smooth, proliferating sympodially, with slightly tapering to flat-tipped apical loci; loci 1.5–2.5 µm wide, not thickened and not darkened. ***Conidia*** solitary, narrowly obclavate to subacicular, straight to curved, (16–)22–54.5(–65) × 3–4.5(–5) µm, 2–6-septate, often constricted at the septa, olivaceous brown, smooth, apex subacute, base truncate to obconically truncate, 1.5–2.5 µm wide, hila not thickened and not darkened.

Table 6. Comparison of *Pseudocercospora sennicola* on *Senna occidentalis* (YMM12) with *Pseudocercospora* species known from *Senna* spp. based on literature [a–g].

Cercospora species	*Leaf spots*, colour, size	Stromata	Conidiophore size (in µm), branching, septa	Conidium sizes (in µm), septa
Pseudocercospora sennicola (YMM12)	Often lacking or indistinct	Lacking to slightly-developed	(16.5–)20.5–92(–98) × (3–)3.5–4.5, branched, 2–6(–8)- septate	(16–)22–54.5(–65) × 3–4.5(–5) µm, 2–6 septa, slightly constricted at the septa
Ps. angustata [ab]	Brownish to dingy grey, 0.5–3 mm.	Small	10–50 × 2–3.5, unbranched, rarely septate	15–75 × 2–4 µm, 3–7 septa
Ps. cassiae-alatae [c]	Present	Small	3–45 × 2.5–3.5, 0–6-septate	15–90 × 1.5–2 µm, 1–10 septa
Ps. cassiae-fistulae [d]	Greyish brown to dark, 0.5–2 mm.	Well-developed	10–30 × 2.5–5, unbranched, 0–2-septate	25–65 × 3–4 µm, 2–8 distinct septa
Ps. cassiae-occidentalis [c]	Indistinct	Absent	60–130 × 4–5, unbranched, 2–6-septate	62–100 × 3.5–4.8, 3–6 septa
Ps. cassiae-siameae [be]	Present	Present	15.3–27.2 × 3.4–4.2, 0–1-septate	28.9–93.5 × 3.4–4.2, 2–8 septa
Ps. nigricans [bdf]	Yellowish discoloration to greyish brown, 2–3 mm wide	Small	15–125 × 3–5, branched, 1–3-septate	20–80 × 3–5, 1–10 septa
Ps. sennae-multijugae [g]	Grey brown, 2–18 mm in diam.	Well-developed (5–67 µm diam.)	11–81 × 3–4, unbranched, 0–2-septate	75–170 × 2–3.5, 2–7 septa
Ps. singaporensis [c]	Yellowish to brownish grey, 0.5–4 mm in diam.	Absent	31–77 × 4.5–5.5, branched, 0–2(–4)-septate.	30–67 × 3.5, 3 (rarely 1 or 4) septa
Ps. taichungensis [d]	Greyish brown, 1–5 mm wide	Well-developed	10–25 × 1–4.3, unbranched, 0–2-septate	20–55–100 × 1.5–3, 1–6 indistinct septa

[a] Lenné (1990), [b] Deighton (1976), [c] Yen and Lim (1980), [d] Hsieh and Goh 1990, [e] Chiddarwar (1959), [f] Cooke and Massee (1883-1884), [g] Silva et al. (2016)

Additional specimen examined. Benin. Atlantique: Cotonou, University of Abomey-Calavi, c. 9 m a.s.l., 6°24'45"N, 2°20'41"E, on *Senna occidentalis*, 26 Sep 2019, Y. Meswaet and A. Tabé, YMM12B (***Paratypes*:** M-0312677; UNIPAR).

Herbarium specimens examined for comparison. On *Senna occidentalis* (as *Cassia occidentalis* L.): USA. South Carolina: Aiken, 1876, Ravenel H. W. s.n. (BPI 439584, ***Holotype*** of *Cladosporium personatum* var. *cassiae* Thüm.).

Host and distribution. On *Senna occidentalis* (Fabaceae) in Benin.

Notes. Currently, eleven *Pseudocercospora* species are known on *Senna* spp. (Fabaceae), namely *Ps. angustata* (Chupp & Solheim) Deighton on *Senna hirsuta* (L.) H.S. Irwin & Barneby, *Ps. cassiae-alatae* (J.M. Yen & Lim) J.M. Yen on *S. alata* (L.) Roxb., *Ps. cassiae-fistulae* Goh & W.H. Hsieh on *Cassia fistula* L. and *S. rizzinii* H.S. Irwin & Barneby, *Ps. cassiae-occidentalis* (J.M. Yen) J.M. Yen on *S. occidentalis*, *Ps. cassiae-siameae* (Chidd.) Deighton on *S. siamea* (Lam.) H.S. Irwin & Barneby, *Ps. nigricans* (Cooke) Deighton on *Senna* spp., *Ps. sennae-multijugae* on *S. multijuga* (Rich.) H.S. Irwin & Barneby, *Ps. sennae-rugosae* A. Hern. Gut., Z.M. Chaves & Dianese on *S. rugosa* (G. Don) H.S. Irwin & Barneby, *Ps. singaporensis* (J.M. Yen) J.M. Yen on *S. occidentalis* (L.) Link, *Ps. taichungensis* Goh & W.H. Hsieh on *S. atomaria* (L.) H.S. Irwin & Barneby (Hernández-Gutiérrez et al. 2015; Farr and Rossman 2021). Among these eleven species of *Pseudocercospora*, only *Ps. nigricans* and *Ps. singaporensis* have some similarity with the species described here (Table 6). *Ps. sennicola*, however, differs from *Ps. nigricans* in causing often indistinct leaf spots, shorter conidiophores [(16.5–)20.5–92(–98) µm versus 15–125 µm in *Ps. nigricans*] with 6(–8) septa and shorter

conidia [(16–)22–54.5(–65) versus 20–80 µm in *Ps. nigricans*] (Hsieh and Goh 1990). *Ps. sennicola* differs from *Ps. singaporensis* by causing often indistinct leaf spots, slightly developed stromata, longer conidiophores [(16.5–)20.5–92(–98) µm versus 31–77 µm in *Ps. singaporensis*] and shorter conidia [(16–)22–54.5(–65) versus 30–67 µm in *Ps. singaporensis*] (Yen and Lim 1980). Moreover, the specimen from Benin has conidia with more septa (2–6 versus strictly 3-septate in *Ps. singaporensis*) and conidial walls constricted at the septa.

In the multi-gene tree (Fig. 1), *Ps. sennicola* is located in a polytomy at the end of a long branch reflecting a long genetic distance to other species included in the analysis. Morphologically, *Ps. sennicola* is distinct from all *Pseudocercospora* species known on species of Fabaceae from Benin by longer conidiophores [(16.5–)20.5–92(–98) µm] and smaller conidia [(16–)22–54.5(–65) µm)].

Based on a MegaBLAST search using the ITS sequence data, the closest matches in NCBI's GenBank nucleotide database were *Pseudocercospora fuligena* on *Lycopersicon* sp. (Solanaceae) from Thailand (GenBank GU214675; Identities 674/687, i.e., 98%), *Pseudocercospora chengtuensis* on *Lycium chinense* (Solanaceae) from South Korea (GenBank GU214672; Identities 674/687, i.e., 98%) and *Pseudocercospora atromarginalis* on *Solanum nigrum* L. (Solanaceae) from South Korea (GenBank GU214671; Identities 673/687, i.e., 97%). Based on the result of our comparative study, we consider the present *Pseudocercospora* species on *Senna occidentalis* from Benin to represent a distinct species, which is described here. However, as sequence data are only available for *Ps. sennae-multijugae*, more molecular sequence data are needed to clarify the species delimitations among these twelve *Ps.* species on *Senna* spp.

Pseudocercospora tabei **Y.Meswaet, Mangelsdorff, Yorou & M.Piepenbr., sp. nov.**
MycoBank No: 839177
Figs 14I, 21

Type. Benin. Borgou: Parakou, c. 360 m a.s.l., 9°20'07"N, 2°38'50"E, on *Vigna unguiculata* (L.) Walp. (Fabaceae), 2 Sep 2019, Y. Meswaet and A. Tabé, YMM220 (***Holotype*****:** M-0312678; ***Isotype*****:** UNIPAR). ***Ex holotype sequences*****.** MW834450 (SSU), MW834434 (LSU), MW834439 (ITS), MW848617 (*tef1*).

Etymology. The epithet *tabei* refers to the person who collected the type specimen, Affoussatou Tabé, mycologist at the University of Parakou, Benin.

Diagnosis. *Pseudocercospora tabei* differs from other *Pseudocercospora* spp. known on *Vigna* spp. by external hyphae, well-developed stromata, as well as the sizes of conidiophores [(20.5–)24–82(–84.5) × 3–4(–4.5) µm] and conidia [(20.5–)24–82(–84.5) × 3–4(–4.5) µm] (Table 7).

Description. ***Leaf spots*** amphigenous, subcircular to irregularly angular, 2.5–7.5 mm diam., occasionally limited by veins, yellowish brown to pale brown, reddish brown to dark brown when old, more evident on the adaxial surface of the leaves, margin indefinite. ***Caespituli*** amphigenous, brown. ***Mycelium*** internal and external. External

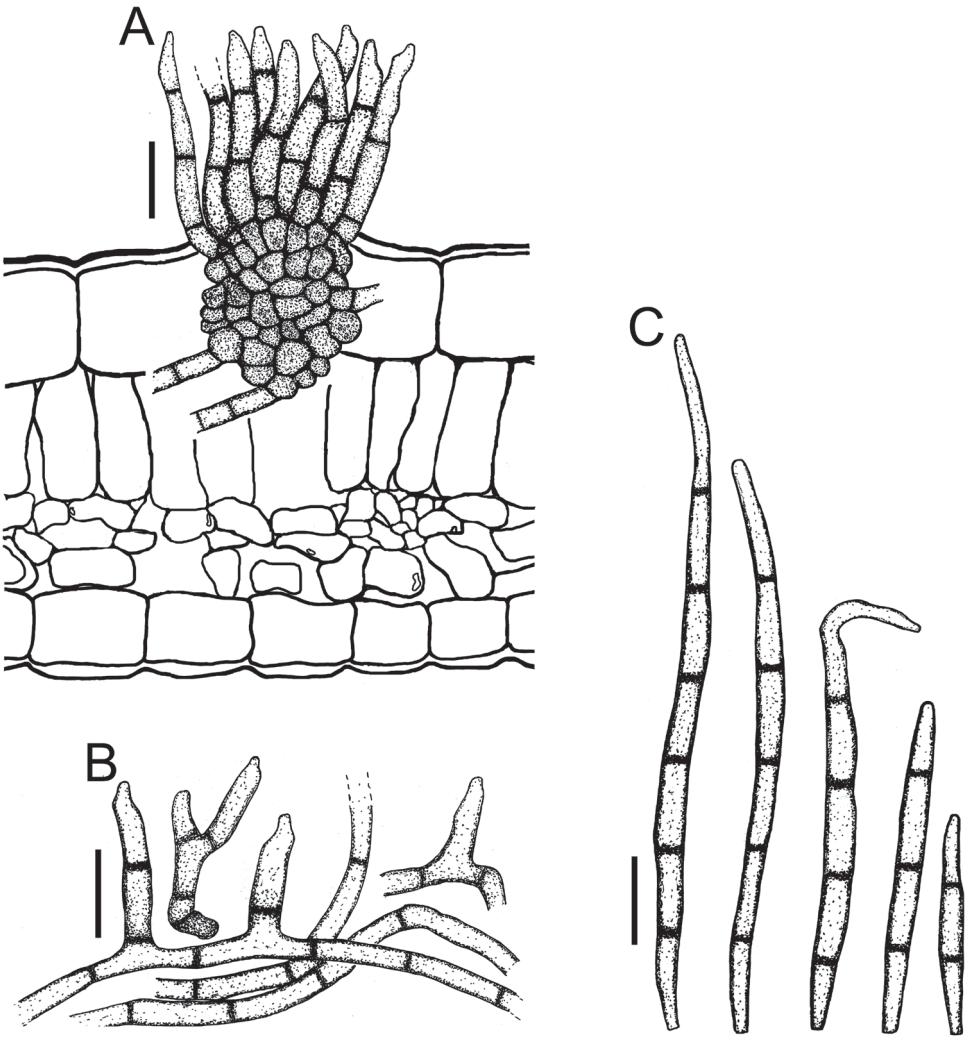

Figure 21. *Pseudocercospora tabei* on *Vigna unguiculata* (YMM220) **A** immersed stroma with conidiophores **B** solitary conidiophores arising from external hyphae **C** conidia. Scale bars: 15 μm (**A**); 12 μm (**B**); 10 μm (**C**).

hyphae branched, 2–2.5(–3.5) μm wide, septate, olivaceous brown to brown, smooth. ***Stromata*** lacking or formed by few aggregated swollen hyphal cells to well-developed, up to approx. 45 μm diam., immersed in the mesophyll or in substomatal chambers, globular to irregular, brown to mostly dark brown. ***Conidiophores*** in small, loose to moderately dense fascicles arising from stromata, breaking through the adaxial epidermis of the leaves or penetrating through stomatal openings, or solitary, arising from external hyphae, straight to sinuous or somewhat geniculate, simple or rarely branched, (11.5–)14.5–40(–44.5) × (3–)3.5–4(–4.5) μm, 0–4-septate, smooth, olivaceous brown to

Table 7. Comparison of *Pseudocercospora tabei* YMM220 on *Vigna unguiculata* with *Pseudocercospora* species known from *Vigna* spp. based on literature [a–d].

***Pseudocercospora* species**	**Stromata**	**Conidiophore size (in µm), branching, septa**	**Conidia size (in µm), septa**
Pseudocercospora tabei (YMM220)	Small or well-developed up to 45 µm diam.	(11.5–)14.5–40(–44.5) × (3–)3.5–4(–4.5), branched, 0–4-septate	(20.5–)24–82(–84.5) × 3–4(4.5), 2–6(–8) septa
Ps. cruenta [a]	Up to 30 µm diam.	10–75 × 3–5, branched, 0–3-septate	25–120 × 2–5, 3–14 septa
Ps. mungo [b]	Up to 30 µm diam.	Up to 90(–130) × 4.5–7.5, branched, 1–3-septate	25–84 × 4.5–7.5, 3–8 septa
Ps. phaseolicola [a]	Absent	3–25 × 1.5–3	20–90 × 1.5–2, indistinctly septate
Ps. shihmenensis[a]	Absent	35–55 × 4–5, branched, 1–4-septate	20–52 × 4–5, 3–8 septa
Ps. vexillatae [ac]	Presen t	10–17 × 4–5, unbranched, continuous or rarely 1-septate	40–100 × 2.5–4, 3–8 septa
Ps. vignae-reticulatae [b]	Small	40–250 × 3.5–5.5, branched	30–95 × 4 –6.5, 1–12 septa
Ps. vignicola [c]	Well-developed	22–75 × 3–5, branched, 0–1-septate	30–60 × 2.5–3, 3–6 septa
Ps. vignigena [d]	Small	22–75 × 3–5, unbranched, 1–3-septate	33–60 × 4–5.5(–6), 3–6 septa

[a] Hsieh and Goh (1990), [b] Deighton (1976), [c] Braun et al. (1999), [d] Yen et al. (1982)

brown, paler towards the tips, sometimes a conidiophore is reduced to a single conidiogenous cell. ***Conidiogenous cells*** terminal or lateral, rarely up to 20 µm long, pale or olivaceous brown, smooth, proliferating sympodially; loci 2–3.5 µm wide, not thickened and not darkened. ***Conidia*** solitary, narrowly cylindrical to obclavate-cylindrical, straight to slightly curved, (20.5–)24–82(–84.5) × 3–4(–4.5) µm, conspicuously 2–6(–8)-septate, olivaceous brown, smooth, apex subacute to rounded and narrower than the rest of the conidium, base truncate, (2–)2.5–3.5 µm wide, hila not thickened and not darkened.

Additional specimens examined. Benin. Borgou: Parakou, c. 354 m a.s.l., 9°20'02"N, 2°38'48"E, on *Vigna unguiculata*, 27 Aug 2019, Y. Meswaet and A. Tabé, YMM232A (***Paratypes*:** M-0312679; UNIPAR). Benin. Borgou: Parakou, c. 391 m a.s.l., 9°22'56"N, 2°37'33"E, same host, 29 Aug 2019, Y. Meswaet and A. Tabé, YMM232B (M-0312680).

Herbarium specimens examined for comparison. *Pseudocercospora cruenta*. On *Vigna unguiculata*: USA. Mississippi: Starkville, Sep 1888, Tracy S. M. s.n. (BPI 435817 ***Paratype*** of *Cercospora dolichi*). On *Phaseolus* sp.: USA. South Carolina: Aiken, Ravenel H. W. s.n (BPI 439619, type of *C. phaseolorum*). *Pseudocercospora stizolobii*. On *Mucuna* sp.: Philippines. Los Baños, 6 Apr 1913, Raimundo M. B. 892 (BPI 441666, ***Holotype*** of *C. stizolobii*).

Host and distribution. On *Vigna unguiculata* (Fabaceae) in Benin.

Notes. On species of *Vigna*, eight species of *Pseudocercospora*, namely *Ps. cruenta*, *Ps. mungo* Deighton, *Ps. phaseolicola* Goh & W.H. Hsieh, *Ps. shihmenensis* (J.M. Yen) J.M. Yen, *Ps. vexillatae* (J.M. Yen) U.Braun, *Ps. vignae-reticulatae* Deighton, *Ps. vignicola* (J.M. Yen, A.K. Kar & B.K. Das) U.Braun and *Ps. vignigena* J.M. Yen, A.K. Kar & B.K. Das are known (Farr and Rossman 2021). Among these species, *Ps. mungo* described on *Vigna radiata*, *V. mungo* from Tanzania (East Africa) (Deighton 1976) and *Ps. phaseolicola* on *Vigna radiata* from China and Taiwan (Hsieh and Goh 1990) are morphologically similar to the present *Pseudocercospora* specimen from Benin (Table 7). Based on the original description by Deighton (1976), *Ps. mungo*, however, differs from the present species in causing leaf spots that form only indefinite chlorotic

areas on the adaxial surface, hypophyllous caespituli, lack of external hyphae and above all, by longer and wider conidiophores [up to 90(–130) × 4.5–7.5 µm)] and wider conidia (4.5–7.5 µm) (Deighton 1976). *Ps. tabei* causes yellowish brown to pale brown leaf spots, that are reddish brown to dark brown, when old, forms amphigenous caespituli, often produces well developed stromata, external hyphae and above all, shorter and narrower conidiophores [(11.5–)14.5–40(–44.5) × (3–)3.5–4(–4.5) µm] and narrower conidia (3–4 µm). *Ps. phaseolicola* differs by producing hypophyllous caespituli, no stromata, non-fasciculate, olivaceous, shorter and narrower conidiophores [3–25 × 1.5–3 µm versus (11.5–)14.5–40(–44.5) × (3–)3.5–4(–4.5) µm in *Ps. tabei*] and narrower conidia [1.5–2 µm versus 3–4 µm in *Ps. tabei*] (Hsieh and Goh 1990).

In the multi-gene phylogeny (Fig. 1), *Ps. tabei* forms part of a polytomy with a large genetic distance (branch length) in relation to other sequences considered in the analysis. In the *tef1* phylogeny, *Ps. tabei* clustered together with the isolates of *Ps. cruenta* on *Vigna* and *Phaseolus* form Benin (see Suppl. material 4). However, morphologically, the present species is clearly distinct from specimens of *Ps. cruenta* by having darker and shorter conidiophores and above all, shorter conidia [(20.5–)24–82(–84.5) µm] (Table 7). It is not possible to distinguish *Ps. tabei* from other numerous *Pseudocercospora* spp. by the phylogenetic analyses based on ITS sequences.

Based on a MegaBLAST search in the NCBI GenBank nucleotide database using the *tef1* sequence, the closest matches were *Ps. cruenta* on *Phaseolus vulgaris* (Fabaceae) from Taiwan (GenBank GU384405; Identities 283 / 312, i.e., 90%), *Pseudocercospora* sp. A on *P. vulgaris* (Fabaceae) from Iran MB-2015(GenBank KM452885; Identities 263 / 292, i.e., 90%) and *Ps. madagascariensis* on *Eucalyptus camaldulensis* (Myrtaceae) from Madagascar (GenBank KF253265; Identities 276 / 314, i.e., 88%).

Key 1: Key to species of *Cercospora* on Fabaceae known for Benin

1	Stromata well-developed, i.e., usually broader than 40 µm diam **2**
–	Stromata lacking or small, i.e., usually less than 20 µm diam **3**
2	Conidiophores branched, with polyblastic conidiogenous cells, conidia mostly 26–160 × 4–5 µm. On *Vigna* ..... ***C. rhynchophora***
–	Conidiophores unbranched, usually with monoblastic conidiogenous cells, conidia mostly 27–70 × 2–3 µm. On *Lablab* ..... ***C.* cf. *fagopyri***
3	Stromata totally lacking, hyphae mainly internal, conidiophores branched, mostly 18–178 × 4–5 µm, conidia mostly 19–88 × 3.5–4.5. On *Desmodium* ... . ***C. parakouensis***
–	Stromata often formed by few aggregated swollen hyphal cells with similar morphology **4**
4	Conidiophores up to 400 µm long. On *Vigna*. **5**
–	Conidiophores usually not longer than 150 µm **6**
5	Leaf spots inconspicuous or absent, caespituli mostly epiphyllous, conidia mostly 38–188 µm long..... ***C. tentaculifera***
–	Leaf spots conspicuous, brown to later with necrotic centre, caespituli mostly hypophyllous, conidia mostly 26–100 µm long ..... ***C. vignae-subterraneae***

6 Conidia up to 330 µm long. On *Calopogonium*, *Vigna* ..... ***C.* aff. *canescens***
– Conidia mostly 20–160 µm long **7**
7 Only internal hyphae **8**
– Internal and external hyphae **9**
8 Internal hyphae often distinct and developed, conidiophores in loose to moderately large and dense fascicles of up to approx. 16. On *Crotalaria* .... ***C. beninensis***
– Internal hyphae often indistinct, conidiophores in small and loose fascicles of up to approx. 6 conidiophores, conidiophores mostly attenuated towards the tips. On *Vigna* ..... ***C. phaseoli-lunati***
9 Conidiophores unbranched, in small, loose or moderately large and dense fascicles of up to approx. 22. On *Vigna* ..... ***C.* cf. *canscorina***
– Conidiophores branched **10**
10 Leaf spots almost lacking or brown discolorations, often uniform in colour and width, conidia hyaline. On *Zornia* ..... ***C. zorniicola***
– Leaf spots often developed, reddish brown, later dark brown by abundant caespituli, conidia often sub-hyaline. On *Phaseolus*..... ***Cercospora* sp. YMM297B**

Key 2: Key to the species of *Pseudocercospora* on Fabaceae known for Benin

1 Conidiophores in synnematous fascicles, synnemata up to 250 µm high, mostly 20–40 µm wide. On *Phaseolus* ..... ***Ps. griseola***
– Conidiophores solitary, fasciculate or in sporodochia **2**
2 Stromata well-developed **3**
– Stromata lacking or very small **4**
3 Leaf spots often lacking or indistinct, conidiophores often narrower towards the tips, mostly 20–92 µm long, conidia, mostly 22–55 µm long, constricted at the septa. On *Senna* ..... ***Ps. sennicola***
– Leaf spots evident, conidiophores, mostly 14–40 µm long, conidia mostly 24–82 µm long. On *Vigna* ..... ***Ps. tabei***
4 Caespituli amphigenous, conidiophores mostly 15–54 µm long, conidia mostly 42–132 µm long. On *Phaseolus*, *Vigna* ..... ***Ps. cruenta***
– Caespituli mainly epiphyllous, conidiophores mostly 13–44 µm long, conidia mostly 38–110 µm long. On *Centrosema* ..... ***Ps. bradburyae***

Discussion

The present study aims to increase the knowledge on the diversity of cercosporoid fungi in tropical Africa. Therefore, cercosporoid fungi collected on fifteen species of plants belonging to ten genera of Fabaceae found in Benin, West Africa, were characterised concerning their morphology, host species and DNA sequence data (18S rDNA, 28S rDNA, ITS and *tef1*). The specimens of cercosporoid species collected in Benin are attributed to groups corresponding to *Cercospora*, *Pseudocercospora* and a heterogeneous

group around *Passalora*. The four-gene phylogenetic tree yielded results consistent with the current knowledge of generic relationships as presented in previous studies (Crous et al. 2013; Groenewald et al. 2013; Nakashima et al. 2016). Species of *Cercospora* and *Pseudocercospora* form morphologically distinct groups that receive moderate support in the phylogenetic analysis (Fig. 1). In the *Cercospora* and *Pseudocercospora* clades, the lengths of branches of most new species (*C. beninensis*, *C. rhynchophora*, *C. vignae-subterraneae*, *C. zorniicola*, *Ps. sennicola* and *Ps. tabei*) are quite long (Fig. 1). This indicates a relatively large genetic and evolutionary distance from neighbouring species included in the analysis. The partial gene sequences of the protein-coding region *tef1* and the combined analysis of four loci provided better results than single gene analyses of ITS and LSU rDNA for the differentiation of species of *Cercospora* and *Pseudocercospora*. Consequently, these molecular sequence data only allow to measure phylogenetic distances between the species. A similar situation has been found for *Cercospora* spp. by Bakhshi et al. (2015, 2018) and for *Pseudocercospora* spp. by Crous et al. (2013a) and Silva et al. (2016).

Fortunately, most species included in this study differ from each other by their morphology and host range. For example, *Cercospora tentaculifera* (YMM75) on *Vigna unguiculata* causes inconspicuous leaf spots and produces adaxial caespituli with large conidiophores (up to 435 µm) that are constricted at the septa (Figs 2H, 11). Thereby, this species is easily distinguishable from other *Cercospora* spp. known on species of *Vigna* and *Phaseolus*. *C. zorniicola* (YMM299) on *Zornia glochidiata* produces external hyphae and conidiophores that are unbranched and uniform in colour and width with usually monoblastic conidiogenous cells (Fig. 13). This is the first species of *Cercospora* known for the host genus *Zornia*.

For the morphological identification of all species included in this study, we examined about 50 type specimens and other specimens loaned from BPI, ILL and NY. As result of these analyses, dichotomous keys to the species of *Cercospora* and *Pseudocercospora* infecting members of Fabaceae known for Benin are presented (see below). The following morphological characteristics are helpful to separate species of *Cercospora* and *Pseudocercospora*: characteristics of leaf spots (distinctiveness, colour, size, form) and sporulation (distinctiveness, position on the leaf), the stroma (size, density), the external hyphae (present/absent), conidiophores (form, size, branching, number and position of conidiogenous loci, form of conidiogenous cells), and conidia (form, size range) (comp. Deighton 1976; Crous and Braun 2003; Crous et al. 2013; Groenewald et al. 2013; Videira et al. 2017).

In order to obtain DNA sequence data, up to now, only cercosporoid fungi available as cultures have been used (Groenewald et al. 2013). Due to the fact that most cercosporoid fungi are not available as cultures, molecular sequences are available only for a small fraction of the species diversity of cercosporoid fungi known by morphological characteristics. It is often difficult to cultivate cercosporoid fungi, as this requires living fungal cells and a sterile environment to avoid contamination. As it was not possible to cultivate cercosporoid fungi in Benin, a technique for DNA isolation from dry specimens has been developed and successfully applied in the context of the present study

for cercosporoid fungi for the first time. This direct DNA extraction method opens interesting possibilities to obtain DNA data of cercosporoid and other fungal plant pathogens especially in tropical countries.

The present study is the first effort towards generating molecular and morphological data for cercosporoid fungi in Benin, West Africa. We found 18 taxa, representing only a small fraction of the yet unknown species diversity of cercosporoid fungi (Piepenbring et al. 2020; Farr and Rossman 2021). Eight taxa found in this study are proposed as species new to science. Ten known species have been identified, including taxa important for agriculture such as *Pseudocercospora cruenta* and *Ps. griseola* on *Phaseolus lunatus* as well as *Nothopassalora personata* and *Passalora arachidicola* on *Arachis hypogaea*. Eight species are reported for Benin for the first time, with three of them namely, *Cercospora* cf. *canscorina*, *C.* cf. *fagopyri* and *C. phaseoli-lunati*, being new for West Africa.

New scientific data, such as species new to science, new records of hosts and for geographic areas, will help plant pathologists to develop efficient and sustainable disease management programs to control these fungal diseases and quarantine officials to take decisions based on scientific evidence. The plethora of novel and newly reported taxa collected on Fabaceae in Benin confirms that mycologists and phytopathologists in Africa have so far not given much attention to the species diversity of fungi occurring on plants, including species of economic relevance, such as those belonging to Fabaceae. Benin and other tropical African countries are likely to harbour highly diverse mycobiomes including cercosporoid fungi that still await discovery (Piepenbring et al. 2020). It is important to investigate them, because these unknown plant pathogens are or may become relevant as agents of emerging diseases that may spread and threaten cultivated plants worldwide. We hope that this study motivates further mycologists to study cercosporoid fungi in Benin, as well as in other countries of tropical Africa, and help to get a better understanding of cercosporoid fungal diversity worldwide.

Conclusions

The present study is a first step for the investigation of the diversity of cercosporoid fungi by an integrative approach including morphological, phylogenetic and ecological information. Taxonomic studies in this work generated eight newly described species, eight new records and the confirmation of two species of cercosporoid fungi that were previously reported from Benin. Previously, 12 cercosporoid fungi were known for Benin. The present work expands this number by adding 16 species of *Cercospora* and *Pseudocercospora* to this list, with a total of 28 species. These records together with herbarium specimens and molecular sequence data form a baseline for further studies in the field of systematics, ecology and phytopathology referring to cercosporoid fungi. This information will help plant pathologists to develop effective disease management programs and evidence-based quarantine regulations. The results obtained for a single family (Fabaceae) in easily accessible vegetation close to settlements suggest that many

more taxa of cercosporoid fungi remain to be discovered on plants belonging to other family of plants in diverse habitats. In the future, more attention should be directed towards collecting cercosporoid and other pathogenic fungi from Benin as well as other parts of tropical Africa.

Acknowledgements

We are grateful to Roland Kirschner, Hermine Lotz-Winter, José Macia-Vicente and Melissa Mardones for fruitful discussions and valuable advice in the context of this study. We thank Carola Glatthorn for her support for the literature search and daily needs. Our special thanks go to Affoussatou Tabé and Ramdan Dramani (Faculty of Agronomy, University of Parakou, Benin) who helped with the sampling of specimens in the field. We acknowledge the support and facilities made available for this study by the Université de Parakou and Université d'Abomey-Calavi, Benin. We are grateful to Adomou Aristide and Paul Yédémohan (National Herbarium of Benin, University of Abomey-Calavi) for their assistance with the identification of host plants. We thank the curators of the US National Fungus Collections (BPI), the Herbarium of the University of Illinois (ILL) and the New York Botanical Garden (NY) for the loans of specimens.

Our participation in summer schools and scientific meetings in tropical mycology 2016, 2017 and 2019 in Benin, along with the field work, has been made possible by financial support from the Volkswagen Foundation (grants Az 90 127 and Az 93 338) and the Freunde und Förderer der Goethe-Universität. A special gratitude goes to the Adolf Messer Foundation for providing a scholarship to the first author. NSY is supported by the German Federal Ministry of Education and Research (BMBF) under the contract number 01DG20015FunTrAf.

References

Aggarwal VD, Pastor-Corrales MA, Chirwa RM, Buruchara RA (2004) Andean beans (*Phaseolus vulgaris* L.) with resistance to the angular leaf spot pathogen (*Phaeoisariopsis griseola*) in southern and eastern Africa. Euphytica 136: 201–210. https://doi.org/10.1023/B:EUPH.0000030678.12073.a9

Agrios GN (2005) Plant Pathology (5th ed.). Elsevier Academic Press, Amsterdam, Boston, 922 pp.

Akoégninou A, van der Burg WJ, van der Maesen LJG [Eds] (2006) Flore analytique du Bénin. Wageningen University papers, 2. Backhuys Publ, Leiden, 1034 pp. https://edepot.wur.nl/281595

Arzanlou M, Groenewald JZ, Gams W, Braun U, Shin H-D, Crous PW (2007) Phylogenetic and morphotaxonomic revision of *Ramichloridium* and allied genera. Studies in Mycology 58: 57–93. https://doi.org/10.3114/sim.2007.58.03

Ávila A, Groenewald JZ, Trapero A, Crous PW (2005) Characterisation and epitypification of *Pseudocercospora cladosporioides*, the causal organism of *Cercospora* leaf spot of olives. Mycological Research 109: 881–888. https://doi.org/10.1017/S0953756205003503

Bakhshi M, Arzanlou M, Babai-Ahari A, Groenewald JZ, Crous PW (2014) Multi-gene analysis of *Pseudocercospora* spp. from Iran. Phytotaxa 184: 245–264. https://doi.org/10.11646/phytotaxa.184.5.1

Bakhshi M, Arzanlou M, Babai-Ahari A, Groenewald JZ, Crous PW (2018) Novel primers improve species delimitation in *Cercospora*. IMA Fungus 9: 299–332. https://doi.org/10.5598/imafungus.2018.09.02.06

Bakhshi M, Arzanlou M, Babai-Ahari A, Groenewald JZ, Braun U, Crous PW (2015) Application of the consolidated species concept to *Cercospora* spp. from Iran. Persoonia – Molecular Phylogeny and Evolution of Fungi 34: 65–86. https://doi.org/10.3767/003158515X685698

Beilharz V, Pascoe I, Parbery D (2002) Three new *Pseudocercospora* species, one with a *Mycosphaerella* teleomorph, from Kennedia in Australia. Mycotaxon 82: 397–408.

Benson DA, Clark K, Karsch-Mizrachi I, Lipman DJ, Ostell J, Sayers EW (2014) GenBank. Nucleic Acids Research 42: D32–D37. https://doi.org/10.1093/nar/gkt1030

Bharadwaj SD (1971) *Cercospora kashiensis* Bharadwaj. Journal of the Indian Botanical Society 49: e119.

Bhat D, Pratibha J (2010) *Cercospora* spp. from Goa and neighbouring areas. Kavaka 37/38: 69–78.

Braun U (1993) New genera of phytopathogenic Deuteromycetes. Cryptogamic Botany 4: 1–14.

Braun U (1995a) A Monograph of *Cercosporella*, *Ramularia*, and Allied Genera (Phytopathogenic Hyphomycetes). IHW, Eching bei München, 333 pp.

Braun U (1995b) Miscellaneous notes on phytopathogenic hyphomycetes (II). Mycotaxon 55: 223–241.

Braun U (1998) A monograph of *Cercosporella*, *Ramularia* and allied genera (phytopathogenic hyphomycetes), additions to host range and distribution. Schlechtendalia 1: 41–43.

Braun U, Crous PW (2005) Additions and corrections to names published in *Cercospora* and *Passalora*. Mycotaxon 92: 395–416.

Braun U, Crous PW (2016) Proposal to conserve the name *Cercospora* (Ascomycota: Mycosphaerellaceae) with a conserved type. Taxon 65: e185. https://doi.org/10.12705/651.18

Braun U, Freire F (2004) Some cercosporoid hyphomycetes from Brazil-III. Cryptogamie Mycologie 25: 221–244.

Braun U, Mouchacca J, McKenzie EHC (1999) Cercosporoid hyphomycetes from New Caledonia and some other South Pacific islands. New Zealand Journal of Botany 37: 297–327. https://doi.org/10.1080/0028825X.1999.9512636

Braun U, Crous PW, Dugan F, Groenewald JZ, De Hoog GS (2003) Phylogeny and taxonomy of *Cladosporium*-like hyphomycetes, including *Davidiella* gen. nov., the teleomorph of *Cladosporium* s. str. Mycological Progress 2: 3–18. https://doi.org/10.1007/s11557-006-0039-2

Braun U, Nakashima C, Crous PW (2013) Cercosporoid fungi (Mycosphaerellaceae) 1. Species on other fungi, Pteridophyta and Gymnospermae. IMA fungus 4: 265–345. https://doi.org/10.5598/imafungus.2013.04.02.12

Braun U, Crous PW, Nakashima C (2015) Cercosporoid fungi (Mycosphaerellaceae) 4. Species on dicots (Acanthaceae to Amaranthaceae). IMA Fungus 6: 373–469. https://doi.org/10.5598/imafungus.2015.06.02.09

Braun U, Crous PW, Nakashima C (2016) Cercosporoid fungi (Mycosphaerellaceae) 5. Species on dicots (Anacardiaceae to Annonaceae). IMA fungus 7: 161–216. https://doi.org/10.5598/imafungus.2016.07.01.10

Cai G, Schneider RW (2008) Population structure of *Cercospora kikuchii*, the causal agent of cercospora leaf blight and purple seed stain in soybean. Phytopathology 98: 823–829. https://doi.org/10.1094/PHYTO-98-7-0823

Carbone I, Kohn LM (1999) A method for designing primer sets for speciation studies in filamentous ascomycetes. Mycologia 91: 553–556. https://doi.org/10.1080/00275514.1999.12061051

Chiddarwar P (1959) Contributions to our knowledge of the *Cercospora* of Bombay State I. Sydowia 13: 152–163.

Chupp C (1954) A Monograph of the Fungus Genus *Cercospora*. Published by the author, Ithaca.

Ciferri R, González-Fragoso R (1926) Hongos parásitos y saprófitos de la República Dominicana (6a serie). Boletín de la Real Sociedad Española de Historia Natural, Biologia 26: 330–341.

Collemare J, Beenen HG, Crous PW, de Wit PJGM, van der Burgt A (2015) Novel intron-like elements in fungi are involved in parallel gains of spliceosomal introns. PLoS ONE 10: e0129302. https://doi.org/10.1371/journal.pone.0129302

Cooke MC, Massee G (1883–1884) Grevillea. Williams and Norgate, London, 130 pp. https://www.biodiversitylibrary.org/item/188030

Crous PW, Braun U (2003) Names Published in *Cercospora* and *Passalora*. Centraalbureau voor Schimmelcultures, Utrecht, 571 pp.

Crous PW, Liebenberg MM, Braun U, Groenewald JZ (2006) Re-evaluating the taxonomic status of *Phaeoisariopsis griseola*, the causal agent of angular leaf spot of bean. Studies in Mycology 55: 163–173. https://doi.org/10.3114/sim.55.1.163

Crous PW, Schoch CL, Hyde KD, Wood AR, Gueidan C, de Hoog GS, Groenewald JZ (2009a) Phylogenetic lineages in the Capnodiales. Studies in Mycology 64: 17–47. https://doi.org/10.3114/sim.2009.64.02

Crous PW, Groenewald JZ, Summerell BA, Wingfield BD, Wingfield MJ (2009b) Co-occurring species of *Teratosphaeria* on *Eucalyptus*. Persoonia – Molecular Phylogeny and Evolution of Fungi 22: 38–48. https://doi.org/10.3767/003158509X424333

Crous PW, Summerell BA, Carnegie AJ, Wingfield MJ, Groenewald JZ (2009c) Novel species of Mycosphaerellaceae and Teratosphaeriaceae. Persoonia – Molecular Phylogeny and Evolution of Fungi 23: 119–146. https://doi.org/10.3767/003158509X479531

Crous PW, Groenewald JZ, Shivas RG, Edwards J, Seifert KA, Alfenas AC, Alfenas RF, Burgess TI, Carnegie AJ, Hardy GEStJ, Hiscock N, Hüberli D, Jung T, Louis-Seize G, Okada G, Pereira OL, Stukely MJC, Wang W, White GP, Young AJ, McTaggart AR, Pascoe IG, Porter IJ, Quaedvlieg W (2011) Fungal planet description sheets: 69–91. Persoonia – Molecular Phylogeny and Evolution of Fungi 26: 108–156. https://doi.org/10.3767/003158511X581723

Crous PW, Summerell BA, Shivas RG, Burgess TI, Decock CA, Dreyer LL, Granke LL, Guest DI, Hardy GEStJ, Hausbeck MK, Hüberli D, Jung T, Koukol O, Lennox CL, Liew ECY,

Lombard L, McTaggart AR, Pryke JS, Roets F, Saude C, Shuttleworth LA, Stukely MJC, Vánky K, Webster BJ, Windstam ST, Groenewald JZ (2012) Fungal planet description sheets: 107–127. Persoonia – Molecular Phylogeny and Evolution of Fungi 28: 138–182. https://doi.org/10.3767/003158512X652633

Crous PW, Braun U, Hunter GC, Wingfield MJ, Verkley GJM, Shin H-D, Nakashima C, Groenewald JZ (2013) Phylogenetic lineages in *Pseudocercospora*. Studies in Mycology 75: 37–114. https://doi.org/10.3114/sim0005

Crous PW, Shivas RG, Quaedvlieg W, van der Bank M, Zhang Y, Summerell BA, Guarro J, Wingfield MJ, Wood AR, Alfenas AC, Braun U, Cano-Lira JF, García D, Marin-Felix Y, Alvarado P, Andrade JP, Armengol J, Assefa A, den Breeÿen A, Camele I, Cheewangkoon R, De Souza JT, Duong TA, Esteve-Raventós F, Fournier J, Frisullo S, García-Jiménez J, Gardiennet A, Gené J, Hernández-Restrepo M, Hirooka Y, Hospenthal DR, King A, Lechat C, Lombard L, Mang SM, Marbach PAS, Marincowitz S, Marin-Felix Y, Montaño-Mata NJ, Moreno G, Perez CA, Pérez Sierra AM, Robertson JL, Roux J, Rubio E, Schumacher RK, Stchigel AM, Sutton DA, Tan YP, Thompson EH, Vanderlinde E, Walker AK, Walker DM, Wickes BL, Wong PTW, Groenewald JZ (2014) Fungal planet description sheets: 214–280. Persoonia – Molecular Phylogeny and Evolution of Fungi 32: 184–306. https://doi.org/10.3767/003158514X682395

Crous PW, Schumacher RK, Akulov A, Thangavel R, Hernández-Restrepo M, Carnegie AJ, Cheewangkoon R, Wingfield MJ, Summerell BA, Quaedvlieg W, Coutinho TA, Roux J, Wood AR, Giraldo A, Groenewald JZ (2019) New and interesting fungi. 2. Fungal Systematics and Evolution 3: 57–134. https://doi.org/10.3114/fuse.2019.03.06

Das A, Gupta S, Parihar AK, Singh D, Chand R, Pratap A, Singha KD, Kushwaha KPS (2019) Delineating genotype × environment interactions towards durable resistance in mungbean against *Cercospora* leaf spot (*Cercospora canescens*) using GGE biplot. Plant Breeding 139: 639–650. https://doi.org/10.1111/pbr.12789

Ddamulira G, Mukankusi C, Ochwo-Ssemakula M, Edema R, Sseruwagi P, Gepts P (2014) Distribution and variability of *Pseudocercospora griseola* in Uganda. Journal of Agricultural Science 6: 1–16. https://doi.org/10.5539/jas.v6n6p16

Deighton FC (1967) Studies on *Cercospora* and allied genera. II. *Passalora*, *Cercosporidium*, and some species of *Fusicladium* on *Euphorbia*. Mycological Papers 112: 1–80.

Deighton FC (1973) Studies on *Cercospora* and allied genera. IV. *Cercosporella* Sacc., *Pseudocercosporella* gen. nov., and *Pseudocercosporidium* gen. nov. Mycological Papers 113: 1–62.

Deighton FC (1974) Studies on *Cercospora* and allied genera. V. *Mycovellosiella* Rangel, and a new species of *Ramulariopsis*. Mycological Papers 137: 1–75.

Deighton FC (1976) Studies on *Cercospora* and allied genera. VI. *Pseudocercospora* Speg., *Pantospora* Cif., and *Cercoseptoria* Petr. Mycological Papers 140: 1–168.

Deighton FC (1979) Studies on *Cercospora* and allied genera VII. New species and redispositions. Mycological Papers 144: 1–56.

Deighton FC (1983) Studies on *Cercospora* and allied genera. VIII. Further notes on *Cercoseptoria* and some new species and redispositions. Mycological Papers 151: 1–13.

Deighton FC (1990) Observations on *Phaeoisariopsis*. Mycological Research 94: 1096–1102. https://doi.org/10.1016/S0953-7562(09)81340-3

Ellis MB (1971) Dematiaceous Hyphomycetes. Commonwealth Mycological Institute, Kew, 608 pp.

Ellis MB (1976) More Dematiaceous Hyphomycetes. Commonwealth Mycological Institute, Kew, 507 pp.

Faris DG (1965) The origin and evolution of the cultivated forms of *Vigna sinensis*. Canadian Journal of Genetics and Cytology 7: 433–452. https://doi.org/10.1139/g65-058

Farr DF, Rossman AY (2021) Fungal Databases, U.S. National Fungus Collections, ARS, USDA. https://nt.ars-grin.gov/fungaldatabases/ [Retrieved January 22, 2021]

Fazekas AJ, Kuzmina ML, Newmaster SG, Hollingsworth PM (2012) DNA barcoding methods for land plants. In: Kress WJ, Erickson DL (Eds) DNA Barcodes. Methods in Molecular Biology. Humana, Totowa, 223–252. https://doi.org/10.1007/978-1-61779-591-6_11

Fortuna-Perez AP, da Silva MJ, de Queiroz LP, Lewis GP, Simões AO, de Azevedo Tozzi AMG, Sarkinen T, de Souza AP (2013) Phylogeny and biogeography of the genus *Zornia* (Leguminosae: Papilionoideae: Dalbergieae). Taxon 62: 723–732. https://doi.org/10.12705/624.35

Fragoso RG (1927) Estudio Sistemático de los Hifales de la Flora Española Conocidos Hasta Hecha Fecha: Memoria. Real Academia de Ciencias Exactas, Físicas y Naturales, Madrid, 377 pp.

Fries E (1849) Summa vegetabilium Scandinaviae, Sectio posterior, 259–572.

Fuckel K (1863) Fungi Rhenani exsiccati, Fasc. I–IV. Hedwigia 2: 132–136.

Gepts P, Beavis WD, Brummer EC, Shoemaker RC, Stalker HT, Weeden NF, Young ND (2005) Legumes as a model plant family. Genomics for food and feed report of the cross-legume advances through genomics conference. Plant Physiology 137: e1228. https://doi.org/10.1104/pp.105.060871

Golato C, Meossi E (1972) A serious leaf infection of beans, *Phaseolus vulgaris*, in Ethiopia. Rivista di Agricoltura Subtropicale e Tropicale 66: 135–138.

Groenewald M, Groenewald JZ, Braun U, Crous PW (2006) Host range of *Cercospora apii* and *C. beticola* and description of *C. apiicola* , a novel species from celery. Mycologia 98: 275–285. https://doi.org/10.1080/15572536.2006.11832700

Groenewald JZ, Groenewald M, Braun U, Crous PW (2010) *Cercospora* speciation and host range. In: Lartey RT, Weiland JJ, Panella L, Crous PW, Windels CE (Eds) *Cercospora* leaf spot of sugar beet and related species. American Phytopathological Society (APS Press), St. Paul, Minn, 21–37.

Groenewald JZ, Nakashima C, Nishikawa J, Shin H-D, Park J-H, Jama AN, Groenewald M, Braun U, Crous PW (2013) Species concepts in *Cercospora*: spotting the weeds among the roses. Studies in Mycology 75: 115–170. https://doi.org/10.3114/sim0012

Grum-Grzhimaylo AA, Georgieva ML, Bondarenko SA, Debets AJM, Bilanenko EN (2016) On the diversity of fungi from soda soils. Fungal Diversity 76: 27–74. https://doi.org/10.1007/s13225-015-0320-2

Guzmán P, Gilbertson R, Nodari R, Johnson WC, Temple SR, Mandala D, Mkandawire AB, Gepts P (1995) Characterization of variability in the fungus *Phaeoisariopsis griseola* suggests coevolution with the common bean (*Phaseolus vulgaris*). Phytopathology 85: 600–607. https://doi.org/10.1094/Phyto-85-600

Guzmán P, Gepts P, Temple S, Mkandawire ABC, Gilbertson RL (1999) Detection and differentiation of *Phaeoisariopsis griseola* isolates with the polymerase chain reaction and group-specific primers. Plant Disease 83: 37–42. https://doi.org/10.1094/PDIS.1999.83.1.37

Hay FS, Maloney E, Vaghefi N, Shivas RG, Pethybridge SJ (2017) First report of *Cercospora* blight of *Asparagus officinalis* caused by *Cercospora asparagi* in New York. Plant Disease 101: e1953. https://doi.org/10.1094/PDIS-05-17-0648-PDN

Hepper FN (1963) Plants of the 1957–58 West African expedition: II. The Bambara Groundnut (*Voandzeia subterranea*) and Kersting's Groundnut (*Kerstingiella geocarpa*) wild in West Africa. Kew Bulletin 16: 395–407. https://doi.org/10.2307/4114681

Hernández-Gutiérrez A, Dianese JC (2008) New cercosporoid fungi from the Brazilian Cerrado 1. Species on hosts of the families Anacardiaceae, Araliaceae, Bombacaceae, Burseraceae and Celastraceae. Mycotaxon 106: 41–63.

Hernández-Gutiérrez A, Dianese JC (2009) New cercosporoid fungi from the Brazilian Cerrado 2. Species on hosts of the subfamilies Caesalpinioideae, Faboideae and Mimosoideae (Leguminosae s. lat.). Mycotaxon 107: 1–24. https://doi.org/10.5248/107.1

Hernández-Gutiérrez A, Chaves ZM, Dornelo-Silva D, Dianese JC (2015) Additions to the cercosporoid fungi from the Brazilian Cerrado: 1. New species on hosts belonging in family Fabaceae, and reallocations of four *Stenella* species into *Zasmidium*. Mycobio 5: 33–64. https://doi.org/10.12664/mycobiota.2015.05.06

de Hoog GS, van den Ende AHGG (1998) Molecular diagnostics of clinical strains of filamentous Basidiomycetes. Mycoses 41: 183–189. https://doi.org/10.1111/j.1439-0507.1998.tb00321.x

Houessou HJH, Beed F, Sikirou R, Ezin V (2011) First report of *Cercospora beticola* on lettuce (*Lactuca sativa*) in Benin. New Disease Reports 23: 1–16. https://doi.org/10.5197/j.2044-0588.2011.023.016

Hsieh WH, Goh TK (1990) *Cercospora* and Similar Fungi from Taiwan. Maw Chang Book Co, Taipei, 376 pp.

Huang F, Groenewald JZ, Zhu L, Crous PW, Li H (2015) Cercosporoid diseases of citrus. Mycologia 107: 1151–1171. https://doi.org/10.3852/15-059

Hunter GC, Wingfield BD, Crous PW, Wingfield MJ (2006) A multi-gene phylogeny for species of *Mycosphaerella* occurring on *Eucalyptus* leaves. Studies in Mycology 55: 147–161. https://doi.org/10.3114/sim.55.1.147

Jenkins WA (1938) Two fungi causing leaf spot of peanut. Journal of Agricultural Research 56: 317–332.

Joshi AS, Jegadeesan S, Chand R, Pawar S (2006) Genetic diversity study of *Cercospora canescens* (Ellis & Martin) isolates, the pathogen of *Cercospora* leaf spot in legumes. Current Science 90: 564–568.

Ju HJ, Choi IY, Lee KJ, Shin HD (2020) First report of *Cercospora malayensis* causing leaf spot on okra in Korea. Plant Disease 104: 1858–1858. https://doi.org/10.1094/PDIS-11-19-2468-PDN

Kearse M, Moir R, Wilson A, Stones-Havas S, Cheung M, Sturrock S, Buxton S, Cooper A, Markowitz S, Duran C, Thierer T, Ashton B, Meintjes P, Drummond A (2012) Geneious Basic: An integrated and extendable desktop software platform for the organization and analysis of sequence data. Bioinformatics 28: 1647–1649. https://doi.org/10.1093/bioinformatics/bts199

Kirschner R (2014) A new species and new records of cercosporoid fungi from ornamental plants in Taiwan. Mycological Progress 13: 483–491. https://doi.org/10.1007/s11557-013-0930-6

Kokalis-Burelle N (1997) Compendium of peanut diseases. APS Press, American Phytopathological Society, St. Paul, Minn, 94 pp.

Kouris-Blazos A, Belski R (2016) Health benefits of legumes and pulses with a focus on Australian sweet lupins. Asia Pacific Journal of Clinical Nutrition 25: 1–17.

Kress WJ, Erickson DL, Jones FA, Swenson NG, Perez R, Sanjur O, Bermingham E (2009) Plant DNA barcodes and a community phylogeny of a tropical forest dynamics plot in Panama. Proceedings of the National Academy of Sciences 106: 18621–18626. https://doi.org/10.1073/pnas.0909820106

Kumar S, Stecher G, Tamura K (2016) MEGA7: Molecular Evolutionary Genetics Analysis Version 7.0 for bigger datasets. Molecular Biology and Evolution 33: 1870–1874. https://doi.org/10.1093/molbev/msw054

Lanfear R, Calcott B, Kainer D, Mayer C, Stamatakis A (2014) Selecting optimal partitioning schemes for phylogenomic datasets. BMC Evolutionary Biology 14: e82. https://doi.org/10.1186/1471-2148-14-82

Lenné JM (1990) A World List of Fungal Diseases of Tropical Pasture Species. Phytopathological Papers (Vol. 31). CAB International, Wallingford.

Levin RA, Wagner WL, Hoch PC, Nepokroeff M, Pires JC, Zimmer EA, Sytsma KJ (2003) Family-level relationships of Onagraceae based on chloroplast *rbc L* and *ndh F* data. American Journal of Botany 90: 107–115. https://doi.org/10.3732/ajb.90.1.107

Liu Z, Braun U, Crous PW, Si J, Zhang Y (2016) Taxonomy and phylogeny of cercosporoid fungi (Mycosphaerellaceae) from China 1. Phytotaxa 278: 212–224. https://doi.org/10.11646/phytotaxa.278.3.2

Marley PS, Diourté M, Neya A, Nutsugah SK, Sérémé P, Katilé SO, Hess DE, Mbaye DF, Ngoko Z (2002) *Sorghum* and pearl millet diseases in West and Central Africa. In: Leslie JF (Ed.) *Sorghum* and millets diseases [based on contributions to the Third Global Conference on *Sorghum* and Millets Diseases in Guanajuato, Mexico, September 2000] (1st ed.). Iowa State Press, Ames, 419–425. https://doi.org/10.1002/9780470384923.ch70

Messina MJ (1999) Legumes and soybeans: overview of their nutritional profiles and health effects. The American Journal of Clinical Nutrition 70: 439s–450s. https://doi.org/10.1093/ajcn/70.3.439s

Meswaet Y, Mangelsdorff R, Yorou NS, Piepenbring M (2019) A new species of *Pseudocercospora* on *Encephalartos barteri* from Benin. Asian Journal of Mycology 2: 101–109. https://doi.org/10.5943/ajom/2/1/4

Miller MA, Pfeiffer W, Schwartz T (2010) Creating the CIPRES Science Gateway for inference of large phylogenetic trees. 2010 Gateway Computing Environments Workshop (GCE). IEEE, New Orleans, 8 pp. https://doi.org/10.1109/GCE.2010.5676129

Montenegro-Calderón J, Martínez Álvarez J, Vieyra-Hernández M, Rangel-Macías L, Razzo-Soria T, Chávez-Herrera R, Ponce-Noyola P, Leal C (2011) Molecular identification of two strains of *Cercospora rodmanii* isolated from water hyacinth present in Yuriria lagoon, Guanajuato, Mexico and identification of new hosts for several other strains. Fungal Biology 115: 1151–62. https://doi.org/10.1016/j.funbio.2011.08.001

Moreno-Rico O, Groenewald JZ, Crous PW (2014) Foliicolous fungi from *Arctostaphylos pungens* in Mexico. IMA Fungus 5: 7–15. https://doi.org/10.5598/imafungus.2014.05.01.02

Mulder JL, Holliday P (1975) *Cercospora canescens*. CMI descriptions of phytopathogenic fungi and bacteria 462.

Nakamura T, Yamada KD, Tomii K, Katoh K (2018) Parallelization of MAFFT for large-scale multiple sequence alignments. Bioinformatics 34: 2490–2492. https://doi.org/10.1093/bioinformatics/bty121

Nakashima C, Motohashi K, Chen C-Y, Groenewald JZ, Crous PW (2016) Species diversity of *Pseudocercospora* from Far East Asia. Mycological Progress 15: 1093–1117. https://doi.org/10.1007/s11557-016-1231-7

Padulosi S, Ng NQ (1990) Wild *Vigna* species in Africa: their collection and potential utilization. IITA, Ibadan, 58–77.

Piątek M, Yorou NS (2018) *Pseudocercospora avicenniicola* on black mangrove (*Avicennia germinans*) in Benin: The first report from Africa. Forest Pathology 49: e12478. [1–4.] https://doi.org/10.1111/efp.12478

Piepenbring M, Maciá-Vicente JG, Codjia JEI, Glatthorn C, Kirk P, Meswaet Y, Minter D, Olou BA, Reschke K, Schmidt M, Yorou NS (2020) Mapping mycological ignorance – checklists and diversity patterns of fungi known for West Africa. IMA Fungus 11: 1–13. https://doi.org/10.1186/s43008-020-00034-y

Quaedvlieg W, Groenewald JZ, de Jesús Yáñez-Morales M, Crous PW (2012) DNA barcoding of *Mycosphaerella* species of quarantine importance to Europe. Persoonia – Molecular Phylogeny and Evolution of Fungi 29: 101–115. https://doi.org/10.3767/003158512X661282

Quaedvlieg W, Verkley GJM, Shin H-D, Barreto RW, Alfenas AC, Swart WJ, Groenewald JZ, Crous PW (2013) Sizing up *Septoria*. Studies in Mycology 75: 307–390. https://doi.org/10.3114/sim0017

Quaedvlieg W, Binder M, Groenewald JZ, Summerell BA, Carnegie AJ, Burgess TI, Crous PW (2014) Introducing the consolidated species concept to resolve species in the Teratosphaeriaceae. Persoonia – Molecular Phylogeny and Evolution of Fungi 33: 1–40. https://doi.org/10.3767/003158514X681981

Ronquist F, Teslenko M, van der Mark P, Ayres DL, Darling A, Höhna S, Larget B, Liu L, Suchard MA, Huelsenbeck JP (2012) MrBayes 3.2: Efficient bayesian phylogenetic inference and model choice across a large model space. Systematic Biology 61: 539–542. https://doi.org/10.1093/sysbio/sys029

Saccardo PA (1878) Fungi italici autographice delineati a Prof. PA Saccardo. Patavii 1878. Fascicoli V-VIII sistentes tab. 161–320. Michelia 1: 326–350.

Saccardo PA (1886) Sylloge fungorum omnium hucusque cognitorum: Additamenta ad volumina I-IV. Sumptibus auctoris Typis seminarii.

Shin HD, Kim JD (2001) *Cercospora* and allied genera from Korea. Plant Pathogens of Korea 7: 1–302.

Silva M, Barreto RW, Pereira OL, Freitas NM, Groenewald JZ, Crous PW (2016) Exploring fungal mega-diversity: *Pseudocercospora* from Brazil. Persoonia – Molecular Phylogeny and Evolution of Fungi 37: 142–172. https://doi.org/10.3767/003158516X691078

Sivanesan A (1990) *Mycosphaerella cruenta*. IMI Descriptions of Fungi and Bacteria, 985 pp.

Soura BH, Gnancadja LSA, Koita K, Gnancadja C (2018) Distribution of *Cercospora oryzae*, the fungus causing *Cercospora* leaf spot or narrow brown leaf spot in southern Benin (advantages and constraints of rice production). Asian Journal of Science and Technology 9(11): 8986–8991.

Spegazzini C (1881) Fungi argentini additis nonnullis brasiliensibus montevideensibusque. Pugillus quartus (Continuacion). Anales de la Sociedad Científica Argentina 12: 193–227.

Spegazzini C (1910) Mycetes Argentinenses (Series V) Deuteromycetes. Anales del Museo Nacional de Buenos Aires 3: e364.

Stamatakis A (2014) RAxML version 8: a tool for phylogenetic analysis and post-analysis of large phylogenies. Bioinformatics 30: 1312–1313. https://doi.org/10.1093/bioinformatics/btu033

Stamatakis A, Hoover P, Rougemont J (2008) A rapid bootstrap algorithm for the RAxML web servers. Systematic Biology 57: 758–771. https://doi.org/10.1080/10635150802429642

Świderska-Burek U, Daub ME, Thomas E, Jaszek M, Pawlik A, Janusz G (2020) Phytopathogenic cercosporoid fungi – from taxonomy to modern biochemistry and molecular biology. International Journal of Molecular Sciences 21: e8555. https://doi.org/10.3390/ijms21228555

Talavera G, Castresana J (2007) Improvement of phylogenies after removing divergent and ambiguously aligned blocks from protein sequence alignments. Systematic Biology 56: 564–577. https://doi.org/10.1080/10635150701472164

Turner PD (1971) Micro-organisms associated with oil palm (*Elaeis guineensis* Jaco.). Phytopathological Papers 14: 1–58.

Vaghefi N, Shivas RG, Sharma S, Nelson SC, Pethybridge SJ (2021) Phylogeny of cercosporoid fungi (Mycosphaerellaceae, Mycosphaerellales) from Hawaii and New York reveals novel species within the *Cercospora beticola* complex. Mycological Progress 20: 261–287. https://doi.org/10.1007/s11557-021-01666-z

Verkley GJM, Quaedvlieg W, Shin H-D, Crous PW (2013) A new approach to species delimitation in *Septoria*. Studies in Mycology 75: 213–305. https://doi.org/10.3114/sim0018

Videira SIR, Groenewald JZ, Braun U, Shin HD, Crous PW (2016) All that glitters is not *Ramularia*. Studies in Mycology 83: 49–163. https://doi.org/10.1016/j.simyco.2016.06.001

Videira SIR, Groenewald JZ, Nakashima C, Braun U, Barreto RW, de Wit PJGM, Crous PW (2017) Mycosphaerellaceae – Chaos or clarity? Studies in Mycology 87: 257–421. https://doi.org/10.1016/j.simyco.2017.09.003

Vu D, Groenewald M, Vries M de, Gehrmann T, Stielow B, Eberhardt U, Al-Hatmi A, Groenewald JZ, Cardinali G, Houbraken J, Boekhout T, Crous PW, Robert V, Verkley GJM (2019) Large-scale generation and analysis of filamentous fungal DNA barcodes boosts coverage for kingdom fungi and reveals thresholds for fungal species and higher taxon delimitation. Studies in Mycology 92: 135–154. https://doi.org/10.1016/j.simyco.2018.05.001

White TJ, Bruns T, Lee S, Taylor J (1990) Amplification and direct sequencing of fungal ribosomal RNA genes for phylogenetics. In: Innis MA, Gelfand DH, Sninsky JJ, White TJ (Eds) PCR Protocols: A Guide to Methods and Applications. Academic Press, New York, 315–322. https://doi.org/10.1016/B978-0-12-372180-8.50042-1

Winter G (1884) Repertorium. *Rabenhorstii* fungi europaei et extraeuraopaei. Cent. XXXI et XXXII. Hedwigia 23: 164–172.

Wortmann CS, Kirkby RA, Eledu CA, Allen DJ (1998) Atlas of Common Bean (*Phaseolus vulgaris* L.) Production in Africa. Centro Internacional de Agricultura Tropical, Cali, Colombia, 133 pp.

Yen JM, Lim G (1980) *Cercospora* and allied genera of Singapore and the Malay Peninsula. The Gardens' bulletin, Singapore 33: 151–263.
Yen JM, Kar A, Das B (1982) Studies on hyphomycetes from West Bengal, India. II. *Cercospora* and allied genera of West Bengal. 2. Mycotaxon 16: 58–79.
Young E (1916) Studies in Porto Rican parasitic fungi–II. Mycologia 8: 42–46. https://doi.org/10.1080/00275514.1916.12018861

Supplementary material 1

Checklist for cercosporoid fungi in West Africa

Authors: Yalemwork Meswaet, Ralph Mangelsdorff, Nourou S. Yorou, Meike Piepenbring

Data type: Checklist

Explanation note: This information is based on the checklist published by Piepenbring et al. (2020) and updated with new results from the present publication and some further publications.

Link: https://doi.org/10.3897/mycokeys.81.67850.suppl1

Supplementary material 2

References for the checklist for cercosporoid fungi in West Africa

Authors: Yalemwork Meswaet, Ralph Mangelsdorff, Nourou S. Yorou, Meike Piepenbring

Data type: text

Explanation note: References for the checklist for cercosporoid fungi in West Africa (Suppl. material 1).

Link: https://doi.org/10.3897/mycokeys.81.67850.suppl2

Supplementary material 3

A Bayesian phylogenetic tree inferred from ITS rDNA sequence data of cercosporoid species

Authors: Yalemwork Meswaet, Ralph Mangelsdorff, Nourou S. Yorou, Meike Piepenbring

Data type: phylogenetic

Explanation note: Nodes receiving Bayesian PP ≥ 0.94 are considered as strongly supported and are indicated by thickened branches. Newly described species are denoted in bold and red text, newly reported species are indicated in blue text.

Link: https://doi.org/10.3897/mycokeys.81.67850.suppl3

Supplementary material 4

A Bayesian phylogenetic tree inferred from *tef1* DNA sequence data of cercosporoid species

Authors: Yalemwork Meswaet, Ralph Mangelsdorff, Nourou S. Yorou, Meike Piepenbring

Data type: phylogenetic

Explanation note: Nodes receiving Bayesian PP ≥ 0.94 are considered as strongly supported and are indicated by thickened branches. Newly described species are denoted in bold and red text, newly reported species are indicated in blue text.

Link: https://doi.org/10.3897/mycokeys.81.67850.suppl4

MycoKeys 81: 139–164 (2021)
doi: 10.3897/mycokeys.139.67773
https://mycokeys.pensoft.net

RESEARCH ARTICLE

A peer-reviewed open-access journal
MycoKeys
Launched to accelerate biodiversity research

Updated description of *Atheniella* (Mycenaceae, Agaricales), including three new species with brightly coloured pilei from Yunnan Province, southwest China

Yupeng Ge[1], Zewei Liu[1], Hui Zeng[2], Xianhao Cheng[1], Qin Na[1]

1 *Shandong Key Laboratory of Edible Mushroom Technology, School of Agriculture, Ludong University, Yantai 264025, China* **2** *Institute of Edible Fungi, Fujian Academy of Agricultural Sciences; National and Local Joint Engineering Research Center for Breeding & Cultivation of Features Edible Fungi, Fuzhou 350014, China*

Corresponding author: Qin Na (naqin19890317@163.com)

Academic editor: Thorsten Lumbsch | Received 23 April 2021 | Accepted 23 June 2021 | Published 14 July 2021

Citation: Ge Y, Liu Z, Zeng H, Cheng X, Na Q (2021) Updated description of *Atheniella* (Mycenaceae, Agaricales), including three new species with brightly coloured pilei from Yunnan Province, southwest China. MycoKeys 81: 139–164. https://doi.org/10.3897/mycokeys.139.67773

Abstract

An updated description of the genus *Atheniella*, combining macro- and micromorphological characters that elaborate on the original generic characterisation, is presented. *Atheniella* is characterised by a brightly coloured pileus, all tissues inamyloid and pileipellis covered with simple to branched excrescences. Previously, nine *Atheniella* species were known globally, of which three species were accepted in China. Three newly-recognised species classified in the genus are here formally described from Yunnan Province: *Atheniella flavida* **sp. nov.**, *A. rutila* **sp. nov.** and *A. taoyao* **sp. nov.** The new species are characterised by a yellow, orange, pink or red pileus, fusiform cheilocystidia and pleurocystidia, non-smooth pileipellis, stipitipellis smooth or with cylindrical ornamentation, caulocystidia fusiform or subglobose, if present and all tissues inamyloid. Morphological descriptions, photographs, line drawings and comparisons with closely-related taxa are presented for the new species. A phylogenetic analysis of sequence data for the rDNA internal transcribed spacer region and nuclear large ribosomal subunit (ITS + nLSU) supported that *Atheniella* is resolved as monophyletic and also supported the taxonomic recognition of the new species. A key to the 12 species of *Atheniella* is also provided.

Keywords

new taxon, polygenes, taxonomy, white basidiospores

Introduction

The genus *Atheniella* Redhead, Moncalvo, Vilgalys, Desjardin & B.A. Perry is a small mycenoid genus, formerly treated as *Mycena* (Pers.) Roussel sect. *Adonideae* (Fr.) Quél., that was elevated to genus rank by Redhead et al. (2012). *Atheniella* is characterised macroscopically by its habit resembling that of *Mycena* owing to the small basidiomata, white lamellae, hollow stipe and is saprophytic on rotten wood or plant debris (Kühner 1938; Smith 1947; Redhead et al. 2012; Aronsen and Læssøe 2016). Redhead et al. (2012) noted that the brightly coloured pileus (e.g. yellow, orange, pink or red) and all tissues unreactive in Melzer's Reagent are diagnostic characters that distinguish *Atheniella* from *Mycena*. Given the change in taxonomic rank, formalisation of new combinations in *Atheniella* was required for species formerly classified in *Mycena* sect. *Adonideae* (Grgurinovic 2003; Redhead et al. 2012; Aravindakshan and Manimohan 2015; Gminder and Böhning 2016; Lehmann and Lüderitz 2018, 2019). In previous publications, nine taxa were recognised in *Atheniella*, comprising three new species and six new combinations, of which *Atheniella adonis* (Bull.) Redhead, Moncalvo, Vilgalys, Desjardin & B.A. Perry is the type species (Grgurinovic 2003; Redhead et al. 2012; Aravindakshan and Manimohan 2015; Gminder and Böhning 2016; Lehmann and Lüderitz 2018, 2019). An infrageneric classification for *Atheniella* has not been proposed since the genus was established (Redhead et al. 2012).

Previous taxonomic studies of *Atheniella* are incomplete because of insufficient species representation and a lack of phylogenetic evidence and only four taxa of *Atheniella* have been included in phylogenetic studies (Moncalvo et al. 2002; Matheney et al. 2006). Based on a phylogenetic reconstruction for more than 800 euagaric taxa derived from a nuclear ribosomal large subunit RNA gene (nLSU) sequence dataset, Moncalvo et al. (2002) established the Mycenaceae (Clade 47) to include 10 genera, including *Mycena*. However, *Mycena aurantiidisca* (Murrill) Murrill (≡ *Atheniella aurantiidisca* (Murrill) Redhead, Moncalvo, Vilgalys, Desjardin & B.A.Perry) and *Mycena adonis* (Bull.) Gray (≡ *Atheniella adonis*) were separated from the Mycenaceae to form an independent lineage termed the "adonis" clade (Clade 26). Matheney et al. (2006) agreed with Moncalvo et al. (2002) in the establishment of the Mycenaceae and that the "adonis" group should be excluded from *Mycena*, but differed in the phylogenetic placement of *Atheniella* spp. *Mycena amabillissima* (Peck) Sacc. (≡ *Atheniella amabillissima* (Peck) Redhead, Moncalvo, Vilgalys, Desjardin & B.A. Perry) and *M. aurantiidisca* (≡ *Atheniella aurantiidisca*) was placed in the "hydropoid" subclade of the Marasmioid clade (IV) (Matheney et al. 2006).

Species of *Atheniella* are widespread in temperate regions, but also distributed in the tropical zone (Smith 1935a, b, c, 1937, 1939; Maas Geesteranus 1980, 1990, 1992a, b; Redhead 1984; Perry 2002; Grgurinovic 2003; Robich 2003; Uehling et al. 2012; Aravindakshan and Manimohan 2015; Osono 2015; Aronsen and Læssøe 2016). Previous studies of *Atheniella* Kühner ex Singer during the last century focused on species distributed in Europe and North America (Murrill 1916; Tyler 1991; Emmett 1992; Gyosheva and Ganeva 2004; Friedrich 2006; Miersch and Karasch 2011;

Miersch 2013; Pérez-De-Gregorio 2015; Norvell 2016; Aime et al. 2018). In contrast, few investigations of *Atheniella* taxa in Australia and Asia have been conducted. However, progress in clarifying the relationship between *Mycena* and *Atheniella* has been achieved in recent years (Miyamoto et al. 1998, 2000; Grgurinovic 2003; Aravindakshan and Manimohan 2015; Na 2019; Na and Bau 2018, 2019a, b).

Three *Atheniella* species, namely *A. adonis*, *A. aurantiidisca* and *A. flavoalba* (Fr.) Redhead, Moncalvo, Vilgalys, Desjardin & B.A. Perry, were previously recognised in China (Bau and Liu 2011; Li et al. 2015; Na 2019). During our ongoing research on *Mycena* s.l., three new mycenoid species belonging to *Atheniella* were discovered in Yunnan Province, southwest China and are formally described here as *A. flavida* Q. Na & Y.P. Ge, *A. rutila* Q. Na & Y.P. Ge and *A. taoyao* Q. Na & Y.P. Ge. In addition, the generic morphological description of *Atheniella* is updated and a key for identification of the 12 species of *Atheniella* currently known is provided.

Materials and methods

Morphological examination

Macroscopic descriptions were prepared, based on freshly-collected specimens, whereas micromorphological descriptions relied on dried material. In the descriptions, colour abbreviations follow Kornerup and Wanscher (1978). Microscopic observations were conducted on dried specimens mounted in 5% potassium hydroxide (KOH) and stained with Congo red when necessary. Melzer's Reagent was used to test whether spores and tissues were amyloid (Horak 2005). Twenty mature basidiospores from each basidiocarp were measured in lateral view and one or two basidiocarps were examined per specimen. The basidiospore dimensions were recorded; the notation [*a*/*b*/*c*] used at the beginning of each basidiospore description indicates that *a* basidiospores from *b* basidiocarps of *c* specimens were measured. Measured dimensions (length × width) are presented as (d) e–**f**–g (h) × (i) j–**k**–l (m), where *d* is the minimum length, *e*–*g* represents the range of at least 90% of values, **f** is the average length and *h* is the maximum length; width (*i*–*m*) is expressed in the same manner. In addition, Q is the length: width ratio of a spore and **Q** ± SD is the average **Q** of all basidiospores ± the sample standard deviation. Authority abbreviations follow those used in Index Fungorum (https://www.indexfungorum.org). Voucher specimens have been deposited in the Fungarium of the Fujian Academy of Agricultural Sciences (**FFAAS**), China.

DNA extraction, PCR amplification and DNA sequencing

Genomic DNA was extracted from tiny pieces of lamellae using the NuClean Plant Genomic DNA Kit (Kangwei Century Biotechnology Co., Beijing, China). The internal transcribed spacer (ITS) region and the nuclear large subunit (nLSU) of rDNA were amplified with the primer pairs ITS1/ITS4 and LROR/LR7, respectively (White

et al. 1990; Hopple and Vilgalys 1999). The PCR thermocycling protocol (for both ITS and nLSU) was 94 °C for 4 min, followed by 34 cycles of 94 °C for 45 sec, 52 °C for 45 sec and 72 °C for 1 min and final extension for 10 min at 72 °C. The new sequences were submitted to GenBank (Table 1). The nBLAST tools (http://blast.ncbi.nlm.nih.gov/Blast.cgi) were used to compare the sequence identity with sequences in the NCBI databases. The GenBank accession numbers for the ITS and nLSU sequences are as follows: *Atheniella flavida* (MW969653–MW969654; MW969665), *A. rutila* (MW969658–MW969659; MW969668) and *A. taoyao* (MW969655–MW969657; MW969666–MW969667).

Sequence alignment and phylogenetic analysis

A dataset comprising concatenated sequences for the ITS and nLSU regions from 45 accessions of three genera (*Atheniella*, *Hemimycena* Singer and *Mycena*) was compiled. A total of 112 sequences downloaded from GenBank and 11 sequences newly generated in this study were aligned and adjusted manually using BioEdit 7.0.4.1 and Clustal X (Thompson et al. 1997; Hall 1999). Gaps in the alignments were treated as missing data. The alignment was deposited with TreeBase (submission ID, 28111; study accession URL: http://purl.org/phylo/treebase/phylows/study/TB2:S28111). *Hydropus scabripes* (Murrill) Singer was chosen as the outgroup. The aligned dataset consisted of 836 ITS and 879 nLSU nucleotide sites (including gaps). The best-fit evolutionary model was determined using Modeltest 2.3 for each of the ITS and nLSU data partitions for Bayesian Inference (BI), which was implemented with MrBayes 3.2.6 (Ronquist and Huelsenbeck 2003; Nylander 2004). Markov Chain Monte Carlo (MCMC) chains sampling every 100th generation until the topological convergence diagnostic value was less than 0.01 (Ronquist and Huelsenbeck 2003). Maximum Likelihood (ML) analysis was performed using raxmlGUI 1.5b1 and topological support was assessed using the rapid bootstrapping algorithm with 1000 replicates (Stamatakis et al. 2004). Topology support values, greater than 75% bootstrap support (ML) and 0.95 Bayesian posterior probabilities (BPP), are shown for relevant branch nodes.

Results

Phylogenetic analysis

The concatenated dataset comprised 45 taxa and 1715 sites. The GTR + G evolutionary model was selected for both ITS and nLSU regions. The optimal evolutionary model for the 5.8S and nLSU partitions was lset nst = 6, rates = invgamma and prset statefreqpr = dirichlet (1,1,1,1). The BI and ML phylogenetic reconstructions were consistent in topology and, thus, only the BI tree is presented (Fig. 1).

The phylogenetic tree contained four major clades. Both *Atheniella* and *Mycena* were resolved as monophyletic. The six species of *Hemimycena* were resolved into two

Table 1. Sequenced specimens used in phylogenetic analysis. New species are marked in bold.

No.	Taxa	Voucher	Locality	ITS Sequences ID	nLSU Sequences ID	Reference
1	*Atheniella adonis* (Bull.) Redhead, Moncalvo, Vilgalys, Desjardin & B.A. Perry	H6036863	FINLAND	MW540691	–	Unpublished
2	*A. adonis* (Bull.) Redhead, Moncalvo, Vilgalys, Desjardin & B.A. Perry	1058	CANADA	KJ705189	–	Unpublished
3	*A. adonis* (Bull.) Redhead, Moncalvo, Vilgalys, Desjardin & B.A. Perry	DAOM174885	–	–	AF261361	Moncalvo et al. (2002)
4	*A. amabillissima* (Peck) Redhead, Moncalvo, Vilgalys, Desjardin & B.A. Perry	AFTOL–ID 1686	USA	DQ490644	DQ457691	Matheny et al. (2006)
5	*A. amabillissima* (Peck) Redhead, Moncalvo, Vilgalys, Desjardin & B.A. Perry	TUR183733	FINLAND	MW540719	–	Unpublished
6	*A. amabillissima* (Peck) Redhead, Moncalvo, Vilgalys, Desjardin & B.A. Perry	BD–2020a	FINLAND	MW540733	–	Unpublished
7	*A. aurantiidisca* (Murrill) Redhead, Moncalvo, Vilgalys, Desjardin & B.A. Perry	UBC: F15202	CANADA	DQ384585	–	Unpublished
8	*A. aurantiidisca* (Murrill) Redhead, Moncalvo, Vilgalys, Desjardin & B.A. Perry	AFTOL–ID 1685	USA	DQ490646	DQ470811	Matheny et al. (2006)
9	*A. aurantiidisca* (Murrill) Redhead, Moncalvo, Vilgalys, Desjardin & B.A. Perry	UBC: F33062	CANADA	MF908459	–	Unpublished
10	*A. aurantiidisca* (Murrill) Redhead, Moncalvo, Vilgalys, Desjardin & B.A. Perry	HMJAU 43811	CHINA	MT497546	–	Unpublished
11	*A. aurantiidisca* (Murrill) Redhead, Moncalvo, Vilgalys, Desjardin & B.A. Perry	MF06837	USA	MT636967	–	Unpublished
12	*A. aurantiidisca* (Murrill) Redhead, Moncalvo, Vilgalys, Desjardin & B.A. Perry	DAOM216791	–	–	AF261360	Moncalvo et al. (2002)
13	*A. flavoalba* (Fr.) Redhead, Moncalvo, Vilgalys, Desjardin & B.A. Perry	604	ITALY	JF908464	–	Osmundson et al. (2013)
14	*A. flavoalba* (Fr.) Redhead, Moncalvo, Vilgalys, Desjardin & B.A. Perry	CBS 359.50	FRANCE	MH856659	MH868175	Vu et al. (2019)
15	*A. flavoalba* (Fr.) Redhead, Moncalvo, Vilgalys, Desjardin & B.A. Perry	CBS 258.53	FRANCE	MH857185	MH868723	Vu et al. (2019)
16	*A. flavoalba* (Fr.) Redhead, Moncalvo, Vilgalys, Desjardin & B.A. Perry	H6032608	FINLAND	MW540661	–	Unpublished
17	*A. flavoalba* (Fr.) Redhead, Moncalvo, Vilgalys, Desjardin & B.A. Perry	H6036822	FINLAND	MW540676	–	Unpublished
18	***A. flavida* Q. Na & Y.P. Ge**	**FFAAS03**50	**CHINA, Type**	**MW969653**	**MW969665**	**This study**
19	***A. flavida* Q. Na & Y.P. Ge**	**FFAAS0355**	**CHINA**	**MW969654**	–	**This study**
20	***A. rutila* Q. Na & Y.P. Ge**	**FFAAS0354**	**CHINA, Type**	**MW969658**	**MW969668**	**This study**
21	***A. rutila* Q. Na & Y.P. Ge**	**FFAAS0356**	**CHINA**	**MW969659**	–	**This study**
22	***A. taoyao* Q. Na & Y.P. Ge**	**FFAAS0351**	**CHINA**	**MW969655**	–	**This study**
23	***A. taoyao* Q. Na & Y.P. Ge**	**FFAAS0352**	**CHINA, Type**	**MW969656**	**MW969666**	**This study**
24	***A. taoyao* Q. Na & Y.P. Ge**	**FFAAS0353**	**CHINA**	**MW969657**	**MW969667**	**This study**
25	*Hemimycena albicolor* (A.H. Sm.) Elborne	MICH 11456	USA	MK169368	–	Unpublished
26	*H. gracilis* (Quél.) Singer	AFTOL–ID 1732	USA	DQ490623	DQ457671	Matheny et al. (2006)
27	*H. lactea* (Pers.) Singer	F33274	CANADA	MH718253	–	Unpublished
28	*H. lactea* (Pers.) Singer	MQ18R237–QFB30753	CANADA	MN992168	–	Unpublished
29	*H. mairei* (E.–J. Gilbert) Singer	CBS 263.47	FRANCE	MH856248	DQ457671	Vu et al. (2019)
30	*H. mairei* (E.–J. Gilbert) Singer	CBS 265.47	FRANCE	MH856249	MH867780	Vu et al. (2019)
31	*H. ochrogaleata* (J. Favre) M.M. Moser	409d	ITALY	JF908431	–	Osmundson et al. (2013)
32	*H. tortuosa* (P.D. Orton) Redhead	PDD:95759	NEW ZEALAND	HQ533011	–	Unpublished
33	*H. tortuosa* (P.D. Orton) Redhead	FRDBI 18076639	UK	MW487985	–	Unpublished
34	*Hydropus scabripes* (Murrill) Singer	GG355_86	NETHERLANDS	GU234149	–	Geml et al. (2009)
35	*Mycena abramsii* (Murrill) Murrill	231a	VENICE	JF908400	–	Osmundson et al. (2013)
36	*M. abramsii* (Murrill) Murrill	HMJAU 43282	CHINA	MH396626	–	Na and Bau (2019)
37	*M. abramsii* (Murrill) Murrill	HMJAU 43468	CHINA	MH396627	–	Na and Bau (2019)
38	*M. adscendens* Maas Geest.	Aronsen120803	NORWAY	KT900140	–	Larsson and Aronsen (2015)

No.	Taxa	Voucher	Locality	ITS Sequences ID	nLSU Sequences ID	Reference
39	*M. adscendens* Maas Geest.	Orstadius329–05	NORWAY	KT900141	–	Larsson and Aronsen (2015)
40	*M. adscendens* Maas Geest.	Aronsen061119	NORWAY	KT900142	–	Larsson and Aronsen (2015)
41	*M. adscendens* Maas Geest.	Aronsen120826	NORWAY	KT900143	–	Larsson and Aronsen (2015)
42	*M. alnetorum* J. Favre (=*M. abramsii* (Murrill) Murrill)	CM14–RG2	USA	KU295552	–	Unpublished
43	*M. amicta* (Fr.) Quél.	4745–HRL 1312	CANADA	KJ705188	–	Unpublished
44	*M. amicta* (Fr.) Quél.	CBS 352.50	FRANCE	MH856655	MH868170	Vu et al. (2019)
45	*M. amicta* (Fr.) Quél.	CBS 254.53	FRANCE	MH857183	–	Vu et al. (2019)
46	*M. amicta* (Fr.) Quél.	H6036851	FINLAND	MW540687	–	Unpublished
47	*M. arcangeliana* Bres.	252b	ITALY	JF908401	–	Osmundson et al. (2013)
48	*M. arcangeliana* Bres.	252f	ITALY	JF908402	–	Osmundson et al. (2013)
49	*M. cinerella* (P. Karst.) P. Karst.	Aronsen051014	SWEDEN	KT900146	–	Larsson and Aronsen (2015)
50	*M. cinerella* (P. Karst.) P. Karst.	173	RUSSIA	MF926553	–	Malysheva et al. (2017)
51	*M. citrinomarginata* Gillet	317h	ITALY	JF908416	–	Osmundson et al. (2013)
52	*M. citrinomarginata* Gillet	AD4TN	TUNISIA	KU973883	–	Unpublished
53	*M. clavicularis* (Fr.) Gillet	615i	ITALY	JF908466	–	Osmundson et al. (2013)
54	*M. clavicularis* (Fr.) Gillet	615b	ITALY	JF908467	–	Osmundson et al. (2013)
55	*M. diosma* Krieglst. & Schwöbel	KA13–1230	KOREA	KR673698	–	Kim et al. (2015)
56	*M. diosma* Krieglst. & Schwöbel	320f	ITALY	JF908417	–	Osmundson et al. (2013)
57	*M. entolomoides* T. Bau	HMJAU 43048	CHINA	MG654736	–	Na and Bau (2018)
58	*M. entolomoides* T. Bau	HMJAU 43052	CHINA	MG654737	–	Na and Bau (2018)
59	*M. entolomoides* T. Bau	HMJAU 43126	CHINA	MG654738	–	Na and Bau (2018)
60	*M. filopes* (Bull.) P. Kumm.	3782	FRANCE	KJ705175	–	Unpublished
61	*M. filopes* (Bull.) P. Kumm.	KA12–1699	KOREA	KR673631	–	Kim et al. (2015)
62	*M. filopes* (Bull.) P. Kumm.	287f	ITALY	JF908410	–	Osmundson et al. (2013)
63	*M. floridula* (Fr.) Quél. (=*Atheniella adonis*)	259	ITALY	JF908405	–	Osmundson et al. (2013)
64	*M. floridula* (Fr.) Quél. (=*Atheniella adonis*)	259a	ITALY	JF908406	–	Osmundson et al. (2013)
65	*M. floridula* (Fr.) Quél. (=*Atheniella adonis*)	CBS 360.50	FRANCE	MH856660	MH868176	Vu et al. (2019)
66	*M. floridula* (Fr.) Quél. (=*Atheniella adonis*)	HMJAU 43193	CHINA	MK309770	–	Unpublished
67	*M. floridula* (Fr.) Quél. (=*Atheniella adonis*)	HMJAU 43213	CHINA	MK309771	–	Unpublished
68	*M. floridula* (Fr.) Quél. (=*Atheniella adonis*)	HMJAU 43613	CHINA	MK309772	–	Unpublished
69	*M. galopus* (Pers.) P. Kumm.	BIOUG19840–F07	CANADA	MF908430	–	Dewaard (2017)
70	*M. leaiana* (Berk.) Sacc.	1028	ITALY	JF908376	–	Osmundson et al. (2013)
71	*M. leaiana* (Berk.) Sacc.	CNH03 (TENN)	USA	MF686520	–	Unpublished
72	*M. meliigena* (Berk. & Cooke) Sacc.	39	ITALY	JF908423	–	Osmundson et al. (2013)
73	*M. meliigena* (Berk. & Cooke) Sacc.	39d	ITALY	JF908429	–	Osmundson et al. (2013)
74	*M. metata* (Fr.) P. Kumm.	313b	ITALY	JF908412	–	Osmundson et al. (2013)
75	*M. olivaceomarginata* (Massee) Massee	GG436–86	NETHERLANDS	GU234119	–	Geml et al. (2012)
76	*M. olivaceomarginata* (Massee) Massee	CBS 228.47	FRANCE	MH856228	MH867756	Vu et al. (2019)
77	*M. olivaceomarginata* (Massee) Massee	CBS 229.47	FRANCE	MH856229	MH867757	Vu et al. (2019)
78	*M. olivaceomarginata* (Massee) Massee	HK47–15	NORWAY	MT153141	–	Thoen et al. (2020)
79	*M. pearsoniana* Dennis ex Singer	FCME25817	USA	JN182198	–	Harder et al. (2012)

No.	Taxa	Voucher	Locality	ITS Sequences ID	nLSU Sequences ID	Reference
80	*M. pearsoniana* Dennis ex Singer	TENN61544	USA	JN182199	–	Harder et al. (2012)
81	*M. pearsoniana* Dennis ex Singer	TENN61384	USA	JN182200	–	Harder et al. (2012)
82	*M. pelianthina* (Fr.) Quél.	CBH164	DENMARK	FN394548	–	Unpublished
83	*M. pelianthina* (Fr.) Quél.	108b	ITALY	JF908379	–	Osmundson et al. (2013)
84	*M. pelianthina* (Fr.) Quél.	108f	ITALY	JF908380	–	Osmundson et al. (2013)
85	*M. plumbea* P. Karst.	JN198391	CHINA	JN198391	–	Wu et al. (2013)
86	*M. plumbea* P. Karst.	420526MF0010	CHINA	MG719769	–	Wang et al. (2017)
87	*M. polygramma* (Bull.) Gray	439b	ITALY	JF908433	–	Osmundson et al. (2013)
88	*M. polygramma* (Bull.) Gray	439f	ITALY	JF908434	–	Osmundson et al. (2013)
89	*M. pura* (Pers.) P. Kumm.	TENN65043	USA	JN182202	–	Harder et al. (2012)
90	*M. pura* f. *alba* (Gillet) Kühner	CBH410	USA	FN394595	–	Unpublished
91	*M. purpureofusca* (Peck) Sacc.	F19748	CANADA	HQ604766	–	Unpublished
92	*M. purpureofusca* (Peck) Sacc.	G. Alfredsen	NORWAY	JQ358809	–	Unpublished
93	*M. rosea* Gramberg	938a	ITALY	JF908488	–	Osmundson et al. (2013)
94	*M. rosea* Gramberg	Champ–21	SPAIN	KX449424	–	Perez-Izquierdo et al. (2017)
95	*M. rubromarginata* (Fr.) P. Kumm.	407q	ITALY	JF908430	–	Osmundson et al. (2013)
96	*M. rubromarginata* (Fr.) P. Kumm.	TL–12780	DENMARK	KX513845	KX513849	Perry (2016)
97	*M. seminau* A.L.C. Chew & Desjardin	ACL136	MALAYSIA	KF537250	KJ206952	Chew et al. (2015)
98	*M. seminau* A.L.C. Chew & Desjardin	ACL308	MALAYSIA	KF537252	KJ206964	Chew et al. (2015)
99	*M. seynii* Quél.	71l	ITALY	JF908469	–	Osmundson et al. (2013)
100	*M. seynii* Quél.	71h	ITALY	JF908470	–	Osmundson et al. (2013)
101	*M. silvae–nigrae* Maas Geest. & Schwöbel	515	ITALY	JF908452	–	Osmundson et al. (2013)
102	*M. silvae–nigrae* Maas Geest. & Schwöbel	CC 13–12	USA	KF359604	–	Baird et al. (2014)
103	*M. stylobates* (Pers.) P. Kumm.	455	ITALY	JF908439	–	Osmundson et al. (2013)
104	*M. supina* (Fr.) P. Kumm.	128a	ITALY	JF908388	–	Osmundson et al. (2013)
105	*M. tenax* A.H. Sm.	p187i	USA	EU669224	–	Unpublished
106	*M. tenax* A.H. Sm.	OSC 113746	USA	EU846251	–	Unpublished
107	*M. vulgaris* (Pers.) P. Kumm.	447h	ITALY	JF908435	–	Osmundson et al. (2013)
108	*M. vulgaris* (Pers.) P. Kumm.	3781	CANADA	KJ705177	–	Unpublished
109	*M. zephirus* (Fr.) P. Kumm.	KA13–1265	KOREA	KR673722	–	Kim et al. (2015)

clades. Each of the four clades corresponded with high statistical support (ML bootstrap [BS] ≥ 84%, BI posterior probability [BPP] = 1).

The *Atheniella* Clade formed a sister group to the *Hemimycena* 1, *Hemimycena* 2 and *Mycena* clades with high statistical support (BS = 84%, BPP = 1.00). Samples of the three new species were placed in the *Atheniella* Clade and formed monophyletic lineages, each with high statistical support (*A. flavida*, BS = 100%, BPP = 1.00; *A. rutila*, BS = 100%, BPP = 1.00; *A. taoyao*, BS = 100%, BPP = 1.00; Fig. 1). The phylogenetic tree resolved *Atheniella flavida* as forming a monophyletic lineage, which was sister to the majority of accessions included within the *Atheniella* Clade, consisting of *A. adonis*, *A. amabillissima*, *A. flavoalba*, *Mycena floridula* and the other two new species. Recognition of *Atheniella taoyao* and *A. rutila* was well supported, with these two

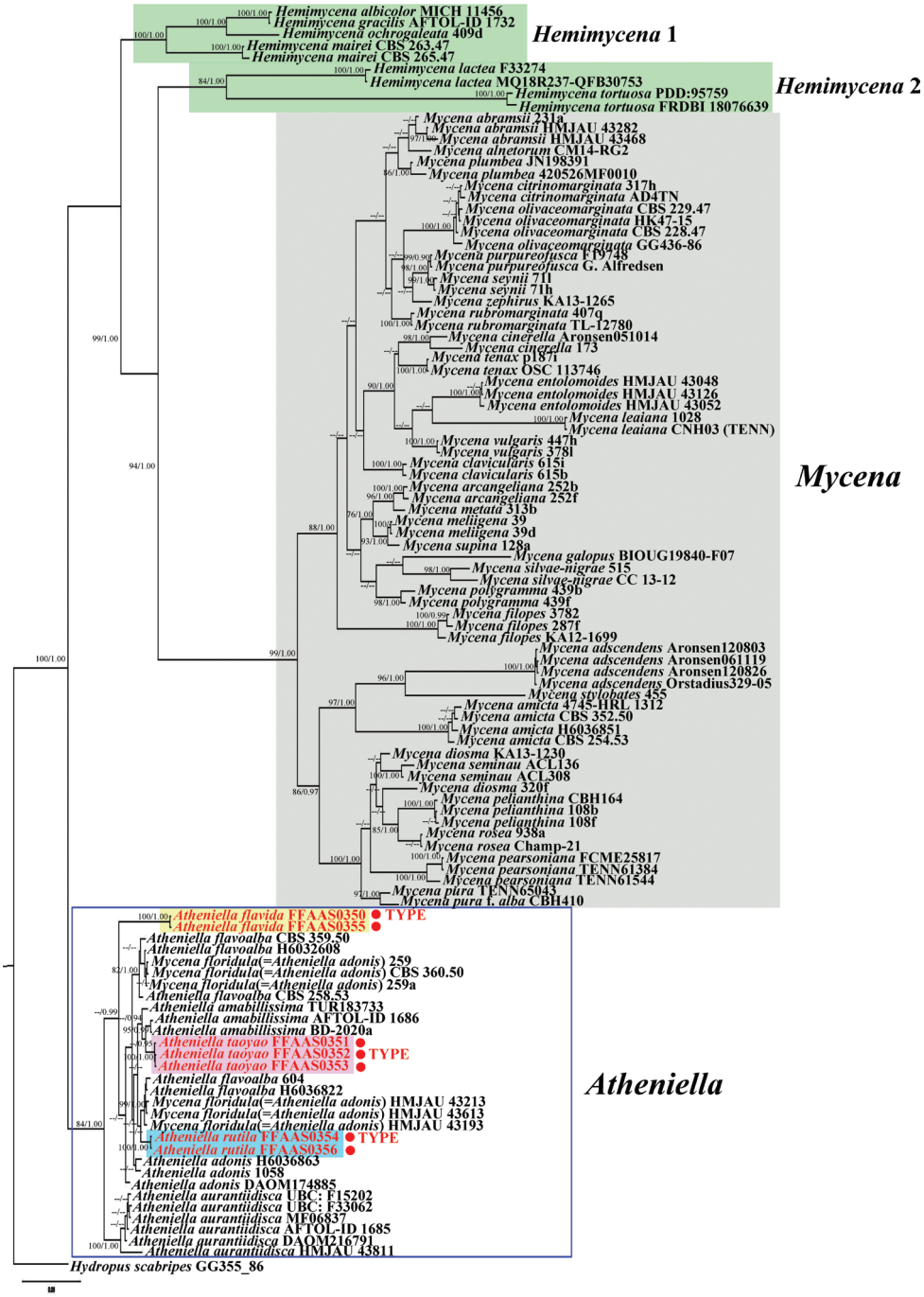

Figure 1. Maximum Likelihood and Bayesian tree concatenated ITS + nLSU dataset (ML ≥ 75%, BPP ≥ 0.90 are indicated). The tree is rooted with *Hydropus scabripes*. The new species are marked by red dot.

species respectively indicated to be sister to accessions of *A. amabillissima* and to accessions of *A. flavoalba* and *Mycena floridula* (Fr.) Quél. *Atheniella flavoalba* was polyphyletic with accessions placed in two distinct lineages together with accessions of *Mycena floridula*. Accessions of *Atheniella adonis* were distributed amongst three lineages and were difficult to distinguish genetically from accessions of *A. flavoalba* in two lineages.

Taxonomy

Atheniella **Redhead, Moncalvo, Vilgalys, Desjardin & B.A. Perry**
MycoBank No: 550101

Diagnosis. Basidiomata small, mycenoid. Pileus conical, campanulate, to hemispherical, often with a small papilla when young, flattening or concave at centre with age; brightly coloured, white, creamy, yellow, orange, pinkish, reddish, sometimes yellow or deep brown at centre when old, the margin frequently fading to white, creamy, yellowish-white or yellow in the mature period; delicately pubescent, pruninose, glabrescent with age, translucent-striate, barely or shallowly sulcate, margin flattened and waved. Context thin and fragile, white. Lamellae ascending, adnate, adnexed, decurrent with tooth, faces concolorous with the sides. Stipe cylindrical, hollow, fragile, pruinose, almost smooth when old, base with coarse fibrils; white, yellow, orange, pink, sometimes base tinged deeper yellow with age. Odour and taste inconspicuous. Basidiospores globose, subglobose, ellipsoid, narrowly ellipsoid to cylindrical, smooth, thin-walled, hyaline, guttulate, inamyloid, white in prints. Basidia clavate, hyaline, thin-walled, 2- or 4-spored. Cheilocystidia fusiform, clavate, subutriform, long-stalked, hyaline, thin-walled. Pleurocystidia similar to cheilocystidia. Pileipellis hyphae covered with simple to branched excrescences, hyaline. Hyphae of the stipitipellis smooth or with simple cylindrical excrescences, hyaline; caulocystidia cylindrical, lageniform, subglobose, if present, hyaline, thin-walled. All tissues non-reactive in iodine. Clamps present or absent.

Habit and habitat. Saprophytic on grass, moss, rotten wood or plant debris (leaves, pine needles and twigs).

Type species. *Atheniella adonis* (Bull.) Redhead, Moncalvo, Vilgalys, Desjardin & B.A. Perry

Etymology. Intentionally spelled to achieve phonetic harmony and uniqueness, the epithet alludes to the mythical goddess Athena (the combination of beautiful colouration, spear-like stature and shield-like pileus) and her ancient Mycenaean origin. Gender: feminine.

Key to species of *Atheniella*

1 Growing on twigs of *Filipendula ulmaria* ..... ***A. ulmariae***
– Growing on lawn or broadleaf-conifer mixed forest **2**

2	Pileus yellowish-white, yellow to orange	**3**
–	Pileus pink or red	**7**
3	Cheilocystidia fusiform, thick-walled in the middle portion	***A. delectabilis***
–	Cheilocystidia fusiform, uniformly thin-walled	**4**
4	Clamps absent in all tissues	***A. flavida***
–	Clamps present in all tissues	**5**
5	Basidiospores broadly ellipsoid	***A. leptophylla***
–	Basidiospores narrowly ellipsoid	**6**
6	Caulocystidia up to 60 µm	***A. flavoalba***
–	Caulocystidia less than 20 µm	***A. aurantiidisca***
7	Lamellae decurrent	***A. taoyao***
–	Lamellae adnate to adnexed	**8**
8	Pileipellis with gelatinous hyphae	***Mycena rohitha*** (≡ ***A. rohitha***)
–	Pileipellis without gelatinous hyphae	**9**
9	Cheilocystidia with several large irregular excrescences or otherwise nodulose	***Mycena wubabulna*** (≡ ***A. wubabulna***)
–	Cheilocystidia entirely smooth	**10**
10	Stipe tinged coral-red and base yellowish with age	***A. amabillissima***
–	Stipe constantly white with age	**11**
11	Stipitipellis smooth; caulocystidia clavate to fusiform	***A. adonis***
–	Stipitipellis with simple cylindrical excrescences; caulocystidia not seen	***A. rutila***

Atheniella flavida **Q. Na & Y.P. Ge, sp. nov.**
MycoBank No: 839378
Figs 2g–i, 3, 4.

Diagnosis. Pileus colour changing from orange-yellow to yellow, slightly concave at centre with age, pruninose. Lamellae narrowly adnate. Stipe densely pruinose. Basidiospores globose to subglobose, inamyloid. Cheilocystidia and pleurocystidia fusiform, thin-walled. Pileipellis with mass of excrescences. Caulocystidia cylindrical or lageniform. All tissues non-reactive in iodine. Clamps absent.

Holotype. China. Yunnan Province, Yuxi City, Xinping County, Mopanshan National Forest Park, 25 Jul 2020, Qin Na, Yupeng Ge and Zewei Liu, *FFAAS0350* (Collection No. MY0182).

Etymology. Refers to the yellow basidiomata.

Description. Pileus 2.6–4.8 mm in diam., conic when young, becoming almost hemispherical and slightly concave at centre with age, orange-yellow (4A8) when young, fading to cream-yellow (3A4–3A6) at maturity, margin light yellow (3A3), sulcate, translucent-striate, delicately pubescent, pruninose, glabrescent with age, margin waved. Context very thin and fragile, pure white. Lamellae narrowly adnate, ascending, cream-white (3A2) to light yellow (3A3), faces concolorous with the sides, decurrent with a short tooth. Stipe slender, 5.5–12 × 0.5–0.8 mm, cylindrical, hollow,

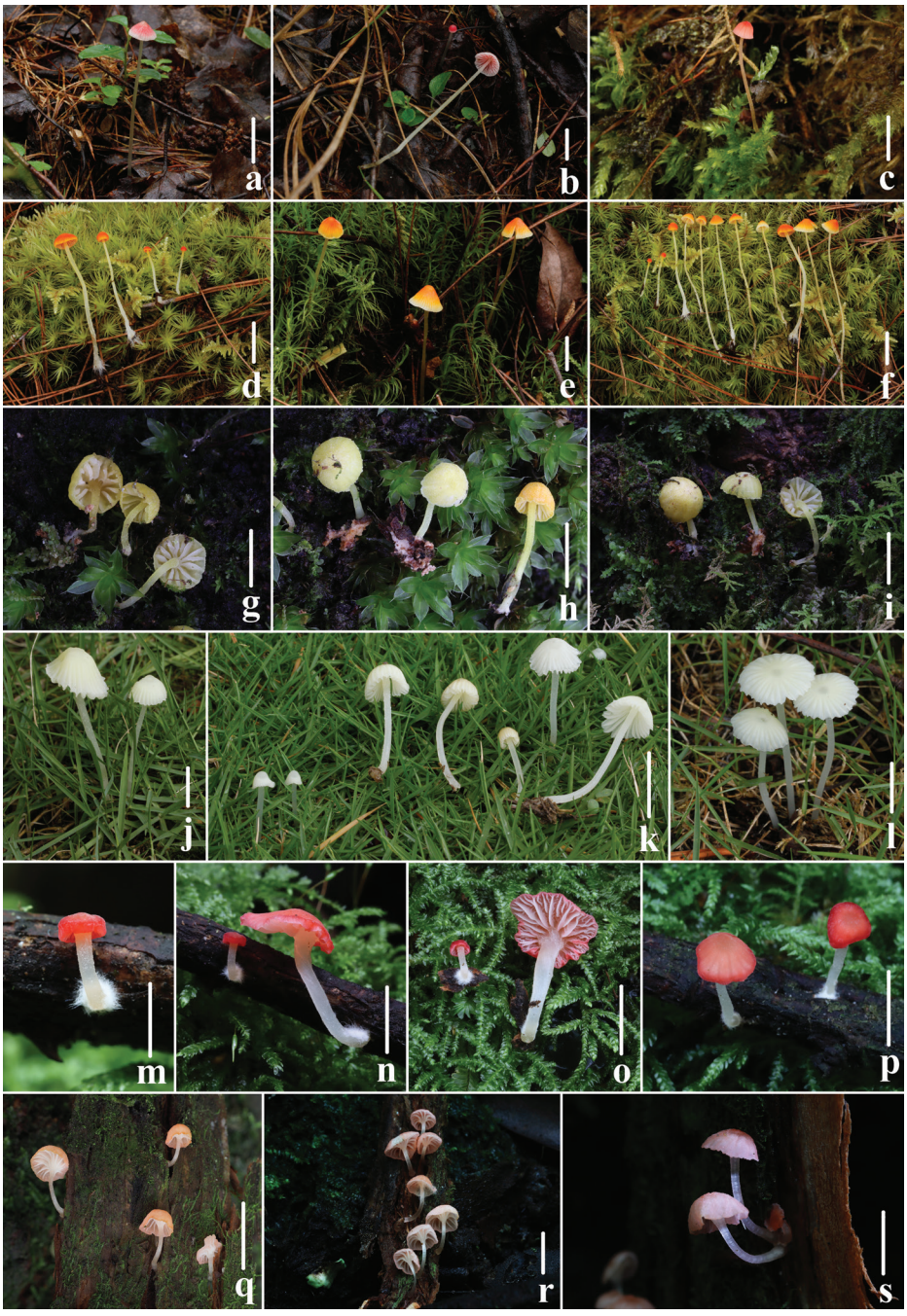

Figure 2. Basidiomata of *Atheniella* species **a–c** *Atheniella adonis* (Bull.) Redhead, Moncalvo, Vilgalys, Desjardin & B.A. Perry **d–f** *Atheniella aurantiidisca* (Murrill) Redhead, Moncalvo, Vilgalys, Desjardin & B.A. Perry **g–i** *Atheniella flavida* Q. Na & Y.P. Ge **j–l** *Atheniella flavoalba* (Fr.) Redhead, Moncalvo, Vilgalys, Desjardin & B.A. Perry **m–p** *Atheniella rutila* Q. Na & Y.P. Ge **q–s** *Atheniella taoyao* Q. Na & Y.P. Ge. Scale bars: 10 mm (**a–f, j–l, n–p**), 5 mm (**g–i, q–s**). Photographs **a,b, d–h, j–o, q, r** by Qin Na; **c, i, p, s** by Yupeng Ge.

fragile, bright yellow (4A6), densely pruinose on the entire surface, almost smooth when old, base with sparse white fibrils. Odour and taste inconspicuous.

Basidiospores [60/3/2] (6.5) 6.7–**7.2**–7.8 (8.3) × (5.7) 5.9–**6.5**–7.1 (7.8) μm [Q = 1.03–1.22, **Q** = ***1.11*** ± 0.043] [holotype [40/2/1] (6.6) 6.7–**7.2**–7.6 (7.9) × (5.8) 5.9–**6.4**–6.9 (7.4) μm, Q = 1.04–1.20, **Q** = ***1.10*** ± 0.041], globose to subglobose, hyaline, guttulate, thin-walled, inamyloid. Basidia 20–29 × 5–8 μm, hyaline, clavate, 2-spored. Cheilocystidia abundant, 36–51 × 8–11 μm, fusiform, long-stalked, hyaline, thin-walled. Pleurocystidia similar to cheilocystidia, 28–43 × 6–10 μm. Pileipellis hyphae 2–6 μm wide, cutis; covered with mass of excrescences, 3.3–8.2 × 1.2–3.4 μm, hyaline. Hyphae of the stipitipellis 2–8 μm wide, hyaline, smooth; caulocystidia cylindrical or lageniform, 14–37 × 5–11 μm, hyaline, thin-walled. All tissues non-reactive in iodine. Clamps not seen in all tissues.

Habit and habitat. Solitary to scattered on rotten wood in evergreen broad-leaf forest, *Cephalotaxus*, *Cunninghamia*, *Keteleeria*, *Podocarpus*, *Pseudotaxus*, *Pseudotsuga*, *Sequoia*, *Taxus*, *Torreya* and *Tsuga*.

Other specimens examined. China. Yunnan Province, Yi Autonomous Prefecture, Chuxiong City, Zixishan, 27 Jul 2020, Qin Na, Yupeng Ge and Zewei Liu, *FFAAS0355* (Collection No. MY0234).

Remarks. *Atheniella flavida* is considered to be a distinct species in *Atheniella* on account of the pileus colour changing from orange-yellow to yellow, globose to subglobose basidiospores and caulocystidia comparatively small (Maas Geesteranus 1980, 1990, 1992a, 1992b; Perry 2002; Robich 2003; Aronsen and Læssøe 2016). Four species with a yellow or orange pileus are recorded: *A. aurantiidisca*, *A. delectabilis* (Peck) Lüderitz & H. Lehmann, *A. flavoalba* and *A. leptophylla* (Peck) Gminder & Böhningare (Smith 1935b; Maas Geesteranus 1980; Robich 2003; Aronsen and Læssøe 2016). *Atheniella flavoalba*, which is the most widely distributed species in the Northern Hemisphere, often seen in northeast China (Fig. 2a–c), shows the most morphological similarities to *A. flavida*; however, the former differs in forming cylindrical spores (6.5–9 × 3–4.5 μm) and the caulocystidia are fusiform and clavate to globose (Perry 2002; Robich 2003; Aronsen and Læssøe 2016; Na 2019). In contrast to *A. flavida*, *A. aurantiidisca*, which had been found in Yunnan Province and Tibet Autonomous Region of China (Fig. 2d–f) and *A. leptophylla* are easily mistaken for the new species (Robich 2003; Aronsen and Læssøe 2016; Na 2019). However, the pileus of *A. aurantiidisca* and *A. leptophylla* is constantly distinctly orange and caulocystidia of the two species are larger (up to 50 μm long) (Robich 2003; Aronsen and Læssøe 2016). *Atheniella delectabilis*, which was formerly named *Hemimycena delectabilis* (Peck) Singer on account of the white to yellowish-white pileus, decurrent lamellae and inamyloid basidiospores, is easily mistaken for *A. flavida* by the light yellowish pileus and the similar shape and size of cheilocystidia and caulocystidia. However, *A. delectabilis* is distinguishable from *A. flavida* by its decurrent lamellae and cylindrical spores (7–9 × 3–4 μm) (Smith 1935b; Malysheva and Morozova 2009). In addition, *A. delectabilis* produces cheilocystidia that are partially thick-walled (Smith 1935b).

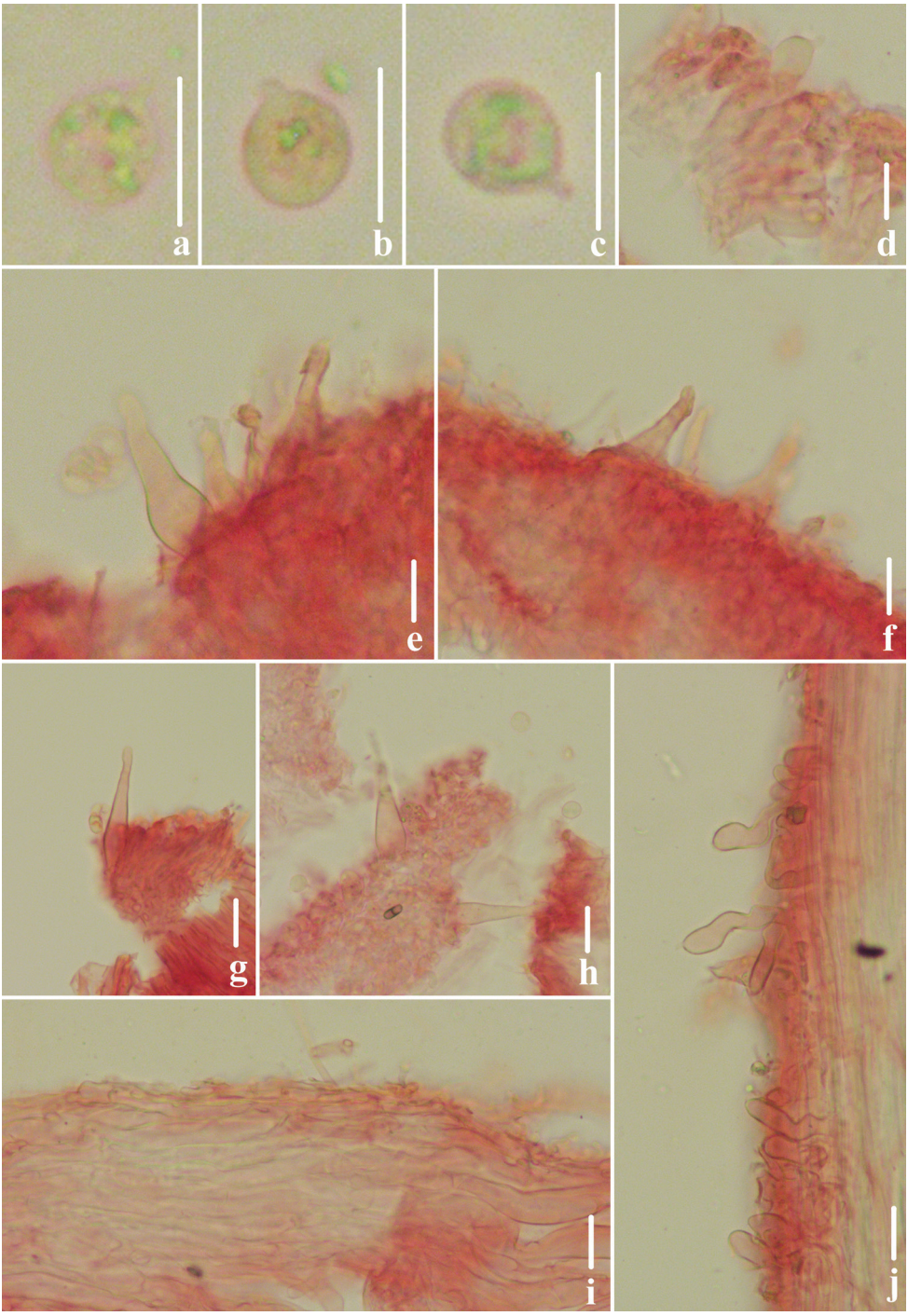

Figure 3. Microscopic features of *Atheniella flavida* (*FFAAS0350*, holotype) **a–c** basidiospores **d** basidia **e, f** cheilocystidia **g, h** pleurocystidia **i** pileipellis **j** stipitipellis and caulocystidia. Scale bars: 10 μm (**a–j**).

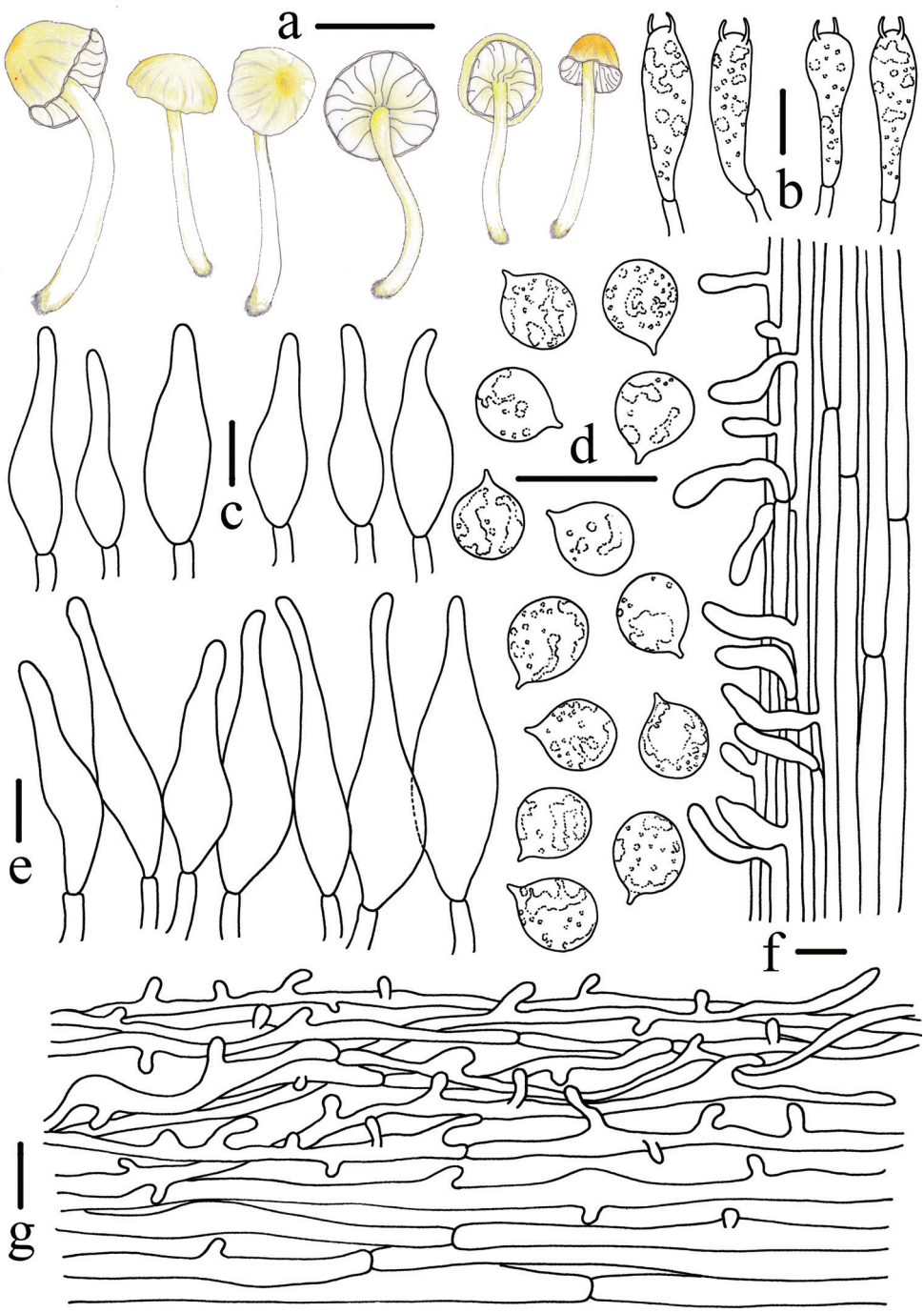

Figure 4. Morphological features of *Atheniella flavida* (*FFAAS0350*, holotype) **a** basidiomata **b** basidia **c** pleurocystidia **d** basidiospores **e** cheilocystidia **f** stipitipellis and caulocystidia **g** pileipellis. Scale bars: 10 mm (**a**); 10 μm (**b–g**). Drawings by Qin Na and Yupeng Ge.

***Atheniella rutila* Q. Na & Y.P. Ge, sp. nov.**
MycoBank No: 839379
Figs 2m–p, 5, 6.

Diagnosis. Pileus campanulate to hemispherical, concave with age, slightly pruinose. Lamellae adnate to adnexed, white. Stipe base with dense white fibrils. Basidiospores cylindrical, inamyloid. Pleurocystidia similar to cheilocystidia, fusiform, with a long neck. Pileipellis covered with numerous excrescences. Hyphae of the stipitipellis with simple cylindrical excrescences. Caulocystidia not seen. All tissues non-reactive in iodine. Clamps absent.

Holotype. China. Yunnan Province, Lincang City, Wulaoshan National Forest Park, 31 Jul 2020, Qin Na, Yupeng Ge and Zewei Liu, *FFAAS0354* (Collection No. MY0210).

Etymology. Refers to the bright red-tinted pileus.

Description. Pileus 2.0–10.2 mm in diam., campanulate to hemispherical, applanate or slightly concave at centre when old, deep salmon (10A7) to bright red (10A8), shallowly sulcate, translucent-striate, delicately pubescent, glabrescent when old. Context white, thin, very fragile. Lamellae broadly adnate to adnexed, ascending, white, concolorous with the sides, basally interveined with age. Stipe 5.0–15.8 × 1.0–2.0 mm, cylindrical, hollow, fragile, transparent, pruninose, glabrescent when old, base slightly swollen, covered with dense white fibrils. Odour and taste indistinctive.

Basidiospores [60/3/2] (7.2) 7.7–**8.6**–9.8 (10.1) × (3.6) 4.1–**4.6**–5.3 (5.5) µm [Q = 1.71–2.05, **Q** = ***1.85*** ± 0.079] [holotype [40/2/1] (7.2) 7.5–**8.5**–9.7 (10.0) × (3.6) 4.1–**4.6**–5.2 (5.5) µm, Q = 1.72–1.99, **Q** = ***1.86*** ± 0.086], narrowly ellipsoid to cylindrical, hyaline in water and 5% KOH, inamyloid, smooth. Basidia 19–28 × 5–8 µm, 2-spored, clavate, hyaline. Cheilocystidia 32–45 × 8–11 µm, abundant, fusiform, with a long neck, thin-walled and hyaline. Pleurocystidia similar to cheilocystidia, 27–42 × 7–12 µm. Pileipellis hyphae 2–5 µm wide, covered with numerous excrescences, 3.2–6.9 × 0.8–1.7 µm, hyaline. Hyphae of the stipitipellis 2–7 µm wide, non-dextrinoid, hyaline, with simple cylindrical excrescences, 4.6–14.3 × 2.9–5.2 µm. All tissues non-reactive in iodine. Clamps absent in all tissues.

Habit and habitat. Scattered on rotten wood in evergreen broadleaf and *Pinus* mixed forest.

Other specimens examined. Yunnan Province, Puer City, Xiaoheijiang National Forest Park, 1 Aug 2020, Qin Na, Yupeng Ge and Zewei Liu, *FFAAS0356* (Collection No. MY0235).

Remarks. *Atheniella rutila* is considered to be a distinct species in *Atheniella* on account of the bright red pileus, white stipe, narrowly ellipsoid to cylindrical and inamyloid spores and characters of the cystidia, pileipellis and stipitipellis (Maas Geesteranus 1980, 1990, 1992a, b; Perry 2002; Grgurinovic 2003; Robich 2003; Aravindakshan and Manimohan 2015; Aronsen and Læssøe 2016). *Atheniella amabillissima* is difficult to distinguish from *A. rutila* owing to the reddish basidiomata, but the pileus of *A. amabillissima* fades to white with age or has a dirty yellowish disc, and the spores are

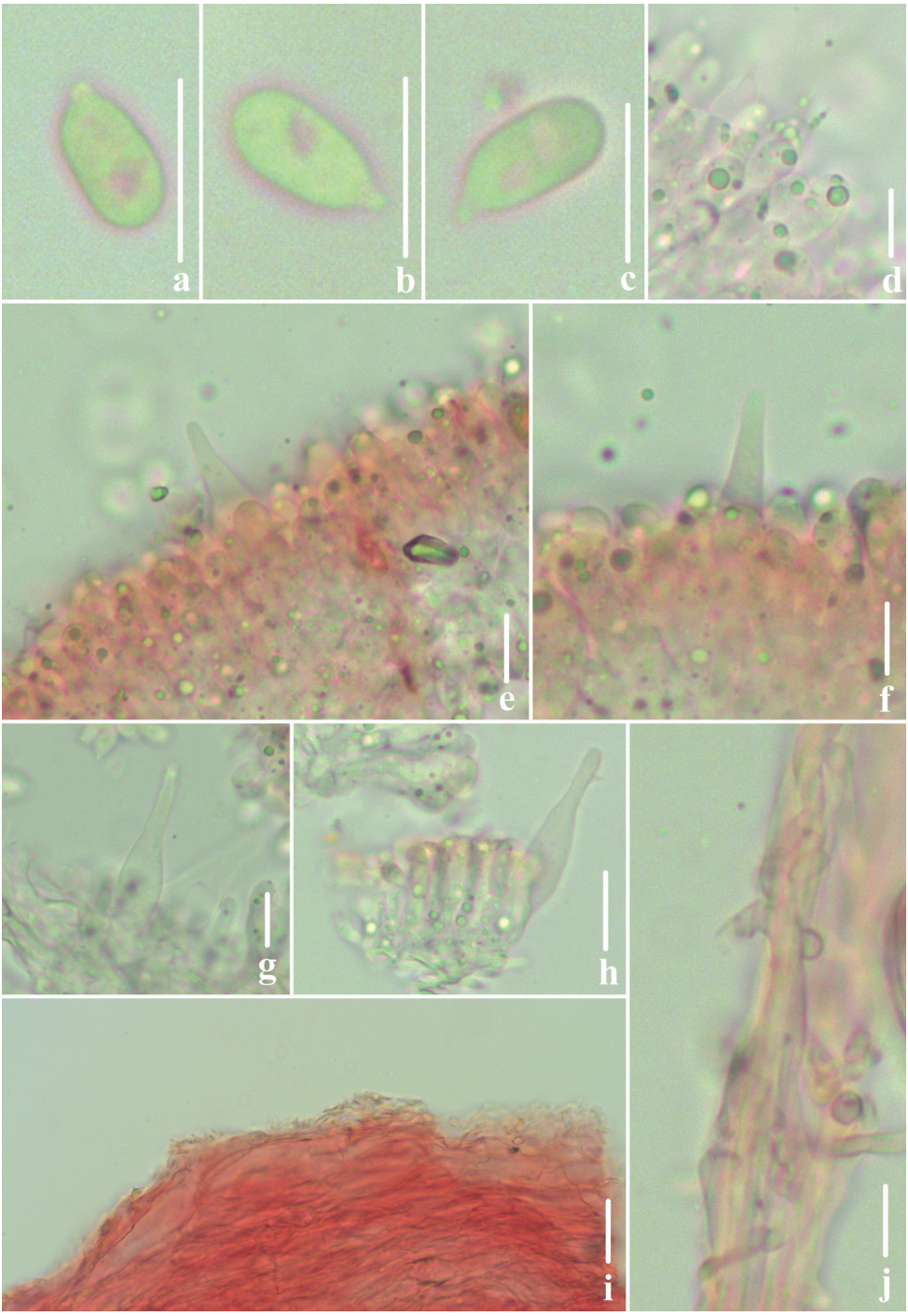

Figure 5. Microscopic features of *Atheniella rutila* (*FFAAS0354*, holotype) **a–c** basidiospores **d** basidia **e, f** cheilocystidia **g, h** pleurocystidia **i** pileipellis **j** stipitipellis. Scale bars: 10 μm (**a–j**).

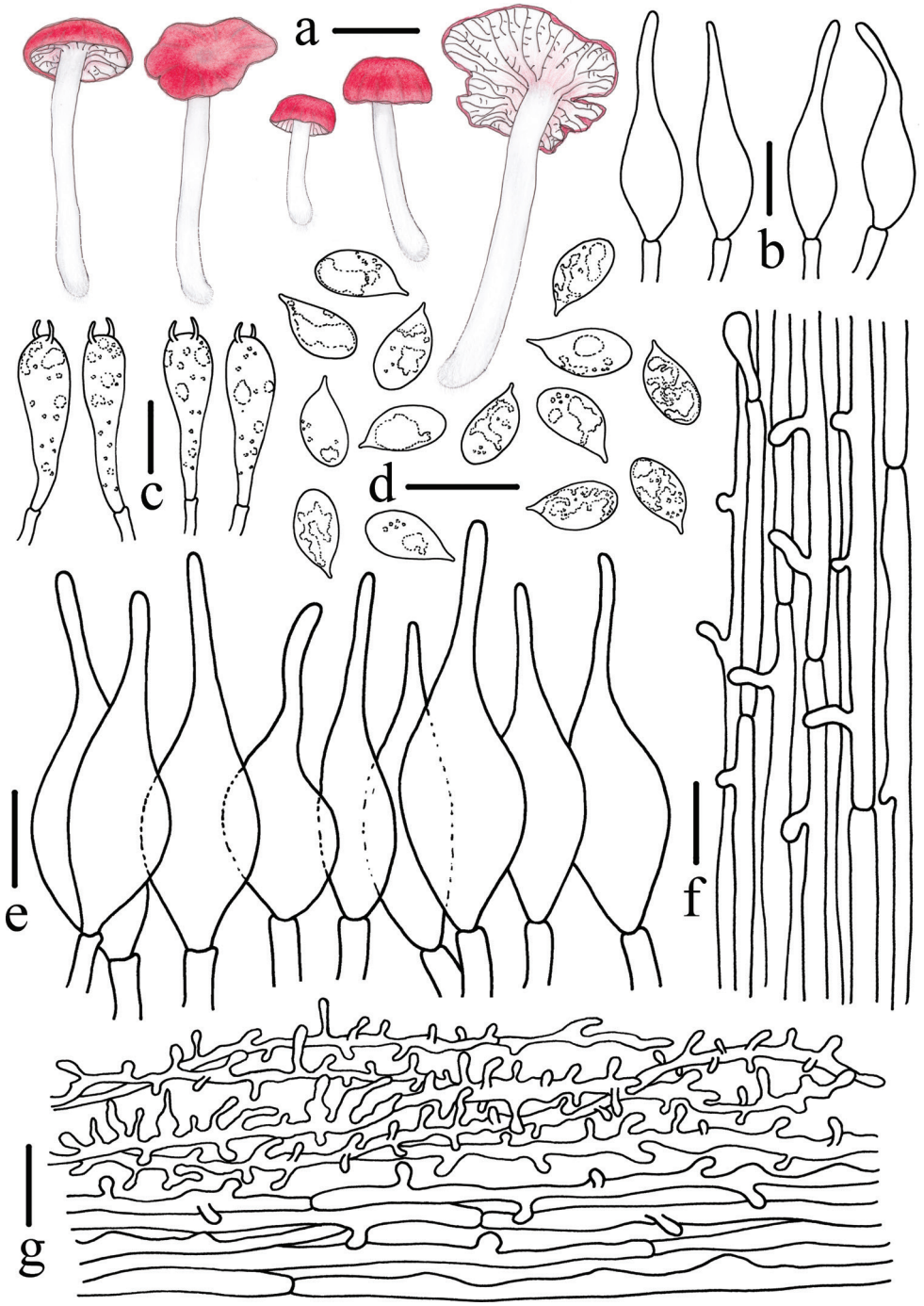

Figure 6. Morphological features of *Atheniella rutila* (*FFAAS0354*, holotype) **a** basidiomata **b** pleurocystidia **c** basidia **d** basidiospores **e** cheilocystidia **f** stipitipellis **g** pileipellis. Scale bars: 5 mm (**a**); 10 μm (**b–g**). Drawings by Qin Na and Yupeng Ge.

smaller (7–9 × 3–4 μm) (Smith 1935b). *Atheniella adonis* shows certain morphological similarities to *A. rutila* in possessing tiny and pinkish-red basidiomata, white lamellae and cylindrical basidiospores. However, *A. adonis* differs in producing a pileus with a white margin, longer stipe and clavate to fusiform caulocystidia (Perry 2002; Robich 2003; Aronsen and Læssøe 2016). In comparison with *Atheniella rutila*, *Mycena rohitha* (≡ *A. rohitha*) and *M. wubabulna* (≡ *A. wubabulna*) have gelatinous pileus hyphae and narrower basidiospores (Grgurinovic 2003; Aravindakshan and Manimohan 2015).

Atheniella taoyao **Q. Na & Y.P. Ge, sp. nov.**
MycoBank No: 839380
Figs 2q–s, 7, 8

Diagnosis. Pileus pinkish to light reddish. Lamellae decurrent. Stipe pruninose, base slightly swollen. Basidiospores narrowly ellipsoid to cylindrical, inamyloid. Cheilocystidia and pleurocystidia fusiform. Pileipellis hyphae covered with excrescences. Stipitipellis smooth, caulocystidia of two types, fusiform or subglobose. All tissues non-reactive in iodine. Clamps absent.

Holotype. China. Yunnan Province, Yuxi City, Xinping County, Mopanshan National Forest Park, 25 Jul 2020, Qin Na, Yupeng Ge and Zewei Liu, *FFAAS0352* (Collection No. MY0184).

Etymology. Refers to the pinkish to reddish basidiomata. Tao Yao is a poem in the "The Book of Songs" that praises a young woman, whose beauty is compared to a flowering peach tree and who will be married and assume a new role in life.

Description. Pileus 1.4–5.8 mm in diam., campanulate or hemispherical, obtusely umbonate in the centre, flattening with age, translucent-striate, light pink-salmon (8A3), light coral red (8B7), fading light pink (8A2) or white to the margin, delicately pubescent, glabrescent with age, with a flat margin. Context pure white, thin, fragile. Lamellae decurrent dentate, ascending, sparse, pure white, edges concolorous with the sides. Stipe 46–58 × 0.5–1.0 mm, central, terete, almost equal, hollow, fragile, transparent, pruninose, glabrescent with age, base slightly swollen, with tiny, white, fine hairs. Odourless, taste mild.

Basidiospores [80/4/3] (7.4) 7.7–**8.3**–9.1 (9.4) × (3.9) 4.1–**4.5**–5.0 (5.5) μm [Q = 1.73–2.08, **Q** = ***1.85*** ± 0.076] [holotype [40/2/1] (7.4) 7.7–**8.2**–9.0 (9.2) × (4.0) 4.1–**4.4**–5.0 (5.4) μm, Q = 1.75–1.99, **Q** = ***1.84*** ± 0.079], narrowly ellipsoid to cylindrical, hyaline, guttulate, thin-walled, inamyloid. Basidia 20–31 × 5–7 μm, hyaline, clavate, 2-spored. Cheilocystidia 23–42 × 5–10 μm, fusiform, long-stalked, hyaline. Pleurocystidia similar to cheilocystidia, 20–40 × 5–9 μm. Pileipellis hyphae 1–5 μm wide, cutis; covered with numbers of cylindrical or fusiform excrescences, 3.5–10.4 × 1.4–4.3 μm, hyaline. Hyphae of the stipitipellis 3–10 μm wide, hyaline, smooth; caulocystidia fusiform, 16.5–24.9 × 5.3–11.5 μm or subglobose, 11.8–16.5 × 9.1–12.9 μm. All tissues non-reactive in iodine. Clamps not seen.

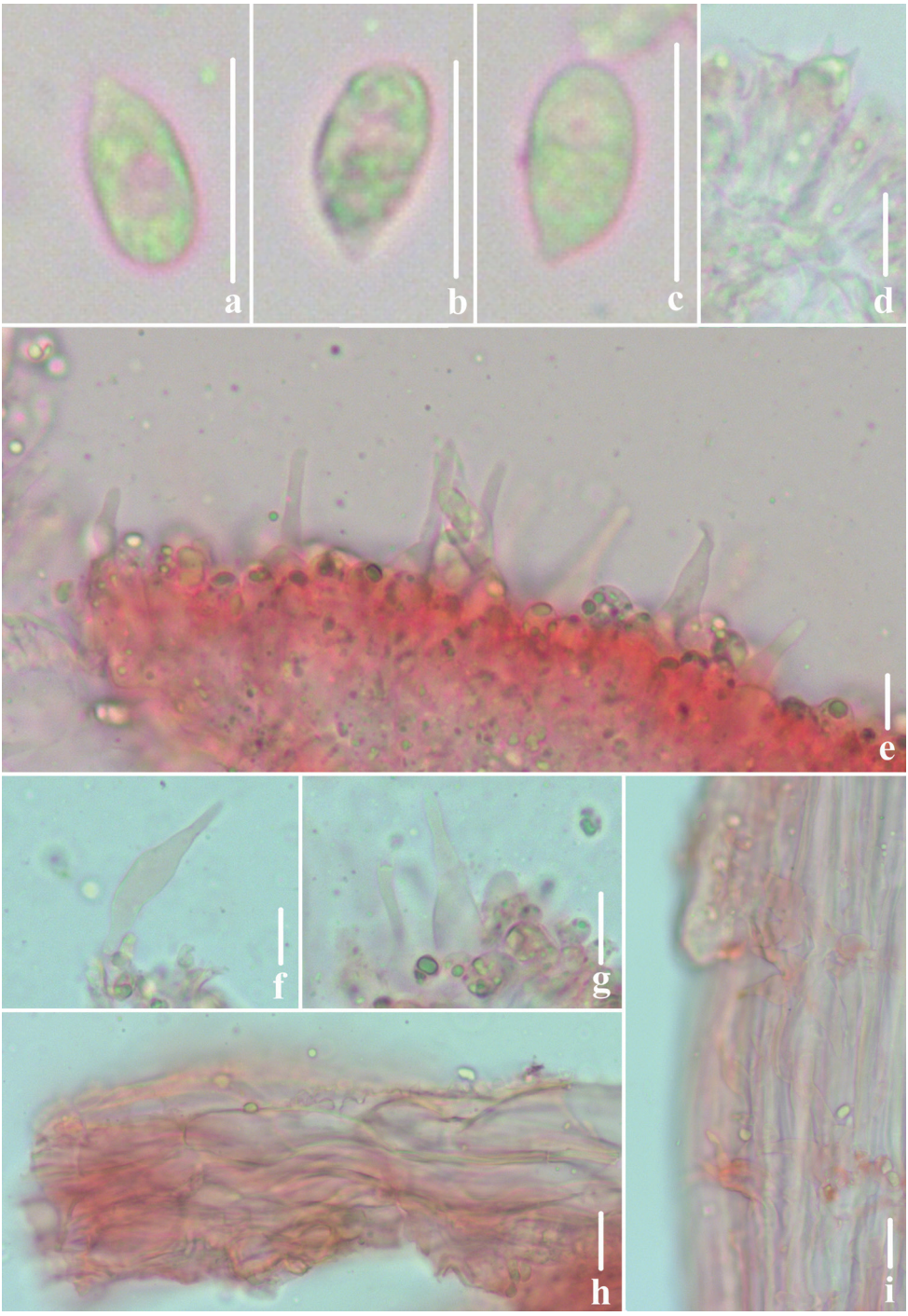

Figure 7. Microscopic features of *Atheniella taoyao* (*FFAAS0352*, holotype) **a–c** basidiospores **d** basidia **e** cheilocystidia **f, g** pleurocystidia **h** pileipellis **i** stipitipellis. Scale bars: 10 μm (**a– i**).

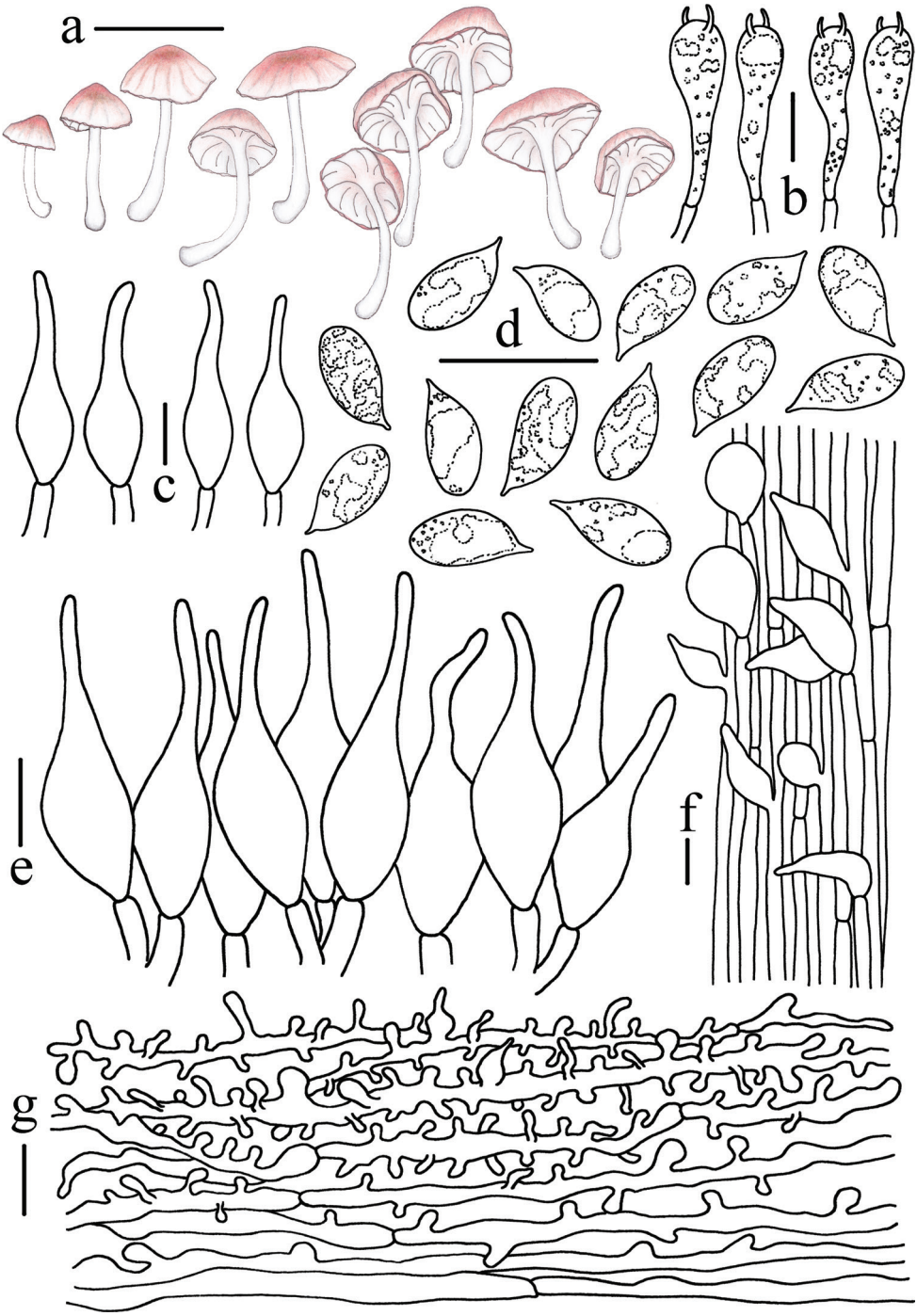

Figure 8. Morphological features of *Atheniella taoyao* (*FFAAS0352*, holotype) **a** basidiomata **b** basidia **c** pleurocystidia **d** basidiospores **e** cheilocystidia **f** stipitipellis and caulocystidia **g** pileipellis. Scale bars: 5 mm (**a**); 10 μm (**b–g**). Drawingsby Qin Na and Yupeng Ge.

Habit and habitat. Scattered to gregarious on living wood in evergreen broadleaf forest, for example, *Cephalotaxus*, *Cunninghamia*.

Other specimens examined. Yunnan Province, Yuxi City, Xinping County, Mopanshan National Forest Park, 25 Jul 2020, Qin Na, Yupeng Ge and Zewei Liu, *FFAAS0351* (Collection No. MY0183); Yunnan Province, Yuxi City, Xinping County, Shimenxia, 26 Jul 2020, Qin Na, Yupeng Ge and Zewei Liu, *FFAAS0353* (Collection No. MY0185).

Remarks. *Atheniella taoyao* is unique in *Atheniella* because of the light pink-salmon pileus, decurrent lamellae and the two types of caulocystidia. *Atheniella adonis* most closely resembles *A. taoyao*, but the former differs in having adnate to adnexed lamellae, stipe with pink at the apex and larger caulocystidia (15–50 × 3.5–13.5 μm) (Aronsen and Læssøe 2016). *Atheniella amabillissima* is closely allied to *A. taoyao*, but differs in the larger basidiomata (pileus 3–20 mm in diam.), pileus fading to white or yellow with age, stipe tinted with coral red and yellow with age and the cheilocystidia are up to 65 μm in length (Smith 1935b). Aravindakshan and Manimohan (2015) described the species *Mycena rohitha* Aravind. & Manim. (≡ *Atheniella rohitha*) collected from India. This taxon differs from *Atheniella taoyao* in its orange stipe and gelatinous pileus hyphae (Aravindakshan and Manimohan 2015). *Mycena wubabulna*, a species described by Grgurinovic (2003) that should be transferred to *Atheniella*, is readily identified by its yellowish stipe base and cylindrical basidiospores (7.5–10.6 × 3.1–4.7 μm; Q = 2.3).

Discussion

The present phylogenetic analysis showed that *Atheniella* formed a distinct clade independent of *Hemimycena* and *Mycena* with high BPP and BS support and, thus, supported segregation of the genus from the Mycenaceae (Moncalvo et al. 2002; Matheney et al. 2006). This finding also supported the view of Redhead et al. (2012) that *Atheniella*, formerly treated as *Mycena* sect. *Adonideae*, should be elevated to generic rank. *Atheniella* is more closely related to *Mycena* than to *Hemimycena*, based on genetic distance, in accordance with the greater similarity of *Atheniella* to *Mycena* spp. in morphological characters. The presence of pileocystidia and the morphological differences of the cheilocystidia, caulocystidia and stipitipellis can be used to distinguish *Atheniella* species from *Hemimycena* and *Mycena*.

Atheniella was originally established by Redhead et al. (2012) to accommodate four species: *A. adonis*, *A. amabillissima*, *A. aurantiidisca* and *A. flavoalba*. In recent years, the number of recognised species of *Atheniella* has increased to nine, but the description of the genus was incomplete and not detailed (Redhead et al. 2012; Gminder and Böhning 2016; Lehmann and Lüderitz 2019). With description of the new species in the present study, the generic description for *Atheniella* requires updating. Amongst *Atheniella* species, the bright colour of the pileus may be uniform or be tinted at the centre, but fades to white at the margin, the lamellae are adnate to decurrent and the stipe colour sometimes changes to yellow or pink towards the base. With regards to

micromorphological characters, *Atheniella* produces globose to cylindrical spores, caulocystidia are present or absent and the stipitipellis is smooth or has projections.

Atheniella is closely allied to *Hemimycena*, *Mycena* sect. *Aciculae* Kühner ex Singer and *Mycena* sect. *Oregonenses* Maas Geest., based on morphology (Maas Geesteranus 1980, 1992a, b). Species of *Hemimycena* lack bright yellow, pink to red basidiomata, produce larger spores and pileocystidia are often seen (Antonín and Noordeloos 2004; Malysheva and Morozova 2009). *M. acicula* (Schaeff.) P. Kumm., which is the sole species classified in *Mycena* sect. *Aciculae*, shares an orange-coloured pileus, non-amyloid spores and ornamentation of the pileipellis, but the stipitipellis is covered with numerous excrescences and is embedded in gelatinous material (Maas Geesteranus 1990; Robich 2003; Aronsen and Læssøe 2016). A longer stipe (up to 60 mm) with yellow fibrils at the base, cheilocystidia fusiform or lageniform with a rounded apex and caulocystidia with yellow contents are morphological characters that distinguish *Mycena* sect. *Oregonenses* from *Atheniella* (Maas Geesteranus 1990).

Morphological and molecular evidence support classification of the three newly-recognised species as members of *Atheniella*. The three species share white lamellae, a pruninose stipe base without a basal disc, inamyloid basidiopores, fusiform and thin-walled cheilocystidia, pileipellis covered with excrescences and are unreactive in Melzer's Reagent. In addition, the three species grow on rotten wood or other plant debris. *A. flavida* is mainly distinguished from *A. taoyao* and *A. rutila* by its distinctly yellowish-orange to yellow pileus and globose spores. The pinkish or reddish basidiomata support the inclusion of *A. taoyao* and *A. rutila* in *Atheniella*. Compared with *A. rutila*, *A. taoyao* is readily discriminated, based on the light pink basidiomata, narrow ellipsoid basidiospores and subglobose or fusiform caulocystidia. *A. amabillissima* shows the most morphological similarities to *A. taoyao* and *A. rutila*; however, *A. amabillissima* has a pileus which fades to white with age, smaller spores and longer cheilocystidia (Smith 1935b).

It is noteworthy that the taxonomic status of *Mycena floridula* remains unresolved (Josserand 1930; Kühner 1938; Aronsen and Læssøe 2016). This species was formerly classified in *Mycena* sect. *Adonideae* as a form of *M. flavoalba* with a pink pileus (Josserand 1930; Kühner 1938; Aronsen and Læssøe 2016). More recently, it was proposed that the name *M. floridula* was a synonym of *A. adonis* (Redhead et al. 2012). The phylogenetic reconstructions in our study and accessions of *M. floridula* indicated that *M. floridula* was closely related to *A. flavoalba*, with little genetic distinction between the two taxa. Therefore, we tentatively accept *M. floridula* as a pink form of *A. flavoalba*, but emphasise that a detailed appraisal of the morphological and molecular variation of *A. flavoalba* is required.

Acknowledgements

This study was supported by the National Natural Science Foundation of China (No. 3190012), the Natural Science Foundation of Shandong Province (No. ZR2020QC001,

No. ZR2019PC028), the Major Scientific and Technological Innovation Projects of Key R & D Programs in Shandong Province (No. 2019JZZY010717) and the Innovation Team of Shandong Agricultural Industry Technology System (2016 No.18). We sincerely thank Drs Jun–qing Yan (Jiangxi Agriculture University, Nanchang) for their kind help during fieldwork.

References

Aime MC, Bell CD, Wilson AW (2018) Deconstructing the evolutionary complexity between rust fungi (Pucciniales) and their plant hosts. Studies in Mycology 89: 143–152. https://doi.org/10.1016/j.simyco.2018.02.002

Antonín V, Noordeloos ME (2004) A monograph of the genera *Hemimycena*, *Delicatula*, *Fayodia*, *Gamundia*, *Myxomphalia*, *Resinomycena*, *Rickenella*, and *Xeromphalina* (Tribus Mycenae sensu Singer, *Mycena* excluded) in Europe. IHW-Verlag.

Aravindakshan DM, Manimohan P (2015) Mycenas of Kerala. SporePrint Books, Calicut, India. doi: http://dx.doi.org/10.13140/RG.2.1.2116.4003

Aronsen A, Larsson E (2016) Studier i släktet *Mycena*-2. Svensk Mykologisk 37(3): 26–31.

Aronsen A, Læssøe T (2016) The Genus *Mycena* s.l. Fungi of Northern Europe (Vol. 5). Narayana Press, Gylling, Denmark.

Bau T, Liu Y (2011) Four new records of *Mycena* from China. Mycosystema 30(4): 653–657. doi: http://dx.doi.org/10.13346/j.mycosystema.2011.04.024

Emmett EE (1992) British *Mycena* species–1. Mycologist 6(2): 72–76. https://doi.org/10.1016/S0269-915X(09)80453-9

Friedrich S (2006) Threatened and protected macromycetes in the Wkrzanska Forest. Acta Mycologica 41(2): 229–240. https://doi.org/10.5586/am.2006.025

Gminder A, Böhning T. (2016) Index Fungorum 302: 1–1.

Grgurinovic CA (2003) The genus *Mycena* in south–eastern Australia. Fungal Diversity Press, Canberra.

Gyosheva M, Ganeva A (2004) New and rare macromycetes and bryophytes from montane peat habitats in Bulgaria. Mycologia Balcanica 1: 9–13.

Hall TA (1999) BioEdit: a user-friendly biological sequence alignment editor and analysis program for Windows 95/98/NT. Nucleic Acids Symposium Series 41: 95–98. https://doi.org/10.1021/bk-1999-0734.ch008

Hopple JS, Vilgalys R (1999) Phylogenetic relationships in the mushroom genus *Coprinus* and dark-spored allies based on sequence data from the nuclear gene coding for the large ribosomal subunit RNA: divergent domains, outgroups, and monophyly. Molecular Phylogenetics & Evolution 13(1): 1–19. https://doi.org/10.1006/mpev.1999.0634

Horak E (2005) Röhrlinge und Blätterpilze in Europa: Bestimmungsschlüssel für Polyporales (pp), Boletales, Agaricales, Russulales. Elsevier, Spektrum Akad Verlag.

Josserand M (1930) Note sur deux mycènes: *M. flavo-alba* (Fr.) Q. et *M. floridula* (Fr.) Q. Bullc. Soc. myc. Fr. 46(1): 38–42.

Kornerup A, Wanscher JHK (1978) The Methuen Handbook of Colour. Eyre Methuen, London.

Kühner R (1938) Le genre *Mycena* (Fries). Encyclopédie Mycologique X. P. Lechevalier.

Lehmann V, Lüderitz O (2018) Index Fungorum 416: 1–1.

Lehmann V, Lüderitz O (2019) Index Fungorum 416: 1–1.

Li Y, Li TH, Yang ZL, Bau T, Dai YC (2015) Atlas of Chinese Macrofungal Resources. Central Chinese Farmer Press, Zhengzhou, China.

Maas Geesteranus RA (1980) Studies in Mycenas–15. Persoonia 11: 93–120.

Maas Geesteranus RA (1990) Conspectus of the Mycenas of the Northern Hemisphere–14, Sections *Adonidae*, *Aciculae*, and *Oregonenses*. Proceedings van de Koninklijke Nederlandse Akademie van Wetenschappen (Ser C), Amsterdam, North–Holland 93(2): 163–186.

Maas Geesteranus RA (1992a) Mycenas of the Northern Hemisphere I. Studies in Mycenas and other papers. Proceedings van de Koninklijke Nederlandse Akademie van Wetenschappen, Amsterdam, North–Holland.

Maas Geesteranus RA (1992b) Mycenas of the Northern Hemisphere II. Studies in Mycenas and other papers. Proceedings van de Koninklijke Nederlandse Akademie van Wetenschappen, Amsterdam, North–Holland.

Malysheva EF, Morozova OV (2009) Notes on *Hemimycena* from European Russia. Czech Mycology 61(1): 27–71. https://doi.org/10.33585/cmy.61103

Matheny PB, Curtis JM, Hofstetter V, Aime M, Moncalvo J, Ge Z, Yang Z, Slot J, Ammirati J, Baroni T, Bougher N, Hughes K, Lodge D, Kerrigan R, Seidl M, Aanen D, DeNitis M, Daniele G, Desjardin D, Kropp B, Norvell L, Parker A, Vellinga E, Vilgalys R, Hibbett D (2006) Major clades of Agaricales: a multilocus phylogenetic overview. Mycologia 98(6): 982–995. https://doi.org/10.1080/15572536.2006.11832627

Miersch J, Karasch P (2011) *Mycena oregonensis* new for Bavaria and *Mycena leptophylla*, two apricot-coloured mycenas. Mycologia Bavaric 12: 19–26.

Miersch J (2013) Records of orange-capped mycena *Mycena aurantiidisca* in Bavaria and Saxony-Anhalt-new for Germany. Mycologia Bavaric 14: 13–21.

Miyamoto T, Igarashi T, Takahashi K (1998) Notes on three species of *Mycena* new to Japan from *Picea* forests of Hokkaido. Mycoscience 3(39): 337–342. https://doi.org/10.1007/BF02464018

Miyamoto T, Igarashi T, Takahashi K (2000) Lignin-degrading ability of litter-decomposing basidiomycetes from *Picea* forests of Hokkaido. Mycoscience 41(2): 105–110. https://doi.org/10.1007/BF02464317

Moncalvo JM, Vilgalys R, Redhead SA, Johnson JE, James TY, Aime MC, Hofstetter V, Verduine SJW, Larsson E, Baroni TJ, Thorn RG, Jacobsson S, Clémençon H, MillerJr OK (2002) One hundred and seventeen clades of euagarics. Molecular Phylogenetics and Evolution 23: 357–400. https://doi.org/10.1016/S1055-7903(02)00027-1

Murrill WA (1916) *Pleurotus*, *Omphalia*, *Mycena* and *Collybia* published in North American Flora. Mycologia 8(4): 218–221. https://doi.org/10.1080/00275514.1916.12018883

Na Q (2019) Taxonomy and Molecular Phylogeny of *Mycena* in China. Doctoral Dissertation of Jilin Agriculture University, Jilin, China. https://doi.org/10.27163/d.cnki.gjlnu.2019.000016

Na Q, Bau T (2018) New species of *Mycena* (Mycenaceae, Agaricales) with colored lamellae and three new species records from China. Phytotaxa 361(3): 266–278. https://doi.org/10.11646/phytotaxa.361.3.2

Na Q, Bau T (2019a) *Mycena* section *Sacchariferae*: three new species with basal discs from China. Mycological Progress 18: 483–493. https://doi.org/10.1007/s11557-018-1456-8

Na Q, Bau T (2019b) Recognition of *Mycena* sect. *Amparoina* sect. nov. (Mycenaceae, Agaricales), including four new species and revision of the limits of sect. *Sacchariferae*. Mycokeys 52: 103–124. https://doi.org/10.3897/mycokeys.52.34647

Norvell LL (2016) Mushrooms of the Redwood Coast–a comprehensive guide to the fungi of coastal northern California. Mycotaxon 131(3): 723–731. https://doi.org/10.5248/131.723

Nylander J (2004) MrModeltest v.2. Program distributed by the author. Evolutionary Biology Centre, Uppsala University, Uppsala.

Osono T (2015) Effects of litter type, origin of isolate, and temperature on decomposition of leaf litter by macrofungi. Journal of Forest Research 20(1): 77–84. https://doi.org/10.1007/s10310-014-0462-1

Pérez-De-Gregorio MÀ (2015) *Mycena leptophylla* from the Iberian Peninsula. Micologia e Vegetazione Mediterrane 29(2): 127–131.

Perry BA (2002) A taxonomic investigation of *Mycena* in California. Doctoral dissertation, San Francisco State University, California, USA.

Redhead SA (1984) Mycological observations, 4–12: on *Kuehneromyces*, *Stropharia*, *Marasmius*, *Mycena*, *Geopetalum*, *Omphalopsis*, *Phaeomarasmius*, *Naucoria* and *Prunulus*. Sydowia 246–270.

Redhead SA, Moncalvo JM, Vilgalys R, Desjardin DE, Perry BA (2012) Index Fungorum 14: 1–1.

Robich G (2003) *Mycena* d'Europa. Associazione Micologica Bresadola, Trento, Italy.

Ronquist F, Huelsenbeck JP (2003) MrBayes 3: Bayesian phylogenetic inference under mixed models. Bioinformatics 19: 1572–1574. https://doi.org/10.1093/bioinformatics/btg180

Smith AH (1935a) Studies in the Genus *Mycena*–I. American Journal of Botany 22(10): 858–877. https://doi.org/10.2307/2435962

Smith AH (1935b) Studies in the Genus *Mycena*–II. Mycologia 27(6): 586–604. https://doi.org/10.1080/00275514.1935.12017103

Smith AH (1935c) Studies in the Genus *Mycena*–III. Mycologia 28(5): 410–430. https://doi.org/10.2307/3754114

Smith AH (1937) Notes on agarics from the western United States. Bulletin of the Torrey Botanical Club 64(7): 477–487. https://doi.org/10.2307/2481096

Smith AH (1939) Studies in the Genus *Mycena*–V. Mycologia 31(3): 267–285. https://doi.org/10.1080/00275514.1939.12017341

Smith AH (1947) North American species of *Mycena*. University Michigan Press, Ann Arbor, Michigan.

Stamatakis A, Ludwig T, Meier H (2004) RAxML–III: a fast program for maximum likelyhood–based inference of large phylogenetic trees. Bioinformatics 21(4): 456–463. https://doi.org/10.1093/bioinformatics/bti191

Thompson JD, Gibson TJ, Plewniak F (1997) The Clustal–X windows interface: flexible strategies for multiple sequence alignment aided by quality analysis tools. Nucleic Acids Research 63: 215–228. https://doi.org/10.1093/nar/25.24.4876

Tyier G (1991) Ecology of the genus *Mycena* in beech (*Fagus sylvatica*), oak (*Quercus robur*) and hornbeam (*Carpinus betulus*) forest of Sweden. Nordic Journal of Botany 11(1): 111–121. https://doi.org/10.1111/j.1756-1051.1991.tb01807.x

Uehling JK, Henkel TW, Vilgalys R, Smith ME (2012) Membranomyces species are common ectomycorrhizal symbionts in Northern Hemisphere forests. Mycorrhiza 22(7): 577–581. https://doi.org/10.1007/s00572-012-0457-8

White TJ, Bruns T, Lee S, Taylor J (1990) Amplification and direct sequencing of fungal ribosomal RNA genes for phylogenetics. In: Innis MA, Gelfand DH, Sninsky JJ, White TJ (Eds) PCR protocols: a guide to methods and applications. Academic, San Diego, 315–322. https://doi.org/10.1016/B978-0-12-372180-8.50042-1

MycoKeys 81: 165–183 (2021)
doi: 10.3897/mycokeys.81.65660
https://mycokeys.pensoft.net

RESEARCH ARTICLE

A peer-reviewed open-access journal
MycoKeys
Launched to accelerate biodiversity research

Cyanescent *Gyroporus* (Gyroporaceae, Boletales) from China

Cong Huang[1,3], Ming Zhang[4], Xing-Liang Wu[5], Gang Wu[1,2], Jian-Ping Xu[6], Zhu L. Yang[1,2], Yan-Chun Li[1,2]

1 *Key Laboratory for Plant Diversity and Biogeography of East Asia, Kunming Institute of Botany, Chinese Academy of Sciences, 650201, Kunming, China* **2** *Yunnan Key Laboratory for Fungal Diversity and Green Development, Kunming 650201, Yunnan, China* **3** *University of Chinese Academy of Sciences, Beijing 100049, China* **4** *Institute of Microbiology, Guangdong Academy of Sciences, Guangzhou 510070, China* **5** *College of Tropical Crops, Hainan University, Hainan 570208, China* **6** *Department of Biology, McMaster University, Hamilton, ON L8S 4K1, Canada*

Corresponding authors: Zhu L. Yang (fungiamanita@gmail.com), Yan-Chun Li (liyanch@mail.kib.ac.cn)

Academic editor: Olivier Raspé | Received 8 March 2021 | Accepted 16 June 2021 | Published 26 July 2021

Citation: Huang C, Zhang M, Wu X-L, Wu G, Xu J-P, Yang ZL, Li Y-C (2021) Cyanescent *Gyroporus* (Gyroporaceae, Boletales) from China. MycoKeys 81: 165–183. https://doi.org/10.3897/mycokeys.81.65660

Abstract

Gyroporus species with cyanescent oxidation reactions were investigated, based on morphology and phylogenetic analysis of DNA sequences from the nuclear ribosomal large subunit (nrLSU), the nuclear ribosomal internal transcribed spacer (ITS) and the mitochondrial adenosine triphosphate ATP synthase subunit 6 (*atp6*). Three species, including two new species, namely *G. alpinus* and *G. flavocyanescens* and one previously-described species, namely *G. brunneofloccosus*, are revealed from China. Collections formerly reported from China as "*G. cyanescens*" are either *G. alpinus* or *G. flavocyanescens*. The new species are documented and illustrated in detail, while the concept of *G. brunneofloccosus* is refined with additional recently-collected materials. Additionally, the cyanescent species *G. pseudomicrosporus*, previously described from China, is shown to be a member of the genus *Gyrodon*, based on re-examination of the type specimen. A key to the cyanescent *Gyroporus* species from China is provided.

Keywords

Boletes, distribution, new taxa, phylogeny, taxonomy

Introduction

The genus, *Gyroporus* Quél., typified by *G. cyanescens* (Bull.) Quél., is a boletoid genus in the monogeneric family Gyroporaceae in the suborder Sclerodermatineae (Boletales) (Binder & Bresinsky, 2002). More than 40 species have been reported and described in this genus (e.g. Li et al. 2003; Kirk et al. 2008; Vizzini et al. 2015; Crous et al. 2016, 2017; Das et al. 2017; Davoodian et al. 2018, 2019, 2020; Magnago et al. 2018). *Gyroporus* is characterised by the initially spongy and then hollow stipe, the white to cream to yellow hymenophore, the white to yellowish context without colour change or with cyanescent or brownish colour change when bruised, the ellipsoid to broadly ellipsoid basidiospores and the presence of clamp connections (Singer 1986; Watling 2008; Magnago et al. 2018). Globally, so far fifteen species have been reported with cyanescent colour changes when bruised. Amongst these, eight species were reported from the Northern Hemisphere: four species originally described from Europe (*G. cyanescens*, *G. lacteus* Quél., *G. pseudolacteus* G. Moreno, Carlavilla, Heykoop, Manjón & Vizzini and *G. pseudocyanescens* G. Moreno, Carlavilla, Heykoop, Manjón & Vizzini), two species originally described from East Asia (*G. brunneofloccosus* T.H. Li, W.Q. Deng & B. Song and *G. pseudomicrosporus* M. Zang), one species originally described from North America [*G. violaceotinctus* (Watling) Blanco-Dios] and one species originally described from Central America (*G. phaeocyanescens* Singer & M.H. Ivory) (Bulliard 1788; Léveillé 1848; Watling 1969; Singer et al. 1983; Zang 1986; Li et al. 2003; Vizzini et al. 2015; Crous et al. 2016, 2017). Seven cyanescent species were reported from Australia (Southern Hemisphere), including four validly-published species (*G. australiensis* Davoodian, N.A. Fechner & Halling, *G. furvescens* Davoodian & Halling, *G. occidentalis* Davoodian, Bougher & Halling and *G. robinsonii* Davoodian) and three undescribed species proposed by Davoodian (2018) with provisional names (*G. allocyanescens*, *G. austrocyanescens* and *G. neocyanescens*) which need additional study when more collections are acquired (Davoodian et al. 2019, 2020). In China, three cyanescent *Gyroporus* have been reported: *G. cyanescens*, *G. brunneofloccosus* and *G. pseudomicrosporus* (Zang 1986; Li et al. 2003). During our recent field investigations of *Gyroporus* across China, we encountered two impressive cyanescent species from south-western China which are apparently different from other species in this genus.

In this study, we used both morphological data and molecular sequences from the nuclear ribosomal large subunit (nrLSU), the nuclear ribosomal internal transcribed spacer (ITS) and the mitochondrial adenosine triphosphate ATP synthase subunit 6 (*atp6*), together with ecological data to evaluate the phylogenetic relationships of the cyanescent species within *Gyroporus* and make morphological and ecological comparisons.

Materials and methods

Sampling and morphological studies

The collections of cyanescent species in *Gyroporus* were collected from Guizhou, Yunnan and Guangdong Provinces, China, in forests dominated by plants of the

family Fagaceae or in the mixed forests dominated by plants of the families Fagaceae and Pinaceae. Fresh basidiomata were photographed and macroscopic characteristics, habitat, colour change when bruised, odour and taste were recorded. Basidiomata were then dried and deposited in the Herbarium of the Kunming Institute of Botany, Chinese Academy of Sciences (**KUN**) and the Herbarium of the Guangdong Institute of Microbiology (**GDGM**). Macroscopic descriptions and microscopic studies followed Naseer et al. (2020), Zhang et al. (2019) and references therein. Colour description was according to Kornerup and Wanscher (1981). The notations and statistics of basidiospores followed Liu et al. (2020). Line drawings were prepared by free hand.

DNA extraction, PCR and sequencing

Genomic DNA was extracted from 100 mg of silica-gel dried samples or herbarium materials using the modified CTAB method (Doyle and Doyle 1987). PCR amplification primers ITS1 and ITS4 were used for the ITS region, LROR and LR5 were used for nrLSU and ATP6-F and ATP6-R were used for *atp6* (White et al. 1990; Davoodian et al. 2018). PCR, amplification conditions, sequencing and sequence alignment followed those in Gelardi et al. (2019), Huang et al. (2021) and Gómez-Zapata et al. (2021).

Phylogenetic analysis

The phylogenetic analyses were based on three fragments (*atp6*, ITS and nrLSU). Two datasets, the *atp6* dataset and the combined nrLSU and ITS dataset, were analysed using RAxML (Stamatakis et al. 2008). DNA sequences of the cyanescent species of *Gyroporus* from China and other continents (Crous et al. 2016, 2017; Das et al. 2017; Davoodian et al. 2018; Magnago et al. 2018) were used to infer the phylogenetic relationships between these species. Since seven cyanescent species have been reported from the Southern Hemisphere continent of Australia and their *atp6* sequences are publicly available, the *atp6* dataset was used to infer relationships of Australian cyanescent species with those from Europe, North America and East Asia in the Northern Hemisphere. The combined dataset was mainly used to infer relationships of species from East Asia, North America and Europe. In our preliminary analysis, the cyanescent species formed a monophyletic clade, thus, *G. longicystidiatus* Nagas. & Hongo without colour change when bruised was chosen as outgroup. For the combined dataset, *Scleroderma areolatum* Ehrenb., *S. duckei* B.D.B. Silva, M.P. Martín & Baseia and *S. laeve* Lloyd were selected as outgroup taxa.

The combined dataset was partitioned into four partitions (nrLSU, ITS1, 5.8S and ITS2). Statistical support for the phylogentic analyses was determined using a rapid bootstrapping with 1000 replicates in Maximum Likelihood (ML) analysis under the partitioned GTRGAMMA model. The scientific names, collection information and GenBank accession numbers for the specimens used in the phylogenetic analyses are presented in Table 1.

Table 1. A tabulation of specimens used for molecular phylogenetic analyses in the present study. Sequences newly generated in this study are indicated in bold.

Species	Voucher	Locality	GenBank Accession No.		
			ITS	LSU	*atp6*
"*Gyroporus allocyanescens*"	REH9700A	Australia	–	–	MF818179
G. alpinus	LI1478-Strain1	China	**MW149435**	**MW151268**	**MW452609**
G. alpinus	LI1478-Strain2	China	**MW149438**	**MW151269**	**MW452610**
G. ammophilus	AH45842	Spain	KX869876	KX869890	–
G. ammophilus	AH45814	Spain	KX869878	KX869892	–
G. australiensis	REH9501	Australia	–	–	MF818183
G. australiensis	REH9559	Australia	–	–	MF818182
G. austrobrasiliensis	ACM1136	Brazil	MF436999	MF437014	–
G. austrobrasiliensis	ACM1144	Brazil	MF437000	MF437015	–
"*G. austrocyanescens*"	REH9700	Australia	–	–	MF818176
G. brunneofloccosus	GDGM74638	China	**MW149437**	**MW151266**	–
G. brunneofloccosus	WU2644	China	**MW149436**	**MW151267**	**MW452611**
G. brunneofloccosus	OR482	China	–	–	MF818146
G. castaneus	AH45841	Spain	KX869875	KX869889	–
G. castaneus	AH45844	Spain	KX869874	KX869888	–
G. cyanescens	MCVE17184 (epitype)	Italy	JF908785	–	–
G. cyanescens	2837	Canada	KM248948	–	–
G. cyanescens	MCVE:28580	Italy	KT363684	KT363685	–
G. cyanescens	MB05-04	USA	–	EU718102	–
G. cyanescens	MG639a	Italy	–	–	MF818172
"*G. cyanescens*"	REH9970	USA	–	–	MF818174
"*G. cyanescens*"	ND11	USA	–	–	MF818173
"*G. cyanescens*"	KH-JPN15-0733	Japan	–	–	MF818191
"*G. cyanescens*"	KH-JPN15-0745	Japan	–	–	MF818192
"*G. cyanescens*"	NY1782681	South Korea	–	–	MF818185
G. flavocyanescens	WXL1182	China	**MW440550**	**MW442950**	**MW452613**
G. flavocyanescens	WXL1187	China	**MW440551**	**MW442951**	–
G. furvescens	REH9673	Australia	–	–	MF818175
G. lacteus	MCVE28582 (epitype)	Italy	KT363682	KT363683	–
G. longicystidiatus	REH8799	Thailand	EU718106	EU718142	MF818147
G. longicystidiatus	EN99-67	Japan	–	–	MF818151
G. occidentalis	REH8821 (holotype)	Australia	EU718103	EU718139	MF818177
G. occidentalis	REH8819	Australia	–	EU718172	–
G. occidentalis	E8164	Australia	–	–	MF818194
G. paramjitii	REH8804	Thailand	EU718101	EU718137	–
G. paramjitii	KD 16-002	India	MF120284	MF120285	–
G. phaeocyanescens	ARB1309	USA	–	–	MF818144
G. pseudocyanescens	AH55729 (holotype)	Spain	KY576808	KY576806	–
G. pseudocyanescens	AH45840	Spain	KY576809	KY576807	–
G. pseudolacteus	AH45848	Spain	KX869867	KX869881	–
G. pseudolacteus	AH39364 (holotype)	Spain	KX869866	KX869880	
G. purpurinus	PRL3737	USA	EU718105	EU718141	–
G. robinsonii	ND13	Australia	–	–	MF818178
G. robinsonii	OKM23719	Australia	–	EU718140	–
G. umbrinisquamosus	BUF-Both3525	USA	–	–	MF818145
Scleroderma areolatum	PBM2208	–	–	EU718150	–
S. duckei	INPA 272127	–	NR_147664		–
S. laeve	ZLR46	China	MW553325	MW553729	–

Results

Molecular analysis

In this study, sixteen new sequences of *Gyroporus* (six for ITS, six for nrLSU and four for *atp6*) were generated. Two datasets were analysed: the combined nuclear ribosomal DNA dataset (nrLSU + ITS) consists of 31 sequences and is 1720 bp long; the mitochondrial *atp6* dataset consists of 23 sequences and is 596 bp long. The alignments were submitted to TreeBASE (27864). Phylograms inferred with RAxML, including the support values, are illustrated (Figs 1, 2). In both of our analyses, species with cyanescent colour changes when bruised cluster together with high support (100% in Fig. 1 and 99% in Fig. 2).

The phylogenetic analysis of *atp6* data indicates that the Australian cyanescent *Gyroporus* species form an independent lineage, while the other cyanescent species from the Northern Hemisphere form another lineage (Fig. 1). It should be noted that the Northern Hemisphere lineage has relatively low bootstrap support (59%) in the *atp6* analysis; however, its two main constituent sub-lineages have high support (70% and 100%) (Fig. 1). Three cyanescent species from China that belong to the Northern Hemisphere lineage are revealed, including two new species, namely *G. alpinus* Yan C. Li, C. Huang & Zhu L. Yang and *G. flavocyanescens* Yan C. Li, C. Huang & Zhu L.

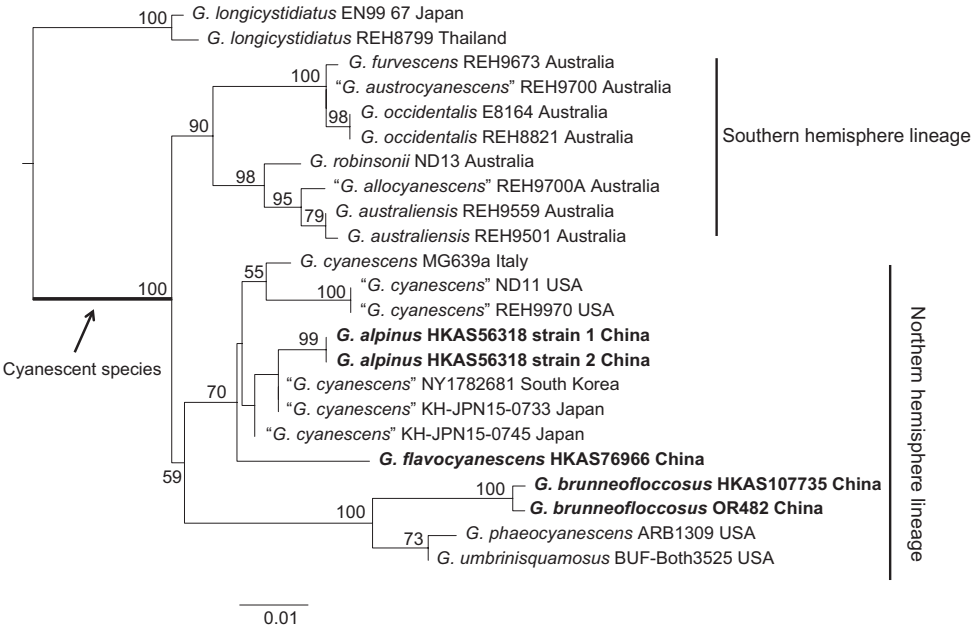

Figure 1. Maximum Likelihood phylogenetic tree of *Gyroporus* inferred from the *atp6* dataset. Bootstrap frequencies (> 50%) are shown above or below supported branches. Newly-sequenced collections are indicated in bold. Species vouchers and countries of origin are provided after the species name successively.

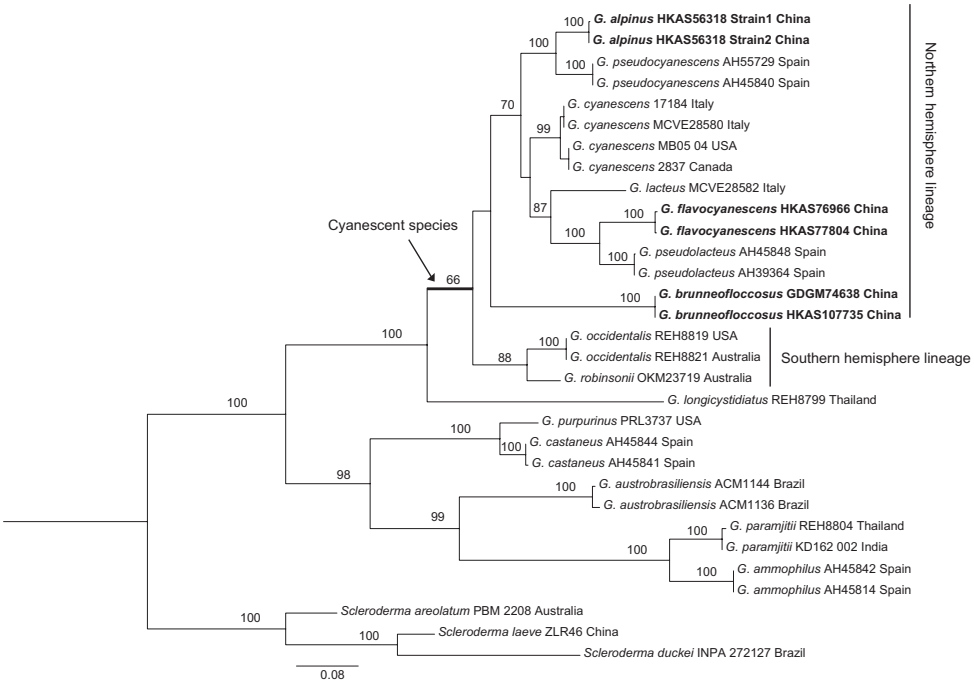

Figure 2. Maximum Likelihood phylogenetic tree of *Gyroporus* inferred from the combined (nrLSU + ITS) dataset. Bootstrap frequencies (> 50%) are shown above supported branches. Newly-sequenced collections are indicated in bold. Species vouchers and countries of origin are provided after the species name successively.

Yang, and one previously-described species, namely *G. brunneofloccosus*. The phylogenetic analysis of the combined (nrLSU + ITS) dataset also indicates that the Australian cyanescent *Gyroporus* species form an independent Southern Hemisphere lineage, while the other cyanescent species from the Northern Hemisphere form another lineage, yet without statistical bootstrap support, but its two main constituent sub-lineages also have high and moderate support (100% and 70%) (Fig. 2). The Chinese species *G. brunneofloccosus* forms one of the two well-supported (100%) sub-lineages, while the other species in Northern Hemisphere form another moderately supported (70%) sub-lineage. The newly-described species *G. alpinus* is closely related to *G. pseudocyanescens* G. Moreno, Carlavilla, Heykoop, Manjón & Vizzini, while *G. flavocyanescens* is closely related to *G. pseudolacteus* G. Moreno, Carlavilla, Heykoop, Manjón & Vizzini.

Taxonomy

***Gyroporus alpinus* Yan C. Li, C. Huang & Zhu L. Yang, sp. nov.**
MycoBank No: 838413
Figs 3a–c, 4

Etymology. The epithet *alpinus* refers to its distribution in alpine forests.

Type. China. Yunnan Province: Deqin, Shangri-La County, Haba Snow Mountain, Yang Fang, alt. 3800 m, 14 Aug 2008, Y.C. Li 1478 (KUN-HKAS 56318, GenBank accession numbers: MW149435 and MW149438 for ITS, MW151268 and MW151269 for nrLSU, MW452609 and MW452610 for *atp6*).

Diagnosis. This species differs from other cyanescent species of *Gyroporus* in its initially ivory yellow to greyish-yellow and then grey-orange to brownish-yellow pileus, scaly to floccose pileal surface, distribution in alpine forests with altitude up to 3800 m, broad basidiospores (5.5–8.5 μm wide) and long and slender basidia measuring 35–55 × 7–12 μm.

Description. Pileus 3–6 cm in diam., sub-hemispherical to convex or plano-convex, ivory yellow (4B3) to greyish-yellow (2B3–4) when young, grey-orange (5B5) to brownish-yellow (5C6–7) when mature; surface dry, densely covered with concolorous appressed scaly to floccose squamules, margin always incurved and slightly extended; context whitish (1A1), staining cerulean blue (23C6–7) to dull blue (23E5–6) when bruised. Hymenophore adnate when young, slightly depressed around apex of stipe when mature; surface white (1A1) when young and then cream to yellowish when mature, staining dull blue (23E5–6) when bruised; pores angular to roundish, fine, 2–3 per mm; tubes 3–8 mm long, whitish (1A1), staining dull blue when bruised. Stipe 6–8 × 1.8–2 cm, sub-cylindrical to clavate, white (2A1) when young, yellowish-white (2A2) to concolorous with pileal surface when mature; surface roughened, staining dull blue when bruised; context white to cream or yellowish, spongy when young and then hollow in age, staining cerulean blue to dull blue when bruised. Odour indistinct and taste mild.

Basidia 35–55 × 7–12 μm, clavate, 4-spored, hyaline in potassium hydroxide (KOH) and yellowish in Melzer's Reagent. Basidiospores [60/3/2] (6.5) 7–10 × 5.5–7.5 (8.5) μm, [Q = 1–1.65 (1.72), Q_m = 1.27 ± 0.23], smooth, ellipsoid to somewhat broadly ellipsoid, yellowish in KOH and primrose yellow in Melzer's Reagent. Cheilocystidia 30–60 × 8–14 μm, clavate to subfusiform, thin-walled, hyaline in KOH and yellowish to yellow in Melzer's Reagent; Pleurocystidia not observed. Tube trama composed of 6–11 μm wide interwoven hyphae, hyaline to yellowish in KOH, yellowish to brownish-yellow in Melzer's Reagent. Squamules on pileus composed of 10–17 μm wide interwoven hyphae, hyaline to yellowish in KOH, yellowish to brownish-yellow in Melzer's Reagent; terminal cells 80–120 × 12–17 μm, clavate to subcylindrical. Clamp connections frequently present in all tissues.

Additional specimen examined. China. Yunnan Province: Deqin, Shangri-La County, Baima Snow Mountain, alt. 3700 m, 11 Jul 1981, L.S. Wang 827 (KUN-HKAS 7756).

Habitat and distribution. Scattered on soil in alpine mixed forests dominated by *Abies* and *Picea* (Pinaceae) and *Quercus* (Fagaceae). Currently known from southwestern China.

Note. *Gyroporus alpinus* is characterised by the initially ivory yellow to greyish-yellow and then grey-orange to brownish-yellow pileus with scaly to floccose squamules, the slightly extended pileal margin, the white pileal context staining cerulean blue to dull blue when bruised, the white to cream or yellowish hymenophore staining dull

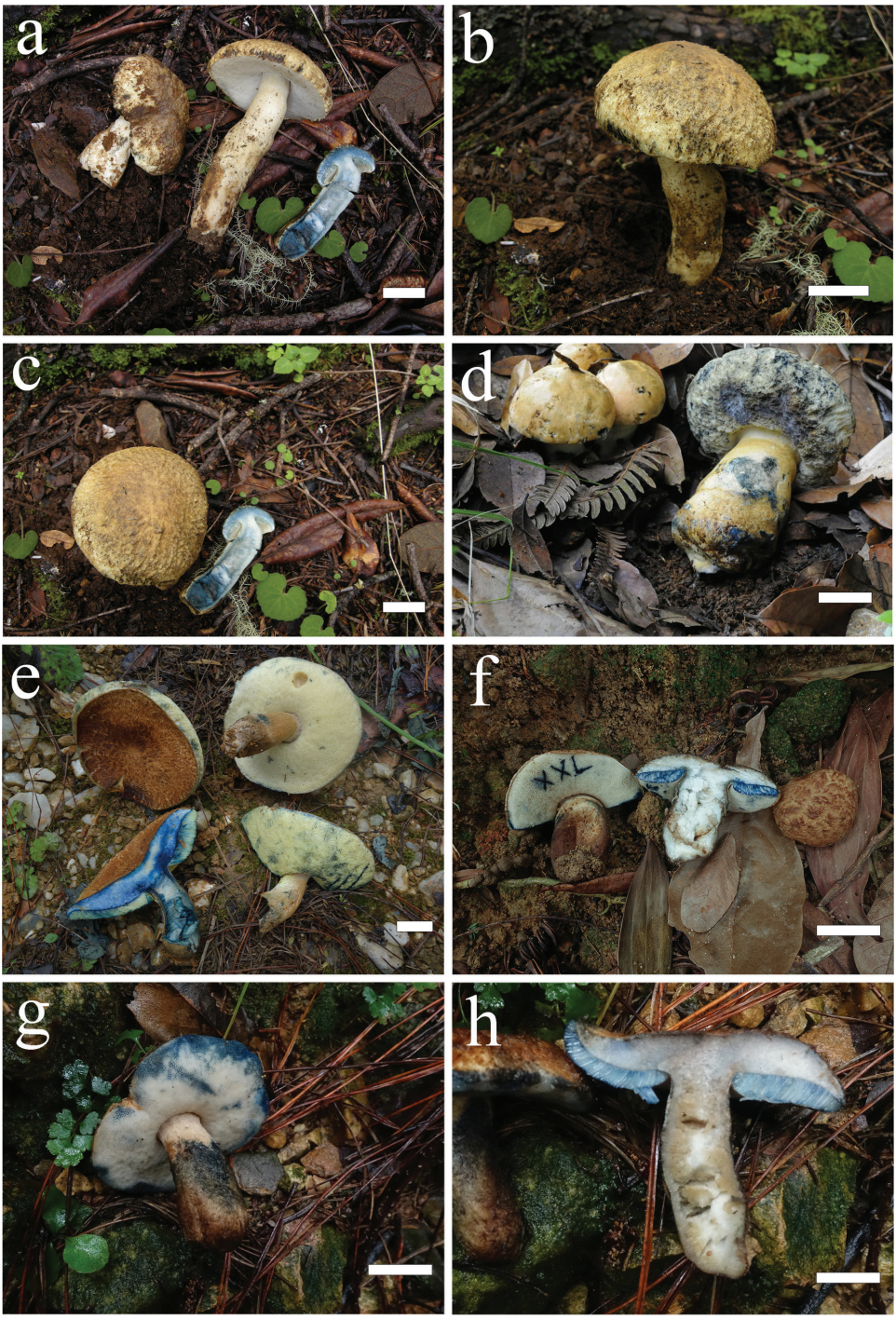

Figure 3. a–c *Gyroporus alpinus* (KUN-HKAS 56318, type, photos by Y.C. Li) **d** *Gyroporus flavocyanescens* (KUN-HKAS 76966, type, photo by X.L. Wu) **e–h** *G. brunneofloccosus* (**e** KUN-HKAS 107735, photo by G. Wu **f** GDGM 77125, photo by J.Y. Xu **g, h** GDGM 74638, photos by J.Y. Xu). Scale bars: 2 cm.

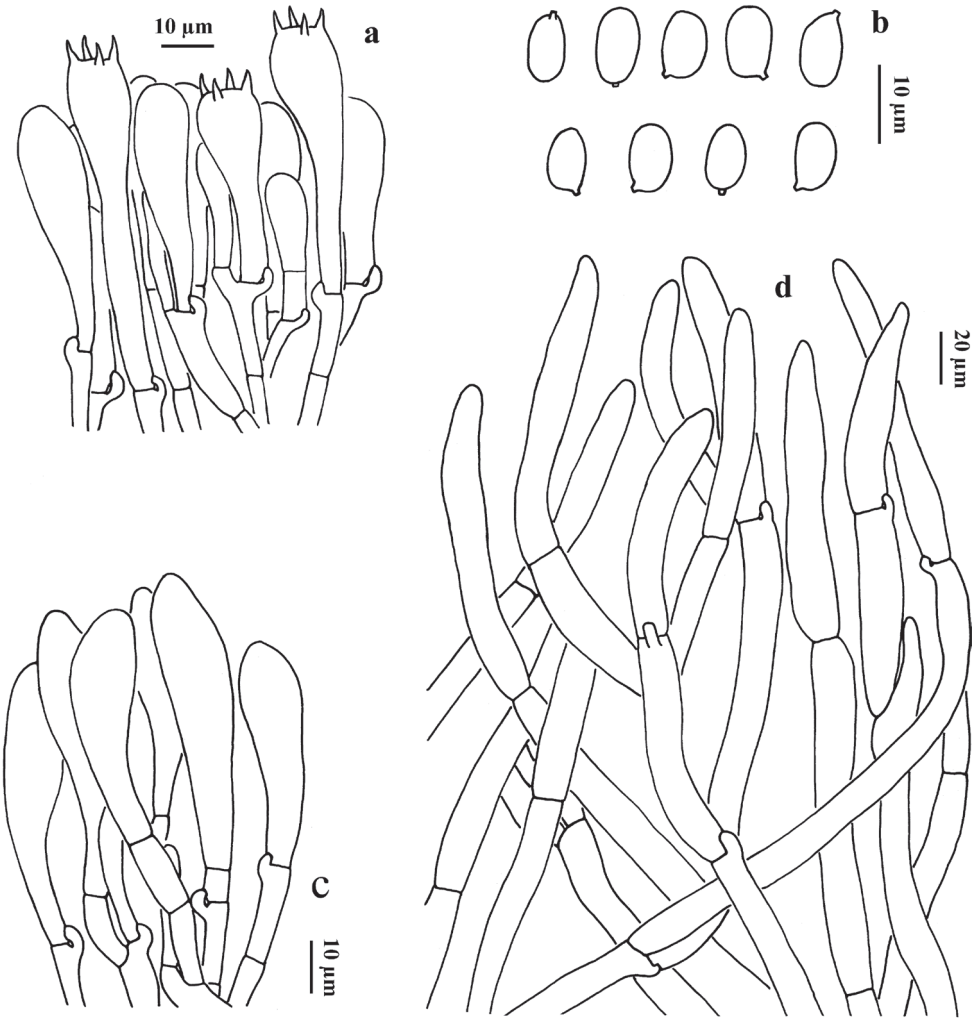

Figure 4. Microscopic features of *G. alpinus* (HKAS 56318, type) **a** basidia and cheilocystidium **b** basidiospores **c** cheilocystidia **d** pileipellis (squamules).

blue when bruised, the white to yellowish-white stipe, the spongy and then hollow context in the stipe, the frequent clamp connections in all tissues, the ellipsoid to somewhat broadly ellipsoid basidiospores and the distribution in alpine forests dominated by plants of the families Pinaceae and Fagaceae. In China, specimens of *G. alpinus* have been identified as *G. cyanescens* (Ying and Zang 1994; Zang 2013). Indeed, *G. alpinus* is closely related to *G. cyanescens* (Figs 1, 2). However, *G. cyanescens*, originally described from Europe, can be distinguished from *G. alpinus* by its relatively large basidiomata which are measuring 5.1–12.7 cm in diam., pale straw-coloured pileus, relatively narrow basidiospores measuring (7) 9–11 × 4.5–6 µm and distribution in forests dominated by *Pinus sylvestris* or *Fagus sylvatia* (Fries 1821; Watling 1970; Vizzini et al. 2015).

In our analysis of the *atp6* dataset, sequences of *G. alpinus* cluster together with sequences labelled as *G. cyanescens* from South Korea and Japan without statistical support (Fig. 1). Nagasawa (2001) treated the Japanese cyanescent taxon as *G. cyanescens* var. *violaceotinctus* Watling, because of the similar colours of their basidiomata and the similar-sized basidiospores. However, *G. cyanescens* var. *violaceotinctus*, originally described from Michigan, USA, is characterised by the white to tan context staining lilaceous and then indigo when bruised, the small basidia measuring 18–23.5 × 8–9 μm, the small cheilocystidia measuring 22.5–27.5 × 4.5–7.5 μm and the distribution in forests dominated by *Acer* (Aceraceae) and *Betula* (Betulaceae) (Watling 1969). These traits are greatly different from those of *G. cyanescens* and, therefore, Blanco-Dios (2018) treated *G. cyanescens* var. *violaceotinctus* as a novel species *G. violaceotinctus* (Watling) Blanco-Dios, while the Japanese taxon differs from *G. violaceotinctus* in its white context staining greyish-blue at first and then blackish-blue when bruised without any lilaceous or violaceous tint, relatively large basidia measuring 24–42 × 9–11 μm, two types of cheilocystidia with the slender type measuring 30–64 × 6–12 μm and the voluminious type measuring 18–55 × 15–20 μm and distributions in mixed forest dominated by *Fagus* (Fagaceae), *Quercus* (Fagaceae), *Betula* (Betulaceae), *Carpinus* (Betulaceae) and *Acer* (Aceraceae) (Nagasawa 2001). The Chinese *G. alpinus* can be distinguished from *G. violaceotinctus* and the Japanese taxon by the dimensions of its basidiospores and basidia, morphology of cheilocystidia and host plants.

Gyroporus alpinus is phylogenetically related and morphologically similar to *G. pseudocyanescens* originally described from Spain in Crous et al. (2017) in our analysis of the combined dataset (Fig. 2). However, *G. pseudocyanescens* has a strawish-cream to yellow cream and then more or less brownish to yellowish-brown pileus, a velutinous pileal surface often cracking at maturity, relatively narrow basidiospores measuring 8–11 × 4.5–6 (6.5) μm, short terminal cells of the hyphae on the surface of the pileus measuring 50–80 × 9–15 μm and a distribution in forests dominated by *Pinus* spp. or *Quercus* spp. (Crous et al. 2017).

Gyroporus brunneofloccosus T.H. Li, W.Q. Deng & B. Song, Fungal Diversity 12: 123 (2013), figs 1–3

Figs 3e–h, 5

Description. Pileus 6–9 cm in diam., hemispherical to sub-hemispherical when young, applanate to plano-convex when mature, dark brown (7E5–6) to brown (6E7–8) when young and brown to light red-brown (8E5–6) when mature; surface covered with concolorous floccose-scaly to coarsely tomentose squamules, always cracked with olivaceous yellow (2D5–6) background exposed when mature or aged, margin always extended; context white (1A1), staining cerulean blue (23C6–7) or greenish-blue (24B6–7) to dark blue (23F7–8) or deep blue (22E6–8) when bruised. Hymenophore adnate to obviously depressed around apex of stipe; surface yellowish (29B3) to

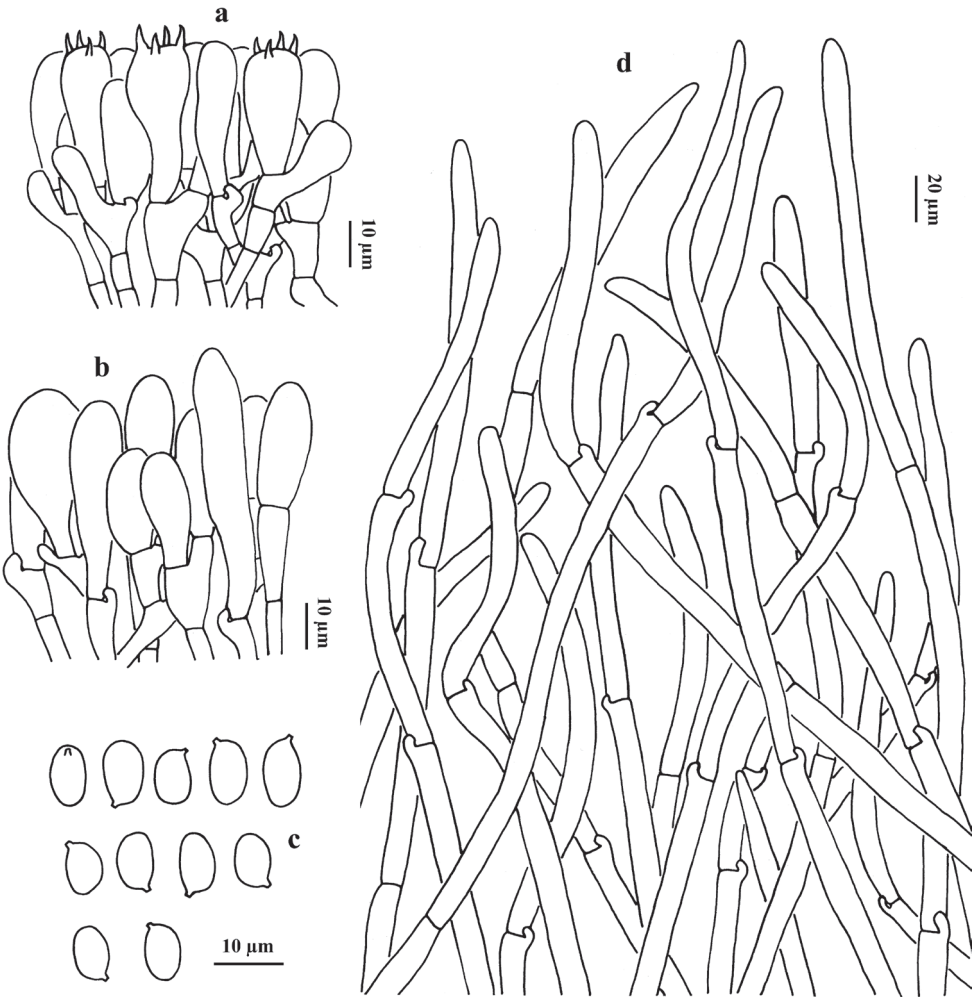

Figure 5. Microscopic features of *G. brunneofloccosus* (HKAS 107735) **a** basidia **b** cheilocystidia **c** basidiospores **d** pileipellis (squamules).

pale yellow (30B3) when young and then greenish-yellow (29B5–6) when mature or aged, staining cerulean blue to greenish-blue when bruised; pores angular to roundish, 1–2 per mm; tubes 3–9 mm long, concolorous with hymenophoral surface, staining cerulean blue to greenish-blue when bruised. Stipe 4.5–6 × 1–2 cm, subcylindrical to clavate, concolorous with pileal surface when mature, but much paler when young; surface covered with tomentose to fibrillose squamules; context white to cream, spongy then hollow when mature, staining cerulean blue to greenish-blue or dark blue to deep blue when bruised. Odour and taste indistinct.

Basidia 22–32 × 8–11 µm, clavate, 4-spored, hyaline in KOH, yellowish in Melzer's Reagent. Basidiospores [60/3/2] (8) 8.5–10 × 5–6 µm, ($Q = 1.42 – 1.90$, $Q_m = 1.62 \pm 0.11$) ellipsoid, smooth, hyaline to yellowish in KOH and primrose yellow to yellow-

ish-brown in Melzer's Reagent. Cheilocystidia 27–44 × 9–12 μm, clavate to subfusiform, thin-walled, hyaline in KOH and yellowish in Melzer's Reagent. Pleurocystidia not observed. Tube trama composed of 8–10 μm wide interwoven hyphae, hyaline in KOH, yellowish in Melzer's Reagent. Squamules on pileus composed of 7–10 μm wide interwoven hyphae, hyaline to yellowish in KOH, yellowish to brownish-yellow in Melzer's Reagent; terminal cells 80–180 × 8–10 μm, clavate to subcylindrical. Clamp connections frequently present in all tissues.

Specimens examined. China. Yunnan Province: Wenshan County, Malipo Village, alt. 1200 m, 14 Oct 2017, Wu 2644 (KUN-HKAS 107735, GenBank accession numbers: MW149436 for ITS, MW151267 for nrLSU, MW452611 for *atp6*). Guangdong Province: Zhaoqing County, Dinghu Shan Nature Reserve, alt. 200 m, 28 Aug 2018, J.Y. Xu (GDGM 74638, GenBank accession numbers: MW149437 for ITS, MW151266 for nrLSU); Shenzhen, Songzikeng Forest Park, alt. 70 m, 19 Jul 2019, J.Y. Xu (GDGM 77125).

Habitat and distribution. Scattered on soil in tropical forests dominated by *Castanopsis* (Fagaceae), *Quercus* (Fagaceae) and *Pinus* (Pinaceae). Currently known from southern and south-western China.

Discussion. *Gyroporus brunneofloccosus*, originally described from southern China, is characterised by the initially dark brown to brown and then brown to light red-brown pileus with concolorous floccose-scaly to coarsely tomentose squamules, the extended pileal margin, the white pileal context staining cerulean blue or greenish-blue to dark blue or deep blue when bruised, the initially yellowish to pale yellow and then greenish-yellow hymenophore staining cerulean blue to greenish-blue when bruised, the brownish to brown or light red-brown stipe, the spongy and then hollow context in the stipe, the frequent clamp connections in all tissues, the ellipsoid basidiospores and the distribution in tropical forests dominated by plants of the families Fagaceae and Pinaceae (Li et al. 2003).

In China, *G. brunneofloccosus* was misidentified as *G. cyanescens* by Bi et al. (1990, 1994), Ying and Zang (1994) and Mao (2000). However, these two species can be separated both by phylogenetic and morphological evidence. Our phylogenetic analysis of *atp6* data (Fig. 1) indicates that *G. brunneofloccosus* is closely related to *G. phaeocyanescens*. However, *G. phaeocyanescens*, originally described from Belize by Singer et al. (1983), has fulvous to snuff brown pileus and relatively large basidiospores measuring 9.3–14.7 × 5.3–6.7 μm (Singer et al. 1983; Li et al. 2003).

Gyroporus flavocyanescens **Yan C. Li, C. Huang & Zhu L. Yang, sp. nov.**
MycoBank No: 838414
Figs 3d, 6

Etymology. The epithet *flavocyanescens* refers to the flavous basidiomata with blue discolouration when bruised.

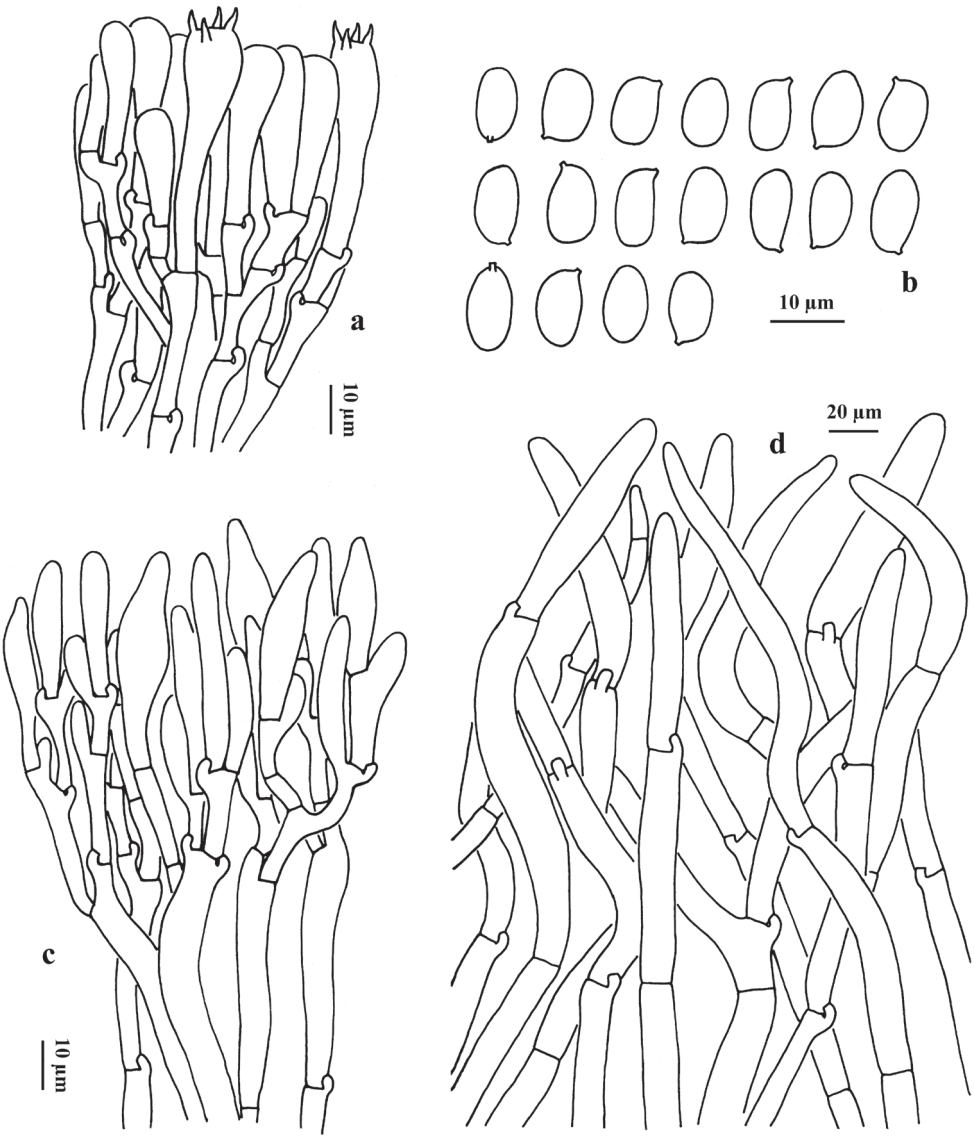

Figure 6. Microscopic features of *G. flavocyanescens* (KUN-HKAS 76966, type) **a** basidia **b** basidiospores **c** cheilocystidia **d** pileipellis (squamules).

Type. China. Guizhou Province: Pan County, alt. 1700 m, 2 Jul 2008, X.L. Wu 1182 (KUN-HKAS 76966, GenBank accession numbers: MW440550 for ITS, MW442950 for nrLSU, MW452613 for *atp6*).

Diagnosis. Differs from other cyanescent species in *Gyroporus* by its initially flavous to dull yellow or grey-yellow and then grey-orange to greyish-orange pileus, nearly glabrous or somewhat fibrillose to finely tomentose pileal surface, relatively small

basidia measuring 21–30 × 9–11 μm, slender basidiospores measuring 8–10 × (5) 5.5–6.5 μm and relatively short and slender chelocystidia measuring 26–35 × 5–9 μm.

Description. Pileus 6–10 cm in diam., hemispherical to sub-hemispherical when young, applanate to plano-convex when mature, flavous (3B3–4) to dull yellow or grey-yellow (2B4–5) when young, grey-orange (5B4–5) to greyish-orange (5B3–4) when mature; surface dry, nearly glabrous or somewhat fibrillose to finely tomentose, margin incurved and slightly extended; context whitish (1A1), staining strong dark blue or indigo-blue (24D4–8) when bruised. Hymenophore adnate when young, depressed around apex of stipe when mature; surface white (1A1) when young and then grey (1B1) to cream when mature, staining cyanine blue (24D4–6) to porcelain blue (23C5–6) when bruised; pores angular to roundish, 1–2 per mm; tubes 4–10 mm long, whitish (1A1), staining cyanine blue to porcelain blue when bruised. Stipe 4–6 × 2.5–4 cm, clavate, enlarged downwards; surface roughened, white to cream when young and then pale yellow (2A3–5) to concolorous with pileal surface when mature or aged; context white to cream or yellowish, spongy when young and then hollow in age, staining cyanine blue to porcelain blue when bruised. Odour indistinct and taste mild.

Basidia 21–30 × 9–11 μm, clavate, hyaline in KOH and yellowish in Melzer's Reagent, 4-spored. Basidiospores [60/3/2] 8–10 × (5) 5.5–6.5 μm, (Q = 1.45–1.81, Q_m = 1.59 ± 0.12), smooth, ellipsoid to somewhat broadly ellipsoid, hyaline to yellowish in KOH and primrose yellow to yellow in Melzer's Reagent. Cheilocystidia 26–35 × 5–9 μm, clavate to subfusiform, thin-walled, hyaline in KOH and yellowish to yellow in Melzer's Reagent. Pleurocystidia not observed. Tube trama composed of 5–9 μm wide interwoven hyphae, hyaline to yellowish in KOH, yellowish to brownish-yellow in Melzer's Reagent. Squamules on pileus composed of 8–17 μm wide interwoven hyphae, hyaline to yellowish in KOH, yellowish to brownish-yellow in Melzer's Reagent; terminal cells 90–140 × 9–17 μm, clavate to subcylindrical. Clamp connections frequently present in all tissues.

Additional specimen examined. China. Guizhou Province: Pan County, alt. 1700 m, 2 Jul 2008, X.L. Wu 1187 (KUN-HKAS 77804, GenBank accession numbers: MW440551 for ITS, MW442951 for nrLSU).

Habitat and distribution. Scattered on soil in the tropical forests dominated by *Castanea* sp. (Fagaceae) and *Quercus* sp. (Fagaceae). Currently known from southwestern China.

Note. *Gyroporus flavocyanescens* is characterised by the flavous to dull yellow or grey-yellow and then grey-orange to greyish-orange pileus, the nearly glabrous to fibrillose to finely tomentose pileal surface, the slightly extended pileal margin, the white pileal context staining strong dark blue or indigo-blue when bruised, the white to grey or cream to yellowish hymenophore staining cyanine blue to porcelain blue when bruised, the white to cream and then pale yellow to flavous stipe, the spongy and then hollow context in the stipe, the frequent clamp connections in all tissues, the ellipsoid to somewhat broadly ellipsoid basidiospores and the distribution in tropical forests dominated by plants of the family Fagaceae.

Gyroporus flavocyanescens is morphologically similar to *G. lacteus* and *G. pseudolacteus*. Indeed, they are phylogenetically related to each other, based on our analysis of combined nrLSU + ITS dataset (Fig. 2), though it should be noted that the bootstrap support is relatively low for the relationship with *G. lacteus* (87%). *Gyroporus lacteus* has large basidiomata (9–17 cm in diam.), ochraceous pileus with scaly tomentose squamules and large cheilocystidia up to 50 × 10 µm (Vizzini et al. 2015). *Gyroporus pseudolacteus* has a whitish to cream white and then more or less yellowish-ochre pileus, relatively large basidia measuring 35–43 × 10–14 µm and large cheilocystidia measuring 35–55 × 8–12 µm (Crous et al. 2017).

In this study, three cyanescent species of *Gyroporus* from China could be recognised and identified. For the convenience of identification of the species, a key is given below.

Key to cyanescent *Gyroporus* species in China

1 Pileus dark brown, brown to light red-brown, without any yellow or orange tinge; squamules on pileus composed of 7–10 µm wide interwoven hyphae.. ..... ***G. brunneofloccosus***

– Pileus ivory yellow to greyish-yellow or flavous to grey-yellow and then grey-orange to brownish-yellow, without brown tinge; squamules on pileus composed of broad interwoven hyphae up to 17 µm wide..... **2**

2 Basidioma distributed in alpine mixed forests dominated by *Abies* sp., *Picea* sp. and *Quercus semicarpifolia*; pileus small to medium-sized 3–6 cm wide, ivory yellow to greyish-yellow and then grey-orange to brownish-yellow, surface with scaly to floccose squamules; cheilocystidia 30–60 × 8–14 µm, clavate to subfusiform; basidia 35–55 × 7–11.5 µm ..... ***G. alpinus***

– Basidioma distributed in tropical forests dominated by *Castanea* sp. and *Quercus* sp.; pileus large 6–10 cm wide, flavous to dull yellow or grey-yellow and then grey-orange to greyish-orange, surface nearly glabrous or somewhat fibrillose to finely tomentose; cheilocystidia relatively small measuring 26–35 × 5–9 µm; basidia relatively short measuring 21–30 × 9–11 µm..... ***G. flavocyanescens***

Discussion

Cyanescent *Gyroporus* species in the Southern Hemisphere form independent lineages in the analyses of *atp6* and combined nrLSU + ITS datasets (Figs 1, 2) and mainly associate with plants of the family Myrtaceae, while the cyanescent species in the Northern Hemisphere also form independent lineages, but without or with low statistical bootstrap support in the analyses of the combined and *atp6* datasets and mainly associate with plants of the families Fagaceae and Pinaceae. Davoodian et al. (2020) suggest that the Southern Hemisphere lineage is derived from the Northern Hemisphere lineage, within which the Southern Hemisphere lineage is embedded. Further field investigations, careful morphological observations and extensive molecular analysis using

multiple genes should help better understand the geographical relationships amongst the cyanescent species.

Sixteen cyanescent *Gyroporus* species were revealed, based on former and present studies, including nine distributed in the Northern Hemisphere and seven distributed in the Southern Hemisphere. Three cyanescent *Gyroporus* have been reported from China before our study, namely *G. cyanescens*, *G. brunneofloccosus* and *G. pseudomicrosporus* (Zang 1986, 2013; Bi et al. 1990, 1994; Ying and Zang 1994; Mao 2000; Li et al. 2003). *Gyroporus cyanescens* was regarded as geographically widespread in Europe, North America and East Asia in the past. Our study identified the disjunct populations of this taxon in Europe and North America, but its distribution in China has not been found yet. The specimens from China labelled "*G. cyanescens*" are either *G. alpinus* or *G. flavocyanescens*. *Gyroporus pseudomicrosporus*, originally described from China by Zang (1986), is characterised by the cyanescent discolouration when bruised, the decurrent hymenophore, the short tubes measuring 2–4 mm long, the eccentric stipe and the small ellipsoid to ovoid basidiospores. These traits match well with those of the genus *Gyrodon* Opat. In conclusion, there are still three cyanescent species in China, but they are *G. alpinus*, *G. brunneofloccosus* and *G. flavocyanescens*.

Acknowledgements

The authors are grateful to Prof. Tai-Hui Li (Guangdong Institute of Microbiology) for his kind assistance in the identification of the species in this genus. The project was supported by the International Partnership Program of Chinese Academy of Sciences (151853KYSB20170026), the National Natural Science Foundation of China (Nos. 32070024, 31750001, 31872618), the Natural Science Foundation of Yunnan Province (2018FB027), the Ten Thousand Talents Program of Yunnan (YNWR-QNBJ-2018-125), the Key Research Program of Frontier Sciences, CAS (QYZDY-SSW-SMC029), the Biodiversity Survey and Assessment Project of the Ministry of Ecology and Environment, China (2019HJ2096001006) and the Science and Technology Project of Guangdong Province (2019B121202005).

References

Blanco-Dios JB (2018) Notas nomenclaturales en los Órdenes Agaricales y Boletales. Tarrelos 20: 28–31.

Bi ZS, Zheng GY (1990) Macrofungus Flora of the Mountainous District of North Guangdong. Guangdong Science and Technology Press, Guangdong, 450 pp. [in Chinese] http://www.ziliaoh.com/zrkx/swkx/ybsq.html

Bi ZS, Zheng GY, Li TH (1994) Macrofungus Flora of Guangdong Province. Guangdong Science and Technology, Guangdong, 879 pp. [in Chinese] https://book.ixueshu.com/book/bf3d5f8d7bd973ed.html

Binder M, Bresinsky A (2002) Derivation of a polymorphic lineage of gasteromycetes from boletoid ancestors. Mycologia 94: 85–98. https://doi.org/10.1080/15572536.2003.11833251

Bulliard JBF (1788) Herbier de la France, 8. Chez l'auteur, Paris, 328 pp. https://core.ac.uk/display/19616989

Crous PW, Wingfield MJ, Burgess TI, Hardy GESTJ, Barber PA, Alvarado P, Barnes CW, Buchanan PK, Heykoop M, Moreno G, Thangavel R, van der Spuy S, Barili A, Barrett S, Cacciola SO, Cano-Lira JF, Crane C, Decock C, Gibertoni TB, Guarro J, Guevara-Suarez M, Hubka V, Kolařík M, Lira CRS, Ordoñez ME, Padamsee M, Ryvarden L, Soares AM, Stchigel AM, Sutton DA, Vizzini A, Weir BS, Acharya K, Aloi F, Baseia IG, Blanchette RA, Bordallo JJ, Bratek Z, Butler T, Cano-Canals J, Carlavilla JR, Chander J, Cheewangkoon R, Cruz RHSF, da Silva M, Dutta AK, Ercole E, Escobio V, Esteve-Raventós F, Flores JA, Gené J, Góis JS, Haines L, Held BW, Jung MH, Hosaka K, Jung T, Jurjević Ž, Kautman V, Kautmanova I, Kiyashko AA, Kozanek M, Kubátová A, Lafourcade M, La Spada F, Latha KPD, Madrid H, Malysheva EF, Manimohan P, Manjón JL, Martín MP, Mata M, Merényi Z, Morte A, Nagy I, Normand AC, Paloi S, Pattison N, Pawłowska J, Pereira OL, Petterson ME, Picillo B, Raj KNA, Roberts A, Rodríguez A, Rodríguez-Campo FJ, Romański M, Ruszkiewicz-Michalska M, Scanu B, Schena L, Semelbauer M, Sharma R, Shouche YS, Silva V, Staniaszek-Kik M, Stielow JB, Tapia C, Taylor PWJ, Toome-Heller M, Vabeikhokhei JMC, van Diepeningen AD, Van Hoa N, Van Tri M, Wiederhold NP, Wrzosek M, Zothanzama J, Groenewald JZ (2017) *Gyroporus pseudocyanescens* sp. nov. Fungal Planet 598. Persoonia 38: 328–329. https://doi.org/10.3767/003158517X698941

Crous PW, Wingfield MJ, Burgess TI, Hardy GESTJ, Crane C, Barrett S, Cano-Lira JF, Le Roux JJ, Thangavel R, Guarro J, Stchigel AM, Martin MP, Alfredo DS, Barber PA, Barreto RW, Baseia IG, Cano-Canals J, Cheewangkoon R, Ferreira RJ, Gene J, Lechat C, Moreno G, Roets F, Shivas RG, Sousa JO, Tan YP, Wiederhold NP, Abell SE, Accioly T, Albizu JL, Alves JL, Antoniolli ZI, Aplin N, Araujo J, Arzanlou M, Bezerra JDP, Bouchara JP, Carlavilla JR, Castillo A, Castroagudin VL, Ceresini PC, Claridge GF, Coelho G, Coimbra VRM, Costa LA, da Cunha KC, da Silva SS, Daniel R, de Beer ZW, Duenas M, Edwards J, Enwistle P, Fiuza PO, Fournier J, Garcia D, Gibertoni TB, Giraud S, Guevara-Suarez M, Gusmao LFP, Haituk S, Heykoop M, Hirooka Y, Hofmann TA, Houbraken J, Hughes DP, Kautmanova I, Koppel O, Koukol O, Larsson E, Latha KPD, Lee DH, Lisboa DO, Lisboa WS, Lopez-Villalba A, Maciel JLN, Manimohan P, Manjon JL, Marincowitz S, Marney TS, Meijer M, Miller AN, Olariaga I, Paiva LM, Piepenbring M, Poveda-Molero JC, Raj KNA, Raja HA, Rougeron A, Salcedo I, Samadi R, Santos TAB, Scarlett K, Seifert KA, Shuttleworth L, Silva GA, Silva M, Siqueira JPZ, Souza-Motta CM, Stephenson SL, Sutton DA, Tamakeaw N, Telleria MT, Valenzuela-Lopez N, Viljoen A, Visagie CM, Vizzini A, Wartchow F, Wingfield BD, Yurchenko E, Zamora JC, Groenewald JZ (2016) *Gyroporus pseudolacteus* sp. nov. Fungal Planet 479. Persoonia 37: 246–247. https://doi.org/10.3767/003158516X694499

Cui YY, Cai Q, Tang LP, Liu JW, Yang ZL (2018) The family Amanitaceae: molecular phylogeny, higher–rank taxonomy and the species in China. Fungal Diversity 91: 5–230. https://doi.org/10.1007/s13225-018-0405-9

Davoodian N, Bergemann SE, Hosaka K, Raspé O, Bougher NL, Fechner NA, Henkel TW, Gelardi M, Soytong K, Naseer A, Ortiz-Santana B, Baroni TJ, Nagasawa E, Smith ME, Halling RE (2018) A global view of *Gyroporus*: molecular phylogenetics, diversity patterns, and new species. Mycologia 110: 985–995. https://doi.org/10.1080/00275514.2018.1511339

Davoodian N, Bougher NL, Fechner NA, Bergemann SE, Halling RE (2019) Three new species of *Gyroporus* (Boletales, Basidiomycota) from Australia. Muelleria 37: 101–107.

Davoodian N, Hosaka K, Raspé O, Bougher NL, Fechner NA, Henkel TW, Gelardi M, Soytong K, Naseer A, Ortiz-Santana B, Baroni TJ, Nagasawa E, Smith ME, Halling RE (2020) Diversity of *Gyroporus* (Gyroporaceae, Boletales): rpb2 phylogeny and three new species. Phytotaxa 434(3): 208–218. https://doi.org/10.11646/phytotaxa.434.3.2

Doyle JJ, Doyle JL (1987) A rapid DNA isolation procedure for small quantities of fresh leaf material. Phytochemical Bulletin 19: 11–15. https://worldveg.tind.io/record/33886/

Das K, Chakraborty D, Vizzini A (2017) Morphological and phylogenetic evidences unveil a novel species of *Gyroporus* (Gyroporaceae, Boletales) from Indian Himalaya. Nordic Journal of Botany 35: 669–675. https://doi.org/10.1111/njb.01628

Fries EM (1821) Systema Mycologicum I. Mauritius, Gryphiswaldiae, 520 pp. https://www.biodiversitylibrary.org/bibliography/71698

Gelardi M, Angelini C, Costanzo F, Dovana F, Ortiz-Santana B, Vizzini A (2019) *Neoboletus antillanus* sp. nov. (Boletaceae), first report of a red-pored bolete from the Dominican Republic and insights on the genus *Neoboletus*. MycoKeys 49: 73–97. https://doi.org/10.3897/mycokeys.49.33185

Hall TA (1999) BioEdit: a user-friendly biological sequence alignment editor and analyses program for Windows 95/98/NT. Nucleic Acids Symposium Series 41: 95–98. https://doi.org/10.1021/bk-1999-0734.ch008

Katoh K, Standley DM (2013) MAFFT multiple sequence alignment software version 7: Improvements in performance and usability. Molecular Biology and Evolution 30: 772–780. https://doi.org/10.1093/molbev/mst010

Kirk PM, Cannon PF, Minter DW, Stalpers JA (2008) Dictionary of the Fungi (10th edn.). CABI Publishing, Wallingford, 771 pp. https://doi.org/10.1038/191109b0

Kornerup A, Wanscher JH (1981) Taschenlexikon der Farben, 3rd edn. Muster-Schmidt Verlag, Göttingen, 243 pp. https://doi.org/10.1002/lipi.19640660234

Léveillé JH (1848) Fragments mycologiques. Annales des Sciences Naturelles Botanique 9: 119–144. https://nbn-resolving.org/urn/resolver.pl?urn:nbn:de:hebis:30-1039071

Li TH, Deng WQ, Song B (2003) A new cyanescent species of *Gyroporus* from China. Fungal Diversity 12: 123–127. https://www.fungaldiversity.org/fdp/sfdp/FD12-123-127.pdf

Li YC (2007) Two noteworthy boletes from China. Mycotaxon 101: 223–228. http://ir.kib.ac.cn:8080/handle/151853/14025

Liu HY, Li YC, Bau T (2020) New species of *Retiboletus* (Boletales, Boletaceae) from China based on morphological and molecular data. MycoKeys 67: 33–44. https://doi.org/10.3897/mycokeys.67.51020

Magnago AC, Alves-Silva G, Neves MA, Mara BDSR (2018) A new species of *Gyroporus* (Gyroporaceae, Boletales) from Atlantic forest in southern Brazil. Nova Hedwigia 107: 291–301. https://doi.org/10.1127/nova_hedwigia/2018/0471

Mao XL (2000) The Macrofungi in China. Henan Science and Technology Press, Zhengzhou, 719 pp. [in Chinese] https://book.douban.com/subject/1433850/

Murrill W (1939) Additions to Florida Fungi-I. Bulletin of the Torrey Botanical Club 66: 29–37. https://doi.org/10.2307/2481013

Naseer A, Garrido-Benavent I, Khan J, Ballarà J, Sher H (2020) *Cortinarius pakistanicus* and *C. pseudotorvus*: two new species in oak forests in the Pakistan Himalayas. MycoKeys 74: 91–108. https://doi.org/10.3897/mycokeys.74.49734

Quélet L (1886) Enchiridion fungorum in Europa media et praesertim in Gallia vigentium. Paris. https://doi.org/10.5962/bhl.title.47025

Singer R (1986) The Agaricales in modern taxonomy, 4th edn. Koenigstein, Germany, 981 pp. https://doi.org/10.2307/1219523

Singer R, Araujo I, Ivory MH (1983) The ectotrophically mycorrhizal fungi of the neotropical lowlands, especially central Amazonia. Beihefte zur Nova Hedwigia 77: 1–352. https://www.cabdirect.org/cabdirect/abstract/19841394943

Stamatakis A, Hoover P, Rougemont J (2008) A rapid bootstrap algorithm for the RAxML web-servers. Systematic Biology 75: 758–771. https://doi.org/10.1080/10635150802429642

Vizzini A, Angelini C, Ercole E (2015) Molecular confirmation of *Gyroporus lacteus* and typification of *Boletus cyanescens*. Phytotaxa 226: 27–38. https://doi.org/10.11646/phytotaxa.226.1.3

Watling R (1969) New fungi from Michigan. Notes from the Royal Botanical Garden Edinburgh 29(1): 59–66. https://agris.fao.org/agris-search/search.do?recordID=US201301225502

Watling R (1970) Boletaceae, Gomphidiaceae and Paxillaceae. In: Henderson DM, Orton PD, Watling R (Eds) British Fungus flora: agarics and boleti, vol. 1. Royal Botanic Garden, Edinburgh, 45–57. https://www.cabdirect.org/cabdirect/abstract/19711101112

White TJ, Bruns T, Lee S, Taylor JW (1990) Amplification and direct sequencing of fungal ribosomal RNA genes for phylogenetics. In: PCR Protocols: a guide to methods and applications. Academic Press, New York, 315–322. https://doi.org/10.1016/B978-0-12-372180-8.50042-1

Wilson AW, Binder M, Hibbett DS (2012) Diversity and evolution of ectomycorrhizal host associations in the Sclerodermatineae (Boletales, Basidiomycota). New Phytologist 194: 1079–1095. https://doi.org/10.1111/j.1469-8137.2012.04109.x

Ying JZ, Zang M (1994) Economic Macrofungi from South-western China. Science Press, Beijing, 422 pp. [in Chinese] https://book.ixueshu.com/book/a3f03cd59a016ac3.html

Zang M (1986) Notes on the Boletales from eastern Himalayas and adjacent of China (2). Acta Botannica Yunnanica 8: 1–22. http://ir.kib.ac.cn:8080/handle/151853/11467

Zang M, Li B, Xi J (1996) Fungi of the Hengduan Mountains. Science Press, Beijing, 348 pp. [in Chinese] http://m.tushu007.com/ISBN-9787030050670.html

MycoKeys 81: 185–204 (2021)
doi: 10.3897/mycokeys.81.68485
https://mycokeys.pensoft.net

RESEARCH ARTICLE

A peer-reviewed open-access journal
MycoKeys
Launched to accelerate biodiversity research

Two new toxic yellow *Inocybe* species from China: morphological characteristics, phylogenetic analyses and toxin detection

Sai Nan Li[1*], Fei Xu[2*], Ming Jiang[1], Feng Liu[2], Fang Wu[1,3], Ping Zhang[1], Yu Guang Fan[4], Zuo Hong Chen[1]

1 *College of Life Sciences, Hunan Normal University, Changsha, Hunan 410006, China* **2** *Ningxia Center for Disease Control and Prevention, Yinchuan, Ningxia 750004, China* **3** *Hunan Edible Fungal Research Institute, Changsha, Hunan 410013, China* **4** *Key Laboratory of Tropical Translational Medicine of Ministry of Education, Hainan Medical University, Haikou, Hainan 571199, China*

Corresponding authors: Yu Guang Fan (fan@hainmc.edu.cn), Zuo Hong Chen (chenzuohong@263.net)

Academic editor: Marc Stadler | Received 13 May 2021 | Accepted 30 June 2021 | Published 3 August 2021

Citation: Li SN, Xu F, Jiang M, Liu F, Wu F, Zhang P, Fan YG, Chen ZH (2021) Two new toxic yellow *Inocybe* species from China: morphological characteristics, phylogenetic analyses and toxin detection. MycoKeys 81: 185–204. https://doi.org/10.3897/mycokeys.81.68485

Abstract

Some species of *Inocybe s. str.* caused neurotoxic poisoning after consumption around the world. However, there are a large number of species in this genus that have not been studied for their toxicity or toxin content. In this study, we report two new toxic yellow *Inocybe s. str.* species from China based on morphological characteristics, phylogenetic analyses and toxin detection. Among the two species, *Inocybe squarrosolutea* is reported as a newly recorded species of China. We also describe a new species, *I. squarrosofulva*, which is morphologically similar to *I. squarrosolutea*. The new species is characterized by its ochraceous squarrose pileus, distinctly annulate cortina on the stipe, nodulose basidiospores and thick-walled pleurocystidia. Muscarine in the fruitbodies was detected by UPLC–MS/MS, the content in *I. squarrosolutea* and *I. squarrosofulva* were 136.4 ± 25.4 to 1683.0 ± 313 mg/kg dry weight and 31.2 ± 5.8 to 101.8 ± 18.9 mg/kg dry weight, respectively.

Keywords

Inocybaceae, muscarine, taxonomy

* Authors contributed equally to this work.

Introduction

The genus *Inocybe* (Fr.) Fr. was established as a "tribe" of *Agaricus* (Fries 1821) and treated as a genus in 1863 (Fries 1863). Recent studies elevated it to the family rank, known as the Inocybaceae (Matheny 2005, 2009; Matheny et al. 2020). The present Inocybaceae (*Inocybe* sensu lato) is composed of seven genera, namely *Auritella*, *Inosperma*, *Mallocybe*, *Nothocybe*, *Pseudosperma*, *Tubariomyces*, and *Inocybe* sensu stricto. *Inocybe s. str.* with about 850 species, turns out to be the largest genus (Matheny et al. 2020), and novel species have continued to be discovered in recent years (Bandini et al. 2020a, 2020b; Fan and Bau 2020; Caiafa 2021; Mešić et al. 2021). Studies on Inocybaceae in China started in the 20th century. From Deng (1963) first reported 15 species of *Inocybe s. l.* Until 2020 about 140 species of Inocybaceae had been reported, of which about 120 belong to *Inocybe s. str*. (Fan and Bau 2010, 2013, 2014a, 2014b, 2017, 2018, 2020; Fan et al. 2013, 2018). Wang (1979) described a new species, *I. flavobrunnea*, which was the first new species of *Inocybe s. str*. in China. After that, Fan et al. have described seven new species of *Inocybe s. str.* in China from 2013 to 2020 (Fan and Bau 2013, 2014a, 2014b, 2020; Fan et al. 2018).

Autonomic toxicity disorder, caused by the ingestion of *Inocybe s. l.* spp., is an important type of neurotoxic mushroom poisoning. Muscarine is the principal toxin in *Inocybe s. l.* (Chen et al. 2016; White et al. 2018). Based on a review of the literature and their own work on toxin detection, Kosentka et al. (2013) reported whether or not muscarine is present in 98 species of Inocybaceae from 1960 to 2013, including 73 species of *Inocybe s. str*. Of these 73 taxa, 57 have been reported to contain muscarine. In China, about 21 species of *Inocybe s. str.* are considered poisonous (Mao 2006; Bau et al. 2014; Xu et al. 2020). However, only three species (*I. asterospora*, *I.* aff. *ericetorum*, *I. serotina*) of *Inocybe s. str.*, causing typically muscarinic poisoning incidents, could be identified as containing muscarine (Chen et al. 1987; Xu et al. 2020; Li et al 2021). Among them, *I. asterospora* and *I.* aff. *ericetorum* are new toxic *Inocybe* species reported in China. In summary, toxins have only been reported for 75 species of *Inocybe s. str.*, and ca. 7% (59 of 850) have been identified as muscarine-containing poisonous mushrooms. Hence, the toxicity of a large number of *Inocybe s. str.* species is still unknown.

In this study, we 1) report *I. squarrosolutea* as a newly recorded species of China, and redescribed this species based on Chinese materials; 2) describe a new species of *Inocybe s. str.*, based on morphological and phylogenetic evidence; and 3) characterize the muscarine content of these two species by UPLC–MS/MS.

Materials and methods

Specimen collection and drying treatment

Most other specimens were collected from Hunan Province; only one specimen was collected from Huang Mountain, Anhui Province. The fresh basidiomata were dried

using an electric dryer EVERMAT operated at 45 °C for 10 h. The dried specimens, along with the holotype of the newly described species, were deposited in the Mycological Herbarium of Hunan Normal University (**MHHNU**), Changsha, China. A small piece of fresh basidioma was also dried with silica gel for molecular analysis.

Morphological studies

Specimens were photographed in situ using a Sony digital camera (LICE-7, Sony, Tokyo, Japan). The macromorphological characters of fresh mushrooms were recorded as soon as possible after collection. Color codes were described following Kornerup and Wanscher (1978). Microscopic structures were studied from dried materials mounted in 5% aqueous KOH, and Congo red was used as a stain when necessary. All the measurements were performed at 1000× magnification, and a minimum of 20–30 basidiospores from each basidioma were measured in side view. Micromorphological investigations were performed by means of a Nikon Eclipse 50i microscope (Nikon, Tokyo, Japan). The measurement methods followed those of Fan et al. (2013). Dimensions of basidiospores and Q values were given as (a) b–c (d), where "b–c" cover a minimum of 90% of the measured values, and "a" and "d" represent extreme values; Q is the ratio of length to width in an individual basidiospore. Qm is the average Q of all basidiospores ± sample standard deviation. The descriptive terms are in accordance with Fan and Bau (2020), Horak et al. (2015), and Matheny et al. (2012). SEM images of basidiospores were obtained using a scanning electron microscope JSM-6380LV (JEOL Ltd., Tokyo, Japan).

DNA extraction, amplification, and sequencing

DNA was extracted from dried basidiomata using a fungal DNA extraction kit manufactured by Omega Bio-Tek (Norcross, GA, USA). The following primer pairs were used for PCR amplification and sequencing: ITS5 and ITS4 for the internal transcribed spacer (ITS) region (White et al. 1990); LR0R and LR5 for the nuclear ribosomal large subunit (nrLSU) region (Vilgalys and Hester 1990); and bRPB2-6F and bRPB2-7.1R for RNA polymerase II second largest subunit (*rpb2*) region (Matheny 2005). PCR protocols for ITS and nrLSU were as described in White et al. (1990), and for *rpb2*, as described in Matheny (2005). PCR products were purified and sequenced by TsingKe Biological Technology Co., Ltd. (Beijing, China).

Sequence alignment and phylogenetic analyses

Thirty-six sequences (12 for ITS, 12 for nrLSU and 12 for *rpb2*) were newly generated for this study and deposited in GenBank (Table 1). The new sequences were subjected to a BLAST search and relevant related sequences retrieved from GenBank (Table1).

The sequences were aligned using MAFFT v7.310 (Katoh and Standley 2013) and manually edited using BioEdit v7.0.5 (Hall 1999). Maximum likelihood (ML) analysis

Table 1. DNA sequences used in this study and their voucher specimen number, geographic origin, toxin status, and GenBank accession numbers.

Species	Voucher	Locality	Muscarine	ITS	nrLSU	*rpb2*	References
Inocybe acriolens	AU10493	Canada	?	NR_153186	NG_057291	N/A	Type material
	JCS071005D	USA	?	N/A	JN974981	MH577492	Unpublished
I. albodisca	PBM1390	USA	–	N/A	EU307819	EU307821	Kropp and Albee-Scott (2010)
I. alienospora	PBM3743	Australia	?	KP171104	KM197209	KM245970	Latha and Manimohan (2017)
	REH9667	Australia	?	KP171105	KM197210	KM245971	Unpublished
I. chelanensis	PBM491	USA	?	N/A	AY239020	AY337368	Matheny (2005)
	PBM2314	USA	?	N/A	AY239021	AY337369	Matheny (2005)
I. giacomi	CLC1321	USA	?	N/A	MK153655	N/A	Unpublished
	JV21543	Sweden	?	N/A	MK153656	N/A	Unpublished
	EL80-12	Sweden	?	N/A	MK153657	N/A	Unpublished
I. grammata	PBM2602	USA	–	N/A	JN974977	N/A	Unpublished
	PBM2558	USA	–	N/A	JQ313562	N/A	Unpublished
	2012038	China	–	N/A	KU764690	N/A	Fan and Bau (2017)
I. hydrocybiformis	TBGT:12318	India	?	KP171130	KP170911	KM245987	Latha and Manimohan (2017)
	ZT10077	Thailand	?	GQ893016	GQ892971	N/A	Unpublished
I. lasseroides	PBM3749	Australia	?	KP171145	KP170924	KM245993	Latha and Manimohan (2017)
	PBM3750	Australia	?	KP171146	KP170925	N/A	Unpublished
I. papilliformis	TBGT:10480	India	?	KP171131	KP170912	KM245988	Latha and Manimohan (2017)
	CAL1372	India	?	KY440096	KY549126	N/A	Latha and Manimohan 2017
I. relicina	JV10258	Finland	?	N/A	AY038324	AY333778	Matheny (2005)
	EL2-05	Sweden	?	N/A	MN296111	N/A	Unpublished
I. sierraensis	DED6101	USA	?	N/A	AY239025	MH249810	Kropp and Matheny (2004)
	DED6477	USA	?	N/A	AY239026	N/A	Kropp and Matheny (2004)
I. soluta	EL10706	Sweden	+	N/A	FN550878	N/A	Unpublished
	JV7811F	Finland	+	N/A	JN974987	N/A	Ryberg and Matheny (2012)
I. sphaerospora	60-774	Japan	?	AB509953	N/A	N/A	Unpublished
	ZRL20151281	China	?	LT716044	KY418860	KY419006	Unpublished
I. sphaerospora	DED8059	Thailand	?	GQ892993	GQ892948	MH577472	Horak et al. (2015)
I. aff. *sphaerospora*	DED8153	Thailand	?	GQ892994	GQ892949	MH577471	Horak et al. (2015)
	PKSR10	India	?	KJ411954	N/A	KJ411970	Unpublished
I. squarrosofulva	MHHNU31548 (holotype)	China	+	MZ050799	MW715814	MW574997	This study
	MHHNU31927	China	+	MZ050802	MW715815	MW729766	This study
I. squarrosolutea	MHHNU8536	China	+	MK250946	MW709445	MW715635	This study
	MHHNU8984	China	+	MK388162	MW709446	MW715636	This study
	MHHNU31006	China	+	MZ050796	MW709457	MW715637	This study
	MHHNU31042	China	+	MZ050800	MW709486	MW715638	This study
	MHHNU31173	China	+	MZ050797	MW715813	MW729760	This study
	MHHNU31427	China	+	MZ050794	MW715804	MW729761	This study
	MHHNU 31434	China	+	MZ050798	MW709488	MW729762	This study
	MHHNU31445	China	+	MZ050801	MW709528	MW729763	This study
	MHHNU31875	China	+	MZ050795	MW709531	MW729764	This study
	MHHNU32151	China	+	MZ050793	MW709532	MW729765	This study
I. stellatospora	PRL2716	USA	?	N/A	EU307840	N/A	Kropp and Albee-Scott (2010)
	EL3004	Sweden	?	AM882747	AM882747	N/A	Unpublished
	PBM963	USA	?	N/A	AY038328	AY337403	Matheny (2005)
Outgroups							
Auritella dolichocystis	Trappe24844	Australia	?	N/A	AY380371	AY337371	Matheny (2005)
	Trappe24843	Australia	?	N/A	AY635764	AY635780	Unpublished
Inosperma calamistratum	PBM2351	USA	–	N/A	AY380368	KM245971	Matheny (2005)
	JV11950	USA	–	N/A	EU555452	KM245971	Unpublished
	PBM1105	USA	–	JQ801386	JQ815409	JQ846466	Matheny et al. (2020)
Mallocybe terrigena	JV16431	Finland	–	N/A	AY380401	AY333309	Matheny (2005)
	PBM1563	USA	–	N/A	MN178550	N/A	Unpublished
Nothocybe distincta	ZT9250	India	?	N/A	EU604546	N/A	Matheny et al. (2020)
Pseudosperma sororium	ADW0063	USA	+	JQ408779	JQ319703	JQ421073	Latha and Manimohan (2017)
	PBM3901	USA	+	N/A	MH220278	MH249810	Matheny et al. (2020)
Tubariomyces inexpectatus	AH20390	Spain	–	N/A	EU569855	GU907088	Matheny et al. (2020)
Crepidotus applanatus	420526MF0534	USA	–	N/A	AF205694	N/A	Kosentka et al. (2013)
	420526MF0689	USA	–	N/A	AY380406	N/A	Matheny et al. (2020)

The new sequences generated in this study are shown in bold. Toxins refer to Kosentka et al. (2013). The "+" indicates the confirmed presence of muscarine, the "?" indicates ambiguous for muscarine, and the "–" indicates a lack of muscarine.

was performed using RAxML v7.9.1 (Stamatakis 2006) under the GTR + GAMMA + I nucleotide substitution model and performing nonparametric bootstrapping with 1000 replicates. Bayesian inference (BI) was performed in MrBayes v3.2 (Ronquist et al. 2012). The optimal substitution model was determined using the Akaike information criterion (AIC) as implemented in MrModeltest v2.3 (Nylander 2004). The selected substitution model for the three partitions was as follows: General Time Reversible + Gamma (GTR + G) for ITS, and General Time Reversible + Proportion-Invariant + Gamma (GTR + I + G) for nrLSU and *rpb2*. The BI analysis was conducted with the following parameters: four simultaneous Markov chains (**MCMC**), each with two independent runs and trees summarized every 1000 generations. The analyses were completed after 1,000,000 generations when the average standard deviation of split frequencies was 0.009808 for the analysis, and the first 25% generations were discarded as burn-in. The phylograms from ML and BI analyses were visualized with FigTree v1.4.3 (Rambaut 2009).

Analysis of toxins by ultrahigh-performance liquid chromatography tandem mass spectrometry

The procedure of toxin extraction and detection followed Xu et al. (2020) with slight modifications. A 0.05 g powdery sample of dried mushroom pileus was mixed with 2 mL of a methanol-water solution (7:3 v/v) and vortexed for 30 min at room temperature. The mixture was treated in an ultrasonic bath for 30 min. After centrifugation at 10,000 rpm for 5 min, the supernatant was purified using a QuCHERS–PP column. Subsequently, the extract was mixed with acetonitrile to a final volume of 1.0 mL. The obtained sample solution was centrifuged at 21,000 rpm for 2 min before UPLC–MS/MS analysis. *Lentinula edodes* was used as a blank sample.

UPLC–MS/MS analysis was carried out with a Waters ACQUITY I-Class UPLC system coupled with a Waters Xevo TQ-S MS/MS system (Waters, Milford, MA, USA). The chromatographic separation was conducted using an ACQUITY UPLC Amide column (2.1 × 100 mm, 1.7 μm; Waters). A gradient elution system used the mobile phase A (acetonitrile) and the mobile phase B (0.05% formic acid aqueous solution) at a flow rate of 0.6 mL/min. The gradient program was as follows: (1) 70–10% A for 1 min, (2) 10% A for 0.5 min, (3) 10–70% A for 0.5 min, and (4) 70% A for 3 min. The analytical column was set to 40 °C, and the injection volume was 2.0 μL. The muscarine content was estimated in the mushroom extract by using standard muscarine (Sigma-Aldrich, St. Louis, MO, USA, Chemical purity ≥ 98%).

A protonated molecular ion ($[M + H]^+$ = 174.2) was chosen as the parent ion as well as two daughter ions of 57.0 and 97.0, which were used for qualitative and quantitative detection, respectively. The MS/MS conditions were as follows: ESI^+ mode; cone, 18 V; collision, 16 V; capillary, 3.0 kV; desolvation temperature, 500 °C; source temperature, 150 °C; desolvation gas flow, 1000 L/Hr; cone gas flow, 150 L/Hr; and collision gas flow, 0.19 mL/min. All the gases were 99.999% pure. Other parameters were used with default values. The product ion confirmation (PIC) was set as follows: scan function; daughter scan; activation threshold level, 500× background

noise; minimum activation threshold, 5000 counts; reset threshold level, 50% of act threshold; mass above parent, 100 Da; minimum mass, 50 Da; centroid; scan speed at 5000 amu/s; PIC duration, 0.5 s; and collision energy, 20 V. The analytical results were reported as X ± U (k = 2, p = 95%), where X is the analytical content and U is the expanded measurement uncertainty (Eurachem 2012).

Results

Phylogenetic data

The combined dataset (ITS, nrLSU, and *rpb2*) contained 1987 total characters and included 58 sequences. The topologies of ML and BI phylogenetic trees obtained in this study were practically the same and the only ML tree with branch lengths and support values is shown in Figure 1. All members of *Inocybe s. str.* in the dataset formed a monophyletic lineage with strong support (MLB = 85%, BPP = 1). Ten specimens of *I. squarrosolutea* from China (MHHNU8536, MHHNU8984, MHHNU31006, MHHNU31042, MHHNU31173, MHHNU31427, MHHNU31434, MHHNU31445, MHHNU31875, MHHNU32151) and two samples labeled as "*I. sphaerospora*" from China (ZRL20151281) and Japan (60-774) grouped together in a well-supported lineage (MLB = 100%, BPP = 1.0). The new species, *I. squarrosofulva*, formed a well-supported distinct lineage from *I. squarrosolutea* (MLB = 100%, BPP = 1.0) and is sister to the lineage of *I. squarrosoluta* with significant support (MLB = 100%, BPP = 1.0).

Taxonomy

Inocybe squarrosolutea **(Corner & E. Horak) Garrido, Bibliotheca Mycologica 120: 177, 1988.**
Figures 2, 3, 6a

≡ *Astrosporina squarrosolutea* Corner & E. Horak, *Persoonia* 10(2): 175, 1979.

Basidiomata. Small to medium-sized. Pileus: 30–60 mm in diameter, bell-shaped to convex when young, and then planar with umbonate center; margin strongly in-rolled or deflexed when young, and then gradually straight when mature; center covered with stout, erect, conic squamules (up to 2 mm high, 1–1.5 mm wide), coarsely fibrillose towards the margin; surface dry, primrose yellow (1A6) to bright yellow (2A5), becoming pale brown (3B6) over the disc. Lamellae crowded (ca. 50–70), 3–5 mm wide, adnexed to adnato-decurrent, often subsinuate; light yellow (1A5) turning to pale yellow-fuscous (2B5), edge concolorous, even. Stipe 35–75 × 4–8 mm, cylindrical or attenuated towards apex, stout, base subbulbous to bulbous, up to 16 mm wide; bright yellow (2A5); apex pruinose, covered with bright

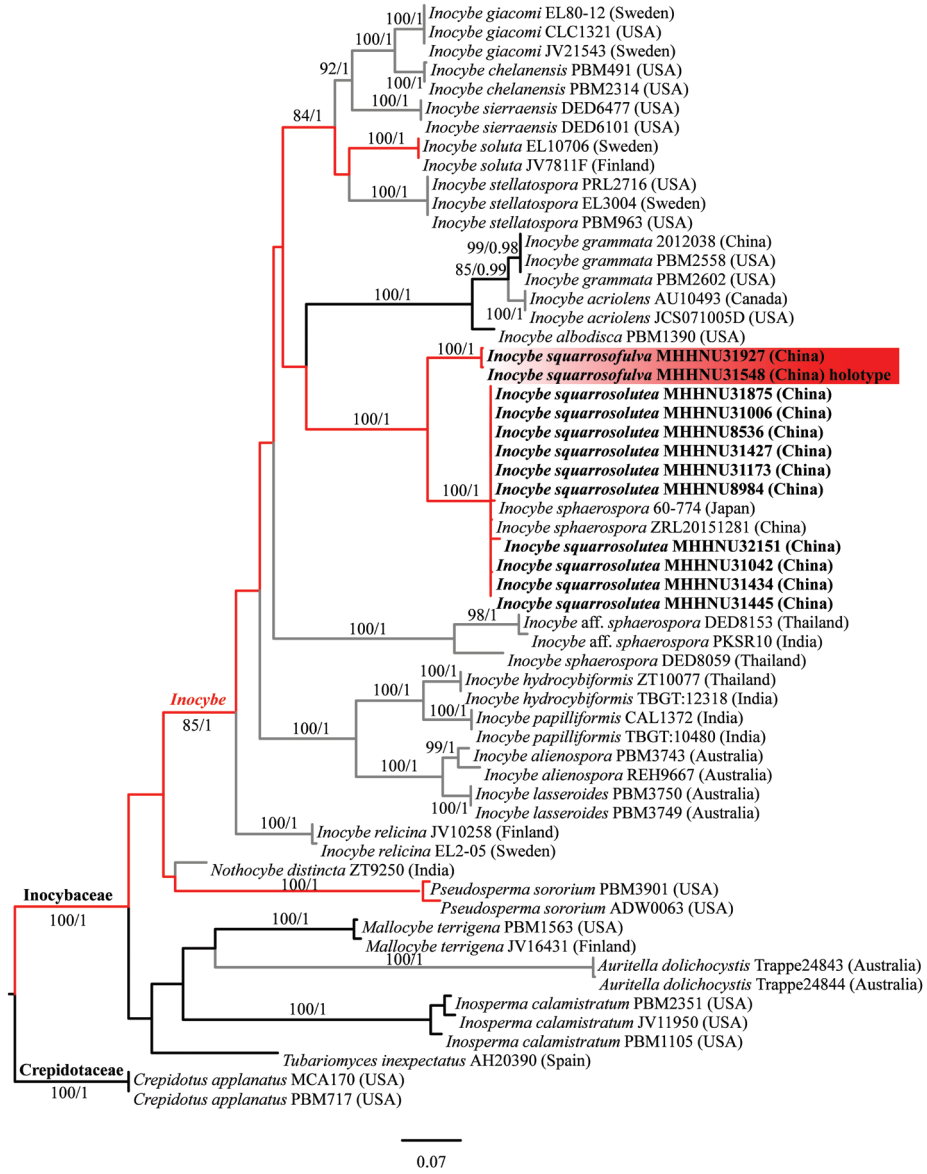

Figure 1. Phylogenetic relationship and placement of *Inocybe squarrosofulva* and *I. squarrosolutea* inferred from the combined dataset (ITS, nrLSU, and *rpb2*) using ML. Bootstrap values ≥80% and Bayesian posterior probabilities ≥0.95 are reported on the branches. Sequences generated in this study are shown in bold. The new species is indicated in red. The red branch indicates the confirmed presence of muscarine, the gray branch indicates ambiguous for muscarine, and the black branch indicates a lack of muscarine.

yellow(2A5) to orange (2A6), longitudinal, floccose-fibrillose fibrils towards base; dry, solid. Cortina conspicuous present in young specimens. Context pale yellow (1A4) in stipe and cuticle.

Figure 2. Basidiomata of *Inocybe squarrosolutea* **a, b** MHHNU8536 **c** MHHNU31006, and **d** MHHNU31427. Scale bars: 10 mm.

Basidiospores. (5.0) 5.5–9.0 (10.0) μm (av. 7.1 μm, SD 1.1 μm) × (4.0) 4.5–6.0 (6.5) μm (av. 5.3 μm, SD 0.6 μm), Q = (1.00) 1.11–1.67 (1.80), Qm = 1.33 ± 0.19 (n = 200 of 10 coll.), nodulose, 6–8 hemispheric knobs, yellow-brown with 5% KOH. Basidia: 17–26 × 7–9 μm, 4-spored, clavate to broadly clavate. Pleurocystidia: 37–67 μm (av. 46.1 μm, SD 3.0 μm) × 10–18 μm (av. 13.4 μm, SD 1.2 μm), Q = 2.80–4.0 (n = 100 of 10 coll.), abundant, broadly fusoid to lageniform; crystalliferous at apex, base usually truncate to obtuse, occasionally tapered into pedicel; metuloid, hyaline, sometimes contain a few small crystals or resinous inclusions, thick-walled, walls up to 1.5 μm thick, bright yellow with 5% KOH. Cheilocystidia similar to pleurocystidia, 35–62 × 9–17 μm; paracystidia: 12–25 × 5–11 μm, abundant, thin-walled, translucent inside, clavate to broadly clavate. Hymenophoral trama: sub-regularly arranged, yellowish with 5% KOH, composed of thin-walled, cylindrical to inflated hyphae 4–23 μm wide. Caulocystidia: 48–98 × 17–22 μm, present at stipe apex, in clusters, similar to those of hymenial cystidia; cauloparacystidia: 20–35 × 10–13 μm, clavate to broadly clavate, thin-walled, nearly hyaline inside, abundant. Pileipellis a trichoderm, regular

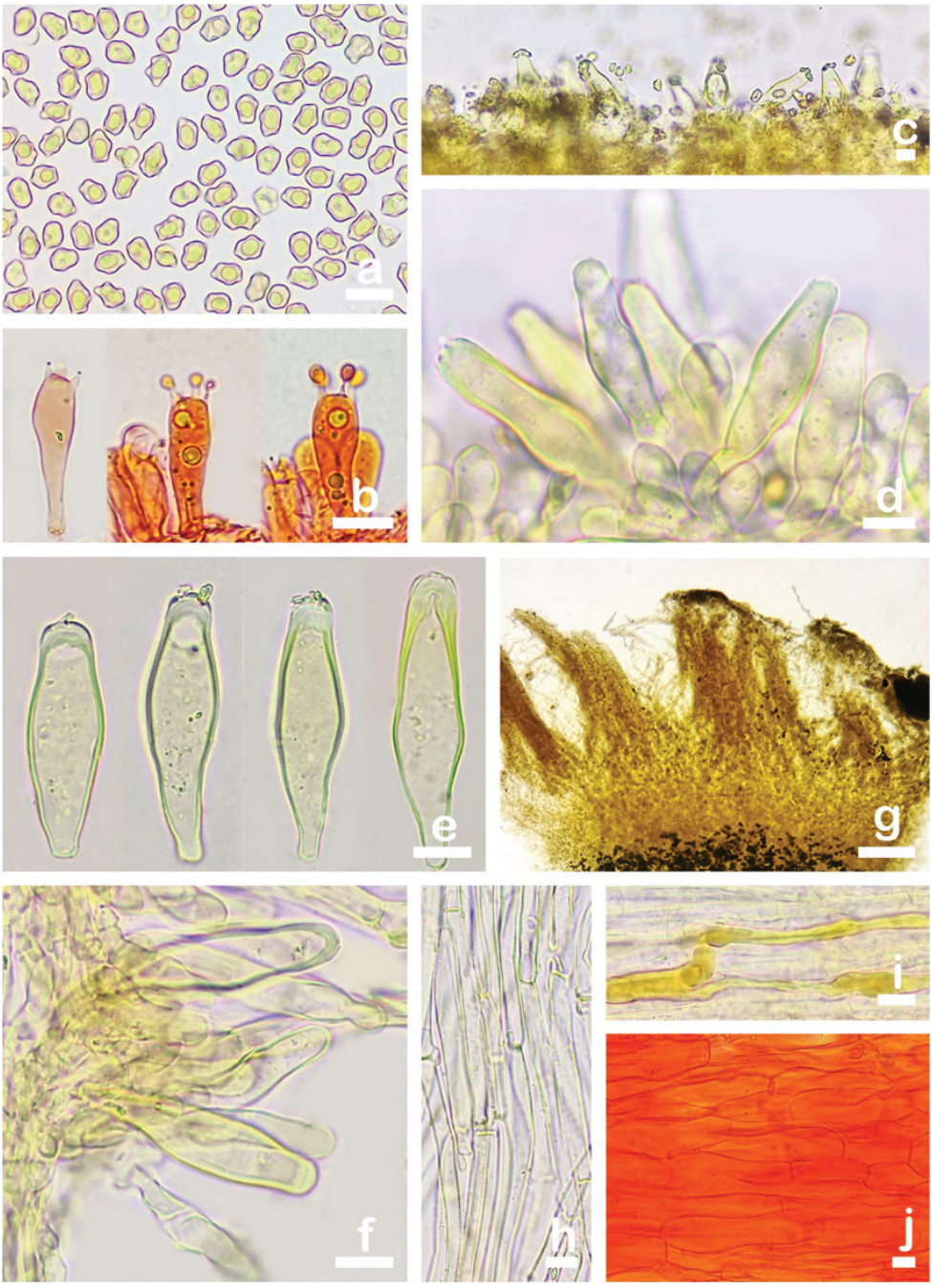

Figure 3. Microscopic features of *Inocybe squarrosolutea* (MHHNU31427) **a** basidiospores **b** basidia with probasidium **c** gill edge **d** cheilocystidia and paracystidia **e** pleurocystidia **f** caulocystidia and caulo-paracystidia **g, h** pileipellis **i** oleiferous hyphae, and **j** hymenial hyphae. Scale bars: 10 μm.

to subregular, pale brown with 5% KOH, composed of smooth, thin-walled, cylindrical hyphae, 4–8 μm in diameter. Oleiferous hyphae present in pileus and stipe trama, 3–10 μm in diameter, branched. Clamp connections present and common in all tissues.

Habitat. Single to scattered in mixed forest dominated by *Pinus* and *Quercus*.

Known distribution. Malaysia (type location) (Horak 1979), China (Hunan Province, Anhui Province).

Specimens examined. China, Hunan Province: Yongshun County, 29 July 2015, MHHNU8536; Yizhang County, 16 September 2016, MHHNU8984; Ningyuan County, 28 May 2017, MHHNU31006; Youxian County, 9 June 2017, MHHNU31042; 18 June 2019, MHHNU31445; Guidong County, 6 July 2018, MHHNU31173; Yongzhou City, 22 May 2019, MHHNU31427; 11 June 2020, MHHNU31875; Qidong County, 2 June 2019, MHHNU31434; Anhui Province, Huangshan City, 11 Aug. 2020, MHHNU32151.

***Inocybe squarrosofulva* S.N. Li, Y.G. Fan & Z.H. Chen, sp. nov.**

MycoBank No: 839726

Figures 4, 5, 6b

Etymology. *Squarrosus* (Latin), squamous; *fulvus* (Latin), brown-orange, referring to its pileus.

Holotype. China. Hunan Province: Zhangjiajie, Badagongshan National Nature Reserve, 29°67.57'N, 109°74.45'E, alt. 1600 m, on ground in subtropical montane forest, 29 July 2019, Z.H. Chen and S.N. Li, MHHNU31548 (GenBank accession no. ITS: MZ050799; nrLSU: MW715814; *rpb2*: MW574997).

Diagnosis. Small to medium-sized basidiomata. Orange-brown to dark brown pileus with squarrose scales. Yellowish brown to brownish , adnexed lamellae. Stipe equal, stout, with distinctly filamentous annulate cortina, pruinose at apex. Odor like raw potatoes. Nodulose basidiospores with six nodules. Hymenial cystidia are broadly fusoid to lageniform, thick-walled. Differs from *Inocybe squarrosolutea* in its orange-brown to dark brown pileus, distinctly filamentous annulus, and less nodulose basidiospores.

Basidiomata. Small to medium-sized. Pileus 25–55 mm in diameter, spherical to bell-shaped when young, and gradually flattened to hemispheric or convex; margin strongly in-rolled when young then decurved or slightly uplifted; yellowish (2A5), center covered with yellow ochre (5C7) to brownish yellow (5C8) erect conical fibrillose scales (up to 1.5 mm high, 1–1.5 mm wide), coarsely fibrillose-rimose towards the margin; pileus with crenellated, nonpersisting fibrillose veil remnants at margin. Lamellae adnexed, crowded (ca. 55–70), up to 4 mm wide; yellowish brown (4C7), becoming brownish (5E4) with age, edge concolorous. Stipe 40–80 × 5–8 mm, cylindrical, equal or slightly enlarged at the base, solid; light yellow (2A3) to yellow ochre (5C7); pruinose with few yellowish-brown (4C7) furfuraceous scales at apex; towards the base covered with numerous, yellow-ochre (5C7), woolly-fibrillose, incomplete

Figure 4. Basidiomata of *Inocybe squarrosofulva* **a, b** MHHNU31548 **c, d** MHHNU31927. Scale bars: 10 mm.

zones; dry. Cortina conspicuous, annulate, composed of yellow ochre (5C7) fibrils, and remains at the upper part of the stipe. Context: pale yellow (2A5) in pileus and stipe. Odor like raw potatoes.

Basidiospores. (4.5) 5.0–7.0 µm (av. 6.6 µm, SD 1.0 µm) × 4.0–6.0 (7.0) (av. 5.3 µm, SD 0.8 µm) µm, Q = (1.00) 1.10–1.67 (1.75), Qm = 1.26 ± 0.16 (n = 80 of 4 coll.), nodulose with six hemispheric knobs, yellowish-brown with 5% KOH, containing a bright yellow oil droplet of uniform size inside. Basidia: 18–24 × 8–10 µm, 4-spored, clavate to broadly clavate. Pleurocystidia: 36–49 µm (av. 43.8 µm, SD 3.9 µm) × 13–18 µm (av. 15.5 µm, SD 2.6 µm), Q = 2.12–3.46 (n = 30 of 2 coll.), mostly hyaline, few with bright yellow oily inclusions, fusiform to broadly fusiform, with crystalliferous apices, obtuse or truncated at base; thick-walled,

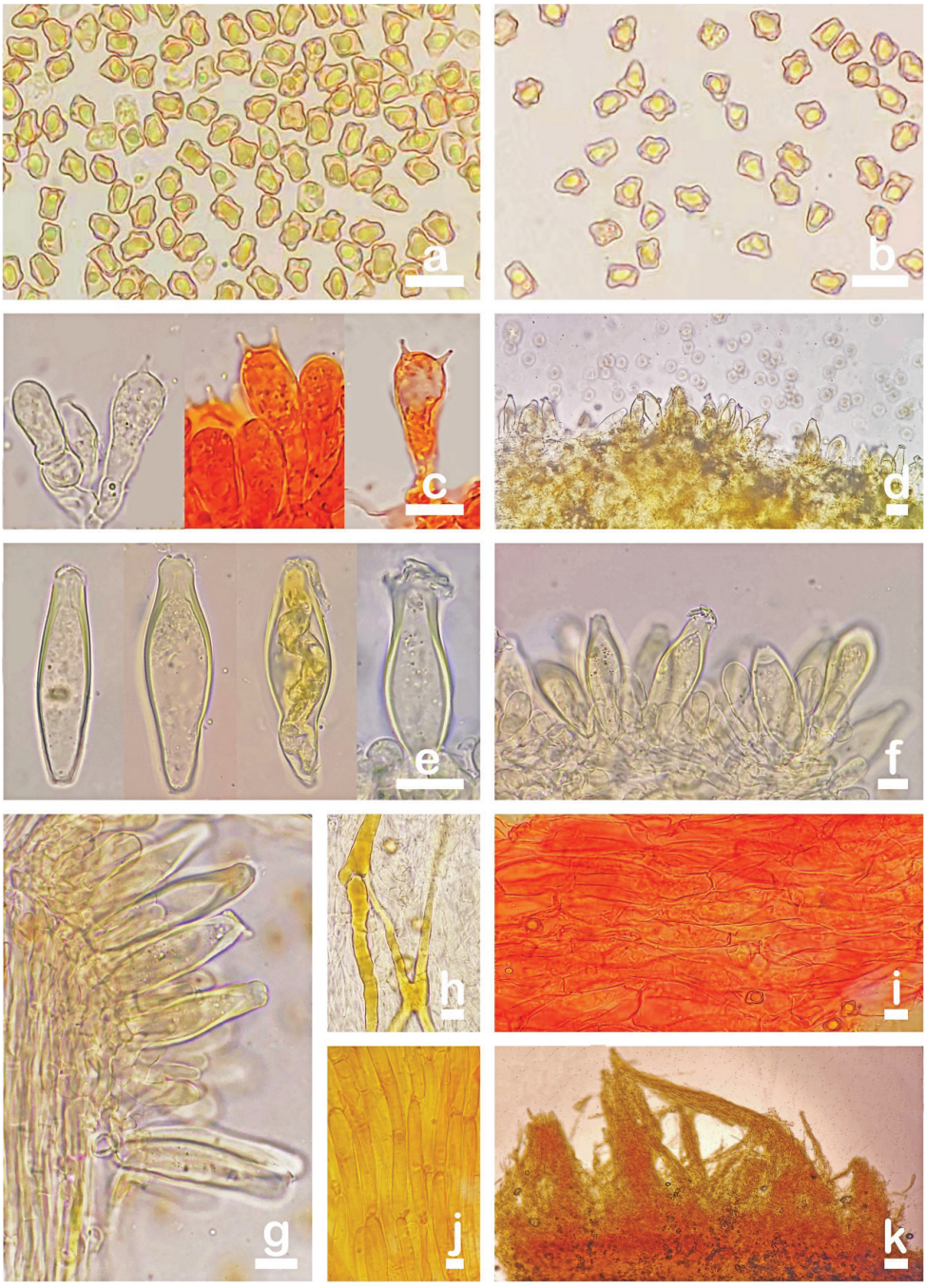

Figure 5. Microscopic features of *Inocybe squarrosofulva* (MHHNU31548, holotype) **a, b** basidiospores, **c** basidia with probasidium **d** gill edge **e** pleurocystidia **f** cheilocystidia and paracystidia **g** caulocystidia and cauloparacystidia **h** oleiferous hyphae **i** hymenial hyphae, and **j, k** pileipellis. Scale bars: 10 μm.

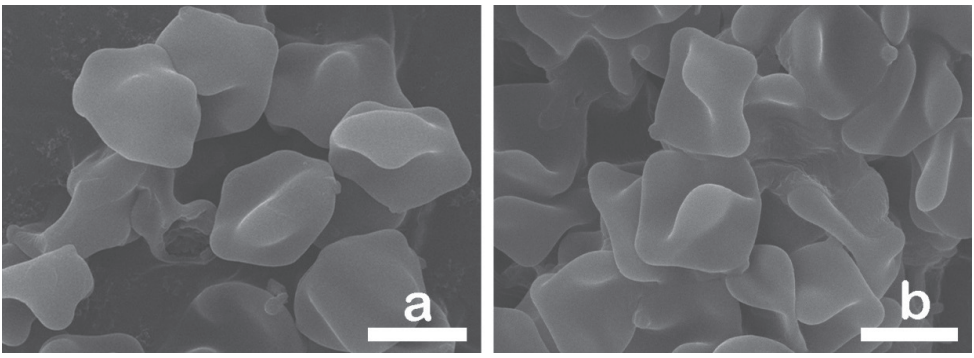

Figure 6. SEM images showing basidiospores of **a** *Inocybe squarrosolutea* **b** *Inocybe squarrosofulva*. Scale bars: 5 μm.

walls bright yellow with 5% KOH, up to 2 μm thick towards apex. Cheilocystidia: 30–48 × 9–19 μm, similar to pleurocystidia, hyaline. Cheiloparacystidia: 10–23 × 6–12 μm, abundant among cheilocystidia, obovate, elliptic to clavate, thin-walled, hyaline. Hymenophoral trama: regular to subregular, composed of inflated hyphae, up to 18 μm wide, hyaline to lightly yellow with 5% KOH, thin-walled. Pileipellis: a trichoderm, subregular, consisting of cylindrical hyphae 5–13 μm in diameter, walls pale yellow brown with 5% KOH, smooth, thin-walled. Caulocystidia: present at stipe apex, 23–49 × 9–21 μm, in clusters, thick-walled, walls thinner than pleurocystidia, hyaline or with pale yellow intracellular contents. Cauloparacystidia: 8–19 × 3–10 μm, clavate or broadly clavate, hyaline, thin-walled. Oleiferous hyphae present in pileus and stipe trama, 4–11 μm in diameter, branched. Clamp connections seen on all hyphae.

Habitat. On soil in subtropical montane forest dominated by *Fagus lucida*.

Known distribution. Known from the type locality.

Other examined specimens. 27 July 2020, Z.H. Chen and S.N. Li, MHHNU31927.

Toxin detection

Through UPLC–MS/MS detection, we found that both *I. squarrosolutea* and *I. squarrosofulva* contained muscarine (Figs 7, 8). In the qualitative analysis, muscarine was identified by comparing the retention time (0.91 min) and relative deviation (0.6%) within the allowable relative range of 25%. The calibration curve in the matrix blank extract given by Y = 69369X + 6849.33, R^2 = 0.9990 (X is injection volume, Y is peak area, and R^2 is correlation coefficient) for muscarine concentration was in the range of 0.5–20 ng/mL. The contents of in *I. squarrosolutea* and *I. squarrosofulva* were 136.4 ± 25.4–1683.0 ± 313 mg/kg dry weight and 31.2 ± 5.8–101.8 ± 18.9 mg/kg dry weight, respectively (Fig. 9). Recovery of muscarine ranged from 72.2 to 93.6%; the average recovery was 83.0%.

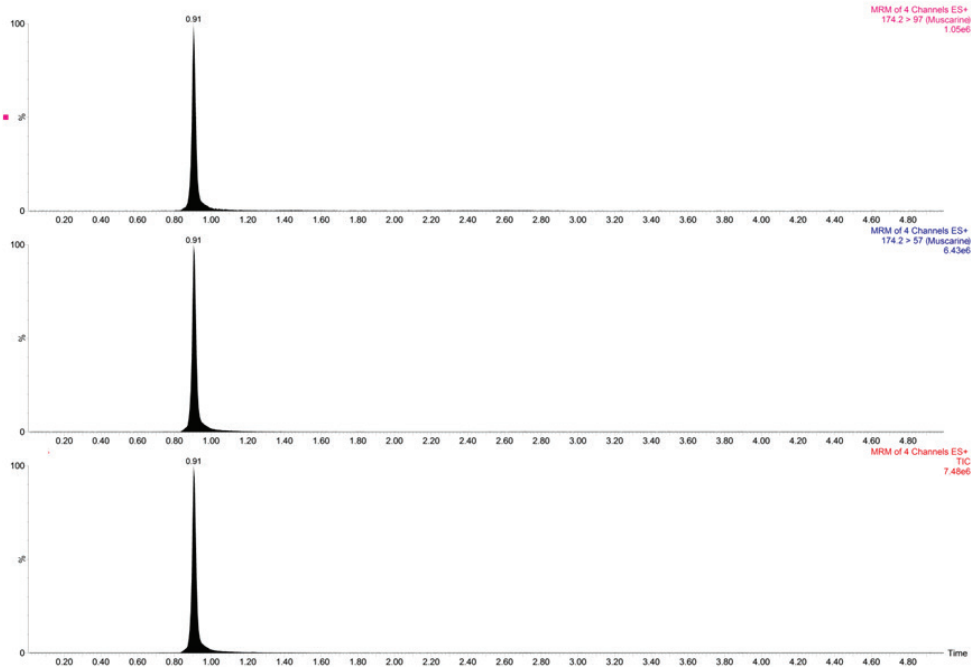

Figure 7. Total ion current (TIC) chromatogram of muscarine in *Inocybe squarrosolutea* (MHHNU31427).

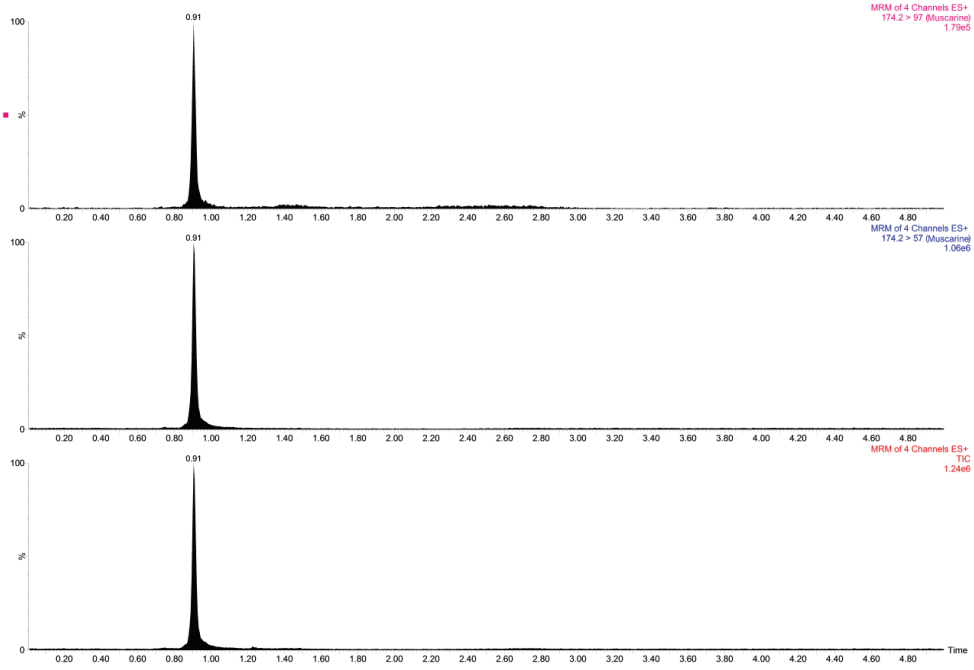

Figure 8. Total ion current (TIC) chromatogram of muscarine in *Inocybe squarrosofulva* (MHHNU31548).

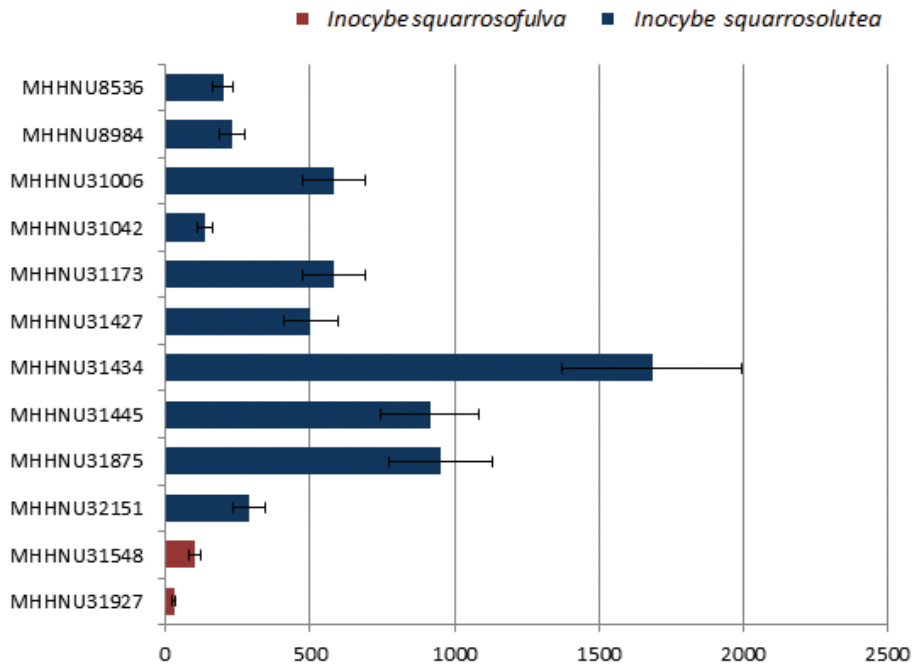

Figure 9. Relative muscarine concentrations measured by UPLC–MS/MS.

Discussion

Species delimitation

Based on the morphological characteristics, the mushroom was identified as *I. squarrosolutea*, which was first described from Cameron Highlands of Malaysia (Horak 1979). According to the original description, this species is characterized by a large-sized basidiomata, a bright yellow coloration and a scaly pileus and orange fibrillose veil remnants on the stipe. Our Chinese materials fit well with the original description in basidiomata size, outwards appearances, and the shape and size of micro-features. Meanwhile, there are some tiny difference between them. The holotype of *I. squarrosolutea* has longer scales (up to 4 mm) in pileus, smaller basidiospores (4–8 × 5–6 μm), finer basidia (18–26 × 5–7 μm), thicker hymenial cystidia (30–60 × 14–25 μm) (Horak 1979). This species is a close relative of *I. lutea* which, by contrast, has a smaller fruiting body, a smooth pileus, and distinctly smaller basidiospores (Kobayasi 1952; Horak 1979). It is easily for people to confuse *I. squarrosolutea* and *I. sphaerospora* because of their similar appearance. In fact, they can be easily distinguished by their basidiospores. The basidiospores of *I. squarrosolutea* are nodulose, while those of *I. sphaerospora* are globose (Kobayasi 1952; Horak et al. 2015). In phylogenetic analysis (Fig. 1) the specimens of *I. sphaerospora* identified by Horak et al. (2015) formed a monophyletic lineage with strong support (MLB = 100%, BPP = 1), and was distinct from *I. squarrosolutea*.

However, the two materials labeled as *I. sphaerospora* from China (ZRL20151281) and Japan (60-774), cluster together with *I. squarrosolutea* in the phylogenetic tree, indicating an inaccurate identification of these two materials.

Inocybe squarrosofulva is characterized by its orange brown to dark brown pileus with squarrose scales, distinctly filamentous annulate cortina in stipe, stipe pruinose only near the apex, nodulose basidiospores with six hemispheric knobs, and its odor like raw potatoes. Phylogenetic analyses revealed that *I. squarrosofulva* is an independent lineage in *Inocybe s. str.* and is sister to *I. squarrosolutea*. However, *I. squarrosolutea* differs in having primrose yellow to bright yellow pileus with less squarrose scales, no distinctly filamentous annulus cortina in the stipe, a subbulbous to bulbous stipe base, a less nodulose basidiospores, and smaller hymenial cystidia. Microscopically, *I. lutea* is similar to new species in shape and size of pleurocystidia and basidiospores, but the pileus of *I. lutea* covered with radially fibrils and pruinate all over the stipe (Kobayasi 1952; Horak 1979). Lastly, a Papua New Guinea material described as *Inocybe luteifolia* (E. Horak) Garrido 1988 (non *Inocybe luteifolia* A.H. Sm. 1941), which is an illegitimate species name, resembles the new species in macromorphology, but it has smaller basidiomata, larger cheilocystidia and pleurocystidia (55–85 × 10–20 μm), no caulocystidia on the stipe, and a fish-like odor (Horak 1979).

Kuyper (1986) recognized two groups on the (informal) level of "supersection", viz. *Cortinatae* and *Marginatae*, according to the different development mode and, hence, absence or presence of a cortina, and the nature of stipe covering. Due to their presence of a cortina and pruinose at the apex of the stipe, both *I. squarrosolutea* and *I. squarrosofulva* might be classified in supersection *Cortinatae*. The morphological characteristics corresponding to the phylogenetic branches are not yet clear (Matheny 2005; Matheny et al. 2020), so the infrageneric framework of *Inocybe s. str.* is still unknown and its characterization requires more research.

Toxicity in *Inocybe*

According to the literature, muscarine was first isolated and identified from *Amanita muscaria*, but the actual muscarine content of *A. muscaria* is very low (usually around 0.0003% of the fresh weight) (Waser 1961). Conversely, muscarine concentrations are much higher in *Inocybe s. l.* spp. (Malone et al. 1962). Brown et al. (1962) detected the muscarine contents of 34 species of *Inocybe s. l.* by paper chromatographic method, ranging from 0.01 to 0.80% in approximately 75% of them. Kosentka et al. (2013) used liquid chromatography–tandem mass spectrometry (LC–MS/MS) to determine whether muscarine was present in 30 new samples of *Inocybe s. l.* Of the 30 species they assayed, eleven species tested positive for presence of muscarine, ranging from ca. 0.00006% to 0.5%. Xu et al. (2020) determined the muscarine content of *I. serotina* by UPLC-MS/MS, and its muscarine content was 324.0 ± 62.4 mg/kg. In our study, the toxin content in each sample was determined using a linear regression equation according to the peak area of the UPLC–MS/MS analysis chromatogram of the test sam-

ple (Figs 7, 8). The results showed that both species contained muscarine; the content of muscarine in *I. squarrosolutea* ranged from 136.4 ± 25.4 to 1683.0 ± 313 mg/kg dry weight and the content in *I. squarrosofulva* was generally lower, ranging from 31.2 ± 5.8 to 101.8 ± 18.9 mg/kg dry weight (Fig. 9). Calculated on a dry-weight basis, the percentage concentrations were 0.01–0.17% for *I. squarrosolutea* and 0.003–0.01% for *I. squarrosofulva*, which is in range of previous reports.

There are some differences in the muscarine content of different poisonous *Inocybe* spp., even within a particular species. The capacity of *Inocybe* species to accumulate muscarine may be influenced by certain hereditary (infraspecific races) or environmental factors (Brown et al. 1962). In this study, the differences in muscarine content among specimens of *I. squarrosolutea* may be related to region and climate. *I. squarrosofulva* MHNNU31548 and *I. squarrosofulva* MHNNU31927 were collected in the same place in different years. The weather was sunny at the time of the collection of *I. squarrosofulva* MHNNU31548, and there was heavy rain at the time of the collection of *I. squarrosofulva* MHNNU31927, so it is presumed that the difference in muscarine content may be related to rainwater washing.

Acknowledgements

This research was funded by the National Natural Science Foundation of China (Grant Nos. 31872616 and 31860009); the Biodiversity Survey and Assessment Project of the Ministry of Ecology and Environment, China (Grant No. 2019HJ2096001006); and the Ningxia Provincial National Natural Science Foundation (Grant No. 2020AAC03437). The authors are very grateful to Dr. Haijiao Li (National Institute of Occupational Health and Poison Control, Chinese Centre for Disease Control and Prevention, China) and Zhengmi He (Kunming Institute of Botany, Chinese Academy of Sciences, China) for critically reviewing the manuscript.

References

Bandini D, Oertel B, Schüssler C, Eberhardt U (2020a) Noch mehr Risspilze: Fünfzehn neue und zwei wenig bekannte Arten der Gattung *Inocybe*. Mycologia Bavarica 20: 13–101.

Bandini D, Vauras J, Weholt Y, Oertel B, Eberhardt U (2020b) *Inocybe woglindeana*, a new species of the genus *Inocybe*, thriving in exposed habitats with calcareous sandy soil. Karstenia 58: 41–59. https://doi.org/10.29203/ka.2020.488

Bau T, Bao HY, Yu LI (2014) A revised checklist of poisonous mushrooms in China. Mycosystema 33: 517–548. https://doi.org/10.13346/j.mycosystema.130256

Brown JK, Malone MH, Stuntz DE, Tyler VE (1962) Paper chromatographic determination of muscarine in *Inocybe* species. Journal of Pharmaceutical Sciences 51: 853–856. https://doi.org/10.1002/jps.2600510908

Caiafa MV, Sandoval-Leiva P, Matheny PB, Calle A, Smith ME (2021) Four new species of sequestrate *Inocybe* from Chilean Nothofagaceae forests. Mycologia 113(3): 629–642. https://doi.org/10.1080/00275514.2020.1859324

Chen JL, Zhang SX, Chen BZ, Zhang HY (1987) Investigation report of poisoning caused by *Inocybe asterospora*. Junduiweisheng Zazhi 5: 36–38. [in Chinese]

Chen ZH, Yang ZL, Bau T, Li TH (2016) Poisonous mushroom: Recognition and poisoning treatment, 1st edn. Science Press, Beijing, 308 pp.

Deng SQ (1963) Fungi of China. Science Press, Beijing, 808 pp. [in Chinese]

Eurachem (2012) CITAC Guide: Quantifying uncertainty in analytical measurement, 3rd edn. 978–0–948926–30–3. http://www.eurachem.org

Fan YG, Bau T (2010) A revised checklist of the genus *Inocybe* (Fr.) Fr. in China. Journal of Fungal Research 8: 189–193.

Fan YG, Bau T (2013) Two striking *Inocybe* species from Yunnan Province, China. Mycotaxon 123: 169–181. https://doi.org/10.5248/123.169

Fan YG, Bau T (2014a) *Inocybe hainanensis*, a new lilac-stiped species from tropical China. Mycosystema 33: 954–960. https://doi.org/10.13346/j.mycosystema.140043

Fan YG, Bau T (2014b) *Inocybe miyiensis*, a new two-spored species in section *Marginatae* from China. Nova Hedwigia 98: 179–185. https://doi.org/10.1127/0029-5035/2013/0135

Fan YG, Bau T (2017) Three newly recorded species of *Inocybe* subg. *Inocybe* in China. Mycosystema 36: 251–259. https://doi.org/10.13346/j.mycosystema.150274

Fan YG, Bau T (2018) Three new species of *Inocybe* sect. *Rimosae* from China Mycosystema 37(6): 693–702. https://doi.org/10.13346/j.mycosystema.180033

Fan YG, Bau T (2020) Two new smooth-spored species of *Inocybe* (Inocybaceae, Agaricales) from Gansu Province, northwestern China Mycosystema 39: 1694–1705.

Fan YG, Bau T, Kobayashi T (2013) Newly recorded species of *Inocybe* collected from Liaoning and Inner Mongolia. Mycosystema 32: 302–308.

Fan YG, Wu RH, Bau T (2018) Two new species and eight newly recorded species of subg. *Inocybe* from China. Journal of Fungal Research 16: 70–83. https://doi.org/10.13341/j.jfr.2018.1211

Fries E (1821) Systema mycologicum. Gryphis waldiae, Lund, 520 pp.

Fries E (1863) Monographia hymenomycetum sueciae. CA LeZer, Uppsala, 355 pp.

Hall TA (1999) BioEdit: A user-friendly biological sequence alignment editor and analysis program for Windows 95/98/NT. Nucleic Acids Symposium Series 41: 95–98. https://doi.org/10.1021/bk-1999-0734.ch008

Horak E (1979) *Astrosporina* (Agaricales) in Indomalaya and Australasia. Rijksherbarium, Leiden 10: 157–205. https://doi.org/10.2307/3759513

Horak E, Matheny PB, Desjardin DE, Soytong K (2015) The genus *Inocybe* (Inocybaceae, Agaricales, Basidiomycota) in Thailand and Malaysia. Phytotaxa 230: 201–238. https://doi.org/10.11646/phytotaxa.230.3.1

Katoh K, Standley DM (2013) MAFFT multiple sequence alignment software version 7: improvements in performance and usability. Molecular Biology and Evolution 30: 772–780. https://doi.org/10.1093/molbev/mst010

Kobayasi Y (1952) On the genus *Inocybe* from Japan. Nagaoa 2: 76–115.

Kornerup A, Wanscher JH (1978) The methuen handbook of colour, 3rd edn. Methuen, London, 252 pp.

Kosentka P, Sprague SL, Ryberg M, Gartz J, May AL, Campagna LR, Matheny PB (2013) Evolution of the toxins muscarine and psilocybin in a family of mushroom-forming fungi. PLoS ONE 8: e64646. https://doi.org/10.1371/journal.pone.0064646

Kropp BR, Matheny PB (2004) Basidiospore homoplasy and variation in the *Inocybe chelanensis* group in north america. Mycologia 96(2): 295–309. https://doi.org/10.2307/3762065

Kropp BR, Albee-Scott S (2010) *Inocybe tauensis*, a new species from the samoan archipelago with biogeographic evidence for a paleotropical origin. Fungal Biology 114(9): 790–796. https://doi.org/10.1016/j.funbio.2010.07.005

Kuyper TW (1986) A revision of the genus *Inocybe* in Europe *I.* subgenus *Inosperma* and the smoothspored species of subgenus *Inocybe*. Rijksherbarium, Leiden 3: 1–247.

Latha KPD, Manimohan P (2017) Inocybes of Kerala. SporePrint Books, Calicut, 181 pp.

Li HJ, Zhang HS, Zhang YZ, Zhou J, Sun CY (2021) Mushroom poisoning outbreaks – China, 2020. China CDC Weekly 3: 41–45. https://doi.org/10.46234/ccdcw2021.014

Malone MH, Robichaud RC, Tyler Jr VE, Brady LR (1962) Relative muscarinic content of thirty Inocybe species. Lloydia 25: 231–237.

Mao XL (2006) Poisonous mushrooms and their toxins in China. Mycosystema 25: 345–363.

Mešić A, Haelewaters D, Tkalčec Z, Liu J, Kušan I, Aime MC, Pošta A (2021) *Inocybe brijunica* sp. nov. a new ectomycorrhizal fungus from mediterranean croatia revealed by morphology and multilocus phylogenetic analysis. Journal of Fungi 7(3): e199. https://doi.org/10.3390/jof7030199

Matheny PB (2005) Improving phylogenetic inference of mushrooms with RPB1 and RPB2 nucleotide sequences (*Inocybe*; Agaricales). Molecular Phylogenetics and Evolution 35: 1–20. https://doi.org/10.1016/j.ympev.2004.11.014

Matheny PB (2009) A phylogenetic classification of the Inocybaceae. McIlvainea 18: 11–21.

Matheny PB, Aime CM, Smith ME, Henkel TW (2012) New species and reports of *Inocybe* (Agaricales) from Guyana. Tomo 37: 23–39.

Matheny PB, Hobbs AM, Esteve-Raventós F (2020) Genera of Inocybaceae: New skin for the old ceremony. Mycologia 112: 1–38. https://doi.org/10.1080/00275514.2019.1668906

Nylander J (2004) MrModeltest v2. Program distributed by the author. Evolutionary Biology Center, Uppsala University.

Rambaut A (2009) FigTree Version 1.3.1. http://tree.bio.ed.ac.uk

Ronquist F, Teslenko M, Mark P, Ayres DL, Darling A, Höhna S, Larget B, Liu L, Suchard MA, Huelsenbeck JP (2012) MrBayes 3.2: Efficient bayesian phylogenetic inference and model choice across a large model space. Systematic Biology 61: 539–542. https://doi.org/10.1093/sysbio/sys029

Ryberg M, Matheny PB (2012) Asynchronous origins of ectomycorrhizal clades of agaricales. Proceedings of the Royal Society B – Biological Sciences 279(1735): 2003–2011. https://doi.org/10.1098/rspb.2011.2428

Stamatakis A (2006) RAxML-VI-HPC: Maximum likelihood-based phylogenetic analyses with thousands of taxa and mixed models. Bioinformatics 22: 2688–2690. https://doi.org/10.1093/bioinformatics/btl446

Vilgalys R, Hester M (1990) Rapid genetic identification and mapping of enzymatically amplified ribosomal DNA from several *Cryptococcus* species. Journal of Bacteriology 172: 4238–4246. https://doi.org/10.1111/j.1096-0031.2010.00329.x

Wang YC (1973) Two new species of Agaricales. Acta Microbiologica Sinica 13(1): 7–10.

Waser PG (1961) Chemistry and pharmacology of muscarine, muscarone, and some related compounds. Pharmacological Reviews 13: 465–515.

White J, Weinstein SA, Haro LD, Bédry R, Zilker T (2018) Mushroom poisoning: A proposed new clinical classification. Toxicon 157: 53–65. https://doi.org/10.1016/j.toxicon.2018.11.007

White TJ, Bruns T, Lee S, Taylor J (1990) Amplification and direct sequencing of fungal ribosomal RNA genes for phylogenies. In: Innis MA, Gelfand DH, Sninsky JJ, White TJ (Eds) PCR protocols: aguidetomethods and applications. Academic Press, San Diego, 315–322. https://doi.org/10.1016/B978-0-12-372180-8.50042-1

Xu F, Zhang YZ, Zhang YH, Guan GY, Zhang KP, Li HJ, Wang JJ (2020) Mushroom poisoning from *Inocybe serotina*: A case report from Ningxia, northwest China with exact species identification and muscarine detection. Toxicon 179: 72–75. https://doi.org/10.1016/j.toxicon.2020.03.003